R-08-86

Water-rock interaction modelling and uncertainties of mixing modelling

SDM-Site Forsmark

Maria J Gimeno, Luis F Auqué,
Javier B Gómez, Patricia Acero
University of Zaragoza, Spain

August 2008

Svensk Kärnbränslehantering AB
Swedish Nuclear Fuel
and Waste Management Co
Box 250, SE-101 24 Stockholm
Tel +46 8 459 84 00

ISSN 1402-3091
SKB Rapport R-08-86

Water-rock interaction modelling and uncertainties of mixing modelling

SDM-Site Forsmark

Maria J Gimeno, Luis F Auqué,
Javier B Gómez, Patricia Acero
University of Zaragoza, Spain

August 2008

Preface

The overall objectives of the hydrogeochemical description for Forsmark are to establish a detailed understanding of the hydrogeochemical conditions at the site and to develop models that fulfil the needs identified by the safety assessment groups during the site investigation phase. Issues of concern to safety assessment are radionuclide transport and technical barrier behaviour, both of which are dependent on the chemistry of groundwater and pore water and their evolution with time.

The work has involved the development of descriptive and mathematical models for groundwaters in relation to rock domains, fracture domains and deformation zones. Past climate changes are one of the major driving forces for hydrogeochemical changes and therefore of fundamental importance for understanding the palaeohydrogeological, palaeohydrogeochemical and present evolution of groundwater in the crystalline bedrock of the Fennoscandian Shield.

Understanding current undisturbed hydrochemical conditions at the proposed repository site is important when predicting future changes in groundwater chemistry. The causes behind of copper corrosion and/or bentonite degradation are of particular interest as they may jeopardise the long-term integrity of the planned SKB repository system. Thus, the following variables are considered for the hydrogeochemical site descriptive modelling: pH, Eh, sulphur species, iron, manganese, carbonate, phosphate, nitrogen species, total dissolved solids (TDS), isotopes, colloids, fulvic and humic acids and microorganisms. In addition, dissolved gases (e.g. carbon dioxide, methane and hydrogen) are of interest because of their likely participation in microbial reactions.

In this series of reports, the final hydrogeochemical evaluation work of the site investigation at the Forsmark site, is presented. The work was conducted by SKB's hydrogeochemical project group, ChemNet, which consists of independent consultants and university researchers with expertise in geochemistry, hydrochemistry, hydrogeochemistry, microbiology, geomicrobiology, analytical chemistry etc. The resulting site descriptive model version, mainly based on 2.2 data and complementary 2.3 data, was carried out during September 2006 to December 2007. Several groups within ChemNet were involved and the evaluation was conducted independently using different approaches ranging from expert knowledge to geochemical and mathematical modelling including transport modelling. During regular ChemNet meetings the results have been presented and discussed.

The original works by the ChemNet modellers are presented in five level III reports containing complementary information for the bedrock hydrogeochemistry Forsmark Site Descriptive Model (SDM-Site Forsmark, R-08-47) level II report.

There is also an additional level III report: Fracture mineralogy of the Forsmark area by Sandström et al. R-08-102.

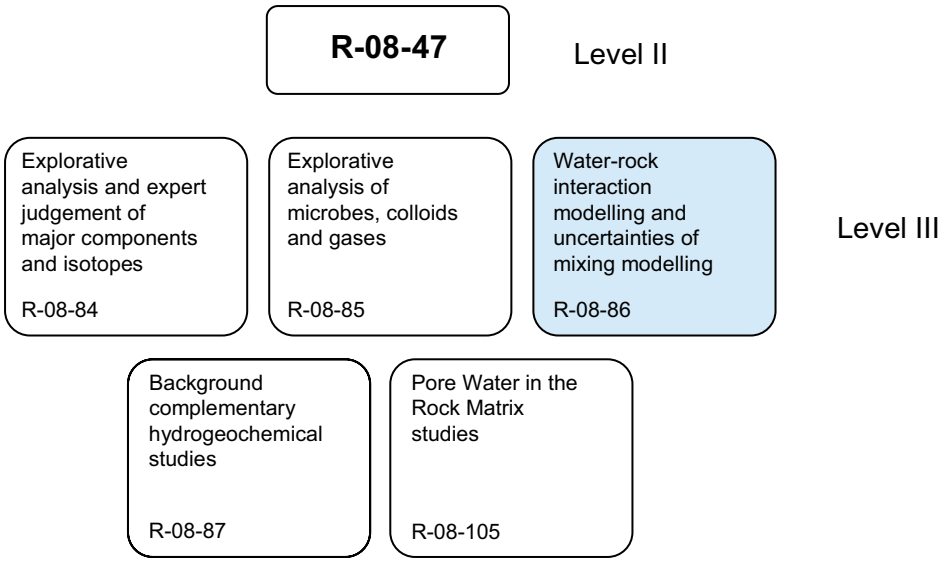

This report presents the modelling work performed by the University of Zaragoza (UZ) group as part of the work planned for Forsmark during stages 2.2 and 2.3.

The chemical characteristics of the groundwaters in the Forsmark and Laxemar areas are the result of a complex mixing process driven by the input of different recharge waters since the last glaciation. The successive penetration at different depths of dilute glacial melt-waters, Littorina Sea waters and dilute meteoric waters has triggered complex density and hydraulically driven flows that have mixed them with long residence time, highly saline waters present in the fractures and in the rock matrix.

A general description of the main characteristics and processes controlling the hydrogeochemical evolution with depth in the Forsmark groundwater system is presented in this report: The hydrochemical characteristics and evolution of the **Near surface waters** (up to 20 m depth) is mainly determined by weathering reactions and especially affected by the presence of limestones. The biogenic CO_2 input (derived from decay of organic matter and root respiration) and the associated weathering of carbonates control the pH and the concentrations of Ca and HCO_3^- in the near-surface environment. Current seasonal variability of CO_2 input produces variable but high calcium and bicarbonate contents in the Forsmark near-surface waters: up to 240 mg/L Ca and 150 to 900 mg/L HCO_3^-. These high concentrations are due to the extensive presence of limestones in the overburden, a feature very uncommon in Swedish soils.

New samples from the extended Forsmark 2.3 data freeze fit with the general picture already drawn with the previous data. Therefore, their inclusion in the conceptual model does not add or modify any of the previous conclusions.

Contents

1 Introduction

This report presents the modelling work performed by the UZ group as part of the work plan for Forsmark 2.2 and 2.3. It has been organised in sections corresponding to the different INSITE (Independent Site Investigation Tracking & Evaluation – the authorities advisory group on site investigation issues), issues in which the UZ group is involved. Issues corresponding to predictive modelling or based on the SR-Can (Safety Assessment) results have been included as appendices. The sections included in this report are the following:

1. *Introduction.*
2. *Palaeohydrogeology.* This chapter contains three main sections which present (a) a comprehensive review of the chemical composition of the end-members, highlighting the main uncertainties encountered during the calculations; (b) the different calculations performed by the UZ group to obtain the chemical composition of the Forsmark groundwaters just before the Littorina stage; and (c) a conceptual model of the temporal evolution of the system. These are basic issues affecting different parts of the work plan:
   - Issue B-2: Alternative end-member selection and uncertainties in end-members.
   - Issue F-1: Glacial vs Littorina in the bedrock, establish Littorina (and Deep Saline in Forsmark) compositions.
   - Issue F-3: Geochemical data used to interpret the groundwater evolution over time.
3. *General overview of the system with the updated information from the 2.2 and 2.3 data freezes.* This section presents the final picture of the system as envisaged using all available data by the time of the last data freeze. A summary of the main conclusions on the distribution of chemical elements and on the main factors controlling the system is also presented. The section is divided into three parts concerning the shallow and near surface groundwater system, the non-redox system in the deep groundwater system, and the redox system This last part provides a general overview of the redox processes controlling some of the important parameters in the system. It summarizes the work done in the previous modelling phases, updating the results with the new data from 2.2 and 2.3 data freezes. It includes the presentation of the different redox parameters and the redox modelling concerning the iron, sulphur, uranium and manganese systems. Therefore, several INSITE issues are dealt with here
   - Issue A-1: Modelling of the existence of a relatively shallow “process zone” capable of buffering the meteoric water with respect to redox and cation exchange.
   - Issue A-4: High uranium content in Forsmark.
   - Issue B-1: Description of models based on reactions and other alternative models.
   - Issue E-1: Spatial variability of hydrochemical data.
   - Issue G-1: Modelling of redox and pH buffering and water-rock reactions at repository depth.
4. *Overall conceptual model for groundwaters evolution.* In this chapter a summary of the main conclusions from the previous sections together with a conceptual model is presented.
5. *References.*

Appendix A. *Eh and pH selection*. This appendix reports the selection of Eh and pH values performed by the UZ group. A comparison with the values proposed in the SICADA database is also reported when information from P-reports is available.

Appendix B. *Groundwater composition at repository depth*. This part summarizes some of the SR-Can modelling results and deals with several issues from the working plan:

- Issue A-2: Present repository conditions redox and alkalinity buffering capacity including discussion on the effects from potassium, sulphide and iron(II) on buffer and the canister.

- Issue D-1: 3D variability of redox, pH and other SKB suitability criteria and buffer capacity at repository depth under current conditions.

Appendix C. *Dilution/concentration of repository groundwaters* to establish the level of variability allowed before SKB suitability criteria are affected. Some results from SR-Can, together with additional predictive equilibrium and reaction path calculations are presented here. This section presents the results concerning issue E-2, but also the main conclusions from two other related issues:

- Issue A-1: Modelling of the existence of a relatively shallow "process zone" capable of buffering the meteoric water with respect to redox and cation exchange.
- Issue A-3: Indications of penetration depths of rain water and glacial water with oxygen intrusion in the bedrock, modelling and description based on observations.

2 Palaeohydrogeology

The chemical characteristics of the groundwaters in the Forsmark and Laxemar sites are the result of a complex mixing process driven by the input of different recharge waters. The successive penetration at different depths of dilute glacial melt-waters, Littorina Sea marine waters and dilute meteoric waters has triggered complex density and hydraulically driven flows that have mixed them with long residence time, highly saline waters present in the fractures and in the matrix of the bedrock.

This complex palaeohydrogeological evolution has affected the groundwater composition at present. Therefore, a review of the main issues related to it is presented here.

Section 2.1 presents a comprehensive review of the chemical composition of the end-members, highlighting the main uncertainties encountered during the calculations. Alternative end-member compositions for sensitivity analysis are also proposed when necessary.

Section 2.2 summarizes the different calculations performed by the UZ group to obtain the chemical composition of the Forsmark groundwaters just before the Littorina stage.

Section 2.3 presents different alternative evolution scenarios for the Forsmark paleohydrogeological system.

All these issues are basic and related to different parts of the work-plan:

- Issue B-2: Alternative end-member selection and uncertainties in end-members.
- Issue F-1: Glacial vs Littorina in the bedrock, establish Littorina (and Deep Saline in Forsmark) compositions.
- Issue F-3: Geochemical data used to interpret the groundwater evolution over time.

2.1 Composition of the end-members

The geochemical study of the Forsmark and Laxemar groundwaters, using either simple conservative elements /Smellie et al. 1995, Laaksoharju and Wallin 1997, SKB 2005a, 2006a/ or more refined isotopic techniques /Louvat et al. 1999, Wallin and Peterman 1999, Négrel and Casanova 2005/ has confirmed the existence of at least four end member waters: an old deep saline water, an old marine water (ancient Littorina Sea), a modern meteoric water (altered meteoric), and a glacial melt-water. As a result, mixing can be considered the prime irreversible process responsible for the chemical evolution of the Forsmark and Laxemar groundwater systems. The successive disequilibrium states resulting from mixing conditioned the subsequent water-rock interaction processes and, hence, the re-equilibration pathways of the mixed groundwaters.

The quantitative assessment of mixing and reaction in these groundwaters can be approached by inverse modelling (mixing and mass balance calculations) with standard geochemical codes like NETPATH /Plummer et al. 1994/ or PHREEQC /Parkhurst and Appelo 1999/ or with PCA-based codes like M3 /e.g. Laaksoharju et al. 1999, Gómez et al. 2006/ A correct selection of the end-member waters is critical in both cases. The uncertainties associated with this selection procedure have already been discussed elsewhere /Luukkonen 2001, Bath and Jackson 2002, Laaksoharju et al. 2004/.

Furthermore, the inclusion of water-rock chemical reactions on top of the first-order process of mixing represents an additional source of uncertainty that must be addressed when analysing the sensitivity of the computed mixing proportions to variable chemical reactions that could contribute to the evolution of the groundwater system. The uncertainties associated with the effects of water-rock chemical reactions in M3 calculations have been previously discussed in /Gómez et al. 2006/.

But there are other evident sources of uncertainty when trying to apply mixing and mass balance calculations to real, complex groundwater systems. One of the most important sources of uncertainty is related to the chemical and physicochemical characteristics of each end-member and their possible spatial and/or temporal chemical variability. The chemical and stable isotope characteristics ($\delta^{18}O$ and $\delta^{2}H$) of the four end-member waters (Deep Saline, Glacial, Littorina and Altered Meteoric) used in the hydrochemical and hydrogeological characterization of Forsmark and Laxemar will be analysed in this review, together with the uncertainties associated with their definition.

Some of these end members (Deep Saline and Altered Meteoric) correspond to real groundwaters sampled in the studied sites, whereas others (Littorina or Glacial) are old waters with compositional characteristics estimated or deduced from diverse geological information. Therefore, the associated uncertainties and their weights can be (and will be) very different depending on the considered end member.

Uncertainties can also have different importance depending on the modelling approach (direct or inverse). Here the uncertainty will be mainly assessed with respect to the needs in the ***M3 inverse approach*** as this code is the standard tool used in mixing calculations at both sites. Results obtained with M3 are useful in the refinement of the mixing and reaction models developed with classical geochemical codes (NETPATH or PHREEQC inverse approaches).

Different uncertainties will also arise depending on the code used for inverse modelling purposes. For example, in the M3 approach no Eh, pH or minor element concentrations are required, whereas pH, Eh, Fe^{2+}, or S^{2-} data would be necessary or, at least, very helpful in NETPATH or PHREEQC.

Some of the uncertainties associated with the ***direct approach*** are not present when performing inverse calculations. For example, dissolved oxygen contents of glacial melt waters (which could affect the redox reactivity of these waters) and their possible effects in the repository, are well known problems and must be addressed by other geochemical lines of reasoning /e.g. Puigdomenech 2001/.Therefore, apart from the uncertainties related to M3 calculations, some others more related to the predictive (direct approach) calculations will also be analysed.

Finally, a Monte Carlo method has been developed to obtain an independent assessment of the chemical composition of the end-member waters. The comparison of the results obtained with this method and the ones obtained in the review serves to build confidence and to reduce the uncertainty in, at least, some compositional characteristics of each end-member.

2.1.1 Deep Saline end-member

Geochemical features

The chemical composition of this end-member corresponds to the deepest and more saline waters sampled in the Laxemar and Forsmark sites. Up to now the deepest and most saline water is a sample from borehole KLX02 in Laxemar at 1,625 m depth with a salinity of 75 g/L TDS. Groundwaters sampled from the deepest part of this borehole are believed to be quite old (1.5 million years estimated from ^{36}Cl data; /Louvat et al. 1997, 1999/) with a Ca-Na-Cl composition and with a significant deviation from the GMWL (Global Meteoric Water Line in $\delta^{18}O$ vs $\delta^{2}H$ plots) due to its long interaction time with the bedrock in a near-stagnant environment /Laaksoharju and Wallin 1997, Laaksoharju et al. 1999/.

In spite of the current controversy about the origin of the salinity in this kind of water in crystalline rocks /Starinsky and Katz 2003, Gascoyne 2004, Casanova et al. 2005, Frape et al. 2005, Négrel and Casanova 2005, Smellie et al. 2006/, it seems reasonable, taking into account their high residence times, to assume that they are, at least, close to equilibrium with the mineralogy of the bedrock /Gimeno et al. 2004/. Moreover, this probable equilibrium situation and the deep and near-stagnant condition allow us to assume a constant chemical composition over the time spans of interest usually considered in performance assessment calculations.

Uncertainty analysis

The above circumstances seem to imply that the definition of the chemical composition of this end-member is simple, as it would be mainly dependent on the raw analytical data. However, there are different uncertainties associated with both the lack of important analytical parameters in the selected sample from KLX02 borehole and the absence of a properly defined Deep Saline end-member in the Forsmark area.

Refinement of the geochemical characteristics of the Deep Saline end-member

The groundwater sample used as the Deep Saline end-member in the Swedish site characterization program lacks aluminium, ferrous iron and sulphide, as well as an in situ determination of pH and Eh. Some of these values have been taken from a different sample from the same borehole (1,420–1,705 m depth section, sample #2731) which does have analytical data for Fe^{2+} and S^{2-} (Table 2-1). This sample is very similar to the sample chosen as end-member, has very low content of drilling water (0.14%) and was taken in a borehole section with physicochemical data from continuous logging of down-hole and surface instruments.

The pH was measured over a period of 28 days and has a value of 8.0 ± 0.2 (more alkaline than the pH measured in the laboratory for the original end member; Table 2-1). The Eh logging shows significant differences between the different electrodes (Pt, C and Au) at the surface and at depth (probably due to oxygen intrusion, as dissolved oxygen concentrations of 0.7 to 1 mg/L were detected over the measurement period). Although the stable reading from the Pt electrode indicates a value of –300 mV (Figure 2-1), this value was not considered representative by /Gimeno et al. 2007/ due to the problems indicated above (see also Appendix A). However, as no other potentiometrically measured value is available for these waters, it has been considered as a plausible Eh value for the Deep Saline end-member.

Table 2-1. Composition of "Deep Saline" groundwaters in Sweden (Laxemar) and Finland (Olkiluoto; /Pitkänen et al. 2004/). Concentrations are expressed in mg/L. Eh value of –300 mV for sample #2731 (Laxemar) was obtained by Chemmac with the Pt electrode (Figure 2-1).

	Deep Saline end-member	Sample 2731 (Laxemar)	Olkiluoto KR4/860/2	Olkiluoto KR4/860/1
Depth (m)	1,631–1,681	1,420–1,705	860–866	860–865
Temp. (ºC)	–	18.0	–	12
pH	7.3 (lab)	8.0	7.0	7.5
Eh (mV)	–	–300	+36	–
Alkalinity	14.1	9.0	8.2	9.2
Cl	47,200	45,500	45,200	43,000
SO_4^{2-}	906.0	832	8.4	1.2
Br	323.66*	312	300	350
Ca	19,300	18,600	18,000	15,100
Mg	2.12	2.7	130.0	108.0
Na	8,500	8,030	9,540	9,200
K	45.5	29.0	28.0	18.0
Si	2.9	4.8	2.62	1.96
Fe^{2+}	–	0.426	3.33	2.4
S^{2-}	–	bdl[1)]	bdl[1)]	bdl[1)]
δ^2H (‰)	–44.9	–47.4	–	–49.5
$\delta^{18}O$ (‰)	–8.9	–8.9	–	–9.3

[1)] below detection limit.

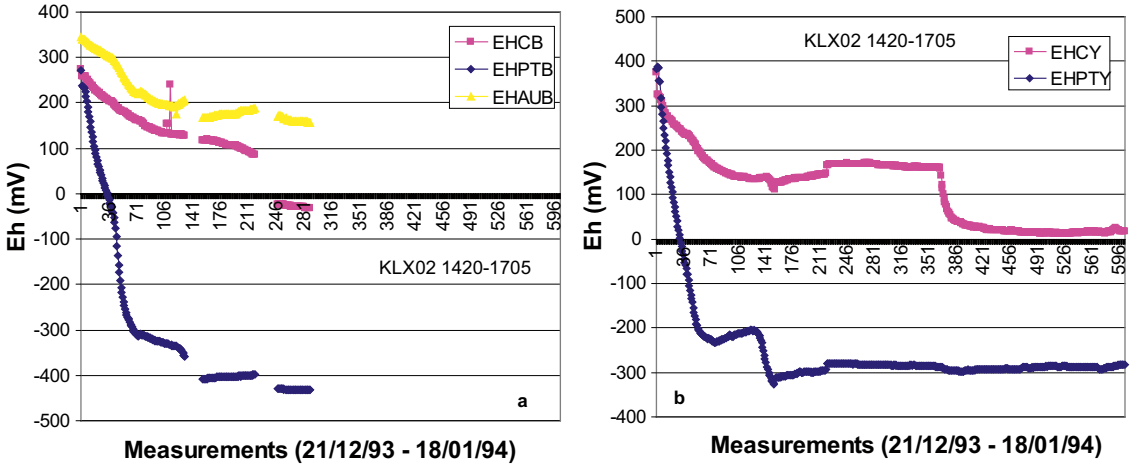

Figure 2-1. *Continuous Eh logs in KLX02 (section 1,420–1,705 m) measured by platinum (EHPTB), gold (EHAUB) and glassy carbon (EHCB) electrodes in the borehole (a) and by platinum (EHPTY) and glassy carbon (EHCY) electrodes at the surface (b) with Chemmac. See appendix A to better understand the way in which these data are taken and managed.*

Compositional and spatial variability of the Deep Saline end-member

An additional uncertainty related to this end-member is the absence of samples (and analytical data) of this type of water in the Forsmark area. In SKB's site characterization programme, the same Deep Saline end-member has been used for mixing and mass balance calculations in Forsmark and Laxemar. However, the most saline waters analysed up to now in Forsmark have much lower salinities (16 versus 47.2 g/L of chloride). Even though this could be explained by the more limited depth of the drilling campaigns in the Forsmark area, it introduces a reasonable doubt about the real composition of the saline waters in the Forsmark area and their similarity to those in Laxemar.

There are very few data of highly saline groundwaters in the Fennoscandian basement useful as a reference to evaluate the degree of homogeneity of saline waters in both sites. Comparison with other crystalline systems does not give an unique answer either. Brines and brackish groundwaters of the Canadian Shield, dominated by a Ca-Na-Cl facies, show similar maximum concentrations of specific species irrespective of the associated major rock types. On the contrary, Finnish saline groundwaters show clear compositional heterogeneity depending on the mafic or felsic nature of the bedrock (/Puigdomenech 2001/ and references therein). Although the situation described in the Finnish shield could be closer to the Swedish area, there are very few highly saline basement locations documented in Sweden compared to Finland, which makes it unclear whether similar hydrogeochemical heterogeneities do occur /Puigdomenech 2001/.

However, the comparative analysis of the compositional trends between Laxemar, Forsmark (Sweden) and Olkiluoto (Finland) is very helpful for an indirect estimation of some possible distinctive compositional features of the Deep Saline end-member in Forsmark.

The main difference between the deep saline groundwaters at Laxemar and Olkiluoto is the SO_4^{2-} content /Gimeno et al. 2004, 2005/. Sulphate concentrations in the Laxemar area increase with chloride, reaching a maximum of about 1,000 mg/L of sulphate (for chloride concentrations of around 15,000 mg/L; Figure 2-2, left) when the waters attain equilibrium with gypsum (Figure 2-2, right). In Olkiluoto, the groundwaters with the highest sulphate content have an intermediate salinity between Laxemar and Forsmark (5,000 to 6,000 mg/L of Cl) and sulphate concentrations decrease to very small values in the most saline groundwaters (lower than 10 mg/L; Table 2-1 and Figure 2-2, left). In Forsmark, groundwater salinities are lower than at Laxemar or Olkiluoto, but they appear to follow the same trend of SO_4^{2-} vs Cl as in Olkiluoto (Figure 2-2, left).

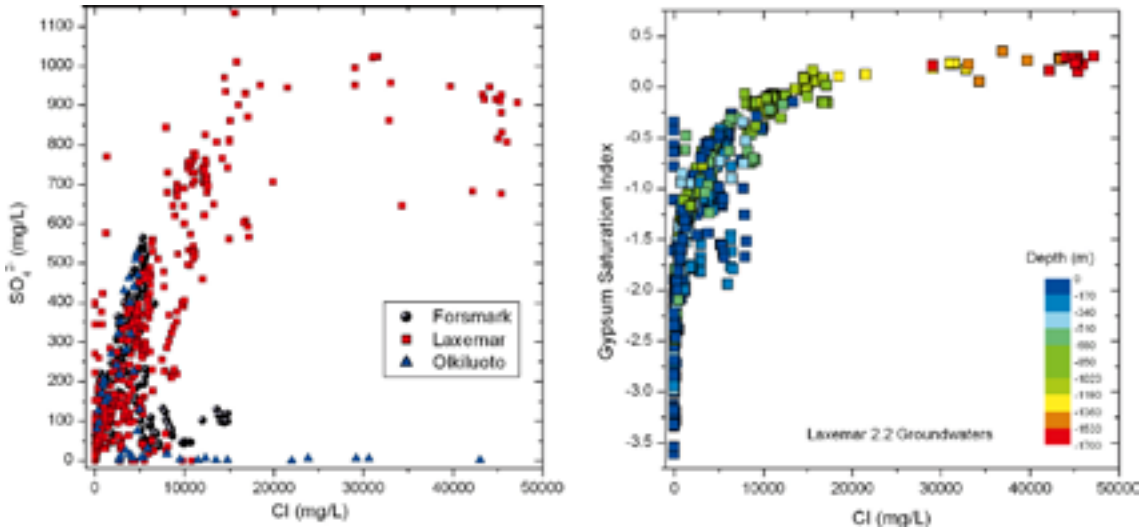

Figure 2-2. *Sulphate contents in Laxemar, Forsmark and Olkiluoto (left) and calculated gypsum saturated indexes in the Laxemar groundwaters (right) as a function of chloride concentration.*

All the deep saline waters from the Finnish shield with TDS values higher than 20 g/L included in the review by /Frape et al. 2005/ have SO_4^{2-} contents lower than 190 mg/L (and most of them lower than 80 mg/L). The highest SO_4^{2-} contents in Laxemar groundwaters seem to be related to the presence of gypsum as fracture fillings /Drake et al. 2006/. This fact suggests that the Deep Saline end-member defined with samples from Laxemar may have an exceptionally high sulphate content (906 mg/L).

In order to take this uncertainty into account, a Deep Saline end-member with a very low sulphate content (10 mg/L, similar to the concentration found in Olkiluoto brines) could be used as an alternative mixing component in the simulations for the Forsmark area (Table 2-14). This approach has been adopted in SR-Can calculations (see /Auqué et al. 2006/ for details of the calculation methodology). Using the mixing proportions of the four end-members (Deep Saline, Glacial, Littorina and Altered Meteoric) as obtained from the hydrogeological model (1.2) for the year 2020, the theoretical composition of the waters in the system, only due to mixing, was calculated using PHREEQC /Parkhurst and Appelo 1999/. Figure 2-3 shows the comparative results when using the two different compositions for the Deep Saline end-member (high and low-sulphate).

The results when using the low-sulphate Deep Saline end-member successfully reproduce the high sulphate concentrations found in the groundwaters with important Littorina signature (Cl about 0.15 mol/kg; 5,318 mg/L). Besides, they reproduce better the sulphate concentration found in the more saline waters (Cl > 0.15 mol/kg), following the trend of the available samples (Figure 2-3, black dots). However, this better agreement is based on a very limited number of clearly saline samples (Cl > 0.25 mol/kg; 8,863 mg/L) from the Forsmark area. A deep saline end-member with SO_4^{2-} concentrations around 400 mg/l (0.0042 mol/kg; extrapolated from the slightly increasing trend of SO_4^{2-} with Cl concentrations in the more saline groundwaters from Forsmark) could also reproduce the observed trend in Figure 2-3 for the most saline groundwaters. Unfortunately, this uncertainty is not resolved with the independent Monte Carlo method presented in Section 2.1.5.

Isotopic characteristics of the Deep Saline end-member

The isotopic composition ($\delta^{18}O$ and $\delta^{2}H$) of the Deep Saline end-member corresponds to the aforementioned saline water sampled in Laxemar (borehole KLX02 at 1,631–1,681 m depth; Table 2-1), which has a significant deviation from the GMWL. The absence of samples of such high salinity in the Forsmark area and the possible compositional and spatial variability of the deep saline waters as discussed in the previous paragraphs also affect the uncertainties in the isotopic values. And, again, a comparison with the isotopic values of brines or deep saline waters from other crystalline systems does not give a unique answer.

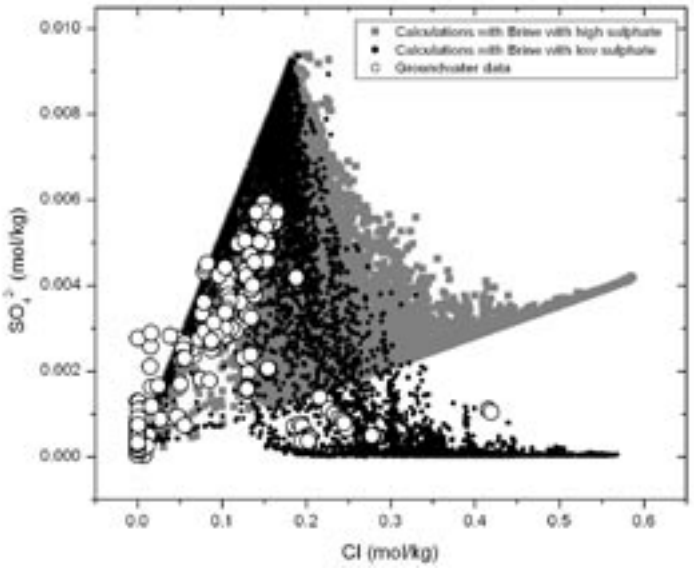

Figure 2-3. *Comparison between simulated (squares and dots) and sampled (open circles) SO_4^{2-} contents plotted against Cl for Forsmark groundwaters. The results obtained using the original high-sulphate Deep Saline end-member are shown in grey squares, whereas the concentrations obtained with a low-sulphate Deep Saline end-member are shown in black dots /from Auqué et al. 2006/.*

In the **Canadian Shield**, the observed linear trends between $\delta^{18}O$ and $\delta^{2}H$ with site-specific slopes (steeper than the GMWL) and different intersects with the GMWL (Figure 2-4) have been interpreted as mixing lines between local meteoric waters and deep brines.

Salinity increases with increasing deviation from the GMWL. Moreover, many of these brines have measurable tritium, indicating that they have mixed with a recent meteoric water, both of natural and anthropogenic origin /Frape and Fritz 1987, Clark and Fritz 1997/. In some cases (Con Mine, Yellowknife; /Douglas et al. 2000/) the brines have even mixed with a glacial melt-water component isotopically depleted with respect to modern meteoric waters. With some note-worthy exceptions (brines from Copper Rand Mine and Keweenaw Peninsula[1], Figure 2-4), the linear trends from the studied Canadian sites seem to converge towards a common end-member (Figure 2-4). This convergence has been used as an argument for supporting the existence of a single chemically and isotopically homogeneous brine in the deep Canadian Shield /Frape et al. 1984, Frape and Fritz 1987, Kloppmann et al. 2002/.

In the **Fennoscandian Shield** (mainly in the Finnish Shield), most site-specific groundwaters fall along mixing lines of $\delta^{18}O$ vs $\delta^{2}H$ with slopes between 10 and 12 (Figure 2-5) but they do not converge towards a hypothetical common end-member. However, Laxemar and Olkiluoto brines seem to define a similar mixing line (Figure 2-5 and Figure 2-6a), with the isotopic values in this trend decreasing with decreasing salinity (or Cl concentrations, Figure 2-6b).

The Forsmark case is somewhat different. As explained before, the most saline waters analysed up to now in Forsmark have salinities clearly lower than in Laxemar or Olkiluoto (Figure 2-6b; Table 2-2). The most saline groundwater samples in Forsmark (#12243, #8843, #12005 and #8152; Figure 2-6 and Table 2-2) intercept the GMWL at an isotopically depleted value with respect to modern meteoric water (Figure 2-6a), suggesting mixing with cooler (glacial-meteoric)

[1] Sealed vugs brines from Copper Rand Mine are considered as residual syntectonic fluids of Proterozoic age trapped and isolated in ‘‘mega-fluid inclusions’’ of several meters diameter and probably they have not mixed with other waters since the formation of the vugs. Therefore, these fluids may represent a pure brine end-member which is supported by the extremely high salinities (> 300 g/L) and one of the most important isotopic shifts from the GMWL ever reported. Fluids from the copper mines of Keweenaw Peninsula show also an important shift from the GMWL the origin of these brines are probably related to the neighbouring sedimentary basins /Kelly et al. 1986, Guha and Kanwar 1987, Kloppmann et al. 2002/.

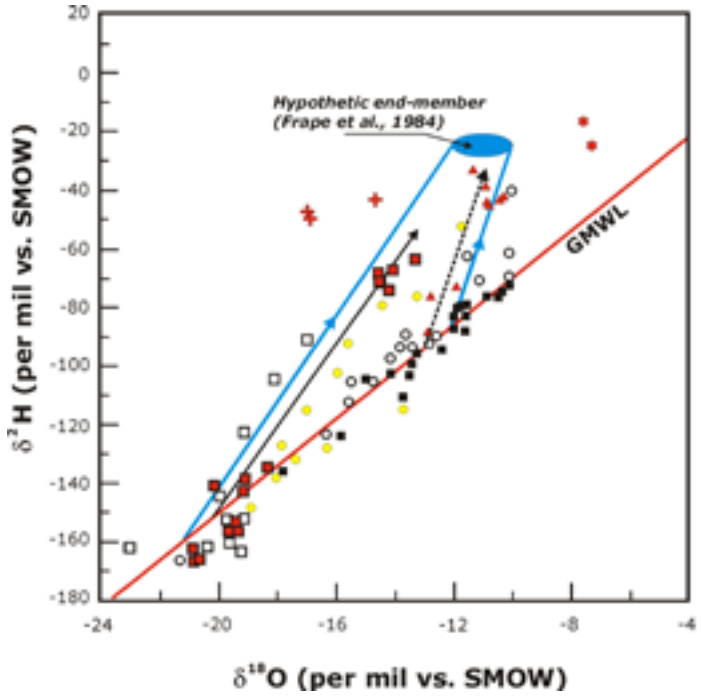

Figure 2-4. *Isotopic compositions ($\delta^{18}O$ vs $\delta^{2}H$) of groundwaters and brines from the Canadian Shield. Arrows indicate mixing paths for Yellowknife (continuous arrow; /Bottomley et al. 1999/) and Sudbury (dashed arrow; /Frape and Fritz 1987/). GMWL is the global meteoric water line. Symbols: crosses, Koper Rand Mine /Guha and Kanwar 1987/; Stars, Keweenaw /Kelly et al. 1986/; red squares, Yellownife /Bottomley et al. 1999/; white squares, Yellownife /Frape and Fritz 1987/; black squares, Esat Bull lake /Bottomley et al. 1990/; triangles, Sudbury /Frape and Fritz 1987/; yellow circles, Thompson /Frape and Fritz, 1987/; white circles, different sites /Bottomley et al. 1994/. Modified from /Clark and Fritz 1997/ and /Kloppmann et al. 2002/.*

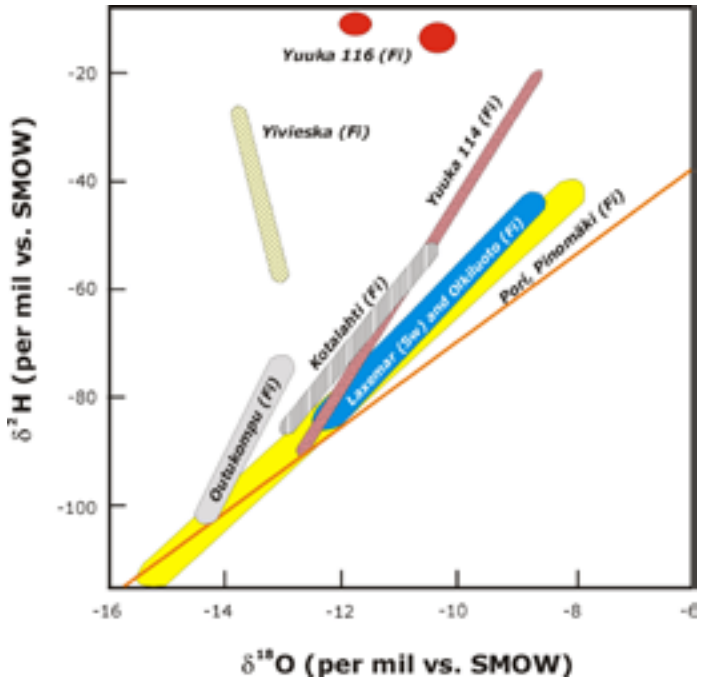

Figure 2-5. *Isotopic compositions ($\delta^{18}O$ vs $\delta^{2}H$) of groundwaters and brines from the Fennoscandian Shield. Most site-specific groundwaters describe mixing lines with slopes between 10 and 12 except the highly concentrated brines of Yuuka and Ylivieska, showing also the highest shifts from GMWL. Modified from /Kloppmann* et al. *2002/.*

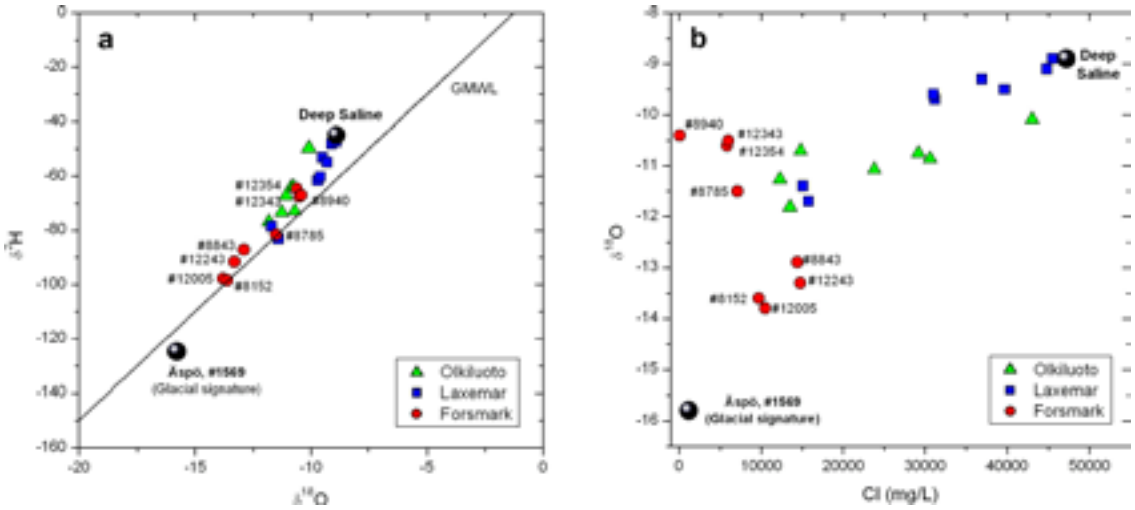

Figure 2-6. *$\delta^{18}O$ vs $\delta^{2}H$ (a), and $\delta^{18}O$ vs Cl (b) for the most saline groundwaters in each site, Forsmark, Laxemar and Olkiluoto. Sample #1569 from KAS02 (Äspö, Laxemar area, 1,220 mg/L Cl), with the strongest cold (glacial) signature ($\delta^{2}H$ = –124.8‰ and $\delta^{18}O$ = –15.8‰) found up to date in the Laxemar and Forsmark areas, is also shown[2]. Numbers in the plots refer to specific water samples from the Forsmark area (see also Table 2-2).*

groundwaters. In any case, these Forsmark data fit fairly well to the Olkiluoto and Laxemar trends and, therefore, they do not contradict the common isotopic composition hypothesis for this Deep Saline end-member.

However, some other less saline groundwaters sampled at Forsmark show a clear shift from the GMWL (samples #12343 and #12354 at 445.17 m depth in borehole KFM01D; Figure 2-6) as usually found in more saline groundwaters with an important Deep Saline component. The shift in these groundwaters with low salinity (around 6,000 mg/L Cl, Table 2-2), cannot be explained by the same dilution trend between the Deep Saline-end member and the most saline groundwaters in Forsmark (with around 15 g/L Cl), in spite of lying on this hypothetic mixing line (Figure 2-6a). A possible explanation is that KFM01D groundwaters represent a Deep Saline component mixed with an old dilute meteoric component, previous to the last glaciation. This meteoric component would be different from the one affecting the clearly saline groundwaters from Forsmark, as the Cl vs $\delta^{18}O$ plot suggests (Figure 2-6b). This hypothesis is consistent with a common isotopic composition for the Deep Saline end-member.

In any case, it must be taken into account that the discussion in the last paragraph is based only on one groundwater sample with a clear deviation from the GMWL. Moreover, these groundwaters are probably the least saline waters with a clear shift from the GMWL ever found (shifts from the GMWL are usually found in groundwaters with Cl concentrations higher than 15 g/L; see the review by Kloppmann et al. 2002). Moreover, a very shallow groundwater sampled in a soil pipe (#8940 from SFM0037), with 87.4 mg/L Cl, has the same shift from the GMWL as one of the samples from KFM01D (Figure 2-6a), which is very difficult to explain. So, in this situation, and until more data become available, it is recommended here to assume a common isotopic composition for the Deep Saline end-member in Forsmark and Laxemar.

[2] Similar cold signatures have been recently found in borehole KLX04 at 484 m depth with $\delta^{18}O$= –15.1‰ (and 1,500 mg/L Cl) and in borehole KLX08 at 480.81 m and 613.75 m depth with $\delta^{18}O$ value around –15.3‰ to –15.6 (Cl concentrations from 1,500 to 2,000 mg/L).

Table 2-2. Chloride, sulphate and stable isotopes for the samples plotted in Figure 2-6.

Site	Borehole	Sample No.	Depth	Cl(mg/l)	$\delta^{18}O$ (‰)	$\delta^{2}H$ (‰)	SO_4^{2-}(mg/l)
Olkiluoto	KR1	KR1_T612_2	–570.44	14,800	–10.70	–72.90	0.84
	KR4	KR4/860/1	–820.17	43,000	–10.09	–49.75	1.2
	KR6	KR6_525_1	–412.09	12,300	–11.27	–73.43	5.3
	KR10	KR10_498_1	–489.53	13,500	–11.81	–76.90	1.4
	KR12	KR12_664_1	–633.44	23,800	–11.07	–67.20	5.4
	KR12	KR12_736_1	–705.60	29,200	–10.75	–64.00	5.5
	KR12	KR12/741/1	–713.24	30,600	–10.86	–64.26	5.1
Laxemar	KLX02	3038	–1,360.93	36,970	–9.30	–54.90	1,205
		2931	–1,322.81	31,230	–9.70	–61.70	1,024
		2930	–1,322.81	31,060	–9.60	–60.20	1,020
		2731	–1,530.98	45,500	–8.90	–47.40	832
		2934	–1,134.60	15,130	–11.40	–83.20	860
		2722	–1,068.24	15,800	–11.70	–78.60	1,010
Forsmark	KFM01D	12354	–445.17	5,800	–10.60	–64.60	38.3
		12343	–445.17	5,960	–10.50	–67.50	31.1
	KFM03A	12005	–969.14	10,500	–13.80	–97.80	47
		8152	–977.67	9,690	–13.60	–98.50	46.7
	KFM06A	8785	–645.34	7,080	–11.50	–81.70	35.5
	KFM07A	8843	–759.92	14,400	–12.90	–87.10	103
	KFM09A	12243	–614.21	14,800	–13.30	–91.60	118
	SFM0037	8940	–1.00	87.4	–10.40	–67.00	38.4
Deep Saline	*KLX02*	*Deep Saline*	*–1,625.77*	*47,200*	*–8.90*	*–44.90*	*906*
Aspo1569	*KAS03*	*1569*	*–121.782*	*1,220*	*–15.80*	*–124.80*	*31.1*

Discussion and conclusions

The chemical and isotopic composition of the Deep Saline end-member for the Laxemar area (Deep Saline-Laxemar; Table 2-14) has been defined from the analytical data of a sample from borehole KLX02 in Laxemar at 1,631–1,681 m depth with the maximum salinity (75 g/L TDS) found in the area up to now. Some of the compositional parameters not determined in this sample (pH, Eh, Fe^{2+} and S^{2-} concentrations) have been taken from a different sample, slightly less saline, from the same borehole KLX02 (1,420–1,705 m depth section, sample #2731).

The absence of a proper deep saline sample from the Forsmark area constitutes one of the main uncertainties associated with this end-member and it casts a reasonable doubt on the real composition of the saline waters in the Forsmark area and their similarity to those in Laxemar. The geochemical studies, the simulations performed in SR-Can for Forsmark /Auqué et al. 2006/ and the review presented here, all suggest the presence of a Deep Saline end-member with a chemical and isotopic composition similar to the one in Laxemar but with a lower sulphate concentration. The precise sulphate concentration is not well constrained and, therefore, a new saline end-member with a very low sulphate concentration (10 mg/L) has been defined to be used in Forsmark (Deep Saline-Forsmark; Table 2-14).

These two end-members can be used for the sensitivity analysis of the mixing proportions calculated in Forsmark. It is also suggested to use the sample KR4/860/1 (Table 2-1) from Olkiluoto (Finland) as an alternative Deep Saline end-member in these sensitivity analysis as it introduces a higher variability in the concentration of Na, K, Ca, Mg, Cl, $\delta^{2}H$ and $\delta^{18}O$.

2.1.2 Glacial end member

Geochemical features

The Glacial end-member represents the chemical composition of a melt-water from an earlier glaciation (>11,000 BC). The composition adopted for this end-member in the site investigation programme (Table 2-3) corresponds to present melt-waters from one of the largest glaciers in Europe, the Josterdalsbreen in Norway, situated on a crystalline granitic bedrock /Laaksoharju and Wallin 1997/. The major element composition of these waters is similar to the one estimated by /Pitkänen et al. 1999, 2004/ in a model study of Olkiluoto (Finland). Glacial melt-waters have a very low content of dissolved solids, even lower than present-day meteoric waters, and they represent the chemical composition of surface melt-waters prior to the water-rock interaction processes undergone during their infiltration into the bedrock.

The $\delta^{18}O$ value (–21‰) is based on test calculations to obtain the best fit to the measured $\delta^{18}O$ content in the Äspö-Laxemar groundwaters /Laaksoharju and Wallin 1997/ and on measured values of $\delta^{18}O$ in calcite surface deposits collected from different geological formations in Sweden and from sub-glacial fracture fillings. The $\delta^{2}H$ value (–158‰) was then deduced from the equation for the global meteoric water line ($\delta^{2}H = 8\,\delta^{18}O + 10$).

Groundwaters with a glacial component are characterized by a low salinity and, mainly, by an isotopically light signature. However, in the Forsmark and Laxemar areas the composition of these groundwaters has been drastically modified by mixing with waters of other origins. Therefore, there are no "undisturbed" glacial melt-water remnants that can be considered as a pure glacial mixing component modified only by water-rock interaction processes.

Furthermore, the evolution of the glacial melt-waters as a result of water-rock interaction processes in the shallower part of the groundwater system could have been affected by factors different from the ones existing at present: higher dissolved oxygen contents, different characteristics of the infiltration zone (erosion rates, soil profiles), etc.

Table 2-3. Chemical composition of the glacial end-members used in the Swedish /Laaksoharju and Wallin 1997/ and Finnish /Pitkänen et al. 1999, 2004/ site characterization programs. The composition of a present meteoric water with very low residence time together with one of the real samples with a clear glacial signature (Äspö groundwater, sample 1569), are also shown. Concentrations in mg/L.

	Glacial end-member (Sweden)	Glacial end-member (Finland)	Meteoric water (HBH02, #1931)	Äspö (KAS03, #1569 at 129–134 m depth)
Temp		1.0	16	10.2
pH	5.8(1)	5.8	6.8	8.0
Eh	–	–	–	–280
Alkalinity	0.12	0.16	63.0	61
Cl	0.5	0.7	5.0	1,220.0
SO_4^{2-}	0.5	0.05	13.2	31.1
Ca	0.18	0.13	15.4	162
Mg	0.1	0.1	1.9	21.0
Na	0.17	0.15	11.5	613.0
K	0.4	0.15	2.3	2.4
Si	–	0.005	3.4	4.9
$\delta^{2}H$ (‰)	–158.0	–166.0	–77.1	–124.8
$\delta^{18}O$ (‰)	–21.0	–22.0	–10.2	–15.8

(1) This value proposed for the Swedish glacial end member comes from the Finnish glacial end-member.

Uncertainty analysis

There are three main sources of uncertainty affecting the definition of this end-member: the dissolved oxygen content (which affects the redox reactivity of these waters), the stable isotope composition (e.g. variable or constant over time) and the extent of the water-rock interaction processes (and their effects in the composition of these waters).

Dissolved oxygen concentrations in glacial meltwaters

Dissolved oxygen concentrations in glacial melt-waters can be high[3], about 1.4 mM or 45 mg/L /Glynn and Voss 1999, Guimerá et al. 1999/. Reduced biological activity in the sub-glacial soil would favour O_2-rich melt-waters and an almost complete cessation in the infiltration of dissolved organic carbon /Puigdomenech 2001/.

O_2-rich glacial melt-waters might penetrate the bedrock through conductive vertical fracture zones and eventually reach the repository, questioning its integrity. This situation, as a possible future scenario, has been widely discussed in different studies and safety assessments in the Scandinavian Shield /Glynn and Voss 1999, Guimerá et al. 1999, Gascoyne 1999, Vieno and Nordman 1999, Puigdomenech 2001/.

However, recent studies have suggested that O_2 is strongly depleted in dissolved gases in basal ice (provided that contact with atmosphere does not occur) and much lower O_2 concentration might be expected in melt-waters recharging the bedrock /Gascoyne 1999/. Moreover, no evidence has been found that oxidising conditions have ever prevailed at depth, neither in Sweden nor in Finland /e.g. Vieno and Nordman 1999, Puigdomenech 2001, Dideriksen et al. 2007/. This indicates that O_2 is already depleted in the near-surface zone.

Isotopic characteristics of the Glacial end-member

The stable isotope composition ($\delta^{18}O$= −21‰ and $\delta^{2}H$= −158‰) considered for the Glacial end-member in the Swedish sites has been deduced indirectly from a range of $\delta^{18}O$ values from glacial precipitates of calcite (from –25 to –21‰; /Tullborg and Larson 1984, Tullborg 1997/). /Pitkänen et al. 1999, 2004/ give a very similar isotopic composition for this end-member at Olkiluoto ($\delta^{18}O$= −22‰ and $\delta^{2}H$= −166‰; Table 2-3) but using again the mean value of the range proposed by /Kankainen 1986/ from data obtained in Hästholmen ($\delta^{18}O$ values between –26 to –18‰ and therefore, $\delta^{2}H$ values between –198 and –134‰).

$\delta^{18}O$ values in ice sheets from Greenland are very low (−33 to –38‰; /Taylor et al. 1992/. In the Canadian Shield a $\delta^{18}O$ value of –28‰ has been derived from different studies as the best value for the glacial end-member of the Laurentide Ice Sheet /Douglas et al. 2000/. However, $\delta^{18}O$ values of the melt-water recharging the bedrock during the deglaciation period (i.e. warmer temperatures) were possibly diluted by rainwater, making these values less negative /Luukonen 2001/. Some analyses from Icelandic glaciers ($\delta^{18}O$ between –22 and –20‰; /Pitkänen et al. 2004/ support the selected values for the glacial end-member in Forsmark and Laxemar areas. But it is noteworthy that the isotopic range deduced for this kind of waters is very wide ($\delta^{18}O$ between –18 and –30‰; /Pitkänen et al. 2004/), probably associated with temporal changes in the isotopic composition of the glacial melt waters during the glacial cycle. Therefore, the $\delta^{18}O$ and $\delta^{2}H$ values selected for the Glacial end-member are reasonable choices but they have important uncertainties.

Sample #1569 (KAS02, Äspö; Table 2-3) has the clearest cold (glacial) signature of all waters found in the Laxemar and Forsmark areas to date ($\delta^{2}H$ = −124.8 and $\delta^{18}O$= −15.8), although similar cold signatures have been recently found in borehole KLX04 at 484 m depth with

[3] For example, ice composition data from the base of the Greenland ice sheet suggests that the melt-waters will be highly enriched in dissolved oxygen, with concentrations at least 3 to 5 times higher than would be obtained at atmospheric equilibrium /Glynn and Voss 1999, Guimerá et al. 1999/.

$\delta^{18}O = -15.1‰$ (and 1,500 mg/L Cl^-) and in borehole KLX08 at 480.81 m and 613.75 m depth with $\delta^{18}O$ value around –15.3 to –15.6 (Cl^- concentrations from 1,500 to 2,000 mg/L). No "glacial" or cold signature below $\delta^{18}O = -16‰$ has been found to date in these sites. Moreover, this "extreme" $\delta^{18}O$ value is in agreement with the value deduced for the pre-Littorina groundwaters both in the Olkiluoto /Pitkänen et al. 1999, 2004/ and Forsmark areas (as displayed in Figure 2-9 below. The linear trend followed by the Littorina-rich groundwaters in both sites suggests that the infiltrated marine water mixed with an existing pre-Littorina groundwater which had a $\delta^{18}O$ value about –16; see also the conceptual model in Section 2.3).

This $\delta^{18}O$ value for the pre-Littorina groundwaters is representative of a mixture of a pure glacial melt-water and an old meteoric water[4] in the studied systems. This is in agreement with the conceptual paleohydrological model proposed by /Smellie et al. 2008/. According to this model, the pre-Littorina groundwaters are the result of mixing between a deep saline component, old meteoric waters, old glacial meltwaters introduced prior to the last Weichselian glaciation, and the glacial meltwaters from the last glaciation.

Effects of water-rock interactions

No "undisturbed" (without mixing) glacial melt-water remnants have been found in Laxemar and Forsmark to be used as a reference to analyse the compositional features of these waters when affected by "pure" water-rock interaction. For example, for the aforementioned sample #1569 (Äspö; Table 2-3) showing the clearest "cold" signature, M3 mixing proportions indicate 56.9% Glacial, 38.5% Altered Meteoric, 3.0% Littorina and 1.6% Deep Saline. Mixing has completely modified the chemistry of this "glacial" water and, for example, the contribution from Deep Saline and Littorina, although very low, represents 78% of the chloride in the sample (950 from the 1,220 mg/l Cl).

Nevertheless, the extent of the expected water-rock interaction processes during the infiltration of melt-waters may be inferred from the study of waters from other zones not affected by mixing. The review and compilation of data and studies carried out for SKB site characterisation program identifies groundwaters of glacial or meteoric origin but with high residence times and corresponding to climates colder than at present (Table 2-4).

Despite the fact that many of the sites studied in the Swedish program lack representative hydrochemical data (e.g. because of contamination with drilling water and/or other groundwaters), some indications of ancient glacial melt-water are apparent. For example, groundwaters below 500 m depth in Fjällveden seem to be residual melt-waters or alternatively meteoric waters from a colder climate /Wallin 1995, Tullborg 1997/. A glacial origin for these groundwaters is suggested in the work of /Bath 2005/ where "apparent" ^{14}C ages of around 12,000 to 14,000 years (i.e. late-glacial) are reported. At Gideå, there seems to be an indication of mixing between meteoric and post-glacial melt-waters /Wallin 1995/. Finally, groundwaters in Lansjärv also show the isotopically light signature ($\delta^2H = -109.3‰$ and $\delta^{18}O = -13.8‰$) typical of glacial or old meteoric waters from colder climates.

Compared with the original composition of glacial melt-waters, all the Swedish waters have a more alkaline pH (≥9) and higher TDS values as a consequence of water-rock interaction. The differences are of orders of magnitude, especially for chloride, sodium and alkalinity. However, the final salt contents are still very low in absolute terms, even taking into account potential contamination. This means that, as expected, water-rock interaction modifies the compositional characteristics in a quite limited scale. Similar conclusions have been obtained when analysing other cold meteoric and glacial waters in crystalline basements.

[4] As the Deep Saline proportion is very low in the groundwaters with the coldest signature (indicated by their low Cl concentrations), the isotopic signature ($\delta^{18}O = –16$) would correspond almost exactly to a 50:50 mixture of "recent" glacial melt-water and ancient meteoric water.

Table 2-4. Compositional data for different groundwaters from a glacial infiltration or simply cold waters in different zones in Sweden and Switzerland. pH and Eh data in the Swedish sites have been obtained from the continuous logging with Chemmac (only pH data in bold and italics correspond to values determined in laboratory). Chemical contents in mg/L.

	Fjallveden[1]		Gidea[2]	Lansjärv	Svartboberget		Switzerland	
	KFJ02 (#267)	KFJ07 (#372)	KGI04 (#194)	KLJ01 (#1410)	KSV04 (#116)	KSV04 (#122)	GTS [3]	Siblingen [4]
Depth (m)	605–607	542–544	404–406	237–500	430–436	630 –633	450	300–1,500
Temp (ºC)	–	–	–	–	–	–	12	up to 55
pH	8.9	***9.2***	9.3	***9.2***	9.1	9.1	9.6	7.6–8.1
Eh (mV)	–	–200	–200	–	–75	–150	–171	–30 to –250
Alk.	83.0	150.0	18	44.0	130.0	126.0	17.1	267–281
Cl	170.0	3.0	178	0.8	8.0	7.0	4.96	15–27
SO_4^{2-}	0.2	bdl.	0.1	4.4	1.2	0.8	5.8	128–146
Ca	12.0	10.0	21.0	7.7	17.0	17.0	6.61	9–12
Mg	0.8	2.0	1.1	1.2	2.0	1.9	0.05	0.4–1.4
Na	130.0	46	105.0	11.3	35.0	35.0	16.1	173–177
K	1.0	3.6	1.9	1.52	0.9	0.7	0.14	3.4–4.6
Si	4.3	n.a.	4.7	3.7	4.3	6.8	5.6	–
Fe	0.34	0.51	0.07	0.01	0.25	0.27	0.06	bdl
δ^2H (‰)	–102.9	–	–99.4	–109.6	–95.0	–95.4	–	–85
$\delta^{18}O$ (‰)	–14.11	–	–13.63	–13.80	–13.0	–13.1	–	–11.9

(1) /Wallin 1995, Tullborg 1997, Bath 2005/.

(2) /Wallin 1995/.

(3) Grimsel Test Site (Switzerland; /Degueldre 1994/).

(4) Sibinglen borehole in Switzerland /Thury et al. 1994/. It corresponds to the ranges used for the reference water in Kristallin-I /NAGRA 1994/.

For example, groundwaters from a recent meteoric origin at 450 m depth in the crystalline rocks of the Grimsel Test Site (Switzerland) are also very diluted /Degueldre 1994, Degueldre et al. 1996/ similar to the ones observed in the Swedish groundwaters (Table 2-4). Also in Switzerland, one of the waters selected as a reference water in the KRISTALLIN-I safety assessment, taken in the Siblingen borehole, represents an old water infiltrated during a cold climatic period 17,000 years ago and possibly during the last glaciation /Thury et al. 1994/ and has exactly the same diluted characteristics as the Swedish groundwaters.

Discussion and conclusions

The effect of the glacial end-member in inverse mixing calculations is mainly a dilution and the influence of the compositional variability of this type of waters would be of minor importance. However, their distinctive stable isotopic signature ($\delta^{18}O$ and δ^2H) is much more important in this type of calculation (e. g. to differentiate between a dilution effect due to mixing with a glacial end-member or with a more recent dilute end-member). As already explained, these values are affected by important uncertainties related to both the possible variation in the isotopic composition of the glacial melt-waters during the glacial cycle and the contribution and superposition of other old meteoric components.

Two glacial end-member compositions are proposed for M3 inverse mixing calculations: (a) the end-member used up to now in the site characterisation studies ($\delta^{18}O$= −21‰ and δ^2H= −158‰) and (b) another glacial end-member with a heavier isotopic signature $\delta^{18}O$= −16‰ and δ^2H= −138‰. With these two end-members part of the wide range of $\delta^{18}O$ values proposed

by /Kankainen 1986/ for the glacial melt-waters is covered for the uncertainty analysis. This alternative "glacial" end-member with $\delta^{18}O = -16‰$ is not a pure end-member but a mixture of a pure glacial melt-water and old meteoric waters. This mixture corresponds to the groundwaters with the coldest isotopic composition found in the studied systems.

The use of this "mixed" end-member is, therefore, analogous to the use of the so-called "reference groundwaters" /e.g. Laaksoharju and Wallin 1997, Pitkänen et al. 1999, 2004/[5] and it can be successfully employed to explain the present hydrochemical variability of the studied systems. In fact, the Monte Carlo method developed in Section 2.1.5 predicts a $\delta^{18}O$ value around –16‰ for the glacial end-member and the hydrological simulations performed considering this heavier isotopic composition in the glacial end-member improve fitting to the real data /Follin et al. 2007/.

2.1.3 Littorina end member

Geochemical features

The chemical composition of seawater during the Littorina stage has been selected as one of the end-members used in the hydrogeological and hydrogeochemical modelling of the Laxemar and Forsmark sites, as well as in other Fennoscandian sites with a similar palaeogeographic evolution (e.g. Olkiluoto in Finland, /Pitkänen et al. 1999, 2004/.

The Littorina stage in the postglacial evolution of the Baltic Sea started when the passage to the Atlantic Ocean opened through Öresund in the southern part of the Baltic Sea and seawater started to intrude at ≈ 6500 BC. The salinity increased more or less continuously until 4,500–4,000 BC, reaching estimated maximum values twice as high as modern Baltic Sea and this maximum prevailed at least from 4000 to 3000 BC. This period was followed by a stage where substantial dilution took place due to freshwaters discharged by rivers or precipitation. During the last 2,000 years the salinity has remained almost constant at the present Baltic Sea values.

Groundwaters with high proportions of Littorina Sea water are identifiable by their higher salinities and $\delta^{18}O$ values than the present Baltic Sea (as well as higher values for other ions such as magnesium and sulphate).

The original major and stable isotope composition of the old Littorina Sea waters was indirectly estimated from palaeontological studies (e.g. fossil assemblages), measurements of $\delta^{18}O$ in molluscs and foraminifera, and $\delta^{18}O$ analysis and trace element content in sediments and minerals (see /Westman et al. 1999/ and references therein). With all these data, an estimation of the salinity (or chloride concentration) and $\delta^{18}O$ values can be obtained. Then, from correlations between the different elements and chloride in sea-water, the rest of the concentrations can also be estimated /Culkin and Cox 1966, Carman and Rahm 1997/.

The Littorina Sea composition used in this work is shown in the first column of Table 2-5. It is based on the maximum salinity estimation of 12‰, or 6,500 mg/L Cl /Kankainen 1986/ deduced from different studies of groundwater salinity, past climate temperature and analyses of microfossils from marine sediments in Hästholmen (southern Finland). The other main element concentrations were obtained by diluting the global mean ocean water /Pitkänen et al. 1999, 2004/.

Stable isotope compositions assigned to the Littorina end-member comes also from the $\delta^{18}O$ value (−4.7‰) proposed by /Kankainen 1986/ analysing fossil shells. The $\delta^{2}H$ value considered for this end-member (−37.8‰) seems to have been obtained in a proportional way from the isotopic composition of the Baltic Sea today ($\delta^{18}O = -7.55‰$ and $\delta^{2}H = -60.8‰$) as it was considered by /Pitkänen et al. 1999, 2004/.

[5] In these works, reference groundwaters are defined as extreme groundwater compositions derived from pure end-members whose composition can no longer be found in the present hydrological system.

Table 2-5. Composition of Littorina end-member and some groundwaters with the highest proportion of Littorina in Forsmark (Sweden) and Olkiluoto (Finland)[6]. Data for the present Baltic Sea are also included (from an average of 94 samples; Pitkänen et al. 1999, 2004). B: Deep Saline, G: Glacial, L: Littorina, AM: Altered meteoric, SG: Subglacial, M: Meteoric. Chemical contents in mg/L.

	Original end member	Forsmark #12004	Forsmark #4724	Olkiluoto OL–KR2/T4	Olkiluoto KR6/135.2	Baltic Sea
Mixing proportions		**DS=4.76; G=22.0; L=48.1; AM==25.2**	**DS=5.29; G=24.4; L=45.0; AM=25.3.**	**DS=0.0; G=18.2; L=57.9; SG=23.9**	**DS=0.0; L=50.2; SG=6.3; M= 25.8.**	
pH	7.6	7.19	7.5	7.5	7.8	7.7
pe	–	–	–170	–	–250	–
Alkalinity	92.5	126	99.5	67.1	129	78.7
Cl	6,500	5,540	5,329.5	4,600	3,480	3,025
SO_4^{2-}	890	507	546.97	523	432	450
Br	22.2	15.8	20.08	18.0	11.5	10.3
Ca	151	890	934	750	661	82.0
Mg	448	224	204	160	184	219.0
Na	3,674	2,160	2,000	1,900	1,440	1,760.0
K	134	36.40	29.2	16	19	66.0
Si	3.94	6.08	6.92	3.6	3.93	0.27
Fe^{2+}	0.002 (Fe tot)	2.26	0.475	0.50	0.78	<0.01
S^{2-}	–	0.066	bdl	0.04	0.03	–
δ^2H (‰)	–37.8	–66.2	–69.3	–69.7	–	–60.8
$\delta^{18}O$ (‰)	–4.7	–8.7	–8.8	–9.2	–	–7.55

Uncertainty analysis

The composition obtained by the above-mentioned methodology corresponds to an old marine water in its basin prior to its infiltration in the groundwater system. Obviously, this compositional estimation presents uncertainties associated with the salinity (chloride contents), stable isotopes ($\delta^{18}O$), and the compositional changes undergone by the marine water due to its reaction with the marine sediments prior to its infiltration into the bedrock.

Salinity during Littorina stage

Littorina composition is based on an estimation of the maximum salinity of these waters. However, the salinity was variable throughout the entire Littorina Sea period. Moreover, as it occurs in the present Baltic sea, salinity also varies with depth[7] and laterally /e.g. Sohlenius et al. 2001/.

This last uncertainty related to the geographic variability can be minimised by restricting the estimation to the areas of interest, that is, the island of Gotland and the Baltic Sea proper. However, the vertical variability is more difficult to deal with. Salinity ranges from 8 to 24‰ for surface and deep sea waters, as deduced from palaeontological and palaeogeochemical studies (Table 2.2 in /Westman et al. 1999/).

[6] Mixing proportions for Forsmark are performed with M3 (*n*-pc mixing algorithm; see /Gómez et al. 2006/ for details). In the Finnish investigations, the subglacial end-member represents the composition of the groundwater previous to the intrusion of the Littorina marine waters /Pitkänen et al. 2004/.

[7] The vertical structure of the present Baltic Sea salinity is strongly dependent on saline water inflow, freshwater inflow and turbulent mixing. Climate change in any of these factors can thus have a large impact on the vertical stratification. Under present climate conditions the Baltic Sea has a typical halocline depth of 60 m. /Westman et al. 1999, Gustafsson 2004/.

The maximum salinity of the surface sea waters during the Littorina Sea stage in the two areas of interest (Gotland and Baltic Sea Proper) seems to have been between 10 and 13‰ (Cl = 5.5 to 7.2 g/L[8]), according to fossil assemblages, $\delta^{18}O$ and trace-element contents in sediments. The question is: How representative is this value for the bottom recharge waters in the Forsmark and Laxemar areas? Shore displacement curves indicate that the Forsmark area was completely covered by the Littorina Sea (reaching maximum depths of around 60 m) whereas the Laxemar area was only partly covered (with maxima depths around 15 m[9]). Since the vertical salinity gradient during the Littorina stage was probably much less pronounced than at present /Westman et al. 1999/, the range of maximum salinities deduced for marine surface waters can be considered adequate for the waters entering the basement in these areas[10].

All these evidences suggest that the chloride concentration assigned to Littorina (6.5 g/L) can be considered representative of a mean value in the more feasible range of uncertainty (Cl = 5.5 to 7.2 g/L) during its stage of maximum salinity. This value is also consistent with the present composition of the groundwaters (and with data from other sources).

In order to analyse the effects of the uncertainties in the chloride content, /Laaksoharju and Wallin 1997/ performed mixing proportion tests considering various possible Cl concentrations for the Littorina seawater. They found that a chloride concentration of 6,100 mg/l and $\delta^{18}O = -5$‰ for the Littorina end-member gave the best fit with the measured values in the groundwaters from the Laxemar zone. /Pitkänen et al. 1999, 2004/ reported evidences that SO_4^{2-} (Littorina)-rich groundwaters at Olkiluoto (Finland) show a clear trend of $\delta^{18}O$ and Cl towards the estimated Littorina composition ($\delta^{18}O = -4.7$‰ and chloride around 6,500 mg/l). Similarly, the $\delta^{18}O$ vs Cl correlations showed by Smellie and Tullborg (2005; pp. 218–221) for the Littorina-rich groundwaters at SFR, Forsmark, Simpevarp, Äspö and Laxemar sites, are also consistent with the chloride and $\delta^{18}O$ values for the Littorina end-member.

Finally, /Sjöberg et al. 1984/ studied the interstitial waters in an outcrop of postglacial black sulphide clays deposited during the early (maximum salinity) Littorina stage (7,400–5,800 yr) and found a Cl concentration of 6,800 mg/l. Therefore, all these estimations made with different methodologies and approaches supply very similar results for the chloride content of the Littorina waters during the maximum salinity stage.

Isotopic characteristics of the Littorina end-member

The oxygen isotope composition and salinity of the present Baltic seawaters are linearly correlated /Frölich et al. 1988/ as it can also be seen in the seawaters of the studied sites (Figure 2-7). The $\delta^{18}O$ values for the Baltic seawaters range from –8.2 to –11.7‰ due to mixing between seawater from the North Atlantic and freshwaters discharged by rivers or precipitation /Frölich et al. 1988, Neumann et al. 2002/. Therefore, just as the stable isotopic composition of Baltic Seawaters is correlated with salinity, the same uncertainties indicated for salinity in the previous section apply here (e.g. spatial vertical and lateral- and temporal variations during the Littorina Sea stage).

---

[8] Very similar to the original estimation of /Kankainen 1986/, with chloride contents between 5.0 and 6.5 g/L (see also /Pitkänen et al. 1999/). However, some estimates based on fossil assemblages suggest a higher maximum salinity of up to 20‰ (11.0 g/L Cl) in the surface water of the Baltic Proper, but the most recent estimates based on the occurrence of cyanobacterial blooms during the entire Littorina Sea phase, even suggest that the salinity in the Baltic proper did not exceed 12‰ (6.6 g/L Cl; /Westman et al. 1999, Brenner 2005/.

[9] This area was only partly covered by the Littorina Sea. Owing to the topography of the area and the on-going isostatic land uplift, the Laxemar subarea was probably influenced only to a small degree, whereas the Simpevarp peninsula was covered for several thousands of years. Eventual emergence during uplift initiated a recharge meteoric water system some 4,000 to 5,000 years ago. This recharge system effectively flushed out much of the Littorina Sea water /Smellie and Tullborg 2005/.

[10] It is recommended checking in more detail whether the Forsmark area could have been below the halocline as it could have influenced the salinity of the recharge marine waters (and even the intensity of the redox processes). For example, the present day salinity in the Baltic Proper is 7–8‰ and the halocline is located at 60–80 m depth. Below this depth the salinity increases to 11–13‰ /Gustafsson 2004/.

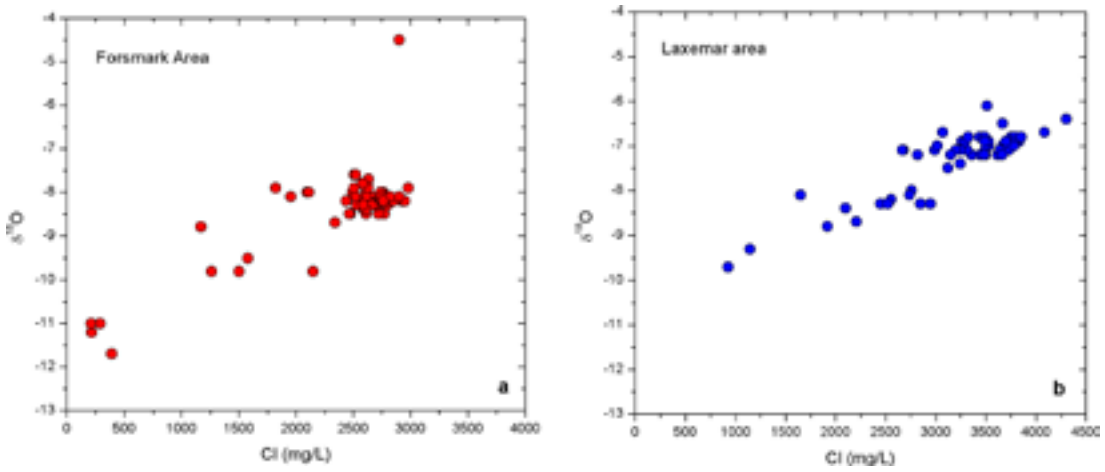

Figure 2-7. *Relation between $\delta^{18}O$ and Cl contents in the present Baltic seawaters from Forsmark (a) and Laxemar (b) areas.*

Moreover, climatic conditions were warmer during that stage (the estimated mean temperature was about 2ºC higher than at present: /Pitkänen et al. 1999, 2004/ and references therein), which favours a heavier isotopic composition of rainwater, which can influence the final composition of seawater. The proposed $\delta^{18}O$ value for the Littorina end-member must take into account these aspects.

The value of $\delta^{18}O$ proposed for the Littorina end-member (−4.7‰; /Pitkänen et al. 1999, 2004/ derives from the estimations performed by /Kankainen 1986/ from fossil shells. This author suggests a range of values between −5.2 and –4.7‰ for salinities between 5.0 and 6.5 g/L in the Littorina stage of maximum salinity. This salinity range is consistent with the results presented in the previous section. Some other studies /Donner et al. 1994/ confirm these values (around –4.5‰) and they are also consistent with the warmer climatic situation during the Littorina Sea period and a heavier isotopic composition of rainwater /Smellie and Tullborg 2005/.

Hydrochemical studies performed in different Fennoscandian sites seem to support this isotopic estimation for the Littorina end-member. As reported above, a Littorina end-member with Cl = 6,100 mg/l and $\delta^{18}O$ = −5‰ has been deduced by /Laaksoharju and Wallin 1997/ with the mixing proportion tests.

In addition, Littorina-rich groundwaters in Forsmark and Olkiluoto show lighter isotopic signatures than the selected end-member (Table 2-5) due to mixing with pre-existing groundwaters (e.g. glacial and/or deep saline waters). The ratios $\delta^{18}O$/Cl /Smellie and Tullborg 2005/ or $\delta^{18}O$/SO_4 (Figure 2-9b) in these kind of waters from both sites are similar to the ratios in the Littorina end-member, which also confirms the consistency of the selected values for this end-member.

Reactions with marine sediments

The composition of the intruding seawater can be modified by reactions in the sediments such as sulphate reduction, carbonate precipitation and cation exchange.

Sulphate reduction is a very feasible process affecting Littorina seawaters during infiltration in the sediments. Microbially mediated sulphate reduction usually takes place in anoxic sea-bed sediments, as in the marine sediments close to Äspö at present /Laaksoharju and Wallin 1997/. This process, represented by the reaction $2CH_2O + SO_4^{2-} \rightarrow 2HCO_3^- + HS^- + H^+$, could reduce considerably the sulphate content and increase the HCO_3^- concentration of the intruding seawater.

Surface water salinity and redox conditions below the halocline have changed drastically several times since the beginning of the Littorina stage /Westman and Sohlenius 1999/. During the most saline phase of the Littorina Sea, anoxic bottom conditions were established at depth below the

halocline and laminated sediments were formed in these anoxic bottoms until 3,000 BC. The study of these marine sediments /e.g. Böttcher and Lepland 2000, Alvi and Winthelhalter 2001/ confirms the existence of sulphate-reduction activity with precipitation of iron sulphides in a seabed rich in organic matter. /Westman and Sohlenius 1999/ indicate the existence of oxic deep water conditions from 2,500 BC to 500 AC, and the subsequent set-up of a second period of anoxic bottom conditions, from that moment to the present.

Oxic conditions of the bottom water have considerable impact on the biogeochemistry of the most superficial sediment layer but they have less influence in the deeper sediment layers if organic matter is available. Anoxic bottom conditions favour anaerobic metabolisms (and hence, sulphate-reduction) in the top of the sediment layers, whereas oxic bottom conditions usually diminish the intensity of anaerobic metabolism and shifts its area of influence some centimetres below the water-sediment interface. This has been verified, for example, in the bottom water of the Gotland Basin during a period of oxic conditions /Piker et al. 1998/.

The second group of geochemical processes able to modify the original composition of intruding seawater is *carbonate precipitation*, which usually controls the alkalinity (HCO_3^-) in marine sediments. Calcite equilibrium is very common and, for example, it is reached at a depth of several centimetres in the anoxic sediments of the present Baltic Sea /Carman and Rahm 1997/. Other carbonates can also participate, and precipitation of sedimentary manganese carbonates[11], such as rhodochrosite and kuthnahorite, $Mn_xCa_{1-x}CO_3$, has long been described in marine sedimentary environments /Li et al. 1969, Suess 1978, Thompson et al. 1986, Gingele and Kasten 1994/, including the Baltic Sea /e.g. Jakobsen and Postma 1989, Lepland and Stevens 1998, Burke and Kemp 2002, Kunzendorf and Larsen 2002, Neumann et al. 2002/. In the Baltic Sea, Mn-carbonate formation has taken place for the last 7,000 yr (Littorina stage) leading to Mn concentrations of up to 10 wt.% in the bulk sediments of the Gotland Basin (/Neumann et al. 2002/ and references therein).

The third type of geochemical process that can modify the original concentrations of major cations (Ca, Mg, Na,K) in the Littorina waters is *cation exchange* /Smellie and Laaksoharju 1992, Carman and Rahm 1997/ alone or mixed with other simultaneous dissolution-precipitation processes.

The existence of all these processes affecting Littorina composition can be deduced from the characteristics of present Littorina rich-groundwaters (or trapped relicts of this marine waters; see below). The extent of this variation is difficult to estimate, even more considering that they could have been heterogeneously distributed in the studied areas. Nevertheless, qualitative estimations can be made for some of the processes.

Sulphate-reduction

Sulphate contents of the Littorina end-member could have decreased as a result of active sulphate-reduction in the marine sediments. As stated above, anoxic bottom conditions were established at depth (below the halocline) during the most saline phase of the Littorina Sea stage. This would favour sulphate-reduction, although the intensity of this process in Forsmark sediments remains unclear. However, some clues on the existence of this process appear to remain in the Littorina-rich groundwaters from Forsmark.

[11] Formation of authigenic rhodochrosite laminae in the Baltic Sea has been related to the periodic renewal of deep waters by inflows of North Atlantic surface waters /Kulik et al. 2000, Heiser et al. 2001, Neumann et al. 2002, Burke and Kemp 2002/. During an inflow event, the anoxic water column is flushed by saline and oxic water which rapidly re-oxidizes the dissolved manganese present, and large quantities of particulate Mn-oxide are deposited at the sediment-water interface. These Mn-oxides supplied from oxic surface sediments are reduced at depth by manganese reducing bacteria when all the available oxygen is consumed. This process produces large in situ Mn^{2+} concentrations and, in combination with high carbonate alkalinity generated by mineralization of organic matter, leads to pore-water conditions in the sediments that are supersaturated with respect to rhodochrosite or to a mixed Ca and Mn-rich carbonate /Burke and Kemp 2002/.

$\delta^{34}S$ values[12] in dissolved sulphate are mainly about 24–26‰ (Figure 2-8a) in Forsmark Littorina-rich groundwaters with SO_4^{2-} contents higher than 350 mg/L. This is clearly higher than the present values of the Baltic Sea in Forsmark (17 to 22‰), which would support the existence of SRB (Sulphate Reducing Bacteria) activity.

Nonetheless, both the saturation states with respect to ferrous iron monosulphides /Gimeno et al. 2007/ and the microbiological analyses performed in these groundwaters, indicate a minor presence or even absence of SRB activity under the present conditions (Figure 2-8b) in agreement with their "isolated" character in the hydrogeological context. Therefore, these isotopic values are better interpreted as an inheritance of a past SRB activity during infiltration of these waters through marine sediments as proposed in Littorina-rich groundwaters from Olkiluoto /Pitkänen et al. 2004/.

In any case, several lines of evidence suggest that the decrease in SO_4^{2-} contents produced by sulphate-reduction in the marine sediments is generally negligible compared with the initial concentrations assumed for this component.

Present groundwaters with clear Littorina signature in Olkiluoto and Forsmark (45 to 60% of this end-member; Table 2-5), have high SO_4^{2-} contents. Since the Deep Saline end-member, and therefore the pre-Littorina groundwaters, in the Olkiluoto area is sulphate-poor /Pitkänen et al. 1999, 2004/, the main contributor to the high sulphate concentrations in the present groundwaters of this zone must be the Littorina end-member. Sulphate contents in these groundwaters can be higher than 500 mg/l (higher than the Present Baltic Sea, Table 2-5) in spite of the possible dilution effects. Something similar could have happened in the Littorina-rich groundwaters in the Forsmark area, where the Deep Saline end-member also probably have low sulphate contents.

Using mass balance calculations with isotopic constraints, /Pitkänen et al. 1999, 2004/ estimated that the extent of sulphate reduction when Littorina seawater passed through the marine sediments only produced a decrease of 0.64 to 1.0 mmol/l (61 to 96 mg/l) of dissolved SO_4^{2-} in

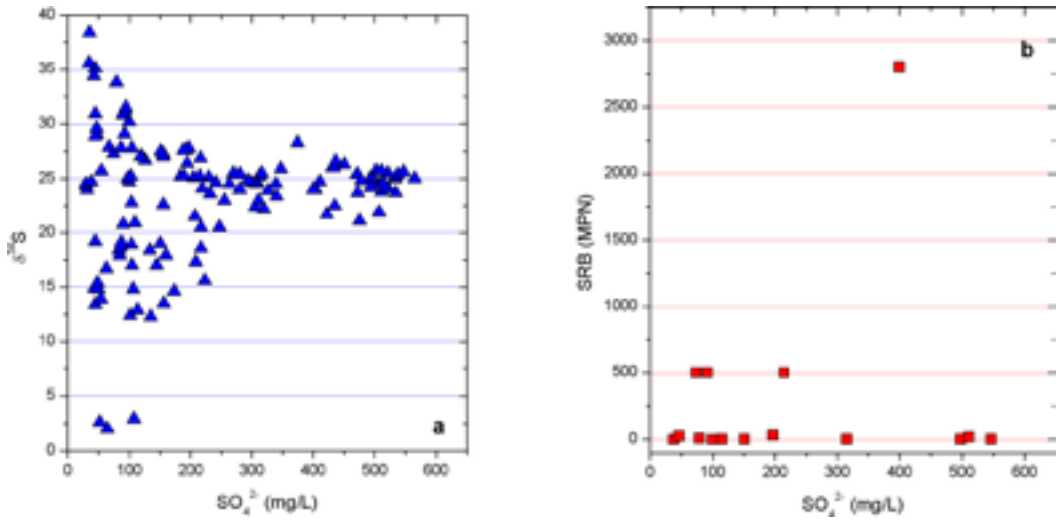

Figure 2-8. *$\delta^{34}S$ (a) and most probable number (MPN) of sulphate reducing bacteria (SRB) (b) with respect to SO_4^{2-} content in groundwaters from Forsmark.*

[12] The activity of the SRB produces a noticeable fractionation of the sulphur isotopes. During sulphate reduction, the lighter isotope (^{32}S) is enriched in the sulphide and the heavier (^{34}S) in the remaining sulphate increasing the $\delta^{34}S$ value in sulphates /Clark and Fritz 1997/.

Olkiluoto groundwaters. This implies a minimal variation on the 890 mg/l SO_4^{2-} initially considered in the end-member (Table 2-5). Assuming a negligible effect of sulphate reduction, these authors extrapolated the $\delta^{18}O$–SO_4^{2-} ratio of the SO_4^{2-} (Littorina) -rich groundwaters in Olkiluoto, to the $\delta^{18}O$ in Littorina (−4.7‰) and the estimated values for sulphate were 900 mg/l (Figure 2-9a), in agreement with the content considered for the end-member.

The behaviour of sulphate seems to be similar at Forsmark (Figure 2-9b), which explains why mixing and mass balance calculations give very good results when this anion is treated as conservative /Gimeno et al. 2004/. This kind of estimation is not possible in the Äspö-Simpevarp-Laxemar area because: (1) there are few groundwaters with an important Littorina signature, and (2) the pre-Littorina groundwaters in that area probably have very high sulphate concentration (from the deep saline contribution). Moreover, the presence of sulphate reducing processes at present in these groundwaters makes it even more difficult to separate the effect of sulphate reduction in the marine sediments.

Rhodochrosite precipitation

The detailed study of the geochemical behaviour of Mn in different granitic systems of the Scandinavian Shield (Forsmark, Laxemar and Finnsjon in Sweden, and Olkilluoto and Palmottu in Finland) performed by /Gimeno et al. 2007/ suggests a clear link between the existence of equilibrium with rhodochrosite and high Littorina proportions (Figure 2-10). This equilibrium situation is very uncommon in the groundwaters of other granitic systems in the Scandinavian Shield, unless the Littorina proportion happens to be in the same range.

Figure 2-10 shows the relationship between rhodochrosite saturation index, Mn concentrations and Littorina proportion as calculated by M3 (n-PC mixing algorithm; Gómez et al. 2006) for a group of selected Forsmark groundwaters. As it is clear from the plots, saline waters with low Littorina proportion (<14%) have low Mn contents and are clearly undersaturated with respect to rhodochrosite. Equilibrium with rhodochrosite is reached only in waters with Littorina proportion larger than 40–50% together with high but variable Mn contents. The variability in Mn concentrations is perhaps related to inorganic re-equilibrium processes after the mixing event.

Only when a high proportion of Littorina remains in the groundwaters the disequilibrium introduced by the mixing event with the previous groundwaters would be small, and re-equilibrium easy. When the proportion of Littorina is small, the undersaturation state with respect to rhodochrosite, typical of the original groundwaters, would prevail.

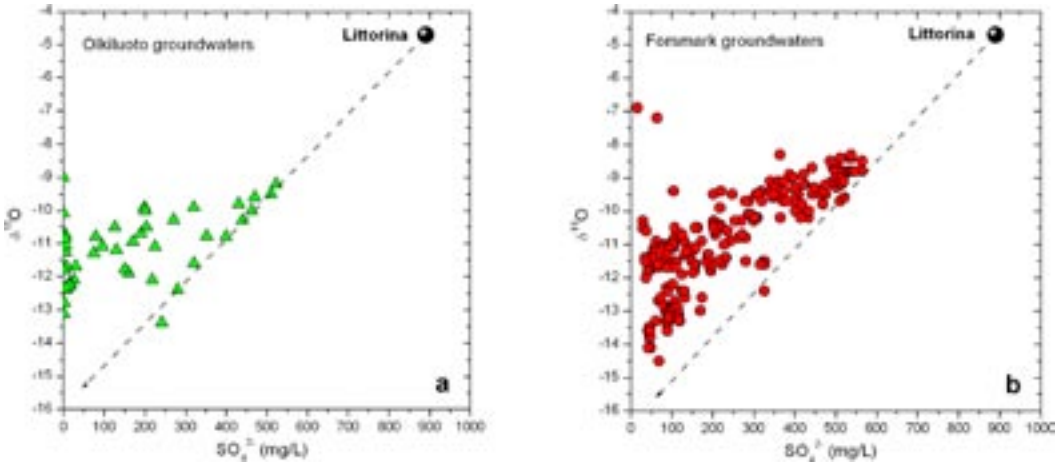

Figure 2-9. *$\delta^{18}O$ versus sulphate concentrations for a) Olkiluoto (Finland) and b) Forsmark (Sweden) groundwaters. The line relates the SO_4^{2-} (Littorina)-rich groundwaters in both sites with the Littorina end member (upper right). Data for Olkiluoto groundwaters from /Pitkänen et al. 2004/.*

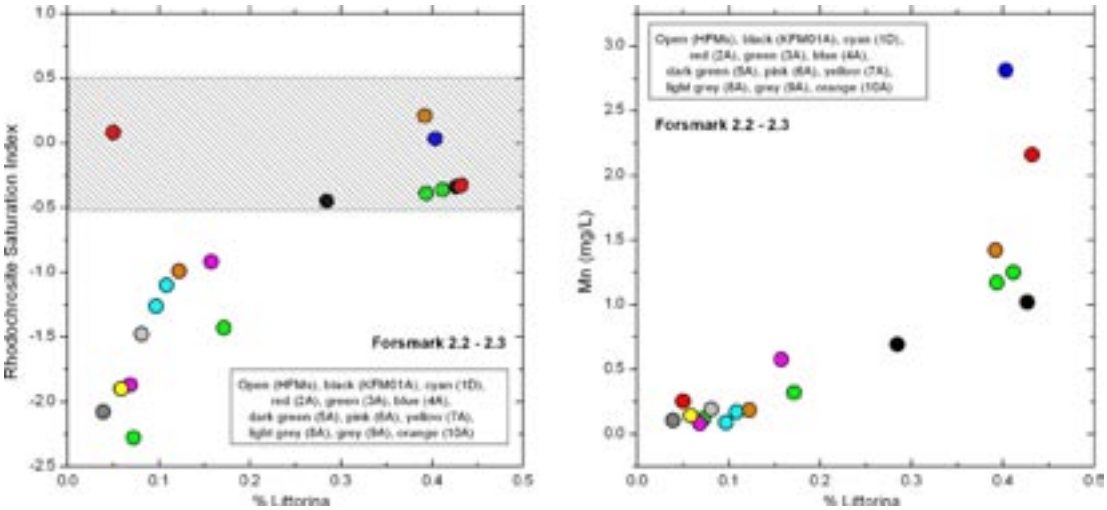

Figure 2-10. *Rhodochrosite saturation indices (left) and Mn concentration (right) in Forsmark groundwaters with respect to Littorina proportion. The solubility value of rhodochrosite used in the calculations is the one included in WATQE4F database /Ball and Nordstrom 2001/, log K =–11.13. The uncertainty range has been fixed in a 5% of the log K value which is represented by the dashed zone in the left panel.*

The low MRB activity in most Forsmark groundwaters would favour the undersaturation state with respect to rhodochrosite in the Littorina-poor groundwaters. The absence of these organisms in most Littorina-rich groundwaters precludes their activity to be considered as the cause of rhodochrosite equilibrium. Therefore, both, the presence of waters with high Littorina proportions (higher than 40%) and the absence of present biological activity (e.g. MRB) in these groundwaters have been probably favoured by the isolated character (pockets) of the analysed groundwater samples.

All this suggests that Mn content and equilibrium with rhodochrosite in brackish groundwaters are characteristics imposed by the superficial marine environment prevailing during the Littorina stage /Gimeno et al. 2007/.

Other processes

The estimation of the possible variation in the rest of the elements is also difficult since there are few data on the composition of the diagenetic interstitial waters in the sediments of the Littorina stage. The only available study on this subject is from /Sjöberg et al. 1984/. They studied the interstitial waters in a 12 m profile from the outcrop of postglacial black sulphide clays deposited during the initial period of maximum salinity of the Littorina stage. Interstitial waters from the six first meters had been affected by the subaereal meteoric alteration over the last 300 years. However, from that depth down, interstitial waters showed a relatively constant composition down to 12 m depth (Figure 2-11), representative of the marine waters that entered the basement and reacted with the sediments of that age.

As displayed in Figure 2-11, chloride contents in the interstitial waters studied by /Sjöberg et al. 1984/ are very close to the value suggested by /Kankainen 1986/ for the end-member and inside the uncertainty range deduced from other studies (Cl = 5,500 to 7,200 mg/l). Sodium, calcium and magnesium contents are slightly lower and K contents slightly higher than the values considered for the Littorina end-member (Table 2-5). These variations between the original marine water (Littorina end-member) and the water analysed in the sediments are the result of diagenetic processes occurring during infiltration. These processes are consistent with observations in reduced marine pore-water environments at present (including those from the Baltic Sea): a depletion in Mg and Na associated with adsorption or exchange processes in clay minerals and an enrichment of K due to the breakdown of K-minerals such as K-feldspar or oligoclase, ubiquitous in the sediments of the Baltic proper (/Carman and Rahm 1997/ and references therein).

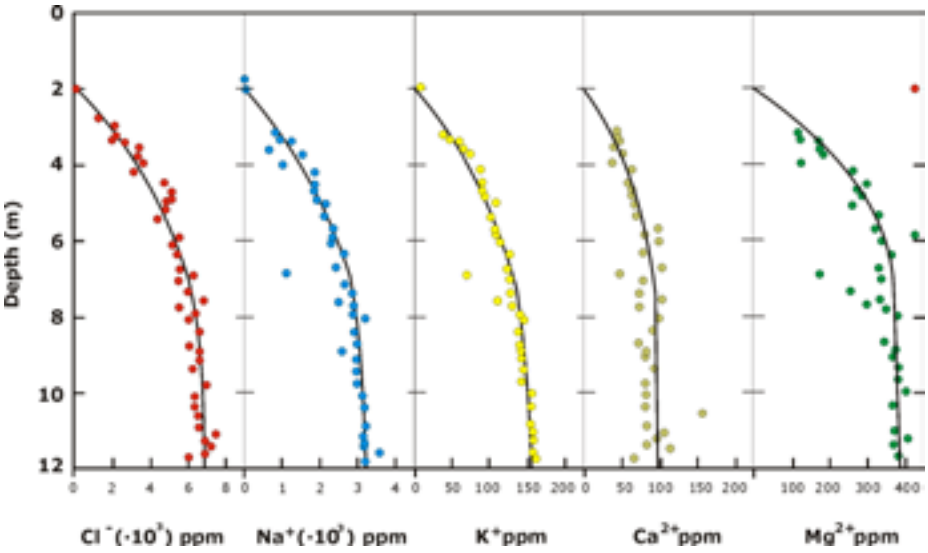

Figure 2-11. *Concentration profiles for major ions in the pore-waters of postglacial black sulphide clays deposited during the Littorina stage /from Sjöberg et al. 1984/.*

In conclusion, the compositional variations produced during the infiltration of Littorina waters through the marine sediments do not seem to be important for the more diagnostic elements for this end-member (SO_4^{2-} and Mg).

Discussion and conclusions

The analysis of the salinity and $\delta^{18}O$ content in the old marine waters from the Littorina Sea stage is the key point on which the rest of the compositional parameters of this end-member are based. The selected chloride value (6,500 mg/l) represents the maximum salinity pulse, at least from 6,000 to 5,000 BP. From then on, salinity decreased owing to climate changes up to the present values in the Baltic Sea. However, the magnitude of the effect of those changes in the salinity and $\delta^{18}O$ values of the seawater entering the basement remains unclear.

Based on shore displacement curves it is clear that the Forsmark area has been covered by the Littorina Sea for a long period of time (around 8,000 years). The low topography favoured that it reached several tens of kilometres further inland for a considerable part of that time. The present meteoric recharge stage following uplift and emergence has only prevailed for the last 1,000 years. The Simpevarp/Laxemar area, in contrast, was only partly covered by the Littorina Sea. Due to the topography of the area and the on-going isostatic land uplift, the Laxemar area was probably influenced only to a small degree, whereas the Simpevarp peninsula was covered for several thousands of years until its eventual emergence during uplift initiated a recharge of meteoric waters some 4,000 to 5,000 years ago /Smellie and Tullborg 2005/. Therefore, groundwaters from most of these areas could be affected by less saline marine intrusions over the time.

Even though the use of an end-member representative of the maximum salinity stage is a simplification, it is reasonable since these waters would have the maximum capacity to penetrate the bedrock. As the maximum salinity, the Littorina stage contained the most saline groundwater, it is assumed to have penetrated more deeply, eventually mixing with the groundwaters already present in the bedrock (Deep Saline waters, Old Meteoric and Glacial). Moreover, the contents of chloride, $\delta^{18}O$ and even sulphate (whose behaviour is quasi-conservative), deduced from the present groundwaters with high Littorina proportions in different sites, are in reasonable agreement with the values proposed for the Littorina end-member.

Diagenetic modifications on the Littorina composition after infiltration through the sediments are difficult to evaluate. The scarce data on interstitial waters of marine sediments from that age /Sjöberg et al. 1984/ and some deductions from the present Littorina-rich groundwaters seem

to indicate that they were not extensive, which is consistent with the high contents of the more diagnostic elements (SO_4^{2-} and Mg) in the groundwaters with high Littorina proportion and with some modelling calculations /Pitkänen et al. 1999, 2004/. However, some of the identified diagenetic processes affecting both present Baltic sediments and old sediments from the Littorina stage, allow us to theoretically obtain some parameters of interest (Eh, pH, etc) by equilibrium calculations (e.g. equilibrium with rhodochrosite, FeS, pyrite or calcite) for these seawaters after interaction with marine sediments /Auqué et al. 2006/.

All the data above seem to indicate that the composition of the Littorina end-member has been properly defined for the studied sites although different uncertainties still hold, mainly related to the salinity variation with time. Therefore, an alternative "Littorina end-member" is proposed for sensitivity analysis in hydrological or hydrochemical mixing calculations: this end-member is the present composition of Baltic seawaters. A large amount of seawater analyses is available for both Forsmark and Laxemar, as well as a Baltic Sea Reference Water (sample ID code SEA01) defined by /Laaksoharju and Wallin 1997/. Since the salinity and compositional characteristics of present Baltic waters are not homogeneous, the alternative end-member proposed is the "average" Baltic seawater obtained by /Pitkänen et al. 1999, 2004/. This "sample" (Table 2-5) is less saline than the aforementioned Baltic Sea Reference Water (3,025 vs 3,760 mg/L Cl) and shows larger differences in the stable isotope contents compared with the one considered in the Littorina end-member.

2.1.4 Altered Meteoric end-member

Geochemical features

In previous modelling efforts with M3, a rain water sample called "Rain 60" or "Precipitation" has been used as a the meteoric end-member /e.g. Laaksoharju and Wallin 1997, SKB 2004abc, 2006a, Puigdomenech 2001/. This water sample corresponds to a modern meteoric water with a modelled high tritium content that represents the rain water from 1960 /Laaksoharju and Wallin 1997/.

This end-member, with an extremely dilute character (Table 2-6), presents the typical composition of rain water just before its interaction with the overburden. Therefore, this water is not representative of the real recharge water which will contact the granite after traversing the soil profile. The real recharge water will show different characteristics depending on the area, the mineralogy and the residence time in the shallow parts of the system.

To minimize this discrepancy, the ChemNet group decided to select different waters representative of shallow groundwaters (less than 100 m depth) of recent meteoric origin after a short interaction with soils, overburden and granite in the studied areas. It is what has finally been called the "Altered Meteoric" (or sometimes "Dilute Granitic Groundwater") end-member.

The selection of a representative composition for this Altered Meteoric end-member has been made from a large amount of available near surface (soil pipes) and shallow dilute groundwater samples from Forsmark and Laxemar. Their tritium content and low chloride concentrations are representative of recent meteoric origin, without mixing with more saline waters. Even though all the groundwaters of this type have low TDS, their chemical composition is very heterogeneous in detail. Therefore, several representative superficial granitic groundwaters have been used for each site.

Sample #8335 (from HFM09 borehole at 17–50 m depth) has been used by the UZ group as the "optimal choice" to compute mixing proportions in the Forsmark area (Table 2-6). More recently, a new, slightly more saline, sample has been proposed in the context of ChemNet: sample #8659 from soil pipe SFM02 at section 4.2–5.2 m depth. The chemical and isotopic characteristics of both samples are stable over six months to several years of monitoring, suggesting proximity to steady state conditions. Additionally, a more dilute sample (#4167; Table 2-6) from HFM03 has been used in the predictive calculations performed in SR-Can /Auqué et al. 2006/ and in the updated strategy for groundwater flow modelling in Forsmark performed by /Follin et al. 2007/ considering alternative end-members.

Table 2-6. Diluted granitic groundwaters from the Forsmark area used in ChemNet modelling work as Altered Meteoric end-members. Rain 60 end-member /from Laaksoharju and Wallin 1997/ is also indicated. Concentrations in mg/L.

	Rain 60	Sample #8335[1]	Sample #8659[2]	Sample #4167[3]	Sample #12281[4]	Sample #4515[5]	Sample #4919[6]
pH	–	7.91	7.08	7.6	7.72	7.69	7.12
Alkalinity	12.2	466.0	346.0	310.0	466.0	536.0	665.0
Cl	0.23	181	51.4	15.7	204.0	17.7	133.0
SO_4^{2-}	1.41	85.1	22.5	18.66	95.1	7.42	43.9
Br	–	0.572	0.21	bdl	0.78	0.071	0.529
F	–	1.6	0.45	1.13	2.45	1.22	0.61
Ca	0.24	41.1	115.0	62.0	45.8	44.3	127.0
Mg	0.1	7.5	7.8	14.0	10.6	11.3	32.7
Na	0.4	274.0	21.7	64.6	276.0	153.0	156.0
K	0.29	5.60	4.79	9.5	7.16	8.55	12.5
Sr	–	0.38	0.171	0.284	0.313	0.169	0.411
Si	–	6.68	6.04	9.78	6.41	7.19	6.89
δ^2H (‰)	–80.0	–80.6	–81.6	–79.6	–81.1	–84.9	–78.6
$\delta^{18}O$ (‰)	–10.5	–11.1	–12.2	–11.8	–11.1	–11.5	–10.5

[1] From HFM09 borehole at section 17–50 m.; [2] From soil pipe SFM02 at section 4.2–5.2 m.; [3] From HFM03 borehole at section 13.1–26 m.; [4] From HFM16 borehole at section 54–67m.; [5] From soil pipe SFM0017 at 4–5 m depth; [6] From soil pipe SFM0037 at 2–3 m depth.

In the Laxemar area, several Altered Meteoric end-members have been prepared. For example, sample HAS05 (Table 2-7) from Äspö usually gives good results in M3 modelling and can be considered a suitable sample for the Äspö and Simpevarp sub-areas. Since this sample is probably too saline for the Laxemar sub-area, the UZ group has also used sample #2030 from Böckholmen (Table 2-7) as a more dilute granitic end-member in sensitivity calculations.

Specific shallow granitic groundwaters from Laxemar have been considered and will be included in the new modelling phase L2.2/L.2.3. Samples #10231 (from HLX28 borehole at section 6.03–154.2 m.) and #7345 (from borehole HLX14 at section 11.9–115.9 m.) have been selected (Table 2-7) for the M3 calculations. Other possible shallow granitic groundwaters for the Laxemar area are shown in Table 2-7.

Uncertainty analysis

Uncertainties affecting this end-member are mainly related to their spatial and temporal compositional variability depending on the site and zone inside each site. A better understanding of the connection between surface waters and groundwaters and of the near-surface reaction zones controlling the chemistry of recharge waters is fundamental to gain confidence in the predictive calculations of future changes in the systems /SKB 2006bc/. Part of the work performed by the UZ group on this problem can be found in Section 3.3. Here only the earlier results relevant to this uncertainty analysis are presented. Two main aspects will be addressed: (1) the influence of the chemical variability of the Altered Meteoric end-member in M3 calculations and the identification of the most suitable altered meteoric end-member for each area, and (2) the influence of the chemical variability and dilute character of these groundwaters in predictive mixing and reaction calculations.

Table 2-7. Shallow granitic groundwaters from Laxemar area used in ChemNet modelling work as Altered Meteoric end-members. Rain 60 end-member /from Laaksoharju and Wallin 1997/ is also indicated. Concentrations expressed in mg/L.

	Rain 60	Sample #10231[1]	Sample #7345[2]	Sample #2030[3]	Sample HAS05[4]	Sample #3904[5]	Sample #2558[6]	Sample #7245[7]
pH	–	8.17	8.11	7.5	8.0	8.23	7.30	7.41
Alkalinity	12.2	265.0	302.0	137.0	370.0	198.0	347.0	217.0
Cl	0.23	23.0	67.9	11.2	119.0	6.3	5.4	12.6
SO_4^{2-}	1.41	35.0	31.3	23.0	118.0	18.7	6.92	20.4
Br	–	bdl	0.415	–	–	bdl	5.2	bdl
F	–	3.85	3.77	–	–	2.75	–	1.22
Ca	0.24	11.2	18.8	38.4	25.0	12.9	45.4	56.7
Mg	0.1	3.6	4.7	4.0	6.0	4.4	8.7	9.2
Na	0.4	110.0	138.0	15.4	237.0	67.7	50.5	38.7
K	0.29	2.97	3.08	2.6	4.0	2.81	3.83	6.64
Sr	–	0.14	0.32	0.22	–	0.116	0.353	0.194
Si	–	6.97	6.69	6.0	–	5.66	8.03	7.66
δ^2H (‰)	–80.0	–76.5	–78.6	–75.3	–73.8	–78.8	–74.4	–79.4
$\delta^{18}O$ (‰)	–10.5	–10.9	–11.2	–9.6	–9.9	–10.9	–9.7	–10.8

[1] From HLX28 borehole at section 6.03–154.2 m; [2] From borehole HLX14 at section 11.9–115.9 m.; [3] From borehole HBH05 at section 11.0–22.0 m.; [4] From borehole HAS05 at section 45–100 m.; [5] From HLX10 at section 0–85 m. [6] From HLX05 at section 19–20 m; [7] From soil pipe SSM000012 at 5–6 m depth.

Chemical variability in the shallow and near-surface groundwaters from Forsmark and Laxemar

The study of the carbonate system in these waters (see Section 3.3) has shown that the biogenic CO_2 input (decay of organic matter and root respiration) and the associated silicate (Laxemar) or silicate + calcite weathering (Forsmark) control pH, Ca and HCO_3^- concentrations in the near-surface groundwaters at both sites.

Seasonal variability of CO_2 input produces variable and high calcium and bicarbonate contents: 5 to 110 mg/L Ca and 1 to 600 mg/l HCO_3^- in Laxemar, and 40 to 240 mg/L Ca and 150 to 900 mg/L HCO_3^- in Forsmark. The higher values in the near surface groundwaters from Forsmark are related to the extensive presence of limestones in the overburden of this area, a feature very uncommon in Swedish superficial materials.

Nevertheless, shallow groundwaters (from 20 to 100–200 m depth) in both sites do not show the same variability and high HCO_3^- or Ca contents as the near surface groundwaters (usually from surface to 20 m depth). Therefore, it could be considered that most of the near surface groundwaters are isolated from, and not hydraulically connected to the shallow groundwater systems. Recharge waters are affected by biogenic CO_2 input but only waters with short residence time in the overburden (fast paths), and therefore, more diluted, are effectively recharging the shallow hydrological systems.

From this situation, the importance of a careful selection of the Altered Meteoric end-member can be deduced, since near surface groundwaters with high Ca (and/or HCO_3^-) contents, even with low or very low Cl concentrations, are not necessarily recharge waters.

As shown in Tables 2-6 and 2-7, the proposed Altered Meteoric end-members for Forsmark and Laxemar include both shallow and near-surface groundwaters with variable Ca contents. The whole compositional variability in the proposed Altered Meteoric end-members will be taken into account in the sensitivity analysis performed with M3 (as required by the inverse approach).

The sensitivity analysis in predictive calculations will be focussed, at this stage, on the calcium concentrations as the most problematic aspect detected in previous studies /Auqué et al. 2006/.

M3 calculations using different Altered Meteoric end-members

A first attempt in identifying the most suitable Altered Meteoric end-member for each site can be obtained with M3. This code calculates the coverage obtained for each set of groundwaters (Laxemar and Forsmark), using different Altered Meteoric end-members. Coverage is defined as the percentage of samples that plot inside the mixing polyhedron. Samples that are located outside the mixing polyhedron cannot be explained by a simple mixture of the chosen end-members.

If the end-members have been correctly chosen for the given dataset, all samples should plot inside the $n-1$-dimensional hyper-volume defined by the n end-members. Only these samples can be "explained" by pure conservative mixing of the selected end-members. The closer the number of explained samples is to the total number of samples, the better the combination is (in the sense that more samples can be explained as a mixing of the selected end-members). In other words, a set of end-members is properly selected for an specific dataset when most of the waters in the dataset are inside the mixing (hyper)polyhedron.

Groundwater samples from Laxemar 2.2 and Forsmark 2.2 data sets have been used to perform these calculations. The end-members used for Forsmark are Altered Meteoric (all samples in Table 2-6) + Deep Saline (low SO_4^{2-}) + Glacial (−21‰ $\delta^{18}O$) + Littorina. For Laxemar the end-members are: Altered Meteoric (all samples in Table 2-7) + Deep Saline (high SO_4^{2-}) + Glacial + Littorina (see Table 2-14). In order to verify the effects on the results of the still poorly understood relations between shallow and deep groundwaters, calculations were performed in both sites with two different data sets: one considering "all groundwaters" (including near-surface groundwaters) and other with "only groundwaters" (excluding near-surface groundwaters).

An allowance parameter[13] of 0.03 is used in all calculations with M3 code. Results are presented in Tables 2-8 and 2-9.

The coverage shown by all the selected Altered Meteoric end-members is higher than 80% in the Forsmark area; and even higher than 88% when using the "only groundwaters dataset". The lower coverage obtained when including the near-surface groundwaters is due to the fact that the chemistry of these shallow groundwaters is mainly controlled by water-rock interaction and not by mixing processes and, therefore, some of them always plot outside the mixing hyper-polyhedron when included in the M3 dataset.

The sample used by the UZ group in previous mixing proportion calculations for the Forsmark area (HFM09, #8335) gives very good results with both datasets (coverage values of 90.5 and 89.2%; the second in the overall rank; Table 2-8). But the most suitable sample for this area appears to be SFM0037 (#4919), from a soil pipe.

Results for the Laxemar area (Table 2-9) are also statistically good for all the selected Altered Meteoric end-members but in some cases the coverage is lower (e.g. 73–75%) than those obtained in Forsmark. Also, in some cases, coverage for the "all groundwaters dataset" is higher than the one obtained for the "only groundwaters dataset" (sample HLX10, #3904 and, specially, sample HBH05, #2030; Table 2-9).

[13] When performing a mixing calculation, some of the samples in the dataset could fall outside the mixing hyper-polyhedron, meaning that they cannot be explained by pure mixing of the chosen end-members. From this set of "outsiders", some samples will fall far from the "walls" of the mixing hyper-polyhedron as they *simply* cannot be explained as a mixture of the selected end-members, but others will fall *just* outside the hyper-polyhedron, very close to any of its walls. These samples are *strictly not* explained by mixing, but the reason in this case is almost certainly due to uncertainties in the composition of the end-members or the samples. In this case it is not unreasonable to "move" these samples to the nearest hyper-polyhedron wall and include them in the mixing calculations. This procedure is implemented in M3 through the so-called ***Allowance Parameter.*** The allowance parameter allows for samples near the mixing hyper-polyhedron (but outside it) to be moved to the nearest wall. The procedure is describe in /Gómez et al. 2006/.

Table 2-8. Coverage results (in percent) of M3 calculations for the Forsmark area. GW means groundwaters and NSGW means near surface groundwaters. See text for the details of calculations.

DGW end-member	GW+NSGW		GW		Overall rank
	Coverage	Rank	Coverage	Rank	
HFM16 (12281)	89.4	4	97.9	4	4
HFM09 (8335)	90.5	2	98.2	2	2
HFM03 (4167)	83.2	5	88.9	5	5
SFM0017 (4515)	90.5	2	98.2	2	2
SFM0037 (4919)	95.7	1	99.3	1	1
SFM0002 (8659)	81.5	6	88.6	6	6

Table 2-9. Coverage results (in percentage) of M3 calculations for the Laxemar area. GW means groundwaters and NSGW means near surface groundwaters. See text for the details of calculations.

DGW end-member	GW+NSGW		GW		Overall rank
	Coverage	Rank	Coverage	Rank	
HAS05	82.3	4	98.7	2	3
HLX10 (3904)	79.7	6	75.2	7	7
HBH05 (2030)	97.5	1	88.9	5	3
SSM000012 (7245)	81.4	5	86.5	6	5
HLX28 (10231)	86.6	2	93.5	3	2
HLX14 (7345)	72.9	7	92.7	4	5
HLX05 (2558)	83.7	3	99.2	1	1

These interesting results are probably due to the hydrological and hydrochemical heterogeneity of the different Laxemar subareas, with the Laxemar sub-area representing and inland recharge area and Simpevarp and Äspö sub-areas a low relief, less hydraulically-active coastal site. In addition, Äspö and Simpevarp groundwaters have been affected by marine waters (old and present Baltic Sea) whereas Laxemar groundwaters were probably influenced only to a small degree by Littorina seawaters due to the topography of the area and the on-going isostatic land uplift (see discussion previously). Samples used by the UZ group in mixing proportion calculations for the Laxemar area (HAS05 and HBH05, #2030) provide good general results. But the most suitable samples are HLX28 (#10231) and HLX05 (#2558), more recently proposed by the ChemNet group.

From these results, sample #4919 can be selected as the most suitable for Forsmark area whereas sample #10231 can be recommended for the Laxemar area (sample #2558 has been removed from the data set in the last Laxemar 2.3 data freeze). But it must be stated that any of the proposed Altered Meteoric end-members (Tables 2-6 and 2-7) can be used in M3 calculations (especially when only groundwaters are used) to obtain an stable set of mixing proportions. M3 calculates the mixing proportion for the different end-members working with the whole set of groundwaters for each site, that is, waters with variable salinity and representative of the different mixing processes effective over the palaeohydrogeological history of the sites. Therefore, the mixing proportions obtained by M3 summarize, at present the whole history and are meaningful only if mixing is the main control on the water chemistry. In this context, the Glacial and Altered Meteoric end-members, compared with Littorina or Deep Saline end-members, mainly promote dilution, independently of their detailed composition. But the situation can be very different in predictive calculations at more reduced temporal and spatial scales, during transient periods – or in local zones – without effective mixing processes.

Discussion and conclusions

The selection of the most suitable Altered Meteoric end-member for each site is affected by different kinds of uncertainties: the lack of a detailed hydrogeochemical model for the near-surface reaction zones (soils and overburden) and the absence of well defined recharge waters that would clarify the connection between surface waters and groundwaters.

These uncertainties are important limitations to the geochemical understanding of the studied sites and some of them have been studied in Section 3.3. Differences found between the hydrogeological systems and the possible recharge waters in Forsmark and Laxemar support the decision of selecting two different Altered Meteoric end-members for the modelling tasks, though their selection will depend on the approach (direct or inverse modelling).

For ***M3 inverse calculations,*** sample #4919 can be selected as the most suitable for the Forsmark area and sample #10231 can be recommended for the Laxemar area. However, the performed sensitivity calculations indicate that the detailed composition (e.g. Ca concentrations) of the selected Altered Meteoric end-member in each zone seems to be of little importance in the M3 results. Different dilute end-members with variable composition provide similar results and, therefore, any of the initially considered Altered Meteoric end-members (Tables 2-6 and 2-7) could be used for M3 calculations.

However, the detailed chemical composition of the selected Altered Meteoric end-member is much more important ***in predictive (direct) calculations***, when transient periods – or local zones – without effective mixing processes must be considered. The performed sensitivity analysis of Ca concentrations indicates that the selection of a proper Altered Meteoric end-member is a critical issue in the dilution scenario predicted for the temperate period.

This selection may be affected by the uncertainties related to the spatial heterogeneities and temporal variability in the composition of present dilute groundwaters at the sites. This is especially true in the Forsmark area. The presence of limestones in the overburden of the Forsmark area promotes Ca concentrations in the recharge waters around 40 mg/L, higher than those observed in the Laxemar area. However, once the carbonates present in the overburden are exhausted, dilute groundwaters reaching the repository depth will probably have lower Ca concentrations. At Laxemar, without calcium carbonate (or with minor amounts) in the overburden, most of the present recharge waters have very low calcium concentrations.

2.1.5 Monte Carlo computation of mixing proportions with uncertain end members

Mixing calculations involve computing the proportions in which two or more end-members are mixed in a sample. Most methods available to compute mixing proportions assume that the composition of the end-members is fully known, which is rarely the case. Often waters representing some of the end-members cannot be sampled, or vary in space and/or time.

Here a method to compute at the same time the mixing proportions of each sample in a dataset and the composition (i.e. the concentration of several input compositional variables) of the end-member waters is presented. The method is based on a Monte Carlo sampling of the end-members' compositional space and the simultaneous calculation of the mixing proportions of *all samples* by a principal component analysis (PCA), trying to find the combination of mixing proportions and end-members' composition that together minimises the residuals with respect to several conservative elements.

The main conclusion to be drawn from this exercise is that most elemental concentrations emanating from the Monte Carlo approach are in full agreement with those derived from the traditional (geochemical) approach. Therefore, most of the groundwater compositions found in the Forsmark area can be justified by the existence of simple mixing processes, being the chemical reactions of minor importance. This conclusion is strongly supported by the results of both independent approaches to the problem, which build confidence on the robustness and feasibility of the general conceptual model proposed.

Methodology

To apply this methodology, a detailed hydrological and geochemical characterization of the groundwater system is needed first. In particular, the number of end-member waters must be known in advance, and also the compositional range of each end-member, although this range can certainly be broad (e.g. from 0 to 6,000 mg/L of chlorine in a "brackish" end-member water). So, the two key elements that the method needs to give meaningful results are: (1) the number of end-members must be known; and (2) the groundwater systems must be dominated by mixing; in other words, the chemical composition of a water sample must be controlled by the composition of the end-members and the mixing proportions, and reactions (mass sinks and sources for elements) must only change the composition of the mixed waters by small amounts. This second restriction is necessary because the method uses both conservative and non-conservative elements in order to increase the discrimination between end-members.

The complete procedure can be subdivided into the following steps:

(1) Select a groundwater dataset. The method works more efficiently when the number of samples is large, as one of the steps in the procedure is a Principal Components Analysis (PCA). In this case, 276 groundwater samples from the Forsmark site have been chosen.

(2) Select the input compositional variables. As already said, this set of variables can include conservative and non-conservative elements in order to maximise the resolution of the end-members. Usually, a combination of major cations and anions, and isotopes is used. Here, the following 9 compositional variables will be used: Na, K, Ca, Mg, HCO_3, Cl, SO_4, ^{2}H and ^{18}O. Ions are expressed in mg/L and isotopes in delta values (per mil deviation).

(3) Select the number of end-members. This is a critical step in the procedure. A wrong selection of the number of end-members would produce spurious results in most cases (M3, the geochemical code that is at the heart of this procedure, can "suggest" the best number of end-members to be chosen with a specific dataset; this is explained in detail in /Gómez et al. 2006/, Section 4.1, dedicated to the End-member Selection Module). It would be assumed here that the correct number of end-members has been already selected, either by expert judgement after a detailed study of the groundwater system, or by using the End-member Selection Module in the M3 code. For the groundwater system at Forsmark, four main end-members have been identified: a saline end-member (Deep Saline), a glacial end-member (Glacial), an fossil sea-water end-member (Littorina), and an altered meteoric water end-member (Altered Meteoric).

(4) Select the compositional range of each end-member. Besides the number of end-members, the site investigation programme should also give an initial guess at the compositional range of each end-member. For the Forsmark site these ranges are listed in Table 2-10. The names "Deep Saline", "Glacial", "Littorina" and "AM" should be understood as labels attached to the end-members in order to distinguish one from the others, and not as particular waters with a known chemical composition. The final composition of each end-member would be given by the procedure itself. As Table 2-10 clearly indicates, the ranges can be very broad (indicating a poorly constrained value from the site investigation programme) or very narrow if the *a priori* knowledge on a compositional variable of an end-member is extensive.

(5) Randomly choose, for each input compositional variable in each end-member, a concentration within the range. It is important to stress here that this selection is completely random and that no correlation between variables is included. A particular, randomly selected, composition of an end-member could be absurd from a geochemical point of view, as Table 2-11 shows (e.g. values of $\delta^{2}H$ and $\delta^{18}O$ do not follow the water dilution line; or very high Cl and very low Ca in the Deep Saline end-member). Actually, *most* randomly selected compositions would be geochemically absurd and the procedure itself would filter them out due to their inherently large residuals.

Table 2-10. Initial compositional range of the end-members.

	Na (mg/L)	K (mg/L)	Ca (mg/L)	Mg (mg/L)	HCO_3^- (mg/L)	Cl (mg/L)	SO_4^{2-} (mg/L)	δ^2H (‰)	$\delta^{18}O$ (‰)
Deep Saline	5,000	15	0.1	5	4	0.1	0.1	–200	–30
	10,000	100	40,000	70	30	10,0000	2,000	–0.1	–0.1
Glacial	0.17	0.4	0.18	0.1	0.12	0.5	0.5	–170	–25
	0.17	0.4	0.18	0.1	0.12	0.5	0.5	–93	–13
Littorina	1,960	95	93	234	90	3,760	325	–59.75	–7
	7,000	260	300	1,000	200	7,000	1,800	–37.2	–4
Altered Meteoric	0.1	0.1	0.1	0.1	0.1	0.1	0.1	–90	–12
	1,000	100	1,000	500	1,000	1,000	1,000	–50	–8

Table 2-11. One random realization of the composition of the end-members.

End-member	Na (mg/L)	K (mg/L)	Ca (mg/L)	Mg (mg/L)	HCO_3 $(mg/L)^-$	Cl (mg/L)	SO_4^{2-} (mg/L)	δ^2H (‰)	$\delta^{18}O$ (‰)
Deep Saline	3,075	94.2	6,825	32.96	16.5	81,896	475.6	–13.5	–22.35
Glacial	0.17	0.4	0.18	0.1	0.12	0.5	0.5	–142.8	–20.77
Littorina	3,235	172.4	279.8	534.6	93.0	5,659	640.7	–38	–5.72
Altered Meteoric	282	84.8	521.3	109.1	996.7	618.7	5.62	–84.2	–11.81

(6) Perform the PCA on the whole dataset and the randomly chosen end-members, and compute the mixing proportions of each sample. The code M3 is used for this purpose. Mixing proportions are computed using the information stored in all principal components. A detailed explanation of the computations can be found in /Gómez et al. 2006/, under the heading "Hyperspace mixing" in Section 3.2. After this step, a list, such as Table 2-12, is obtained, where each sample has either a set of mixing proportions or is blank. Blank samples can not be explained by pure mixing of the chosen end-members (i.e., they fall outside the mixing polyhedron, as sample #3 in the example of Table 2-12).

(7) Compute *d*, the difference between the real and the calculated concentration of each conservative element in each sample. Calculated concentrations are obtained from the mixing proportions. For example, the Cl concentration in sample *i* is:

$$Cl_{i,calc} = (\%Deep\ Saline_i \times Cl_{Deep\ Saline} + \%Glacial_i \times Cl_{Glacial} + \%Litt_i \times Cl_{Litt} + \%DGW_i \times Cl_{DGW.})/100$$

From there, it is straightforward to compute *d*:

$$d_{i,Cl} = Cl_{i,real} - Cl_{i,calc},$$

and the same for the rest of conservative elements (^2H, and ^{18}O in this case):

$$d_{i,2H} = {}^2H_{i,real} - {}^2H_{i,\ calc},$$

$$d_{i,18O} = {}^{18}O_{i,\ real} - {}^{18}O_{i,\ calc}.$$

Table 2-12. Mixing proportions of each sample in the dataset as computed by M3.

Sample	Deep Saline (%)	Glacial (%)	Littorina (%)	Altered Meteoric (%)
1	6.69	7.52	10.42	75.37
2	30.06	41.70	6.08	22.15
3	–	–	–	–
...				
276	1.35	4.56	55.20	38.89

(8) For the whole dataset, compute Δ_k, the total deviation of conservative element *k*. In other words, each sample's deviation d_i is squared and divided by the calculated concentration. The result for each sample is added together and then normalised by the number of samples inside the mixing polyhedron, n:

$$\Delta_{\mathrm{Cl}} = \frac{1}{n}\sum_{i=1}^{n}\frac{d_{i,\mathrm{Cl}}^2}{\mathrm{Cl}_{i,\mathrm{calc}}}$$

$$\Delta_{2\mathrm{H}} = \frac{1}{n}\sum_{i=1}^{n}\frac{d_{i,2\mathrm{H}}^2}{{}^{2}\mathrm{H}_{i,\mathrm{calc}}}$$

$$\Delta_{18\mathrm{O}} = \frac{1}{n}\sum_{i=1}^{n}\frac{d_{i,18\mathrm{O}}^2}{{}^{18}\mathrm{O}_{i,\mathrm{calc}}}$$

This is a chi-square statistics for a variable (the concentration of a conservative element) whose variance is proportional to its mean value (i.e., the assumption is made that concentrations are known with a fixed percent precision). As an example, if the Cl concentration of a sample is 6,000 mg/L, it is assumed that this value is known with an uncertainty of $\sqrt{6000} = 77$ mg/L; and if the Cl concentration is 20 mg/L, its associated uncertainty is $\sqrt{20} = 4.5$ mg/L. This is of course not the *analytical accuracy*, but the sum of all uncertainties, including conceptual ones as the non-constant end-member composition, or the uncertainty in the computed mixing proportions /Carrera et al. 2004/.

The number of samples inside the mixing polyhedron, n, is also computed by M3 and output as a *coverage* (percentage of samples inside the mixing polyhedron: see /Gómez et al. 2006/ Section 4.1).

(9) Repeat steps 5 to 8 a large number of times (usually several millions). Each run is composed of four numbers: three Δs and a coverage, as Table 2-13 shows. Coverage is not only important to compute Δ_k, but also to assess the quality of a particular composition of the end-members: if the coverage is low, that means that few samples can be explained as a mixture of the chosen end-members, irrespective of the value of the total deviations (think, for example, of a run that only explains 1% of the samples but these have low deviations: Δ_k would be low, but the chosen composition of the end-members would not be good at explaining the dataset as a whole). For example, run#2 in Table 2-13 has low values of the three total deviations but the coverage is very low: this run will be discarded because of the low coverage, irrespective of the total deviations.

(10) Discard all runs with a coverage below a critical value. This value is system-dependent, but should always be close to the maximum coverage. In our case, only runs with a coverage of 100% (all 276 sample) have been kept, as the number of runs with this coverage was significantly higher than with 275 samples, or 274, and so on, as Figure 2-12 clearly shows.

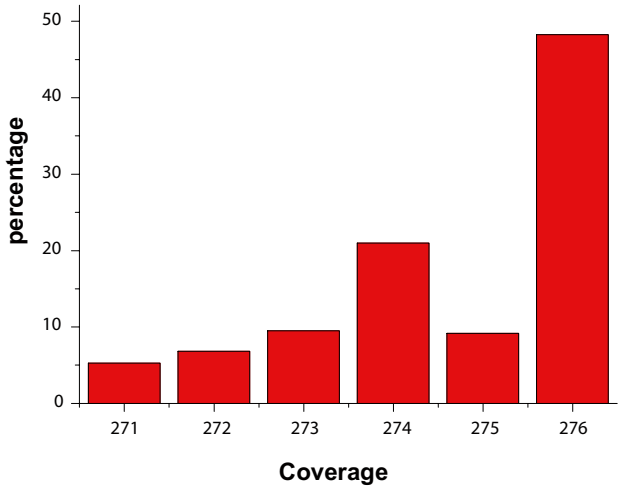

Figure 2-12. *Percentage of runs with the number of samples inside the mixing polyhedron in the range 271–276 (i.e. coverage from a 98% to a 100% of samples). Only runs with all samples inside the mixing polyhedron have been kept.*

Table 2-13. Example of output for every Monte Carlo run: three ∆s and a coverage.

Run #	Δ_{Cl}	$\Delta_{\delta^2 H}$	$\Delta_{\delta^{18} O}$	Coverage
1	663.3	0.527	1.144	84%
2	216.4	0.513	0.497	6%
3	2,424.9	0.805	1.356	78%
...	...	...	...	...
5,000,000	153.0	0.403	0.848	94%

(11) For each remaining run, compute *R*, the weighted normalised log-deviation with respect to all conservative elements:

$$R = \Delta^*_{\mathrm{Cl}} + \frac{1}{2}\Delta^*_{\mathrm{2H}} + \frac{1}{2}\Delta^*_{\mathrm{18O}}$$

where

$$\Delta^*_i = \frac{\log \Delta_i - \overline{\log \Delta_i}}{\sigma_{\log \Delta_i}},\ i = \mathrm{Cl},\ ^2\mathrm{H},\ \text{or}\ ^{18}\mathrm{O}$$

A log transformation of the variable has been used to make the distribution of deviations more Gaussian. Figure 2-13 plots on the left the histogram of Cl deviations and the histogram of the log-transformed variable on the right. It is easy to see that the log-transformed variable has a more symmetric distribution than the original variable.

After log-transformation, the variable is normalized by subtracting the mean $\overline{\log \Delta_i}$ and dividing by the standard deviation $\sigma_{\log \Delta_i}$. This step is necessary because Cl and the isotopes are measured in different units (mg/L for Cl and delta-values for the isotopes). Figure 2-14 shows on the left the log-transformed variables and on the right the final histograms for the three normalised log-transformed variables (Cl, ^{2}H, and ^{18}O).

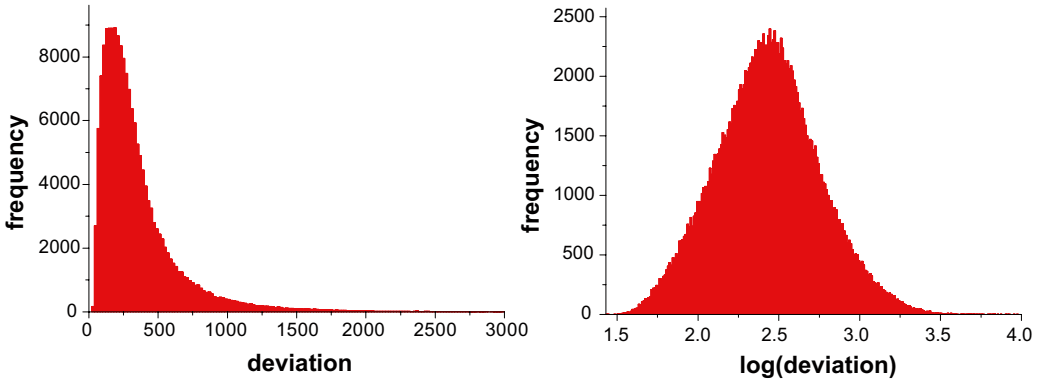

Figure 2-13. *Result of the log-transformation of the deviation. The log-transformed variable (right panel) has a more symmetric (gaussian) distribution.*

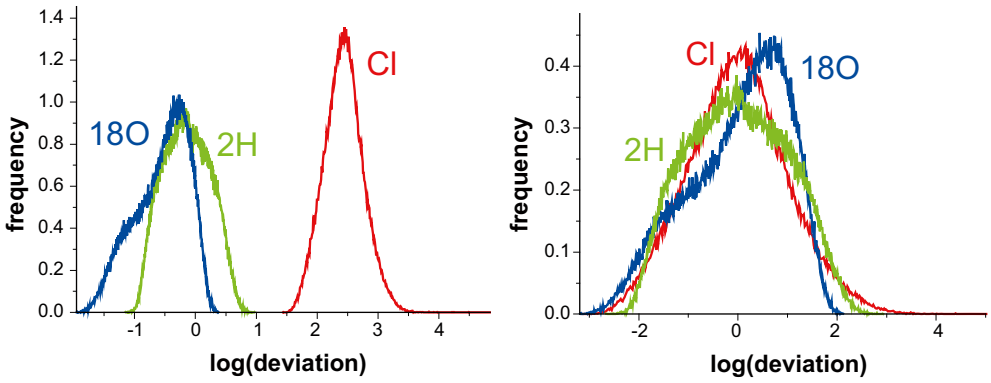

Figure 2-14. *Histogram of the log-transformed variables before (left) and after (right) normalisation.*

The weights 1, 1/2 and 1/2 that appear in the expression for *R* above are intended to give the same importance to chlorine and to the isotopes in the computation of the residual. These weights also acknowledge the strong correlation that exists between deuterium and oxygen-18 in most non-saline water samples. Because the correlation is so good, not much information is gained by using ^{18}O after having used ^{2}H.

(12) Sort the remaining runs in ascending order of *R* and keep the best 100. Figure 2-15 shows graphically how this is done for the case of chlorine in the Deep Saline end-member. The left panel is a plot of the Cl log-deviation for the 5 million Monte Carlo runs. Each dot is a different run and is colour-coded according to its coverage (dark blue means 100% coverage, the only runs that have been kept). The vertical red line separates the best 100 runs, where "best" means with the lowest residual. The right panel is a histogram of these best 100 runs binned with respect to the concentration of Cl. The maximum is around 50,000 mg/L of chlorine, meaning that this is the most probable concentration of Cl in the Deep Saline end-member. The blue arrow in the histogram points to the Cl content of the water that have been traditionally used as Deep Saline end-member in Forsmark.

Results

This section presents the results of the above procedure for all the elements in the form of histograms binning the 100 best runs. These histograms have been constructed in exactly the same manner as the right panel of Figure 2-15. Each histogram has either one blue arrow pointing to a particular concentration value or two arrows spanning a range of concentrations. These are the values that characterise the composition of the proposed end-members (Deep Saline, Glacial, Littorina and Altered Meteoric) as explained in Sections 2-1 to 2-4 above.

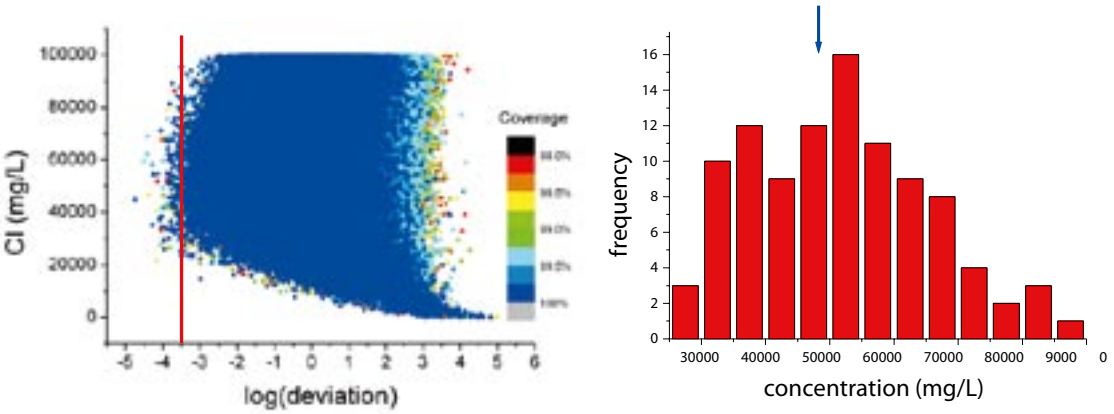

Figure 2-15. *Left: Cl content as a function of the total residual [log(deviation)]of each of 5×10^6 Monte Carlo runs. The lower the residual, the better at explaining the Forsmark dataset is the corresponding set of end-members. Right: histogram of the best 100 runs (to the left of the red line in the left panel). Chlorine concentrations of around 50,000 mg/L are most probable. The blue arrow points to the Cl content of the Deep Saline end-member traditionally used in Forsmark.*

The following 4 figures (Figures 2-16 to 2-19) summarise the results of the above procedure to compute the composition of the end-member waters that have been produced by mixing all the present groundwater analyses in the Forsmark groundwater system. The blue arrow in each histograms points to the concentration of the given element in the end-member traditionally used to compute the mixing proportions in Forsmark. These traditional end-members, as explained in the previous sections, can be real waters, extrapolations from real waters, or theoretical waters constructed by applying several geochemical constraints and assumptions. The present approach can, then be considered as an independent assessment of the feasible composition of each end-member, to be compared with the composition derived form the traditional approach.

The main conclusion to be drawn from this exercise is that most elemental concentrations emanating from the Monte Carlo approach are in full agreement with those derived from the traditional approach, as the coincidence between the position of the blue arrow and the maximum in the histogram suggests. There are, however, some discrepancies which will be discussed below.

Several elements are not very well constrained by the method. This means that almost any concentration inside the used range is compatible with a low residual. In other word, the use of any value inside the range will give the same mixing proportions and the residuals will be low. What follows is a summary of the main conclusions, end member by end-member.

Deep Saline end-member (Figure 2-16). Magnesium and bicarbonate are not constrained by the method and any value inside the range (Table 2-10) give similar residuals. Sodium is also poorly constrained, although it seems that values below 8,000 mg/L are less probable. As for calcium, it is only constrained in its lower end, with values below 15,000 mg/L being very improbable. Most probable values for K are around 40–50 mg/L, exactly matching the value used in the proposed end-member.

Chlorine is around 50,000 mg/L, very close to the 47,000 mg/L selected for the Deep Saline end-member; and sulphate must be above 200 mg/L and below 800 mg/L, possibly eliminating the low-sulphate end-member suggested above. Finally, the isotopes are well constrained and in good agreement with the values used in the proposed end-member.

Glacial end-member (Figure 2-17). Only the isotopes are of concern here, due to the very low contents of all other major ions. The most probable value for deuterium is between –110 and –115, and the most probable value for ^{18}O is around –15. Considering that no correlation among variables was included during the Monte Carlo calculations, the selection by the method of a pair of δ^2H and $\delta^{18}O$ values that lay on the GWDL is another proof of the suitability of the method. The problem is that these most probable values are in disagreement with those used in the Glacial end-member ($\delta^2H = -160‰$ and $\delta^{18}O = -21‰$).

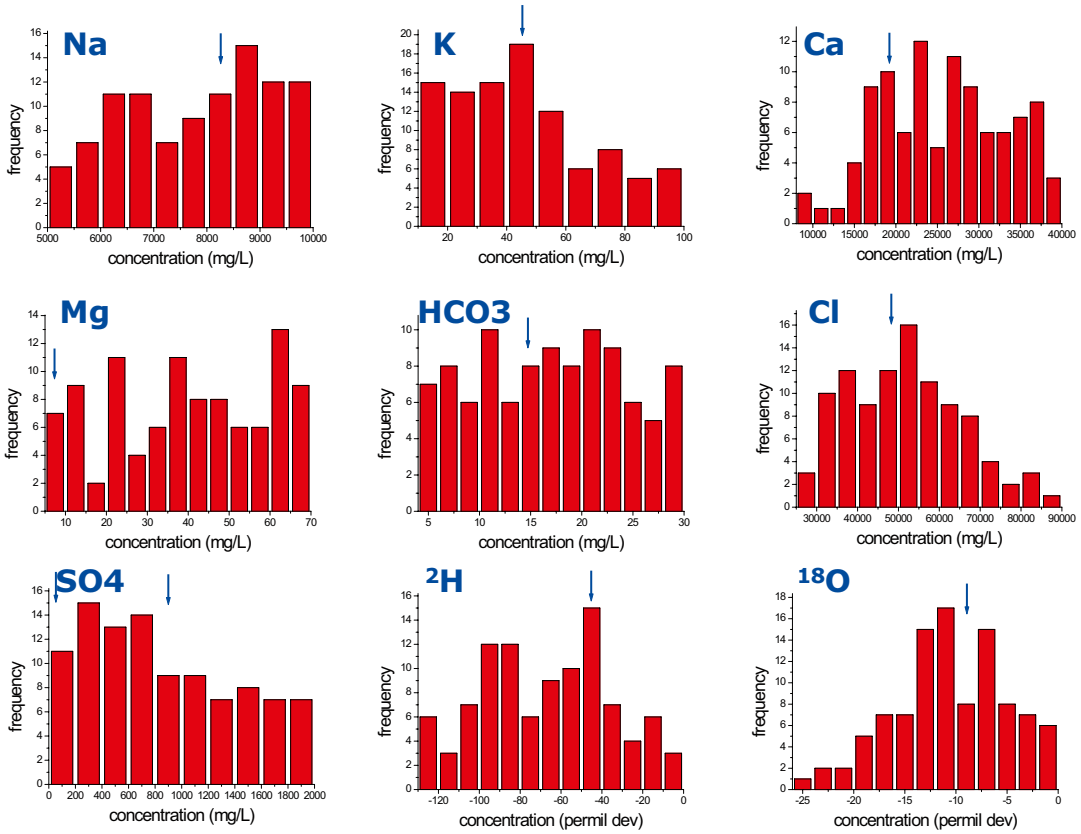

Figure 2-16. *Composition of the Deep Saline end-member. The blue arrow in each histogram points to the concentration of the given element in the end-member traditionally used to compute the mixing proportions in Forsmark.*

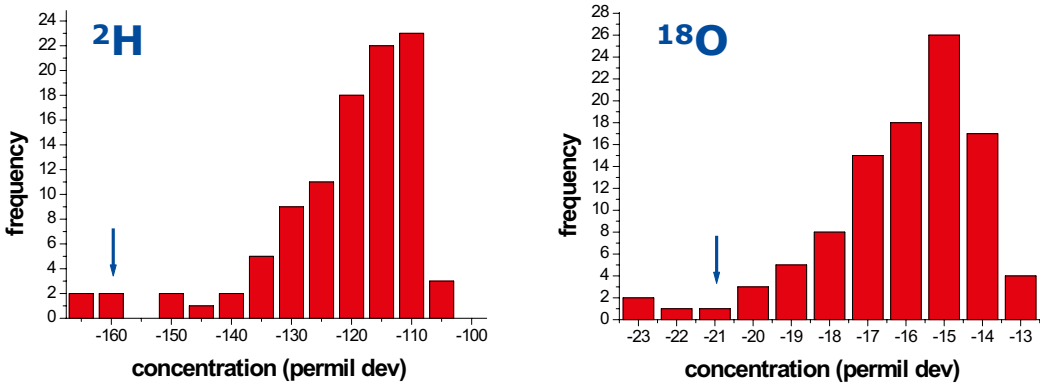

Figure 2-17. *Composition of the Glacial end-member. The blue arrow in each histogram points to the concentration of the given element in the end-member traditionally used to compute the mixing proportions in Forsmark.*

The discrepancy could be related to the "mixed" nature of the glacial end-member, being $^{18}O = -16‰$ already a mixture of a real glacial melt-water with a $\delta^{18}O$ of −21‰ and an old meteoric water with a $\delta^{18}O$ of −11‰. A 50–50% mixture of these two waters could give rise to the "glacial" water with a $\delta^{18}O$ of −16‰. This explanation is compatible with the paleohydrological history of the Forsmark site.

Littorina end-member (Figure 2-18). The values for Cl, SO_4 and ^2H are not constrained by the method.

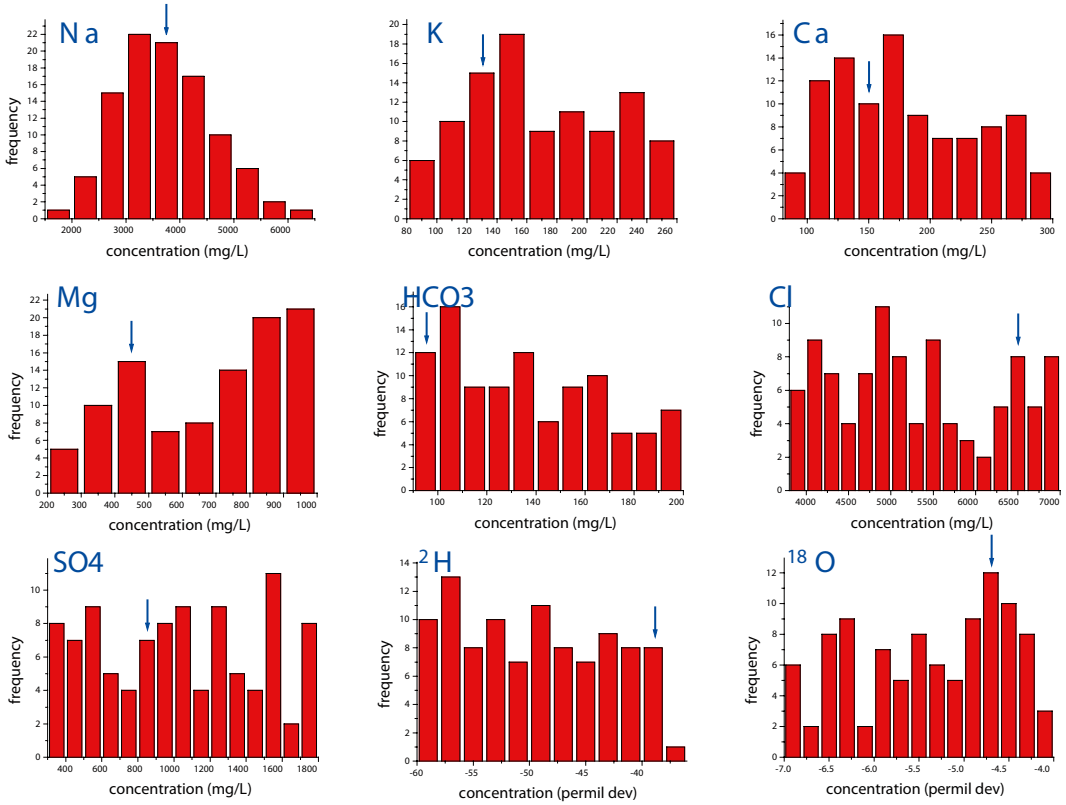

Figure 2-18. *Composition of the Littorina end-member. The blue arrow in each histogram points to the concentration of the given element in the end-member traditionally used to compute the mixing proportions in Forsmark.*

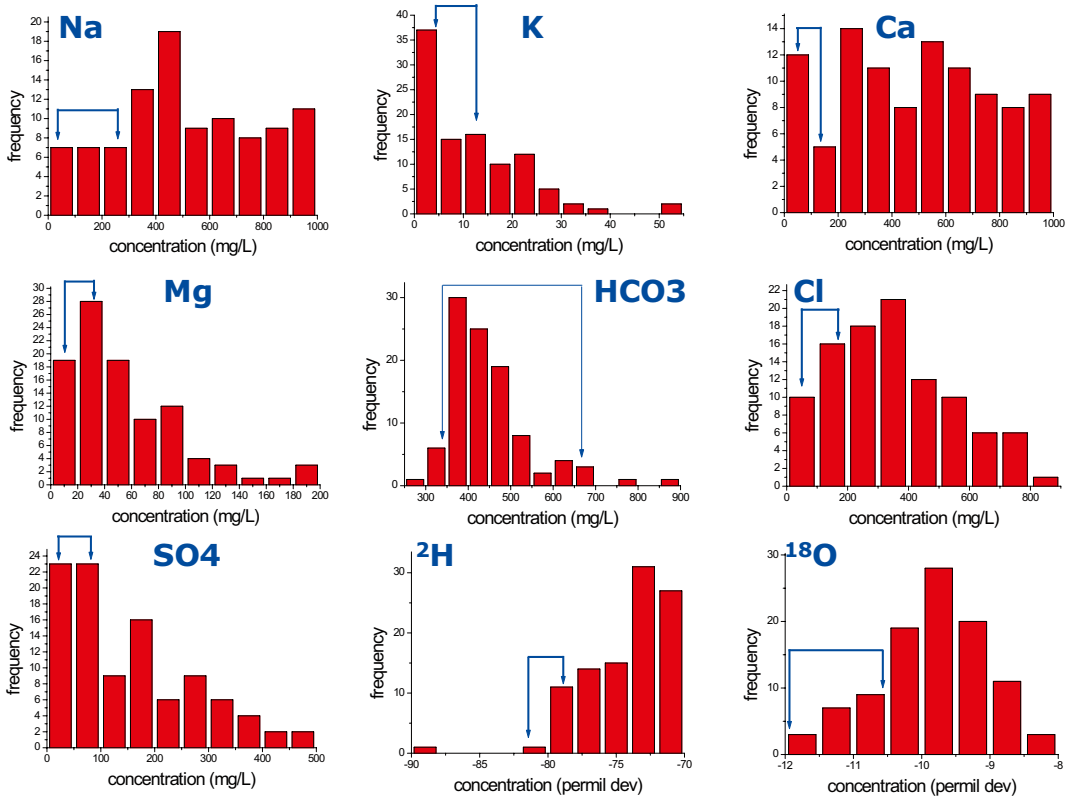

Figure 2-19. *Composition of the Altered Meteoric end-member. The blue arrow in each histogram points to the concentration of the given element in the end-member traditionally used to compute the mixing proportions in Forsmark*

Magnesium seems to have two sets of possible values: one around 450 mg/L (coincident with the value used in the proposed end-member) and another between 800–1,000 mg/L. Potassium must be below 160 mg/L and above 120 mg/L; calcium must be between 100 and 175 mg/L; bicarbonate is quite scattered, but the most probable value seems to be below 150 mg/L. Sodium is very well constrained, with a most probable value between 3,000 and 4,000 mg/L.

Finally, the isotope ^{18}O has a maximum at –4.75, just where the value used in the proposed end-member lies. In summary, either the most probable value coincides with the proposed value, or the element is not constrained by the method.

Altered Meteoric end-member (Figure 2-19). The only element not constrained by the method is calcium. Sodium must be between 300 and 500 mg/L, slightly above the value used in the proposed end-member. Potassium must be below 5 mg/L, value which is slightly below the one used in the proposed end-member. Magnesium is between 20 and 30 mg/L (the proposed value depends on the chosen real sample, with a range of 7.5–32 mg/L). Bicarbonate is very well constrained by the method, with a range of possible values from 350 to 500 mg/L; the lower limit coincides with the lower limit of the proposed end-member, and the upper limit is more stringent than the proposed one (which is 665 mg/L).

Chlorine is also well constrained inside the range 100–400 mg/L, with the upper limit more probable than the lower one. Proposed Cl values are inside the range 51–181 mg/L, lower but compatible with the other range. Sulphate perfectly matches the proposed range of 22–85 mg/L.

The isotopic values are well constrained by the method, with values of −70 to −75‰ for ^{2}H, and −9.25 to −10.25‰ for ^{18}O. In both cases the most probable values are less negative than the proposed ones (around −80‰ for ^{2}H and between −10.5 and −12.2 for ^{18}O). This is the most serious discrepancy between both methods, although the less negative values compatible with the proposed end-member ($\delta^{2}H = -78‰$ and $\delta^{18}O = -10.5‰$) are not far from the most negative ones as suggested by the Monte Carlo method ($\delta^{2}H = -74‰$ and $\delta^{18}O = -10.25‰$).

Discussion and conclusions

The Monte Carlo method introduced here gives an independent assessment of the chemical composition of the end-members Deep Saline, Glacial, Littorina, and Altered Meteoric. The comparison of these results with the ones obtained by more traditional approaches (as summarised in Sections 2.1.1 to 2.1.4 in this report) serves to build confidence and reduce the uncertainty in their compositional characteristics, and at the same time place rather strict lower and upper limits for some of the elements. The value suggested by the Monte Carlo method is in most cases inside the range for the proposed end-members. All the elements constrained by the method in the Deep Saline end-member are inside the range of the composition of the proposed end-member. The same conclusion applies to the Littorina end-member, although in this case more elements are not constrained by the Monte Carlo method. The only noteworthy discrepancies are thus the following:

1. For the Glacial end-member, the isotopes have less negative values in the Monte Carlo method. As explained, this could mean that the “glacial” end-member is not a pure end-member but a mixture of a pure glacial melt-water and an old meteoric water. This is supported by the paleohydrological history of the Forsmark site. The most probable value of −16‰ for ^{18}O could then be a roughly 50–50% mixture of a glacial melt-water and an old meteoric water.
2. For the Altered Meteoric end-member, all the elements except calcium are well constrained by the Monte Carlo method and most of them are compatible with the proposed composition of the Altered Meteoric end-member. Chlorine seems to be higher than the value presently used (<181 mg/L) and the isotopes are again less negative than presently used, although the discrepancy is not large in any of the cases.

2.1.6 General conclusions and summary

The chemical characteristics of the groundwaters in the Forsmark and Laxemar areas are the result of a complex mixing process driven by the input of different recharge waters since the last glaciation. The successive penetration at different depths of dilute glacial melt-waters, Littorina Sea waters and dilute meteoric waters has triggered complex density and hydraulically driven flows that have mixed them with long residence time, highly saline waters present in the fractures and in the rock matrix, see /Smellie et al. 2008/.

Mixing can be considered the prime irreversible process responsible for the chemical evolution of the Forsmark and Laxemar groundwater systems. Therefore, the successive disequilibrium states resulting from mixing conditioned the subsequent water-rock interaction processes and, hence, the re-equilibration pathways of the mixed groundwaters.

The geochemical study of the Forsmark and Laxemar groundwaters, using either simple conservative elements or more refined isotopic techniques has confirmed the existence of at least four end member waters: an old deep saline water, an old glacial melt-water, a marine water (ancient Littorina Sea), and a modern meteoric water.

The quantitative assessment of mixing and reaction in these groundwaters can be approached by mixing and mass balance calculations with standard geochemical codes (NETPATH or PHREEQC) or with PCA-based codes like M3. A correct selection of the composition of the end-member waters is critical in both cases. The uncertainties associated with this selection procedure and with the effects of chemical reactions have already been discussed elsewhere /Luukkonen 2001, Bath and Jackson 2002, Laaksoharju et al. 2004, Gómez et al. 2006/.

Here, other sources of uncertainty related to the chemical and physicochemical characteristics of each end-member and their possible spatial and/or temporal chemical variability have been dealt with.

Some of these end members (Deep Saline and Altered Meteoric) correspond to real groundwaters sampled in the studied sites, whereas others (Littorina or Glacial) are old waters with compositional characteristics estimated or deduced from diverse geological information. Therefore, the associated uncertainties and their weights can be (and will be) very different, depending on the considered end-member.

Uncertainties can also have different importance depending on the modelling approach (direct or inverse). Here the uncertainty hasl been mainly assessed with respect to the needs in the ***M3 inverse approach*** as the standard tool used in mixing proportion calculations in both sites. However, some other uncertainties more related to the predictive (direct approach) calculations have also been analysed.

Finally, a Monte Carlo method has been developed to obtain an independent assessment of the chemical composition of the end-members Deep Saline, Glacial, Littorina, and Altered Meteoric. The method computes at the same time the mixing proportions of each sample in a dataset and the composition (i.e. the concentration of several input compositional variables) of the end-member waters. It is based on a Monte Carlo sampling of the end-members' compositional space and the simultaneous calculation of the mixing proportions of *all samples* by a Principal Component Analysis (PCA), trying to find the combination of mixing proportions and end-members' composition that together minimises the residuals with respect to several conservative elements.

The main conclusion to be drawn from this exercise is that most elemental concentrations emanating from the Monte Carlo approach are in full agreement with those derived from the traditional (geochemical) approach. This serves to build confidence and reduce the uncertainty in their compositional characteristics and, at the same time, places rather strict lower and upper limits for some of the elements. The values suggested by the Monte Carlo method are in most cases inside the range of the proposed end-members. In the cases where discrepancies have been found, the values suggested by the Monte Carlo analysis come to support other independent lines of evidence that already point to these values as problematic. This is specially true for the isotopes in the Glacial end-member and the chloride content in the Altered Meteoric end-member.

Deep Saline end-member

The groundwater sample used as the Deep Saline end-member in the Swedish site characterization program corresponds to a 1,623 m depth sample from borehole KLX02 (Laxemar) which has the maximum salinity found in the area to date. Some of the compositional parameters not analysed in this sample (pH, Eh, Fe^{2+} and sulphide concentrations) have been taken from a different sample, only slightly less saline, from the same borehole and at a similar depth (1,531 m depth, sample #2731).

The absence of a proper deep saline sample in the Forsmark area to be used as an end-member constitutes one of the main uncertainties associated with this end-member and it casts a reasonable doubt on the real composition of the saline waters in the Forsmark area. The review presented here, the simulations performed in SR-Can for Forsmark /Auqué et al. 2006/ and the Monte Carlo results, all suggest the presence of a Deep Saline end-member with a chemical and isotopic composition similar to the one defined and used in Laxemar.

However, all the studies reported here indicate that the composition of the Deep Saline end-member defined for Forsmark should have a lower sulphate concentration than the end-member used in Laxemar. The precise sulphate concentration is not well constrained by any of the methods, therefore, a new saline end-member with a very low sulphate concentration (10 mg/L) has been defined to be used in Forsmark (Deep Saline-Forsmark; Table 2-14).

The two end-members could be used for the sensitivity analysis of the computed mixing proportions in Forsmark. The sample KR4/860/1 (Table 3.1.1) from Olkiluoto, Finland, is also suggested to be used as an alternative Deep Saline end-member in these sensitivity analyses as it introduces a higher variability in the concentration of Na, K, Ca, Mg, Cl, δ^2H and $\delta^{18}O$.

Glacial end-member

The Glacial end-member represents the chemical composition of a melt-water from a previous glaciation (>11000 BC). The composition adopted in the site investigation programme corresponds to present melt-waters from one of the largest glaciers in Europe, the Josterdalsbreen in Norway, situated on a crystalline granitic bedrock /Laaksoharju and Wallin 1997/. The major element composition of these waters is similar to that estimated by /Pitkänen et al. 1999, 2004/ in a model study of Olkiluoto (Finland).

Table 2-14. Final composition of the end-members selected for the mixing calculations in the Forsmark area. All the concentrations are in mg/L.

	Deep Saline		Littorina	Glacial	Glacial + Old meteoric	Altered meteoric	
	Laxemar	Forsmark				Forsmark #4919	Laxemar #10231
pH	8	8	7.6			7.91	7.30
Alkalinity	14.1	14.1	92.5	0.12	0.12	466.0	347.0
Cl	47,200	47,200	6,500	0.5	0.5	181	5.4
SO_4^{2-}	906.0	10	890	0.5	0.5	85.1	6.92
Br	323.66*	323.66*	22.2			0.572	5.2
Ca	19,300	19,300	151	0.18	0.18	1.6	–
Mg	2.12	2.12	448	0.1	0.1	41.1	45.4
Na	8,500	8,500	3,674	0.17	0.17	7.5	8.7
K	45.5	45.5	134	0.4	0.4	274.0	50.5
Si	2.9	2.9	3.94	–	–	5.60	3.83
Fe^{2+}	–	–	0.002 (Fe tot)			0.38	0.353
S^{2-}	–	–	–			6.68	8.03
δ^2H (‰)	–44.9	–44.9	–37.8	–158.0	–118	–80.6	–74.4
$\delta^{18}O$ (‰)	–8.9	–8.9	–4.7	–21.0	–16.0	–11.1	–9.7

Glacial melt-waters have a very low content of dissolved solids, even lower than present-day meteoric waters, and a very light isotopic signature, and they represent the chemical composition of surface melt-waters prior to water-rock interaction during infiltration in the basement.

In the Forsmark and Laxemar areas the composition of the groundwaters with a glacial component are characterized by a relatively low salinity and an isotopically light signature (although not as light as the original Glacial end-member) but they have been extensively modified by mixing with waters of other origins. Therefore, there are no "undisturbed" glacial melt-water remnants that can be considered as a pure glacial mixing component modified only by water-rock interaction processes. However, the final salt contents are still very low which means that, as expected, water-rock interaction modify the compositional characteristics to a limited degree. Similar conclusions have been obtained when analysing other old meteoric or glacial waters in crystalline basements.

With respect to the isotopic values for this end-member, the study presented here based on the hydrochemical variability of the systems and on the Monte Carlo results, suggests the possibility of considering two different isotopic signatures for this Glacial end-member (Table 2-14):
(a) the one used up to now in the site characterisation studies ($\delta^{18}O$= −21‰ and $\delta^{2}H$= −158‰) and (b) a heavier isotopic signature ($\delta^{18}O$= −16‰ and $\delta^{2}H$= −118‰). With these two end-members part of the wide range of $\delta^{18}O$ values proposed by /Kankainen 1986/ for the glacial melt-waters is covered during uncertainty analysis.

The alternative "glacial" end-member with $\delta^{18}O$= −16‰ is not a pure end-member but a 50:50 mixture of a pure glacial melt-water with and an old meteoric water. This mixture corresponds to the groundwaters with the coldest isotopic composition found in the studied systems.

Littorina end-member

The chemical composition of seawater during the Littorina stage has been selected as one of the end-members used in the hydrogeological and hydrogeochemical modelling of the Laxemar and Forsmark sites, as well as in other Fennoscandian sites with a similar palaeogeographic evolution (for example, Olkiluoto in Finland; /Pitkänen et al. 1999, 2004/.

The Littorina stage in the postglacial evolution of the Baltic Sea started when the passage to the Atlantic Ocean opened through Öresund (in the southern part of the Baltic Sea) and seawater started to intrude at ≈ 6500 BC. The salinity increased until 4500–4000 BC, reaching estimated maximum values twice as high as modern Baltic Sea and this maximum prevailed at least from 4000 to 3000 BC. This period was followed by a stage where substantial dilution took place. During the last 2,000 years the salinity has remained almost constant to the present Baltic Sea values.

Based on shore displacement curves it is clear that the Forsmark area has been covered by the Littorina Sea for a long period of time (around 8,000 years). The Littorina Sea composition used in this work is shown in Table 2-14. It is based on the maximum salinity estimation of 12‰ or 6,500 mg/L Cl /Kankainen 1986/. The other main element concentrations were obtained by diluting the global mean ocean water /Pitkänen et al. 1999, 2004/. Stable isotope composition assigned to the Littorina end member comes also from the $\delta^{18}O$ value (−4.7‰) proposed by /Kankainen 1986/ and from the $\delta^{2}H$ value considered by /Pitkänen et al. 1999, 2004/ for this end-member (−37.8‰).

Even though the use of an end-member representative of the maximum salinity stage is a simplification, it is reasonable since these waters would have the maximum capacity to penetrate the bedrock. Moreover, the contents of chloride, $\delta^{18}O$ and even sulphate (whose behaviour is quasi-conservative), deduced from present groundwaters with high Littorina proportions in different sites are in reasonable agreement with the values proposed for the Littorina end member.

The composition obtained using the above mentioned methodology corresponds to an old marine water prior to its infiltration into the groundwater system. Obviously, this compositional estimation presents uncertainties associated with the salinity (chloride contents), stable isotopes ($\delta^{18}O$), and the compositional changes undergone by the marine water due to its reaction with the bottom sediments prior to its infiltration in the bedrock. However, the compositional variations produced during infiltration of Littorina waters through the marine sediments or during the subsequent diagenetic processes do not seem to be important for the most diagnostic elements for this end-member (SO_4^{2-} and Mg).

All the data above seem to indicate that the Littorina end-member composition has been properly defined for the studied sites although different uncertainties still hold, mainly related to the salinity variation with time. These uncertainties have also arisen from the Monte Carlo analysis. Therefore, an alternative "Littorina end-member" is proposed to perform sensitivity analysis in hydrological or hydrochemical mixing calculations: the present composition of Baltic seawaters. Since the salinity and compositional characteristics of present Baltic waters are not homogeneous, the alternative end member proposed is the "average" Baltic seawater obtained by /Pitkänen et al. 1999, 2004/.

Altered Meteoric end-member

In previous modelling works with M3 a rain water sample called "Rain 60" or "Precipitation" has been used as the meteoric end-member /e.g. Laaksoharju and Wallin 1997, SKB 2004abc, 2006a, Puigdomenech 2001/. This water corresponds to a modern meteoric water with a modelled high tritium content that represents the rain water from 1960 /Laaksoharju and Wallin 1997/. This end-member, with an extremely dilute character, presents the typical composition of rain water just before its interaction with the overburden. Therefore, it is not representative of the real recharge water after interaction with the shallower parts of the system.

To minimize this discrepancy, the ChemNet group has selected different samples representative of shallow groundwaters (less than 100 m depth) of recent meteoric origin after a short interaction with soils, overburden and granite in the studied areas. This is what has been finally called the "Altfered Meteoric" (or sometimes "Dilute Granitic Groundwater") end-member.

The differences found between the hydrogeological systems and the possible recharge waters in Forsmark and Laxemar support the decision of using two different Altered Meteoric end-members for the modelling tasks (Table 2-14).

For ***M3 inverse calculations,*** the performed sensitivity calculations indicate that the detailed composition of the selected Altered Meteoric end-member in each zone seems to be of little importance. Different dilute end-members with variable composition provide similar results and, therefore, any of the initially considered Altered Meteoric end-members could be used for M3 calculations. This can be attributed to the fact that the main effect of the Glacial and Altered Meteoric end-members in mixing is promoting dilution, independently of their detailed composition.

However, the detailed chemical composition of the selected Altered Meteoric end-member is much more important ***in predictive (direct) calculations***, when transient periods – or local zones – without effective mixing are considered. The sensitivity analysis performed over calcium concentrations indicates that the selection of a proper Altered Meteoric end-member is a critical issue in the dilution scenario predicted for the temperate period.

The results from the Monte Carlo method indicate that all the elements except calcium are well constrained and most of them are compatible with the proposed composition of the Altered Meteoric end-member. Chlorine seems to be higher than the value presently used (<181 mg/L) and the isotopes are again less negative than presently used, although the discrepancy is not large in any of the cases.

2.2 Pre-Littorina groundwaters

Different calculations performed by the UZ group by request of the SKB hydrogeologists are presented here. They needed the chemical composition of groundwaters in Forsmark just before the input of Littorina waters. The reconstruction of that scenario is developed here.

Moreover, this calculation is directly related to the work presented by the UZ group in Appendix 3 of the ChemNet report for Forsmark 2.1 /SKB 2007/, where the special situation of a set of samples characterised by an important Littorina contribution and a more or less constant chloride content (with variable amounts of the rest of the chemical components) was analysed. From this analysis (a summary of which is presented below), it was found that those waters seem to have had a very constant Deep Saline to Glacial ratio just before different amounts of Littorina waters mixed with them. Therefore, the calculations presented in this section could be useful for any modelling on the state of the system previous to Littorina.

The request of the hydrogeologists was:

- A plot (or several plots) showing the mixing proportions calculated with M3 for the selected samples. This has been done using different kinds of plots, which are presented in Subsection 2.2.1.
- The concentration of some of the main components (including stable isotopes), for the selected samples, just before the input of Littorina in the system (Subsection 2.2.2). The starting point were the mixing proportions calculated for the samples at present. Two different options were suggested:
  - To eliminate the Littorina and Altered Meteoric mixing proportions from the present values and then re-calculate the Glacial and Deep Saline proportions as a 100% assuming that they were the only waters existing in the system before the Littorina stage. Once these mixing proportions are calculated, the corresponding chemical composition is readily obtained for each sample.
  - To consider not only Glacial and Deep Saline when Littorina entered the system, but also some "old" meteoric water. This option consists in considering a different isotopic composition for the Glacial end member. A heavier isotopic composition could be interpreted as a mixture of "old meteoric waters" including under this term, not only the glacial waters but also all the previous meteoric or glacial inputs to the system before the last glaciation.

A complementary set of calculations were also performed in the light of the previous results in order to assess the feasibility of Littorina Sea waters penetration into the bedrock considering the salinity and density of the pre-Littorina groundwaters. These results can be found in Subsection 2.2.3.

2.2.1 Mixing proportions at present

Based on the conclusions from Section 2.1 on the composition of the end-members, two different Glacial compositions have been used for any mixing calculation: one representing a pure glacial melt-water and called "Glacial" (the one used up to now with the lightest isotopic signature; see Table 2-14) and the other with a heavier isotopic signature representing the previous mixture with old meteoric waters, called "Old meteoric-Glacial".

This section summarises the results of mixing calculations considering these two possible glacial end-members. M3 calculations were performed using Forsmark 2.2 groundwater dataset, the common set of variables (Na, K, Ca, Mg, HCO_3^-, Cl, SO_4^{2-}, Br, δ^2H and $\delta^{18}O$) and the four end members Deep Saline (low in sulphate), Glacial, Littorina, and Altered Meteoric (sample HFM09). The same calculations were carried out by changing the isotopic compositions of the Glacial end-member (from $\delta^{18}O = -21‰$ to $\delta^{18}O = -16‰$), that is using what has been called "Old meteoric-Glacial". The composition of the end members is shown in Table 2-14. The results are shown in Subsection "Mixing proportions".

The calculated and measured concentrations for the conservative elements Cl and the stable isotopes, and some other elements of interest (SO_4^{2-} and Mg) are compared in the subsection "Comparison of the calculated and measured contents". The degree of agreement between them will give an idea of the confidence in the reconstruction of the water composition. Poor reproduction of the actual values would invalidate any other calculation based on these mixing proportions.

Mixing proportions

Results obtained by using the two different Glacial end-members are shown in Figures 2-20 and 2-21. As stated above, both sets include Deep Saline (low sulphate), Littorina and Altered Meteoric, but one of the sets uses the original Glacial end-member with the lighter isotopic signature and the other one uses the "Old meteoric-Glacial" end-member with the heavier isotopic signature.

The first interesting outcome from the comparison of the the two models is that by changing the isotopes in the Glacial end-member, the mixing proportion of this end-member increases significantly, and only at the expense of the Altered Meteoric end-member (see Figure 2-20 and upper panels of Figure 2-21). The other two mixing proportions remain almost constant (Figure 2-20 and lower panels of Figure 2-21). The numeric results are included in Table B-1 (Appendix B).

Figure 2-21 shows, as a function of depth, the proportion of each end-member as a result of using the first or the second set of end-members (Glacial with circles and Old meteoric-Glacial with squares). These figures clearly show that the differences only affect the two dilute end member's proportion (Altered Meteoric and Glacial), while the Deep Saline and Littorina end-members remain almost identical irrespective of the isotopic values used for the Glacial end-member.

In the case in which a pure Glacial end-member ($\delta^{18}O = –21‰$) is used, all the meteoric contributions (from old and recent meteoric waters) are included in the Altered Meteoric end-member. On the contrary, if an Old meteoric-Glacial end-member, representing a mixture of true glacial meltwaters ($\delta^{18}O = -21‰$) and old meteoric waters ($\delta^{18}O = -10‰$ or $-11‰$) is used, the Altered Meteoric end-member represents only the contribution of recent meteoric waters. Therefore, subtracting one simulation from the other allows to partition the Altered Meteoric mixing proportion of any sample into two contributions: one coming from a recent Altered Meteoric water, and other coming from an old meteoric water. This is graphically shown in the two upper panels of Figure 2-21.

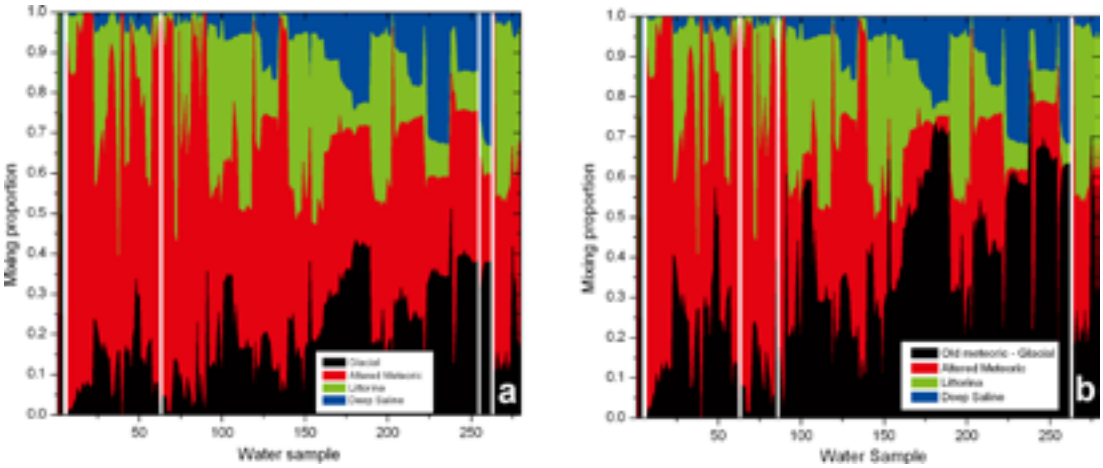

Figure 2-20. *Comparison of the mixing proportions calculated using exactly the same model, set of samples and variables, except for the isotopic composition of the Glacial end member. a: Results obtained with the Glacial end-member ($\delta^{18}O = –21‰$). b: Results obtained with the Old meteoric-Glacial end-member ($\delta^{18}O = –16‰$). The mixing proportions are plotted with respect to sample ID number.*

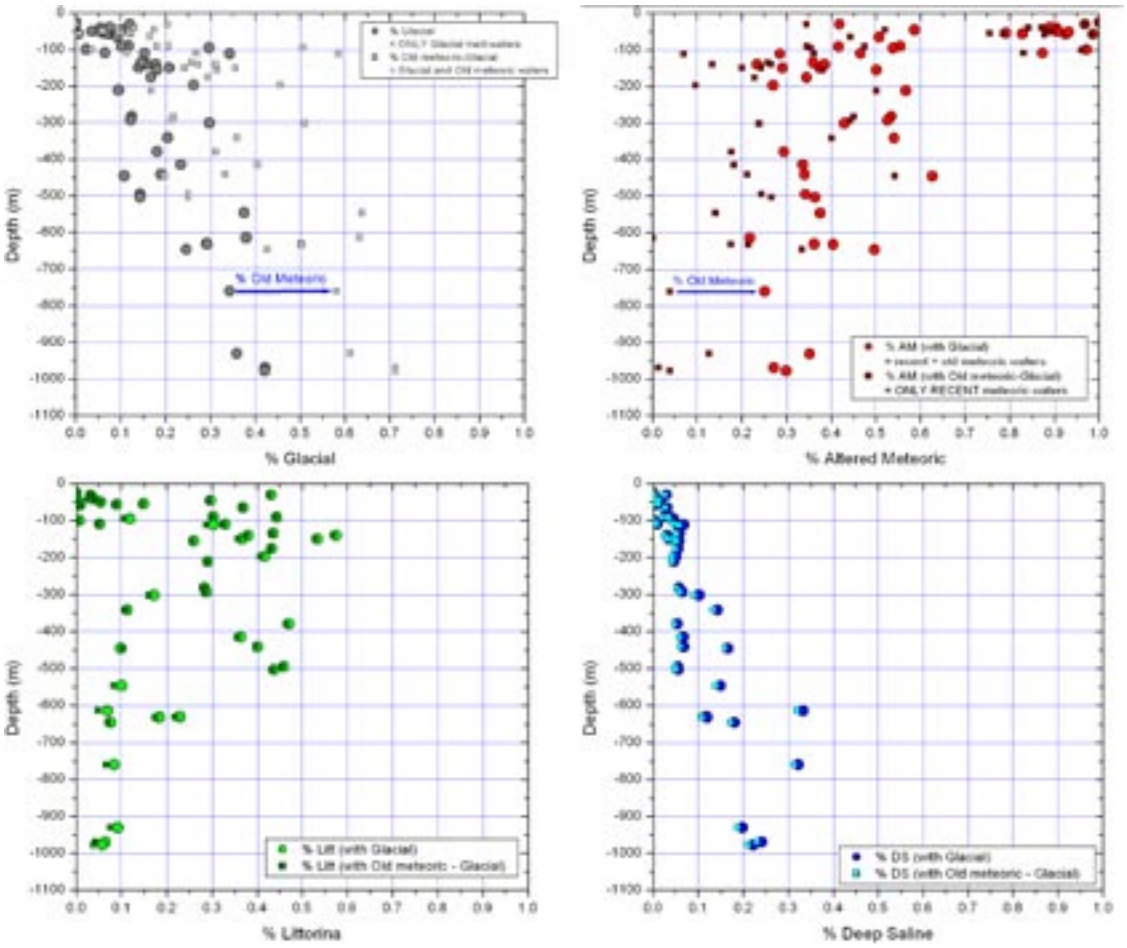

Figure 2-21. *Mixing proportions for the selected groundwaters calculated with the two end-members combination.*

This partition of the Altered Meteoric contribution is very important when reconstructing the salinity of the waters in the pre-Littorina stage in order to calculate the maximum penetration depth of the Littorina waters. Section 2.3 is entirely dedicated to this important topic.

Comparison of the calculated and measured contents

In order to assess the quality of the calculated mixing proportions, a comparison of the calculated concentrations (based on this mixing proportions) with the concentrations measured in the real samples for the conservative elements Cl and $\delta^{18}O$ and other elements of interest has been made. Results are displayed in Figure 2-22, showing the computed values using the two different Glacial end-members (squares for the case of using the original Glacial and circles for the case of Old meteoric-Glacial).

The results obtained for Cl using the original Glacial end-member show an acceptable agreement but, for $\delta^{18}O$ the results obtained by using the Old meteoric-Glacial (heavier isotopes) are much closer to the actual measurements.

2.2.2 Reconstruction of waters before Littorina stage

In this section the calculation of the values (for some of the main components, including isotopes) for selected samples just before the input of Littorina waters into the system is presented.

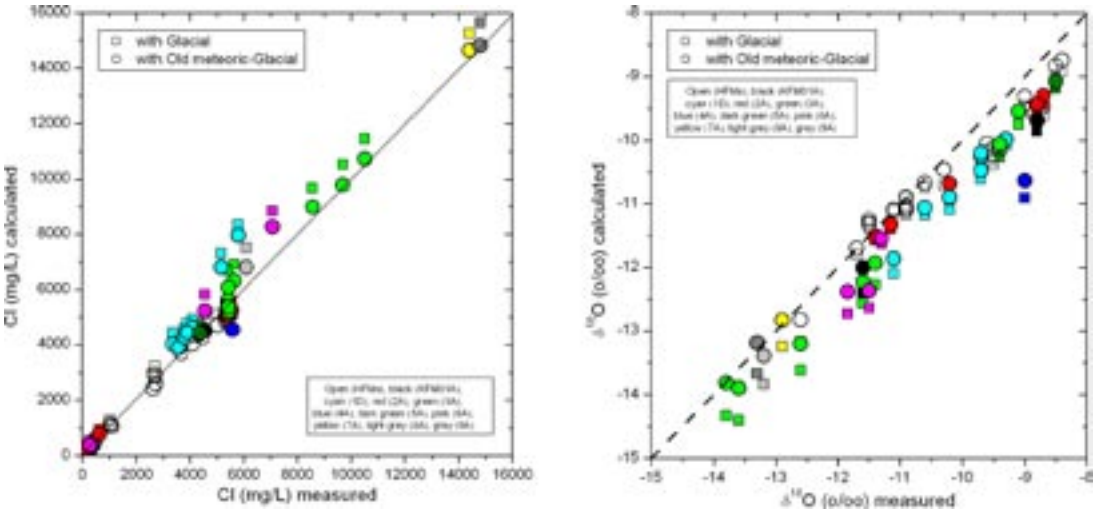

Figure 2-22. *Comparison of the chloride and $\delta^{18}O$ contents measured in the real samples and computed with M3 for the two combinations of end-members (DS+Lit+AM+Gl and DS+Lit+AM+Old meteoric-Gl). Note that in most cases the circles (which represent the M3 calculations with the Old meteoric-Glacial) are closer to the real values than the squares.*

Different approaches and methodologies have been used in order to assess the degree of confidence which can be placed on the results and to assess the degree of uncertainty. The first approach (subsection "PHREEQC calculations") uses PHREEQC and calculates the Pre-Littorina composition for waters with a chloride content of around 5,500 mg/L and the highest Littorina mixing proportions. The second approach (subsection "M3 approach") uses M3 to calculate the Pre-Littorina contents using the rationale explained in Section 2.2.1. The third uses the tritium content in the waters to partition the meteoric contribution into a recent and an old component; and the fourth follows the methodology suggested by /Pitkänen et al. 1999/. The two last approaches have been only applied to the groundwater sample with the highest Littorina mixing proportion.

PHREEQC calculations

In the ChemNet's report concerning Forsmark 2.1 /Gimeno et al. 2007/, the UZ group presented a hypothesis to explain the roughly constant chloride content of several groundwaters at different depths. These brackish groundwaters, located between 100 and 600 m depth in the Forsmark area (mainly in the Deformation Zone) and characterised by an important Littorina contribution (Figure 2-23, label beside each point) presented a chloride content of 5,500 ± 600 mg/L (shadowed area in Figure 2-23a and b) In spite of this constant chloride content, the concentrations of the other elements vary.

The calculations presented in /Gimeno et al. 2007/ suggests that this behaviour could be the result of pure mixing of different proportions of Littorina waters (with a chloride content of 6,500 mg/L) with a previous mixture of Glacial (Gl) + Deep Saline (DS) (giving a similar Cl concentration). The intrusion of variable amounts of Littorina (from 20% to a maximum of 55%) would not modify very much the Cl concentration of the previous Gl+DS mixture, *but* it would modify the concentrations of all remaining elements.

Different PHREEQC mixing calculations were carried out starting with different mixing proportions of Gl and DS (8 to 12% DS vs 92 to 88% Gl) until the chloride content of the mixture was in the range 4,000–6,000 mg/L. Then, different Littorina mixing fractions from 20 to 60% (as computed by M3 for Forsmark samples) in steps of 10% were used to calculate the concentration of selected elements (20–60% Litt vs 80–40% DS+Gl). The results are compared with the data for the real waters with a chloride content of 5,500 ± 600 mg/L. Figure 2-24 shows the results for SO_4^{2-} and Mg as an example.

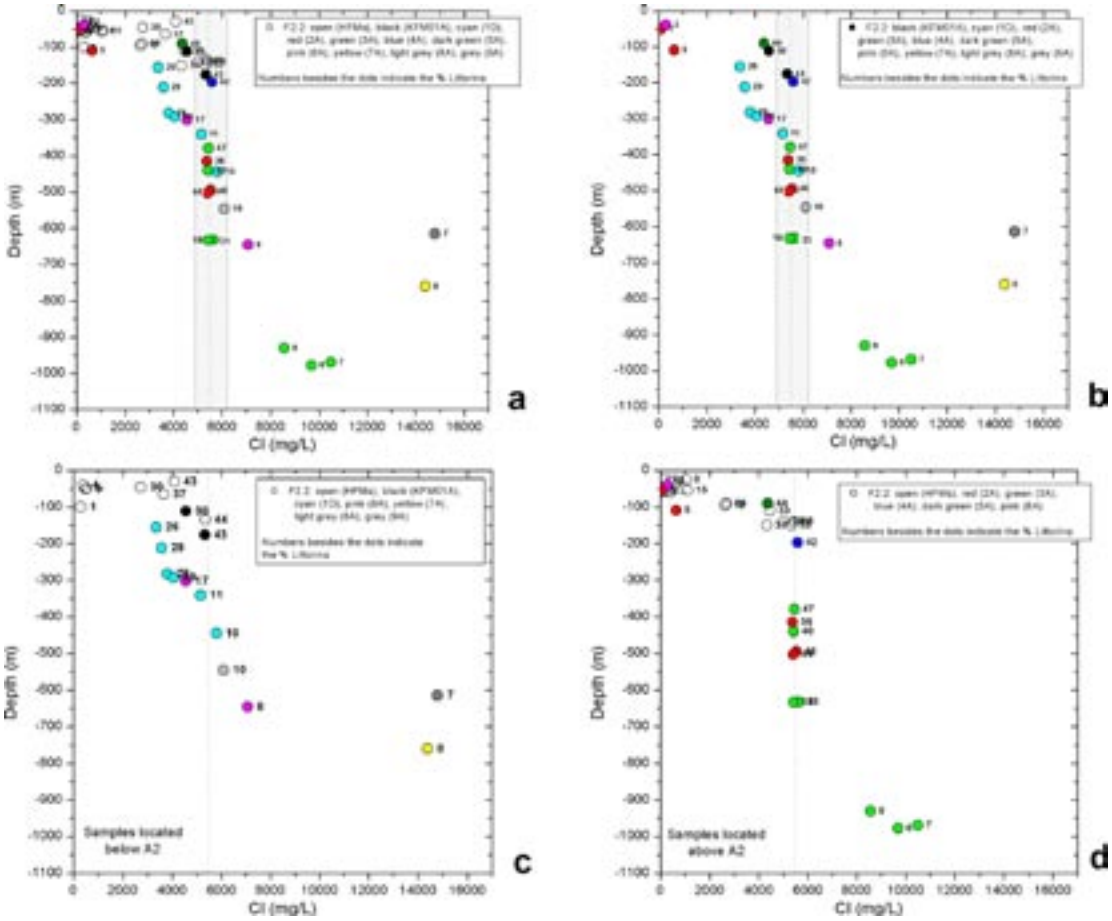

Figure 2-23. *Chloride distribution with depth in the Forsmark 2.2 selected groundwaters. The colour code indicates the borehole and the number next to the symbol gives the percentage of Littorina in the mixture. Grey spheres are the simulation results and coloured squares are the actual analytica data. Panels a and b show all the samples, including (a) or not (b) the percussion borehole samples. c: samples located below Deformation Zone ZFMA2 (Fracture domain waters). (d) samples located above that deformation zone (Deformation Zone waters).*

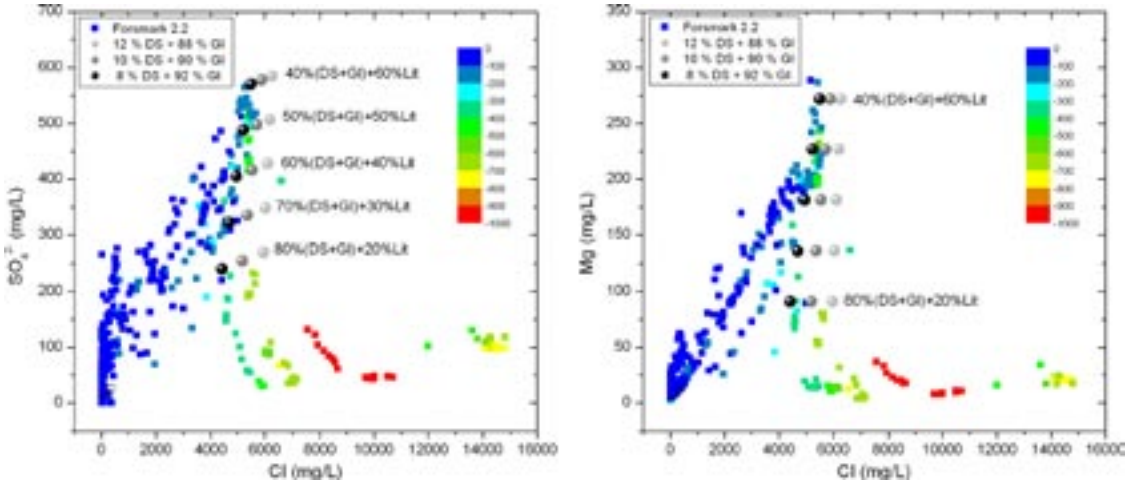

Figure 2-24. *Computed concentrations (grey spheres) of selected major ions (left: SO_4^{2-}, right: Mg) in calculated mixtures of Lit+DS+Gl with a Cl content of 5,500 ± 600 mg/L. The different mixing proportions plotted as grey spheres correspond to different initial ratios between DS and Gl (horizontal variation; see the legend) and then to different Littorina proportions (vertical variation). The computed range matches the observed range (coloured squares) in a Cl interval around 5,500 mg/L. Real samples are colour coded according to depth.*

As can be readily observed, calculations closely reproduce the observed ranges of these elements between 100 and 500 m depth (Figure 2-23). In all cases the range of values of the calculated samples matches the observed range, confirming that a simple mixing hypothesis can explain the geochemical behaviour of the constant-Cl depth range in Forsmark area. All this was already presented in the Forsmark 2.1 report /Gimeno et al. 2007/.

Based on the mixing proportions obtained with PHREEQC, the ^{2}H and ^{18}O values have been calculated and compared with the real values (Figure 2-25). As displayed in Figure 2-25, the calculated values (grey spheres) do not reproduce accurately the measured isotopic contents. Only the results obtained with the highest Littorina proportion are inside the measured range. So, in spite of having reproduced fairly well the chemical composition of these waters, the simulations were not able to explain the isotopic composition of the real data.

In order to improve the agreement between isotopic calculations and measurements, the isotopic composition of the dilute end-member considered in the calculations (that is, the Glacial end-member) was modified to represent a heavier isotopic signature. Therefore, the second option for the glacial component is used here again, that is the "Old Meteoric-Glacial" end-member (OM-Gl in the plots). In this case, the resultant isotopic composition fits much better the range of values measured in the real samples (triangles in Figure 2-25).

From these results, a range of pre-Littorina compositions for the groundwaters with Cl concentrations around 5,500 mg/L and located between 100 and 500 m depth can be obtained (Figure 2-26). The most probable values correspond to the lowest Deep Saline proportion of the range presented in Figure 2-26, that is, the result of a mixture of 8% Deep Saline and 92% Old meteoric-Glacial.

M3 approach

Two different calculations have been performed with the Forsmark 2.3 dataset (289 groundwater samples) in order to split the meteoric mixing proportion between a recent and an old component. Both simulations use the four end-members (Deep Saline, Glacial, Littorina and Altered Meteoric) but, whereas simulation #1 uses $\delta^{18}O = -15‰$ and $\delta^{2}H = -111‰$ as the isotopic composition of the Glacial end-member (Old meteoric-Glacial), simulation #2 uses $\delta^{18}O = -21‰$ and $\delta^{2}H = -160‰$ (Glacial). This difference has important implications.

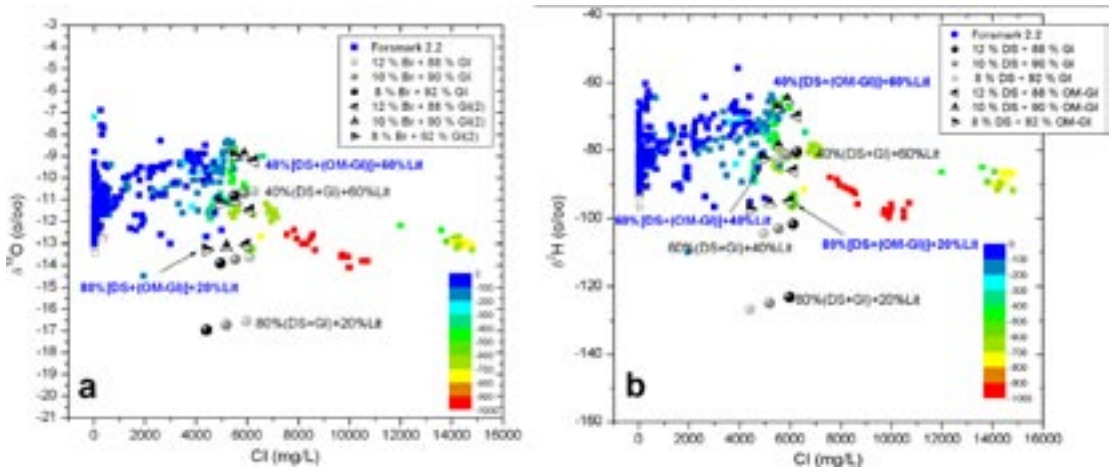

Figure 2-25. *Computed concentrations (grey spheres and triangles) of stable isotopes (a: $\delta^{18}O$, and b: $\delta^{2}H$) in calculated mixtures with a Cl content of 5,500 ± 600 mg/L. The different mixing proportions correspond to the ones described in Figure 2-24. The difference between the spheres and the triangles is in the isotopic composition of the Glacial end member used for the calculations. The range computed with the second Glacial end member (Old meteoric-Glacial) matches much better with the observed range in the real samples.*

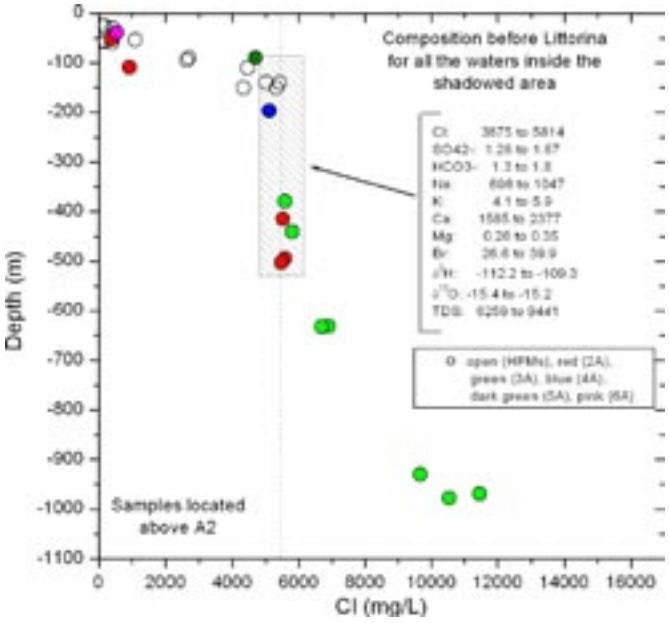

Figure 2-26. *Simulated water composition for some of the waters before the Littorina Stage (calculated with PHREEQC) on the plot shown in Figure 2-23.*

Simulation #1 assumes that the "Glacial" end-member is already a 50–50 mixture of a pure glacial melt-water end-member (with $\delta^{18}O = -21‰$) and an old meteoric end-member (with $\delta^{18}O = -10$ to$-1‰$). In other words, the old meteoric component is included in the mixing proportion of the "Glacial" end-member of simulation #1 and, as a consequence, the Altered Meteoric end-member represents only the contribution of a recent meteoric component.

Simulation #2 assumes that the glacial end-member is a true glacial melt-water. Therefore, all the meteoric components (recent and old) are included in the Altered Meteoric end-member.

Subtracting, for a given sample, the Altered Meteoric mixing proportion of simulation #1 from the Altered Meteoric mixing proportions of simulation #2, the percentage of old meteoric end-member will be obtained. The Altered Meteoric mixing proportions of simulation #1 gives directly the percentage of recent meteoric component. In other words, with this procedure, the mixing proportions of 5 end-members (two of them with identical composition) will be obtained for a given sample: deep saline, true glacial, Littorina, old meteoric (pre-Littorina stage) and recent meteoric (post-Littorina stage).

In both cases, the starting points was the mixing proportions calculated for the groundwater samples at present, but using the two different sets of end-members. Subsequently, the Littorina and Altered Meteoric mixing proportions are eliminated from the present values and the Glacial and Deep Saline proportions re-calculated to 100%, assuming that they were the only waters existing in the system before the Littorina stage. The difference between them is that in simulation #1, the waters existing previous to Littorina input would be a deep saline water, an old meteoric water and a glacial melt-water, whereas in simulation #2, the old meteoric influence is not considered. Once these mixing proportions are calculated in the two simulations, the corresponding chemical compositions are obtained for each sample.

The results of these two types of calculations are shown in Figure 2-27. The main conclusion is that an important variability in chemical and isotopic contents is obtained depending on the conceptual model assumed. Another important uncertainty is directly associated with the M3 calculations, which have important limitations for the set of samples with low chloride contents (shallow groundwaters), not controlled by mixing and without a contribution of the Deep Saline end-member. For those waters, M3 always gives some Deep Saline proportion which, even being very low, has important effects on the calculated concentrations (in general higher contents than measured). Due to this limitation, the reconstruction presented here makes sense only at depths below 100 m.

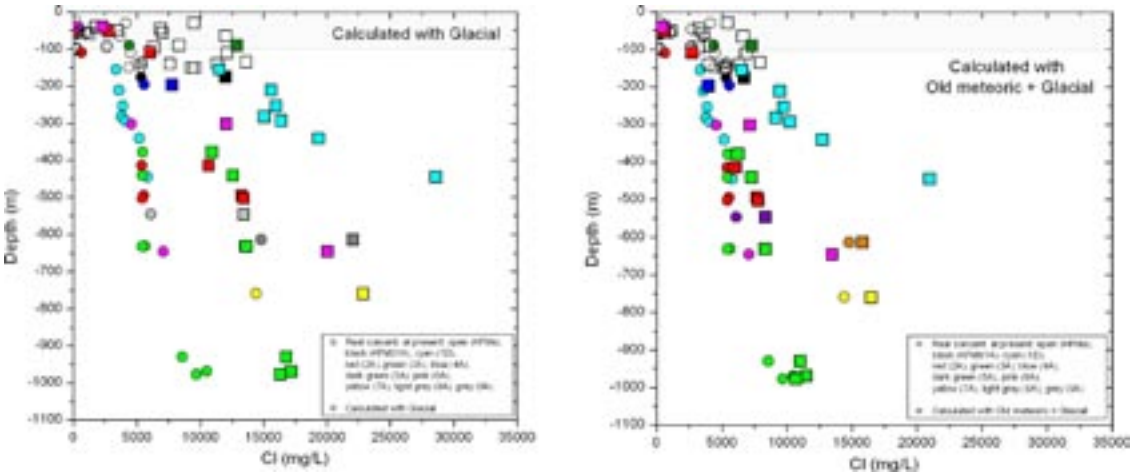

Figure 2-27. *Computed values of choride in the selected waters before Littorina stage using the two alternative reconstructions. Left: Deep Saline and Glacial; Right; Deep Saline and Old meteoric+Glacial. Circles are for the real composition and squares for the calculated ones. Notice how the right panel, using the Old meteoric+Glacial as end-member, gives a much better agreement.*

In the light of the results presented in Figure 2-27, it seems clear that the first scenario (the presence of an "old meteoric" water already present in the system before the last glaciation) gives more reasonable results concerning the possibility of Littorina input in the waters with real Littorina signature at present.

A summary of the ranges of values obtained with these two types of simulations and with the PHREEQC approach explained in the previous sub-section is presented in Table 2-15. From this comparison it is clear that the assumption of the existence of an old meteoric water provides better agreement with the PHREEQC results.

Table 2-15. Reconstruction of contents before Littorina stage in the samples analysed with PHREEQC in the section above. Concentration (mg/L) ranges calculated with PHREEQC as they are shown in Figure 2-26, compared with the values obtained from the M3 mixing proportions for the same set of samples.

	PHREEQC	M3	
		Deep Saline + (Old meteoric-Glacial)	Deep Saline + Glacial
Cl	3,875 to 7,800	3,900 to 7,800	7,590 to 13,400
SO_4^{2-}	1.28 to 1.67	1.29 to 2.07	2 to 3.17
HCO_3^-	1.3 to 1.8	1.29 to 2.43	2.3 to 4.1
Na	689 to 1,047	686 to 1,353	1,320 to 2,327
K	4.1 to 5.9	4.17 to 7.84	7.6 to 13
Ca	1,585 to 2,377	1,614 to 3,185	3,100 to 5,500
Mg	0.26 to 0.35	0.27 to 0.43	0.42 to 0.67
Br	26.6 to 39.9	27.1 to 53.4	27.1 to 53.4
δ^2H	–112.2 to –109.3	–113 to –100	–139 to –128
$\delta^{18}O$	–15.4 to –15.2	–15.6 to –14.3	–19 to –17.6

Two additional approaches to the composition of Pre-Littorina waters

The two other approaches used here consist of (a) using the tritium content of each sample as a proxy for the proportion of recent meteoric water, and (b) applying the aproach proposed by /Pitkänen et al. 1999/ to the sample with the strongest Littorina signature (sample #4522, HFM08 borehole at 150 m depth).

Tritium method

Tritium is assumed to be a signature of recent meteoric water input. Old meteoric waters (pre-Littorina) would have, on the other hand, zero tritium. In other words, the tritium content of a sample should correlate only with the recent Altered Meteoric end-member, not with the Old Meteoric one. So, if a sample has a 50% of meteoric water (recent or old) and 50% of other waters (all of them "old" from the tritium point of view), and its tritium content is, say, 8 TU, then because we know that recent precipitation has a tritium content of 16 TU, this would immediately imply that all the meteoric component in the sample is recent (none is old). If the obove sample has a triutium content of 6 TU, that would imply that its meteoric component must be a mixiture of recent and old meteoric water, specifically 75% of recent meteoric and 25% of old meteoric.

Recent precipitation has a mean ^{3}H content of 16 TU. From M3 calculations (which do not use tritium as an input compositional variable) an Altered Meteoric percentage of 23.4% is obtained for sample #4522. This Altered Meteoric percentage is the sum of the recent Altered Meteoric and the Old Meteoric percentages. Sample #4522 has a tritium content below detection limit, which is 0.8 TU; so the maximum percentage of recent meteoric component is 7% (assuming a tritium content equal to the detection limit) and the minimum recent meteoric component is 0% (assuming a tritium content of zero). Subtracting the Littorina percentage and a range of 0–7% of recent Altered Meteoric in order to compute the pre-Littorina Cl content gives a range of Cl from 2,815 to 3,344 mg/L.

Method proposed by /Pitkänen et al. 1999/

This very simple method is based on a plot of SO_4^{2-} versus $\delta^{18}O$, similar to Figure 2-28. In this figure, the dashed line represents a binary mixing line between the Littorina end-member (cyan circle at the right end of the line) and a dilute pre-Littorina water with $\delta^{18}O = -16‰$. The rightmost sample is sample #4522, and from its position on the mixing line it can be concluded that its Littorina mixing proportion is 63%, in agreement with M3 calculations. From this value (63% Littorina), the Cl content of the sample (5,422 mg/L), and the assumption that it is a binary mixture of Littorina and a pre-Littorina water component, a pre-Littorina Cl concentration of 3,415 mg/L is obtained.

Considering only the sample used in these approaches the following results are obtained:

PHREEQC calculations: the pre-Littorina waters corresponding to these samples would have had a Cl content of 3,600 to 4,500 mg/L, using the 8% Deep Saline and the 10% Deep Saline, respectively (considering that the Deep Saline end-member has a Cl content of 45,500 mg/L).

M3 calculations: using the results from simulations #1 and #2 for the sample with the strongest Littorina signature (sample #4522) the following percentage for the five end-members would be:

Deep Saline	Glacial	Littorina	Recent Meteoric	Old Meteoric
2.5%	16.0%	58.1%	13.3%	10.1%

Sample #4522 has a present Cl content of 5,422 mg/L. Subtracting the recent Altered Meteoric and Littorina components gives a pre-Littorina Cl content of 4,040 mg/L.

The four methods presented here give a rather wide range of possible chloride contents for the pre-Littorina waters above repository depths. The range goes from 2,800 to 4,500 mg/L of Cl.

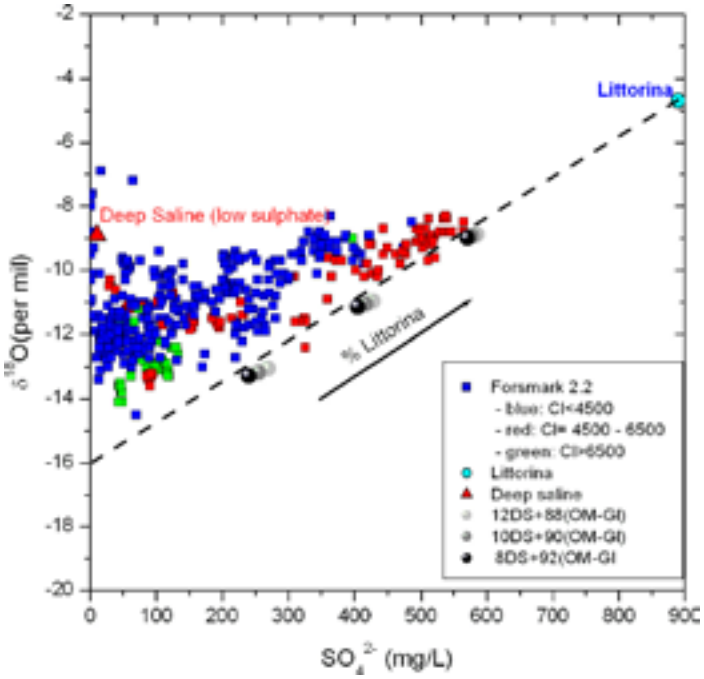

Figure 2-28. *Plot of SO_4 versus $\delta^{18}O$ for Forsmark groundwaters.*

The lowest value is obtained with the tritium method, but it must be taken with caution since it has been obtained with a "below detection limit" tritium value. The upper limit of the range calculated with the tritium method is 3,344 mg/L Cl, more consistent with other results. Without the lower value, the pre-Littorina Cl range for waters between the surface and the depth of the repository is between 3,500 and 4,500 mg/L. Taking into account that Littorina waters have a Cl content of around 6,500 mg/L, there is no hydrodynamic inconsistency in these results as Littorina waters could have penetrated pre-Littorina groundwaters of such chlorine content. The feasibility of this Littorina penetration is further investigated in the next section.

2.2.3 Feasibility of Littorina penetration: Density calculations

It seems clear that the density of the Littorina end-member must be higher than the density of the pre-Littorina groundwaters to allow effective Littorina penetration and mixing. In order to check the feasibility of this process within the frame of the proposed model of groundwater evolution, some simple calculations about the density of pre-Littorina groundwaters have been carried out.

For these calculations, the salinity of pre-Littorina groundwaters has been reconstructed from present groundwater samples. Pre-Littorina groundwater compositions considered here were the result of the calculations performed with M3 with the simulation #1 described in the previous section, that is, considering the Glacial end-member with the heavy isotopic composition (Old meteoric-Glacial). The salinity of the resulting groundwaters has been then calculated and compared with the salinity of the Littorina end-member, as defined in Section 2.1. In this system, a minimum difference of salinity of around 1,000 mg/L between both types of groundwaters seems to be necessary to allow an effective penetration and mixing (Sven Follin, pers. comm., Sept, 2007).

As shown in Figure 2-29, most of the pre-Littorina groundwater samples above 500 m in FFM02 and FFM03, and above 300 m in FFM01 display salinities more than 1,000 mg/L below Littorina salinity. For all those groundwaters, and according to the criterion of minimum salinity difference, mixing can be justified theoretically by simple salinity contrast between pre-Littorina and Littorina groundwaters. This is consistent with the penetration depth for the Littorina end member in the two zones deduced from mixing proportions and actual analytical data in previous sections.

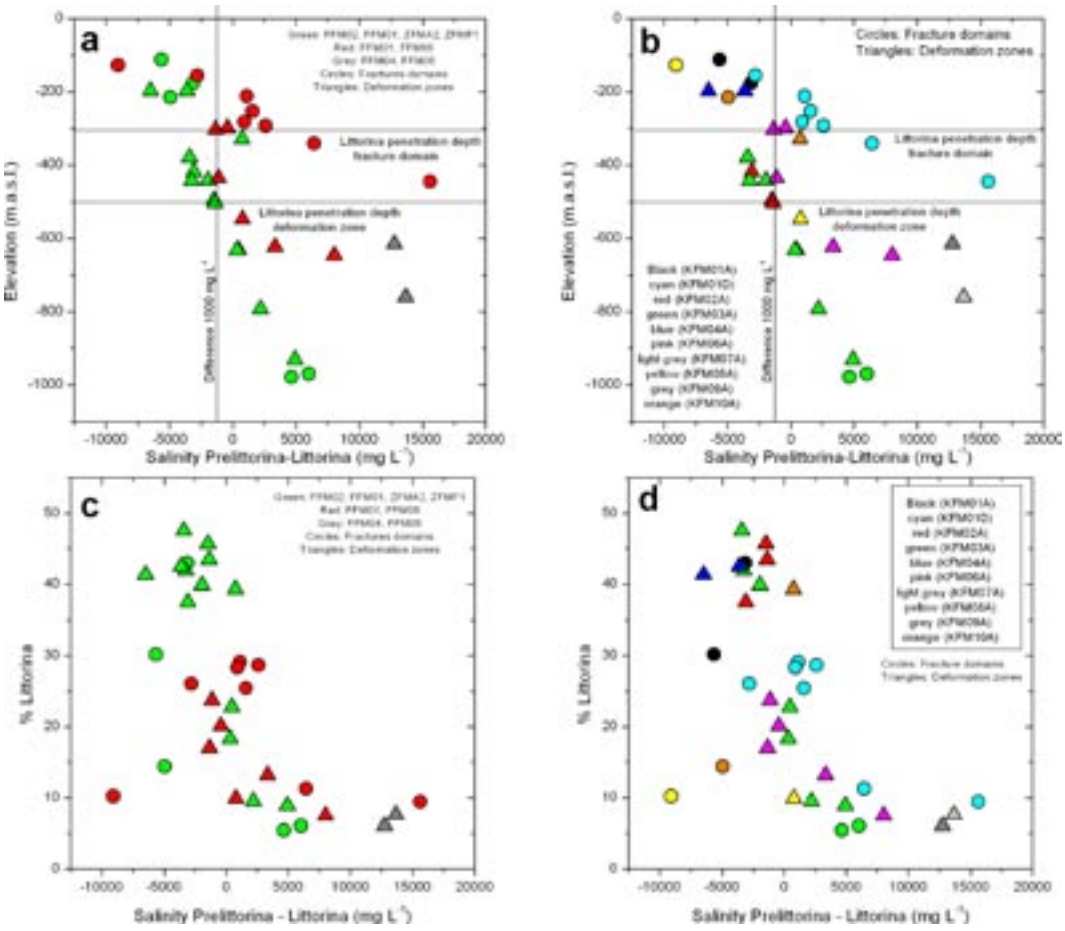

Figure 2-29. *Salinity differences between the reconstructed pre-Littorina groundwaters and the Littorina end-member vs depth (a and b) and vs Littorina percentage (c and d) in the Forsmark groundwaters colour-coded by their location in the system (a and c) or by the borehole (b and d). The vertical line indicates the limit of 1,000 mg/L of difference in salinity, therefore samples located left-side to the line had lower salinity that Littorina (allowing the input of this water), and the ones located right-side higher than it. The methodology for the reconstruction of pre-Littorina groundwaters is detailed in the text.*

It can be expected that the samples with a larger salinity difference between the pre-Littorina groundwaters and the Littorina waters should exhibit larger proportions of Littorina contribution at present. This hypothesis has been explored in the samples plotted in the panels c and d of Figure 2-29. As a general trend, the samples for which the pre-Littorina groundwaters had larger salinities than the Littorina end-member display Littorina proportions smaller than 10%, whereas for the rest of groundwaters the Littorina contribution is generally larger (up to 50%).

However, some apparent inconsistencies emerge when the plots are examined in more detail. In the first place, it should be noted (Figure 2-29c and d) the great dispersion of values for Littorina proportion for water samples presenting similar differences in salinity between the pre-Littorina and Littorina stages. Second, an important amount of groundwater samples with Littorina contribution larger than 10% seem to have had a pre-Littorina salinity similar or even larger than the Littorina end-member.

These two apparent inconsistencies with the general model may indicate that salinity difference is not the only factor triggering mixing processes. In the light of the distributions observed in Figures 2-29, other factors or processes seem also to be controlling and favouring the mixing of the Littorina waters with previous groundwaters (e.g. density differences induced by temperature gradients). Although this hypothesis cannot be checked with the data available at present, it should be explored further in the future with the assistance of hydrogeological models able to cope with variable density flow and taking into account temperature differences between the pre-Littorina groundwaters already in the bedrock and the waters in the bottom of the Littorina Sea.

2.3 Temporal evolution of mixing

Based on the general conceptual model for the groundwater evolution at Forsmark developed by /Smellie et al. 2008/, additional supporting evidence to this model is presented here.

The proposed conceptual model is based on the observation that in this natural system there is no simple binary mixture between the different types of waters but a more complicated one, with at least five different end-members involved. These possible end-members are: (1) a deep saline groundwater, (2) an old meteoric water, (3) a glacial melt-water, (4) a Littorina Sea water, and (5) a recent altered meteoric water. The chemical characteristics of each end-member water are reviewed in Section 3, and the existence of an old meteoric component is confirmed in Section 4.

In the light of the results presented in the previous sections, the following temporal evolution of mixing has been constructed (Figure 2-30).

A deep saline groundwater is formed in the crystalline bedrock (covered by several kilometres of sediments) over hundreds of millions of years mainly by water-rock interaction /Smellie et al. 2008/. This is the Deep Saline end-member. Subsequent erosion reduced this sedimentary cover until, in the Late Tertiary, the present bedrock was exposed once again /Lidmar-Bergström 1996/ resulting in a progressive dilution of the brine in the upper 1,000 m (or more) of the bedrock and the consequent salinity gradient with depth (Figure 2-30a).

During the last three million years, a succession of glacial and interglacial periods has triggered the alternating or simultaneous input into the upper part of the crystalline basement of glacial melt-waters and meteoric waters. Because of the complex and rapid change of climatic conditions, these two end-member waters (the Glacial and the Old Meteoric) are always mixed in different proportions, but they never appear as pure end-member waters. The second panel

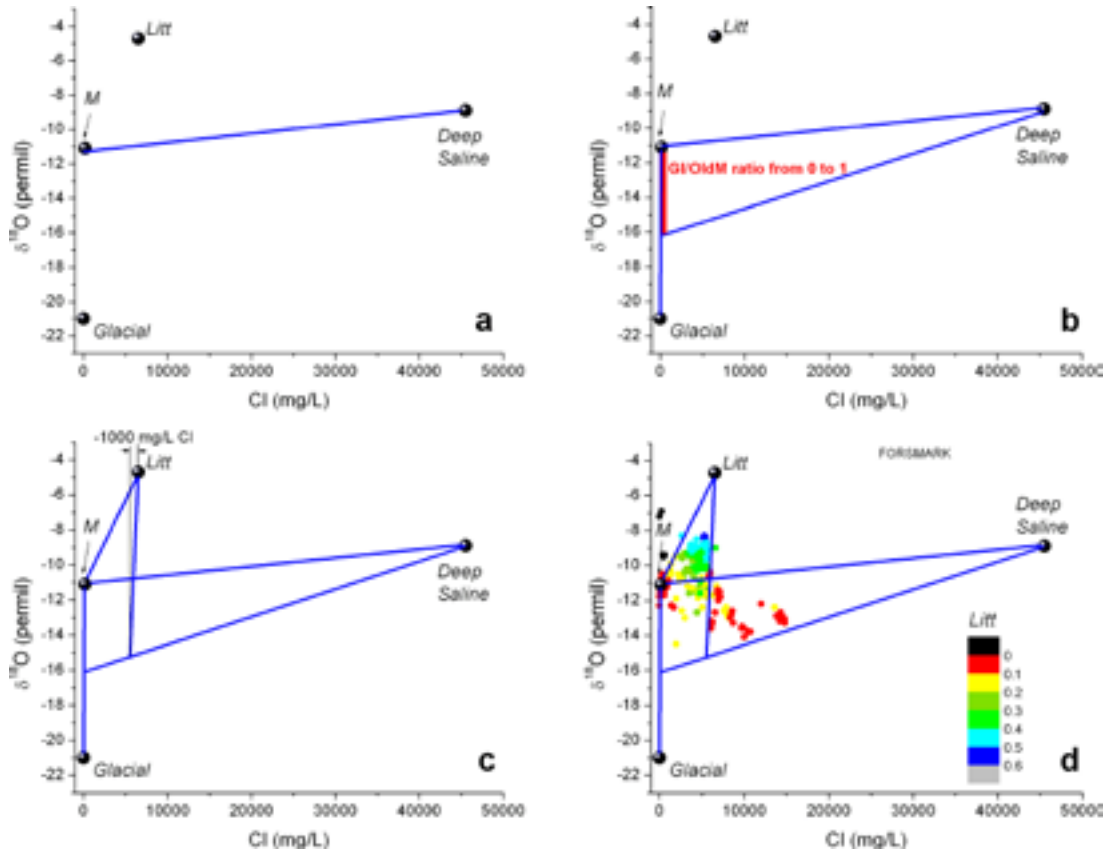

Figure 2-30. *Temporal evolution of mixing at Forsmark. See text for details.*

in Figure 2-30 shows in red the mixing line between the Glacial and the Old Meteoric end-members on a plot with chlorine in the horizontal axis and oxygen-18 in the vertical axis. Except for one water found in Palmottu (with $\delta^{18}O = -19‰$; /Blomqvist et al. 2000/), no groundwater in the Scandinavian Shield has been found with a $\delta^{18}O$ value lower than −16‰, which means that the binary mixtures of Glacial and Old Meteoric waters have a maximum Glacial contribution of 50% (based on their isotopic values).

Any of the dilute mixtures of glacial and meteoric waters formed during the previous stage can mix, if pushed downwards by gravity or forced by the weight of glaciers, with the saline groundwaters that occupy most parts of the deeper basement. In theory then, any mixture inside the wedge depicted in Figure 2-30b can be formed. This wedge has as vertices the Deep Saline end-member, the (Old) Meteoric end-member (M in the figure), and the 50:50 mixture of Glacial and Old Meteoric which gives a $\delta^{18}O$ signature of −16‰. These mixing events would generate a rather steep salinity gradient in the groundwater system, with diluted waters in the upper part, brackish waters in the middle, and saline waters in the lower part.

8,000 year ago, after the last glacial period, a brackish sea (the Littorina Sea) was established in what is today the Baltic Sea. The Forsmark area was under the waters of this sea for 8,000 years and, as a consequence, Littorina Sea waters percolated down into the basement. Because of the salinity gradient already present in the basement, Littorina waters could penetrate down only until encountering groundwaters with a chlorine content of around 5,500 mg/L. This mixing cut-off is marked in Figure 2-30c and sets a drastic limit to the feasible mixing lines between the Littorina end-member (Litt in the figure) and the previous water mixtures.

After the Forsmark area emerged from the Littorina Sea as a result of post-glacial rebound and uplift less than 1,000 years ago, modern meteoric waters started to penetrate into the upper part of the groundwater system. These waters became the Recent Altered Meteoric end-member after reacting with the soil and overburden materials, and mixed with the Littorina and pre-Littorina groundwaters. The composition of this Recent Altered Meteoric end-member is thought to be very similar to the Old Meteoric one, and so it occupies the same position in the graphs of Figure 2-30, where it has been simply labelled “Meteoric” (M). Because this end-member water (or its elder sibling, the Old Meteoric end-member) has already mixed with the other three end-members, it does not add new areas on the Cl versus $\delta^{18}O$ graph of Figure 2-30 where the waters can lie.

As a consequence of this mixing history, the only permitted area on the Cl versus $\delta^{18}O$ graph for real water samples to be plotted in are those inside the mixing polyhedron marked by blue lines in Figure 2-30. Figure 2-30d shows the position of the Forsmark samples colour-coded by their Littorina end-member mixing proportion as computed with M3. Two observations are readily apparent: (1) almost all samples are inside “the permitted area”; and (2) samples with Littorina are located only in the sub-area where Littorina waters could have penetrated. These two observations add confidence to the proposed mixing history.

A third observation that adds consistency to this account is this: if samples from two other areas in the Scandinavian Shield, Laxemar and Olkiluoto (Figure 2-31) are also plotted it is observed how, again, most samples are inside the “permitted perimeter” and very few plot in the forbidden areas.

However consistent this temporal evolution could sound, there are several points that are far from clear. The most intriguing one is: why the mixing events between Glacial and Old Meteoric waters are restricted to a maximum of 50% Glacial end-member (i.e., to a minimum value of $\delta^{18}O$ of −16‰)?

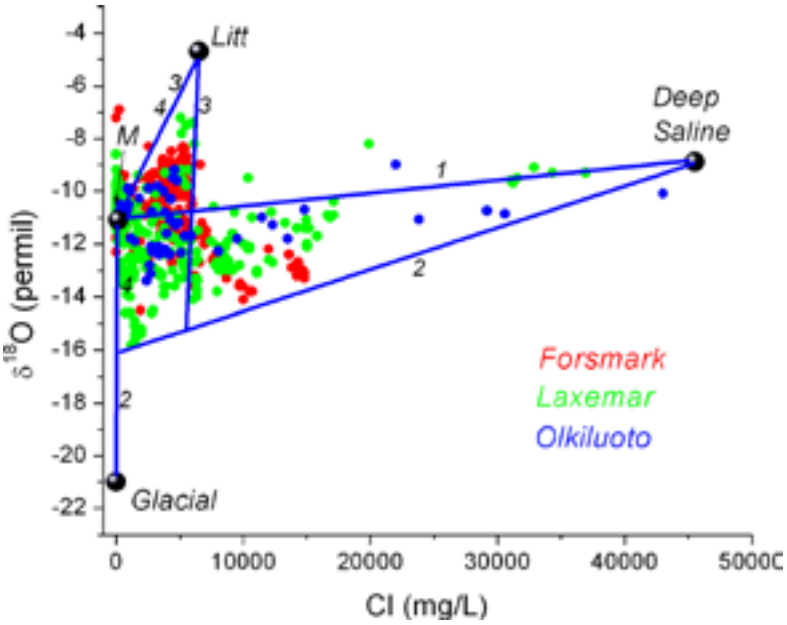

Figure 2-31. *Representation of the groundwaters from three different sites in the framework of the different mixing lines proposed in the conceptual model. Blue lines are mixing lines between water end-members (black spheres). Numbers beside the mixing lines give the temporal order of mixing: 1 indicates the first mixing event, 2 the second mixing event, and so on. The area outside the mixing polygons are forbidden for waters in this scenario. Filled circles are actual water data from Forsmark (red), Laxemar (green) and Olkiluoto (blue).*

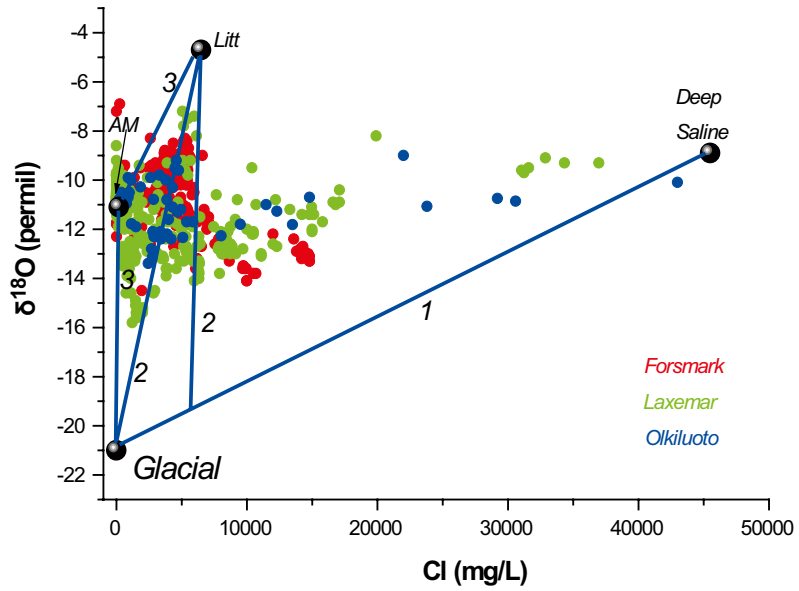

Figure 2-32. *Different evolution of mixing events not considering the presence of an Old Meteoric end member. Blue lines are mixing lines between water end-members (black spheres). Numbers beside the mixing lines give the temporal order of mixing. The area outside the mixing polygons are forbidden for waters in this scenario. Filled circles are actual water data from Forsmark (red), Laxemar (green) and Olkiluoto (blue).*

The necessity of an Old Meteoric end-member has been discussed in depth in Section 2.2. Here this topic is revisited and an additional possible temporal evolution scenario with no Old Meteoric end-member is constructed in order to show that the real groundwater samples from Forsmark, Laxemar and Olkiluoto mostly fall outside the permitted perimeter. This scenario is shown in Figure 2-32. It is assumed that a deep saline groundwater exists, mostly undisturbed and very homogeneous in composition until the last glaciation. Then, glacial melt-waters intrude into the system, mixing with the deep saline groundwaters. This is marked in Figure 2-31 by mixing line "1" between the Glacial and the Deep-Saline end-members. Next, the Littorina Sea stage begins; the Littorina waters sink into the basement until encountering waters of similar salinity (<5,500 mg/L of chlorine), as was explained before. This mixing event generates a wedge defined by the mixing lines labelled "2" in the figure. Finally, when the Forsmark area emerged by glacio-eustatic uplift, meteoric waters penetrated into the upper part of the bedrock, producing the mixing lines labelled "3".

So, the "permitted perimeter" in this scenario is restricted to the polyhedron defined by the two mixing lines labelled "3" plus the rightmost mixing line "2". All the samples to the right of the of this last line fall outside the permitted perimeter and thus cannot be explained by mixing the proposed end-members. Thus, it is clear that earlier episodes of old meteoric water input is necessary to explain the location of the samples on the Cl versus $\delta^{18}O$ plot.

Finally, as /Smellie et al. 2008/ indicate, the above description is valid for areas in the Forsmark bedrock where first Holocene glacial meltwater and than later Littorina Sea water have been introduced; the brackish sea water has only been able to intrude (by density turnover) were fresh water (mainly glacial) had previously filled the fractures. Therefore two different systems have developed in the Forsmark area:

1) The higher transmissive deformation zones and the more fractured domains (FFM03 and parts of FFM01/02), where all water types (Saline, Old Meteoric ± Old Glacial + Saline, Holocene glacial, Littorina and present altered Meteoric) can be found to have interacted to various degrees, and
2) The target area (FFM01), where at least parts of the aquifer have been isolated and therefore only Saline and Old Meteoric ± Old Glacial + Saline groundwaters can be identified.

This two different systems show slightly (but important) different chemical characters and geochemical processes which will be shown in the following Section.

3 General overview of the hygrogeochemical system

This section presents the final picture of the system with all the data available by the time of 2.3 data freeze. A summary of the main conclusions on the chemical elements distribution, their main controls and the results of geochemical modelling is also presented.

The section is divided into three parts concerning the shallow and near surface groundwater system, the deep groundwater system and the redox modelling. This last part provides a general overview of the redox processes controlling some of the important parameters in the system. It summarizes the work done in the previous modelling phases, updating the results with the new data from the 2.2 and 2.3 data freeze. It includes the presentation of the different redox parameters and the redox modelling concerning the iron, sulphur and uranium systems. Therefore, several issues are dealt with here:

- Issue A-1: Modelling of the existence of a relatively shallow "process zone" capable of buffering the meteoric water with respect to redox and cation exchange.
- Issue A-4: High uranium content in Forsmark.
- Issue B-1: Description of models based on reactions and other alternative models.
- Issue E-1: Spatial variability of hydrochemical data.
- Issue G-1: Modelling of redox and pH buffering and water-rock reactions at repository depth.

Before starting with the description of the hydrogeochemistry of the system, two important points must be clarified. The first refers to the geological and structural position of the samples in this complex system. To deal with this complexity the concept of *fracture domains* has been used /Olofsson et al. 2007/. A summary of this work and its application to our modelling approach is presented in Section 3.1.

The second refers to the set of waters included in this study and its subdivision into a "shallow system" and a "deep groundwater system". This is explained in Section 3.2. This section also includes the list of samples that comprise the "Final Set of Selected Forsmark Groundwaters".

The main geochemical features of the shallow and deep groundwater systems are reported in Sections 3.3 and 3.4, respectively. Finally the redox modelling is extensively presented in Section 3.5.

3.1 Fracture domains: implications for the hydrogeochemical modelling

During previous model versions of Forsmark, significant spatial variability in the fracture pattern was observed which sparked the need for a subdivision of the model volume into sub-volumes for a more precise treatment of geological and hydrogeological data. Subsequent analyses of data collected up to data freeze 2.1 led to a better understanding of the site and a concept for the definition of fracture domains based on geological characteristics matured /SKB 2006c/.

The fracture domain report /Olofsson et al. 2007/ was written as a support for modelling in the 2.2 stage and it was intended to constitute a basis for any subsequent modelling work. Fracture domains are identified and described on the basis of geological data together with the compilation of hydrogeological, hydrogeochemical and rock mechanics data within each fracture domain.

On the basis of borehole data, six fracture domains (FFM01–FFM06) have been recognized inside and immediately around the candidate volume. Three of these domains (FFM01, FFM02 and FFM06) lie inside the target volume for a potential repository in the north-western part of the candidate area; domain FFM03 is outside the target area in the south-eastern part of the candidate area; and domains FFM04 and FFM05 occur on the edges of the target volume.

A representation of the fracture domain model, which shows the geometrical relationships between the domains FFM01, FFM02, FFM03 and FFM06, is shown in Figure 3-1. Fracture domain FFM01 is coloured in light grey while the volume coloured in dark grey shows the position of FFM06. The uppermost part of the bedrock, in the north-western part of the model, is fracture domain FFM02 (in blue). This domain dips gently towards the south. Fracture domain FFM03 (in green) is situated directly above the gently dipping and sub-horizontal zones ZFMA2 and ZFMF1 at depth, and above domain FFM02 close to the surface. Two of the main steeply dipping fractures are also shown in Figure 3-1 (ZFMENE0060A and ZFMENE0062A).

The main features characterising these domains are the following:

- *Fracture Domains FFM01 and FFM06*: Both are situated beneath the gently dipping and sub-horizontal zones ZFMA2 and ZFMF1, and beneath the near-surface fracture domain FFM02. They are distinguished solely on their alliance to separate rock domains, RFM029 and RFM045 (/see Olofsson et al. 2007/ for more detailed description). These domains present steeply dipping, minor fault zones with sealed fractures and low fracture frequency between zones whereas gently dipping or sub-horizontal deformation zones are not common.
- *Fracture Domain FFM02*: This domain is situated close to the surface inside the target volume, directly above fracture domain FFM01 (Figure 3-1). The domain is characterized by a complex network of gently dipping and sub-horizontal, open and partly open fractures, which are known to merge into minor zones beneath drill site 7 (DS 7 in Figure 3-1).
- *Facture Domain FFM03*: This domain is situated within rock domains RFM017 and RFM029, outside the target volume. It is characterized by a high frequency of gently dipping, minor deformation zones containing both open and sealed fractures.

Several interesting observations, very useful in our work, were pointed out in /Olofsson et al. 2007/ report concerning the hydrochemical data:

(1) There is a relatively low total number of observations and investigated borehole sections (fractures or fracture zones or joints) in each borehole.

(2) Most hydrochemical data (70% of the sampled borehole sections) originate from geological entities interpreted as deformation zones (henceforth represented by triangles in the hydrochemical plots) in the geological model, whereas only 30% are associated with interpreted fracture domains (henceforth represented by circles in the hydrochemical plots).

(3) The gently dipping deformation zone ZFMA2 was identified as a major structural feature steering both the hydrogeological and fracture properties at the site /SKB 2005a/.

(4) The conditions close to the surface in the north-western part of the model volume appeared to be different from the conditions observed at depth.

(5) The sections of the two well-investigated boreholes KFM01D and KFM03A represent what seems to be two extremes: (1) the impermeable bedrock of the modelled fracture domain FFM01 in the target area; and (2) the gently dipping deformation zones penetrating fracture domain FFM03.

(6) Finally, the two more saline waters sampled at the site are located at 700–800 m depth in deformation zones from the fracture domains FFM04 (KFM09A) and FFM05 (KFM07A; henceforth represented by grey colours).

With all these observations in mind, a general division of the hydrochemical data was proposed:

- Data from fracture domains FFM01 and FFM06 (dark blue area in Figure 3-2). Most of them are located below ZFMA2 and ZFMF1 and they are plotted together either by boreholes (different colours) or as an homogeneous group (Group 1 in sinthetic plots, in red). In all

the cases a different symbol (triangles or circles) is used to indicate if they correspond to deformation zones or fracture domains, respectively. Together with these waters, the deep groundwater data associated with the deformation zones adjacent to the strongly foliated rocks constituting fracture domains FFM04 and FFM05 along the margins of the target area, are also included but using a different colours (in grey).

- Data representing conditions within the deformation zones ZFMA2, ZFMF1 and the gently dipping deformation zones in the south-east part of the candidate area (FFM03; green area in Figure 3-2) as well as within fracture domain FFM02 (turquoise area in Figure 3-2). The only deep flow anomaly assigned to fracture domain FFM03 (KFM03A at 969 m, circles in the plots) is also included in this group. Therefore, all the waters located in these areas are plotted together either by boreholes (different colours) or as an homogeneous group (Group 2 in some sinthetic plots, in green) indicating in both cases if they correspond to deformation zones (triangles) or fracture domains (circles).

The following sections will summarise the main hydrogeochemical characteristics of the waters taking into account their location in the different zones. When possible, they will be separated by the categories described above.

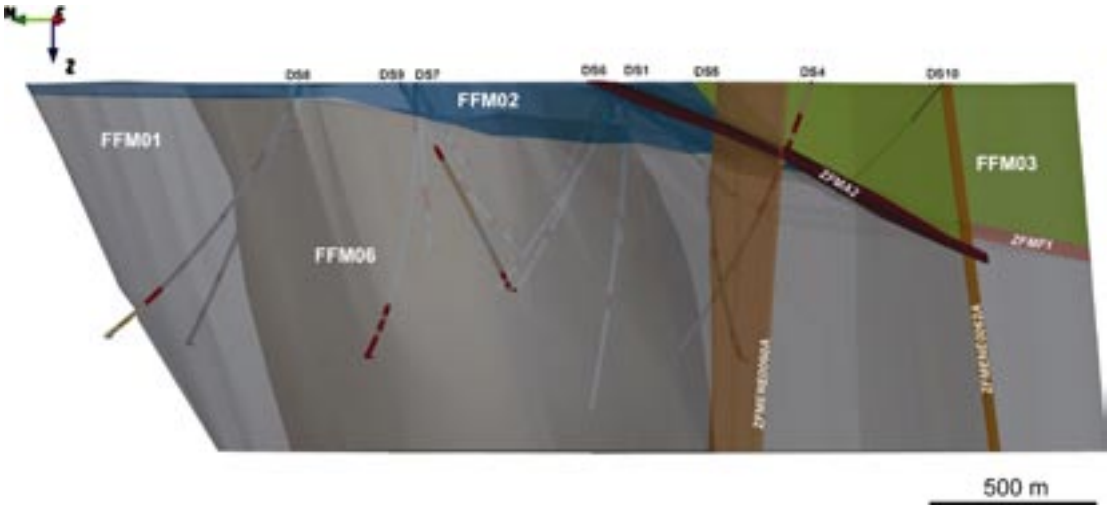

Figure 3-1. *Image of the fracture domain model. Fracture domains FFM01, FFM06, FFM02 and FFM03 are coloured grey, dark grey, blue and green, respectively. The gently dipping and sub-horizontal zones ZFMA2 and ZFMF1 as well as the steeply dipping deformation zones ZFMENE0060A and ZFMENE0062A are also shown (taken from /Olofsson et al. 2007/).*

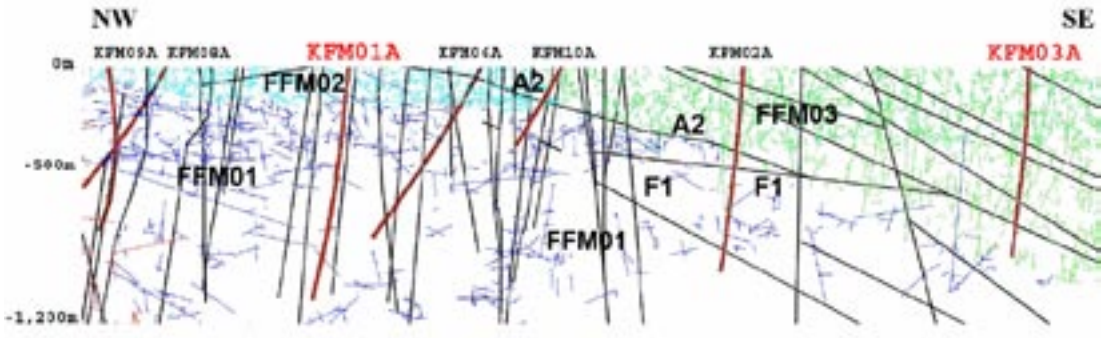

Figure 3-2. *NW-SE cross-section along the central part of the candidate volume showing an example of DFN model realisation with connected open fractures in fracture domain FFM01 (dark blue), FFM02 (turquoise) and FFM03 (green). The cored boreholes KFM01A and KFM03A penetrated the footwall and hanging wall bedrock segments, respectively, on each side of the gently-dipping deformation zones A2 and F1 /Follin et al. 2007b/. Both boreholes KFM01A and KFM03A are drilled subvertically and reaches c. –1,000 m RHB 70. Note the absence of connected open fractures in KFM01A below c. –300 m RHB 70.*

3.2 Final set of data for the "shallow" and "deep" groundwater systems

For this new modelling stage (Forsmark 2.2–2.3), the dataset supplied by SICADA as Data Freeze 2.2 and 2.3, include old (Data Freeze 2.1; July 2005) and new (post-Data Freeze 2.1) samples. Data Freeze 2.2 was delivered in October 2006 and Data Freeze 2.3 in April 2007.

Samples from 2.2 Data Freeze are used for the modelling work and new data from 2.3 Data Freeze are used for comparison, updates and verification. The main advantage of having more data is the possibility of studying the spatial distribution of different parameters, with the aim of associating their values to the processes controlling them in the different areas of the studied system.

Table 3-16 summarises the main information on the samples included in the two last data freezes (2.2 and 2.3). The number of samples indicated here do not include those samples with incomplete major ions chemical data.

The whole set of waters has been evaluated by /Smellie et al. 2008/ and, after an exhaustive analysis of the data quality, an assignment to different categories was made. This categorisation has been fundamental to the selection of the samples used here for modelling purposes.

As a general rule, only samples included in categories 1 to 4 have been used in this work. Only when a specific analysis on the evolution of a sample over time required it, the whole time series has been used. The need of field measurements of pH (and sometimes even of Eh) has reduced very much the available set of samples for speciation-solubility calculations.

The next two sections describe the main chemical characteristics of the whole set of groundwaters separated in two groups: near surface and shallow groundwaters in Section 3.3, and the deep groundwaters in Section 3.4. The samples included in each group and the reason for their inclusion is explained at the beginning of each section.

3.3 Near-surface and shallow groundwaters

Under the term Near-surface groundwaters (NSGW), samples taken in soil pipes from the surface down to 20 meters depth are included. Shallow groundwaters (SGW) are those sampled between 20 and 200 m depth and include waters taken in percussion boreholes but also a few packered samples from cored boreholes. These waters represent the part of the system where the interaction between the superficial groundwaters and the deep groundwaters takes place.

Table 3-16. Number and type of samples included in the final table of Forsmark. The different columns indicate the number of samples delivered in each data freeze (2.1, 2.2 and 2.3) or updated between one data freeze and the next (2.1–2.2 and 2.2–2.3).

	F 2.1	2.1–2.2	F 2.2	2.2–2.3	F 2.3	Total
Percussion Boreholes	45	25	62		22	154
Cored Boreholes	27	78	41	6	26	178
Process Control	4	9				13
Drilling sample	5	2				7
Tube sampling	17	34	14			65
NSGW	188	73	31	7	18	317
Sea Water	71	177	21	4	4	277
Lake Water	319	27	49	6	3	404
Stream Water	315	26	45	4	8	398
Precipitation	23		3	5		31

Due to the hydrological and structural complexity that characterize the Forsmark site, these two groups of waters include a very heterogeneous set of chemical compositions that in part reflect their diverse origin: (a) recent infiltrating waters (recharge system) in different evolution stages; (b) recent waters with important marine influence from the Baltic sea; (c) old waters, originally from deeper depths, that are discharging towards the surface (discharge zones); and (d) pockets of old waters isolated from the main hydrogeological fluxes.

The reason why these samples are evaluated separately from the deep groundwaters (next section) is that the processes controlling their chemical characteristics are quite different. The accepted hypothesis is that reactions mainly take place near the surface, where infiltrating meteoric water is buffered with respect to redox, alkalinity and other geochemical parameters. After these surface reactions, the composition of these waters is mainly altered by mixing with other groundwaters.

A detailed study of the main compositional features and controlling processes in the near surface and shallow system in Forsmark has already been presented in /Tröjbom et al. 2007/. Therefore, this section will only focus on the origin of some contrasting features of these groundwaters and on the effects of these near-surface groundwaters as possible recharge terms of the deep system. With this aim, a description of the compositional variability induced by the carbonate system in the Forsmark near-surface and shallow systems is presented in Subsection 3.3.1. Moreover, a summary of the main conclusions pertaining to the redox state of these waters is presented in Subsection 3.3.2.

3.3.1 Chemical variability and the carbonate system in the shallow and near surface groundwaters from Forsmark

Present calcium concentrations at Forsmark increase rapidly with depth in the top ≈ 100 m of the bedrock (Figure 3-3a) and a similar trend has been observed in Olkiluoto (Figure 3-3b). This is partly related to the contribution of calcium from recent marine waters /Smellie and Tullborg 2005/ or from brackish groundwaters present in discharge zones or as trapped remnants of Littorina waters. These contributions explain the very high TDS and calcium concentrations found in many shallow groundwaters at Forsmark (almost 5,000 mg/L Cl and 900 mg/L Ca, Figure 3-3a). The influence of marine relics of high salinity is especially clear in the topographically "lower" soil tubes (presumably discharge areas). Hence, near-surface groundwaters with chloride contents higher than 200 mg/L have not been included in the subsequent discussion to avoid the "noise" coming from the presence of relict marine waters.

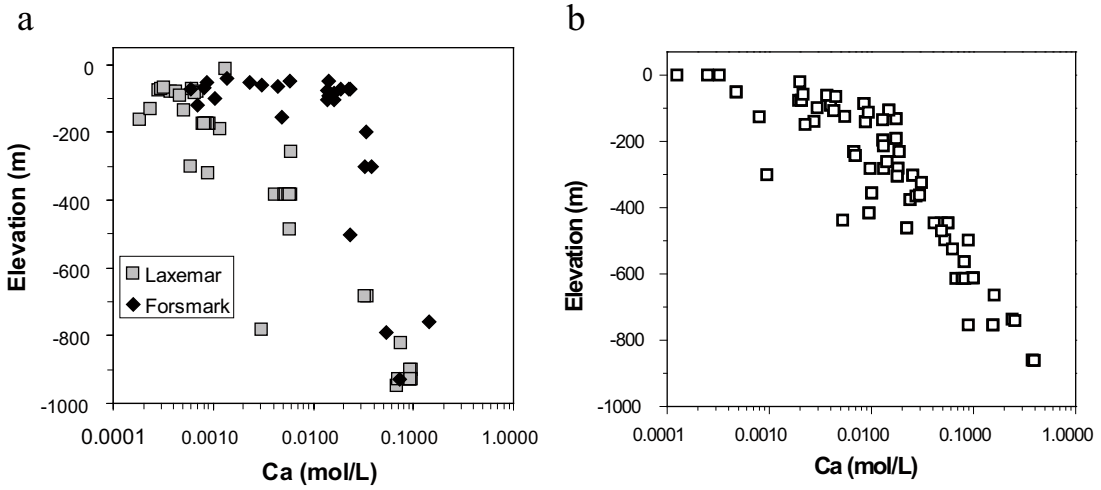

Figure 3-3. Calcium concentrations in groundwaters sampled in Forsmark and Laxemar (a) and Olkiluoto (b) as a function of depth /from Auqué et al. 2006/.

In this subset of near surface groundwaters, calcium concentrations found in Forsmark up to 100 m depth are usually higher than in the equivalent groundwaters in the Laxemar subarea (Figure 3-3a). This can be attributed to the presence of carbonate materials in the Forsmark Quaternary overburden. The Forsmark area contains minor bedrock outcrops (less than 10%) and therefore, till deposits and soils dominate the surface. Immature soil types (young soils) are also frequent. Soils and glacial till deposits from Forsmark show an important influence of calcareous materials from Ordovician limestones present at the sea bottom towards the North of the Forsmark area[14] /Lundin et al. 2004, SKB 2005b/. Most till samples at Forsmark contain between 10–30% calcite (calcium carbonate) per dry weight, which is about 30 times higher than the median value of the Swedish reference data /Tröjbom and Söderbäck 2006/ and also higher than in the Laxemar area.

The presence of calcite in Forsmark soils leads to higher pH values (Table 3-17), higher calcium contents and higher amounts of exchangeable calcium than in the rest of Swedish soils. The bicarbonate contents are also higher in Forsmark than in other Swedish areas, including Laxemar. Therefore, calcite oversaturation is very frequent in Forsmark (Figure 3-4).

Oversaturation with respect to calcite can be reached after calcite dissolution if other sources of Ca or DIC are present (from silicate weathering, evapoconcentration, etc). Degassing of soil waters /Appelo and Postma 2005/ may also lead to calcite oversaturation. However, if the system only reaches a slight oversaturation with respect to calcite (SI < 1), kinetic barriers will inhibit precipitation and will maintain the oversaturation state (Figure 3-4c, d and e; highest oversaturation states around 0.75).

One of the main processes controlling the composition and evolution of the Forsmark near-surface system is the generation of biogenic CO_2 by decay of organic matter (e.g. plant debris) or by root respiration, as indicated by the isotopic signature of waters in most soil tubes ($\delta^{13}C$ values generally between –15‰ and –10‰; SKB, 2007). This input of CO_2 promotes the decrease of pH and, in turn, leads to undersaturation with respect to calcite in the soil waters. Therefore, if this phase is available in the system, it is dissolved, increasing the Ca and HCO_3^- (or DIC) concentrations in soil waters and consuming CO_2. In open-system conditions (high input of CO_2 in the pedogenic environment), the input of CO_2 replenishes the gas consumed during calcite dissolution, enhancing dissolution and increasing the concentrations of Ca and HCO_3^- further than in closed-system conditions.

Therefore, when calcite is available, its dissolution in the near-surface groundwaters is controlled by the existence of open or closed-system conditions with respect to biogenic CO_2. The intensity of biogenic CO_2 production and its effect vary throughout the year (high intensity in summer and low in winter) and also with the pedogenic profile depth. The result is a partially open-system (or mixed open-closed) evolution, typical of natural systems /Clark and Fritz 1997/.

Table 3-17. Average values of soil pH in different horizons of the Forsmark and Laxemar areas compared with the average values in Swedish soils (data from /Lundin et al. 2004, 2005/).

	Forsmark	Laxemar	Sweden
O-horizon (0–30 cm)	6.2 ± 1.1	4.3 ± 0.7	4.2 ± 0.7
B-horizon (0–10 cm)	6.5 ± 1.0	5.2 ± 0.5	4.9 ± 0.5
B-horizon(10–20 cm)	6.7 ± 0.8	5.3 ±0.4	4.9 ± 0.5
C-horizon (55–65 cm)	7.2 ± 0.9	5.2 ± 0.6	5.3 ± 0.6

[14] Calcite in the Forsmark area originates from the seafloor of Gävlebukten, a bay to the Baltic Sea located about 100 km north of the Forsmark site and covered by Cambrian and Ordovician sedimentary bedrock. The calcium-rich material was transported from Gävlebukten and deposited in the Forsmark area during the latest glacial period /Tröjbom and Söderbäck 2006/.

This group of reactions related to the carbonate system explains many of the compositional features of the Forsmark near-surface system. In those parts of the system where the pCO_2 is high (open system) and calcite is available, near surface waters have higher Ca and HCO_3^- (or DIC). On the contrary, in the parts of the pedogenic system where biogenic CO_2 is low or calcite is not available, the concentrations of Ca and HCO_3^- (or DIC) are lower (Figure 3-4).

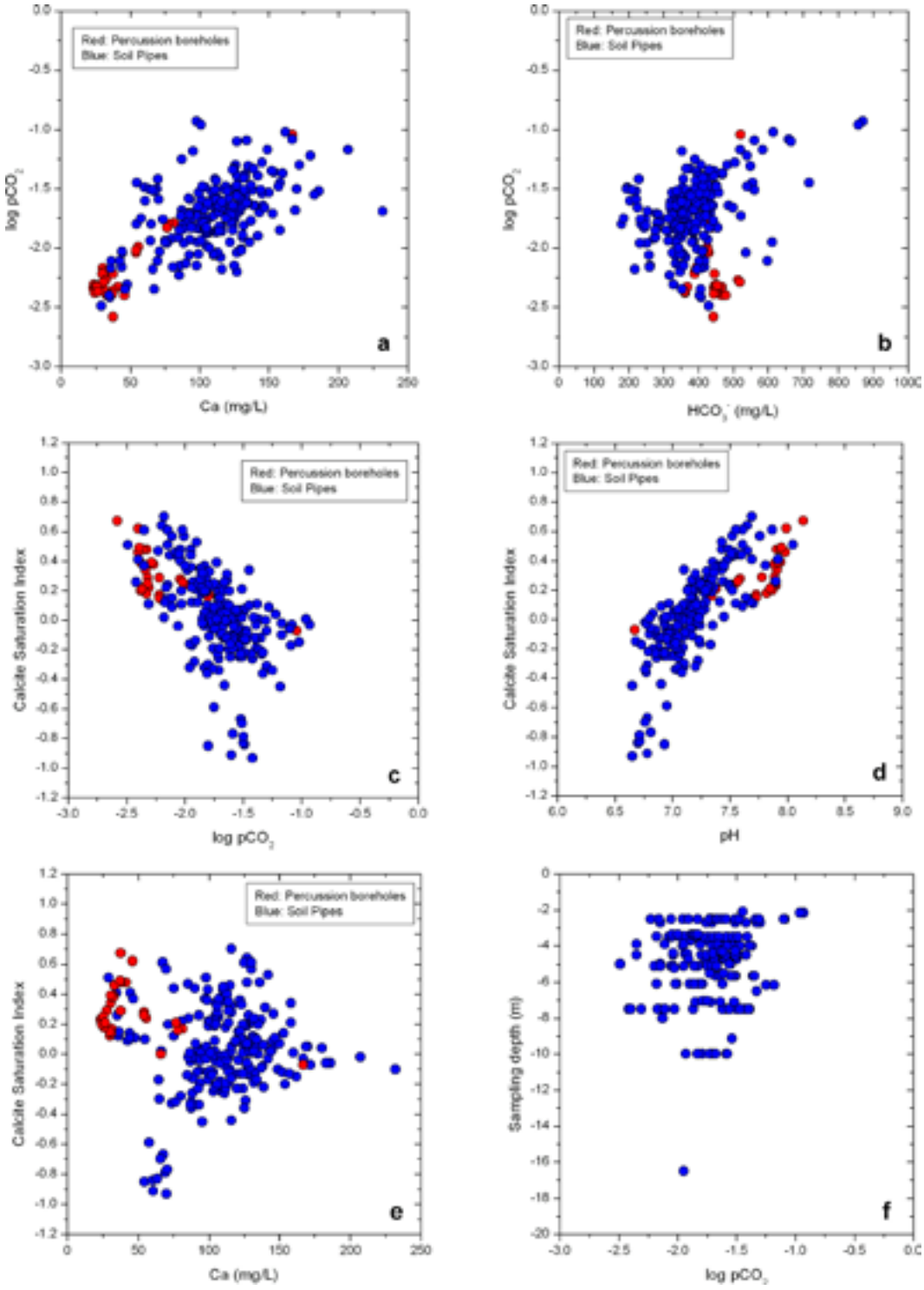

Figure 3-4. *Main chemical features of the carbonate system for the near surface and shallow groundwaters (less than 100 m depth) from Forsmark. log pCO_2 values vs Ca (a) and HCO_3^- (b); calcite saturation index vs pCO_2 (c), pH (d) and Ca (e); and log pCO_2 vs depth of the soil pipes (f).*

The connection between the near-surface groundwaters (up to 20 m depth; soil pipe samples) and the shallow groundwater system (20 to 100–200 m depth, percussion borehole samples) in Forsmark is not clear and a better understanding of the reactions and paths followed by the recharge waters is needed. However, a first approach is to compare the chemical features of both types of waters. Some of theses features are displayed in Figures 3-4 and 3-5.

Shallow groundwaters in Forsmark are characterized by bicarbonate values of 400–500 mg/L (Figure 3-5b). Such high HCO_3^- concentrations cannot derive from calcite dissolution alone and, therefore, suggest the existence of a biogenic CO_2 input. Calcium contents in the shallow groundwaters are, in general, in the lower limit of the range defined by the near-surface groundwaters (30–50 mg/L; Figure 3-5a). This indicates that the waters recharging the shallow hydrological system are those less affected by carbonate dissolution in the overburden. With regard to pH and pCO_2, shallow groundwaters in Forsmark have the highest pH values and the lowest CO_2 partial pressures (Figure 3-4c and d, respectively), suggesting that these waters have evolved under more or less CO_2 closed conditions until reaching equilibrium (or oversaturation) with calcite and showing low calcium concentrations (Figure 3-4e). Thus, it can be inferred that only waters with short residence time in the overburden (fast paths), and therefore, more diluted, are effectively recharging the shallow hydrological systems.

The main implication for the shallow groundwaters (and, indirectly, for the deep groundwater system) is that, even if the presence of carbonates in the overburden may justify the high calcium concentration in the Forsmark shallow groundwaters, its influence is smaller than expected from the calcium concentrations measured in the near-surface groundwaters.

3.3.2 Redox characterisation of the near surface and shallow groundwaters at Forsmark

The study or the redox state of these waters (<200 m depth) is limited by the number (and type) of suitable data: there are field potentiometrical measurements in soil pipes but, due to lack of information about the methodology used, they are not useful for modelling purposes; and there are no field Eh measurements for the samples taken in percussion boreholes. Therefore, the redox characterisation of these waters is based on data from redox-sensitive parameters (redox pairs, microbes and mineralogy). The only available data of direct Eh measurements (with Chemmac) in waters from these depths correspond to packed samples from cored boreholes and they are studied with the rest of the deep groundwaters in the following sections.

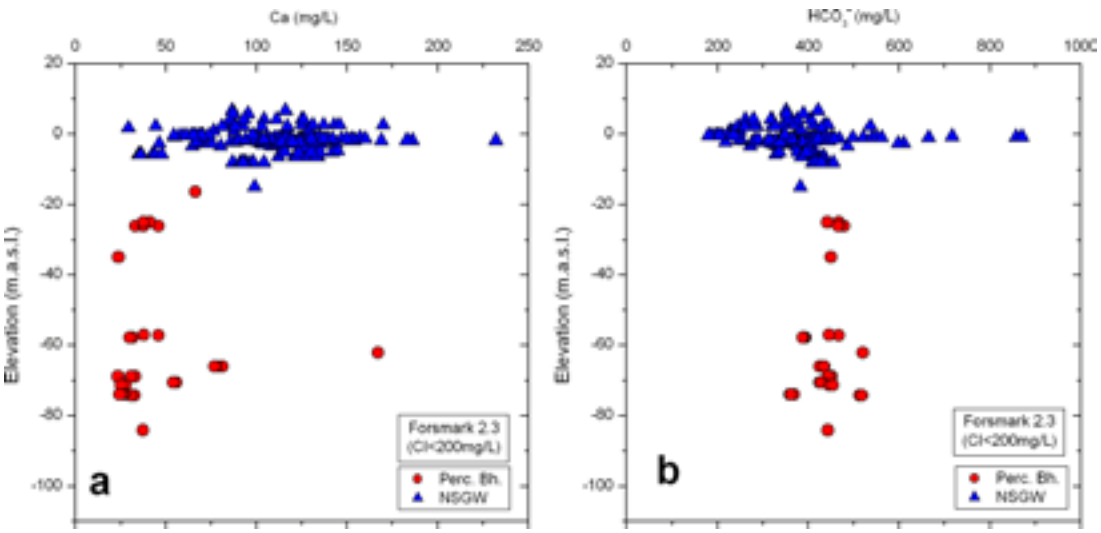

Figure 3-5. *Calcium(a) and bicarbonate (b) distribution with depth (elevation expressed as meters above sea level) in the Near Surface Groundwaters (soil pipes) and other shallow groundwaters from percussion boreholes (100–200 m depth) with Cl concentrations less than 200 mg/L in Forsmark.*

With respect to pH, there are good field pH data for soil pipes, but only laboratory values for percussion borehole samples, which may induce misleading results in speciation-solubility calculations.

Apart from the limitations derived from Eh and pH measurements, the study of the redox state (as happens with the rest of the modelling) is complicated by mixing between a "recharge system" (constituted by Na-HCO_3^- dilute groundwaters of meteoric origin) and a possible "discharge system" (with "old" brackish Na-Ca-Cl-SO_4^{2-} waters). Due to all these shortcomings, only a simplified model of the effective redox state and processes in this shallow system is proposed here.

Concentrations of Fe^{2+} and Mn are variable but high. High Fe^{2+} concentrations in shallow groundwaters are indicative of reducing conditions, since the original source for iron is the reductive dissolution of Fe(III)-silicates or ferric oxyhydroxides. Although reductive processes may proceed abiotically, microbially-mediated reactions through dissimilatory iron reduction seem to play a key role in Fe^{2+} mobilisation /Banwart 1999, Larsen et al. 2006/. With regard to Mn, its high concentration in all the shallow groundwaters seems to be the result of anaerobic oxidation of organic matter by microbes. Consistent with this hypothesis of a biological contribution to the high Fe and Mn concentrations in Forsmark groundwaters, iron-reducing and manganese-reducing bacteria (IRB and MRB, respectively) have been detected in some of these waters /Hallbeck and Pedersen 2008/.

The behaviour of Fe and Mn is also affected by the precipitation of carbonate minerals, since a generalized equilibrium with respect to siderite and rhodocrosite is found in the shallow Forsmark groundwaters. Similar equilibrium situations have been reported with respect to siderite during the Äspö Large-Scale Redox Experiment /Banwart 1999/ and with respect to rhodochrosite in the shallow and superficial groundwaters from other Swedish and Finnish sites /Gimeno et al. 2007/.

For sulphide (S^{2-}), concentrations are highly variable in the shallow groundwaters from Forsmark but, in general, low contents are detected, suggesting a limited activity of sulphate-reducing bacteria (SRB). Therefore, equilibrium with respect to "amorphous" or disordered mackinawite (indicative of the existence of present sulphate-reducing activity in the system) is attained only locally. In any case, more detailed sampling would be necessary to clearly identify the location of the sulphidic zones in the shallow groundwater system.

Feasible redox potentials for the shallow groundwaters in post-oxic conditions may be inferred from $Fe(OH)_3/Fe^{2+}$ heterogeneous redox pair (with the solubility value deduced by /Banwart 1999/, with values between –135 and –147 mV.

All these data suggest the existence of a generalized anoxic state in the shallow groundwaters. Although mineralogical data (distinctive presence of goethite in some fracture fillings; /Drake et al. 2006/) support the existence of "old" oxidising water inputs through fractures in the shallow system, these oxidizing events seem not to have been intense enough to exhaust the reducing capacity of the mineral phases present in the fracture fillings (Fe^{2+}-minerals such as chlorite or even pyrite).

3.3.3 Summary of the near surface and shallow groundwaters

The study of the carbonate system has shown that the biogenic CO_2 input (decay of organic matter and root respiration) and the associated weathering of silicates + calcite control the pH and the concentrations of Ca and HCO_3^- in the near-surface groundwaters.

Seasonal variability of CO_2 input produces variable but high calcium and bicarbonate contents in the Forsmark near-surface waters: up to 240 mg/L Ca and 150 to 900 mg/L HCO_3^-. These high concentrations are due to the extensive presence of limestones in the overburden, a feature very uncommon in Swedish soils.

Shallow groundwaters (from 20 to 100–200 m depth) do not show the same variability and high HCO_3^- or Ca contents as the near-surface groundwaters. Therefore, most near-surface groundwaters are isolated and not hydraulically connected to the shallow groundwater systems. Only waters with short residence time in the overburden (fast paths), and therefore, more diluted, are effectively recharging the shallow hydrological systems.

Weathering reactions in the overburden are tightly coupled to the biogenic CO_2 input. This CO_2 input is an important source of acidity that is consumed through mineral reactions, increasing the dissolved contents of the waters. But, even so, recharge waters are not affected by important increases in their chemical contents. Therefore, if biological activity becomes more restricted (e.g. during glaciations) reactions will mainly proceed inorganically and recharge waters will probably be even more dilute.

Although more detailed studies are necessary to complete the redox characterisation of the shallow groundwater system, tentative calculations allow inferring the existence of a generalised anoxic state with possible episodic inputs of oxidising waters. However, these oxidising episodes have not been intense enough to exhaust the reducing capacity of fracture filling minerals (such as Fe-II chlorite or pyrite) still present in the shallow system.

For calculation purposes in the Forsmark shallow system, the use of the heterogeneous pair $Fe(OH)_3/Fe^{2+}$ seems to produce consistent Eh values.

3.4 Non-redox system in the deep groundwaters

Under the term “deep groundwaters” all samples taken approximately below 100 m depth are included, which correspond to waters sampled both in percussion boreholes and in cored-boreholes. It means that some of the waters considered as “shallow” waters in the previous sections are also analysed here. The reason to include them also here is that they represent the first stage of groundwater evolution and the connection with the upper part of the bedrock system. In other words, they are used as “initial” or “boundary” conditions for the subsequent evolution.

The distribution of the main non-redox chemical components, together with the description of their geochemical controls is shown next. For this purpose, apart from the chemical data, mixing proportions of the end-member waters and solubility controls are also used when necessary.

Mixing proportions have been calculated with M3 using the Forsmark 2.3 groundwater dataset, the common set of variables (Na, K, Ca, Mg, HCO_3^-, Cl, SO_4^{2-}, Br, δ^2H and $\delta^{18}O$) and the four end members Deep Saline (low in sulphate), Old Meteoric-Glacial ($\delta^{18}O = -16‰$), Littorina, and Altered Meteoric (sample HFM09). Mixing proportion results are shown in Table 3-18. Speciation-solubility calculations have been performed with the code PHREEQC /Parkhurst and Appelo 1999/ and the WATEQ4F thermodynamic database /Ball and Nordstrom 2001/.

The hydrochemical data have been graphically displayed using X-Y plots to derive trends that may facilitate interpretation. Since chloride is generally conservative in normal groundwaters, its use is appropriate to study hydrochemical evolution trends when coupled to ions, ranging from conservative to non-conservative, to provide information on mixing, dilution, sources and sinks. Moreover, here chloride acts as a tracer of the main irreversible process operating in the system – mixing –, which will be demonstrated below. Therefore, many of the X-Y plots involve chloride as one of the variables.

However, due to the important heterogeneity of the system, visualization of the spatial distribution of different geochemical parameters is not an easy task. Therefore, after these X-Y plots, the following figures will show the distribution with depth of different parameters in the sampled sections and these plots will be based on the basic division of domains already presented in Section 3.1. For each parameter two different plots are used: one for the waters corresponding to fracture domains FFM01 and FFM06, and to the deep waters located in the margins of the target area (fracture domains FFM04 and FFM05, represented by boreholes KFM07A and 09A, coloured in grey); and another one for the waters corresponding to fracture domains FFM02 and FFM03 and to the gently dipping deformation zones.

Table 3-18. Mixing proportions calculated with M3.

Borehole	SampleNo	Depth (m)	%Deep Saline	%Old Meteoric + Glacial	%Littorina	%Altered Meteoric
HFM02	12006	–43.25	0.2	9.0	3.6	87.3
HFM03	4167	–21.25	0.4	14.2	1.9	83.5
HFM04	12003	–61.75	0	12.3	0	87.7
HFM05	12374	–153.25	2.6	39.0	33.5	24.9
HFM06	4618	–70	0	9.7	14.5	75.8
HFM08	4535	–89.75	1.6	22.0	30.0	46.3
HFM08	4522	–138.5	2.3	27.9	56.7	13.1
HFM10	4965	–117.5	4.0	28.9	32.3	34.8
HFM12	8018	–117	4.0	58.0	10.2	27.8
HFM13	12009	–163	4.3	33.4	37.2	25.1
HFM16	12379	–59	0	1.8	1.6	96.6
HFM17	8246	–31.25	0.1	0	3.2	96.8
HFM19	12010	–176.25	2.7	25.3	52.6	19.4
HFM22	12076	–62.75	1.9	13.7	27.9	56.5
HFM24	12222	–33.75	0.1	6.1	5.4	88.3
HFM27	12506	–54.4	0.8	16.6	29.1	53.5
HFM32	12286	–18	2.5	19.7	38.7	39.2
HFM32	12285	–63.24	3.0	23.5	40.3	33.2
HFM32	12288	–147.68	5.5	46.3	31.9	16.2
HFM32	12284	–29.05	2.6	20.5	42.5	34.4
HFM33	12247	–136.25	4.6	27.9	43.0	24.5
HFM36	12550	–58	1.0	31.5	5.4	62.1
KFM01A	12397	–115.79	4.5	39.1	32.2	24.3
KFM01A	4724	–176.27	4.2	32.1	42.7	21.0
KFM01A	4538	–111.75	5.4	59.8	28.5	6.3
KFM01B	4951	–36.61	0.0	7.8	1.9	90.3
KFM01D	12316	–340.87	12.4	39.1	10.9	37.7
KFM01D	12366	–253.31	5.4	25.2	25.2	44.1
KFM01D	12360	–293.12	5.5	23.2	28.4	42.9
KFM01D	12362	–282.32	4.8	23.6	28.1	43.6
KFM01D	12343	–445.17	14.9	26.3	9.7	49.1
KFM01D	12361	–155.69	4.5	33.5	25.5	36.5
KFM01D	12363	–211.45	3.8	18.4	28.9	48.9
KFM02A	4398	–51.67	0.1	9.8	0.8	89.3
KFM02A	12004	–494.97	4.3	27.3	45.4	23.0
KFM02A	12002	–417.8	5.6	42.5	36.6	15.3
KFM02A	8100	–108.86	0.6	11.7	5.0	82.7
KFM02A	8016	–503.34	4.4	27.3	43.2	25.2
KFM03A	8284	–442.35	5.1	40.2	41.1	13.5
KFM03A	12001	–631.1	10.1	52.2	21.5	16.2
KFM03A	8744	–792.11	14.1	62.0	7.9	16.0
KFM03A	8273	–631.91	10.1	52.9	17.2	19.8
KFM03A	8011	–379.06	4.2	33.4	46.8	15.6
KFM03A	12005	–969.14	22.3	72.4	3.7	1.6
KFM03A	8152	–977.67	20.2	72.9	3.2	3.7
KFM03A	8281	–930.5	17.9	63.1	7.2	11.9
KFM03A	8017	–440.79	5.4	35.8	39.3	19.5

KFM04A	8267	–197	4.2	35	42	19
KFM04A	8267	–197	3.6	47.4	40.3	8.7
KFM05A	8332	–90.41	2.9	19.8	44.1	33.2
KFM06A	8785	–645.34	16.2	45.7	6.8	31.4
KFM06A	12399	–298.54	8.3	47.1	19.1	25.5
KFM06A	12398	–622.78	13.1	52.4	12.1	22.4
KFM06A	8809	–301.99	8.5	53.2	15.8	22.5
KFM06A	8187	–39.37	0.1	13.2	2.9	83.8
KFM06C	12500	–434.84	7.7	46.7	22.7	22.8
KFM07A	8843	–759.72	30.2	59.9	5.8	4.0
KFM08A	12000	–546.42	13.1	65.6	8.1	13.2
KFM08A	8786	–127.33	3.4	87.1	7.4	2.2
KFM09A	12243	–614.21	31.1	65.0	3.9	0
KFM10A	12552	–214.77	7.5	74.6	12.3	5.7
KFM10A	12509	–328.08	4.1	20.8	39.2	35.9

This subdivision is based on the main conclusions presented in Section 3.1 which consider also the indications from /Smellie et al. 2008/, about the two different systems developed in the Forsmark area: (a) the higher transmissive deformation zones and the more fractured domains (FFM03 and parts of FFM01/02), and (b) the target area (FFM01), where at least parts of the aquifer have been isolated.

3.4.1 Ion-ion plots

This section is a summary of previous works from /Gimeno et al. 2005/ and /Smellie and Tullborg 2005/ developed for SDM version 1.2 in Forsmark. However, here an update of the data together with their overall interpretation (including modelling results) and an indication of their location in the framework of the structural model of the system, is also included. Then, the following ion-ion plots show the relationship between different non-redox chemical parameters (in some cases also saturation states for minerals of interest) and chloride in two different plots, one showing the values coloured by the borehole and the other one with the values coloured by the structural domain. In most cases the values corresponding to the Littorina and the Deep Saline end-members are also shown.

Sodium shows an overall positive correlation with chloride (Figure 3-6a and b), which reflects that mixing is the main process controlling Na content. But, in detail, two different trends can be seen: the first represented by the more saline groundwaters (clearly affected by the Deep Saline end-member) and the second clearly visible from the brackish groundwaters with 5,500 mg/L of chloride (with an important contribution of the Littorina end-member).

These two mixing trends are even more clearly recognizable in the case of sulphate (Figure 3-6c and d) or magnesium (Figure 3-6e and f). These two components have a clear contrast between the contents in the pre-Littorina waters (low values from previous mixtures between deep saline and more dilute groundwaters) and the Littorina end-member (comparatively higher).

For these three elements the plots showing the different structural domains indicate that waters from the more transmisive deformation zones (triangles) from FFM02 and FFM03 (green colours) follow the trend towards Littorina influence in a higher degree than the waters from the other system dominated by fracture domain waters from FFM01. The most saline waters samples in the system (up to now) are located outside the target area (FFM04 and 05) and correspond to boreholes KFM07 and KFM09. They show a clear trend towards the Deep Saline end-member.

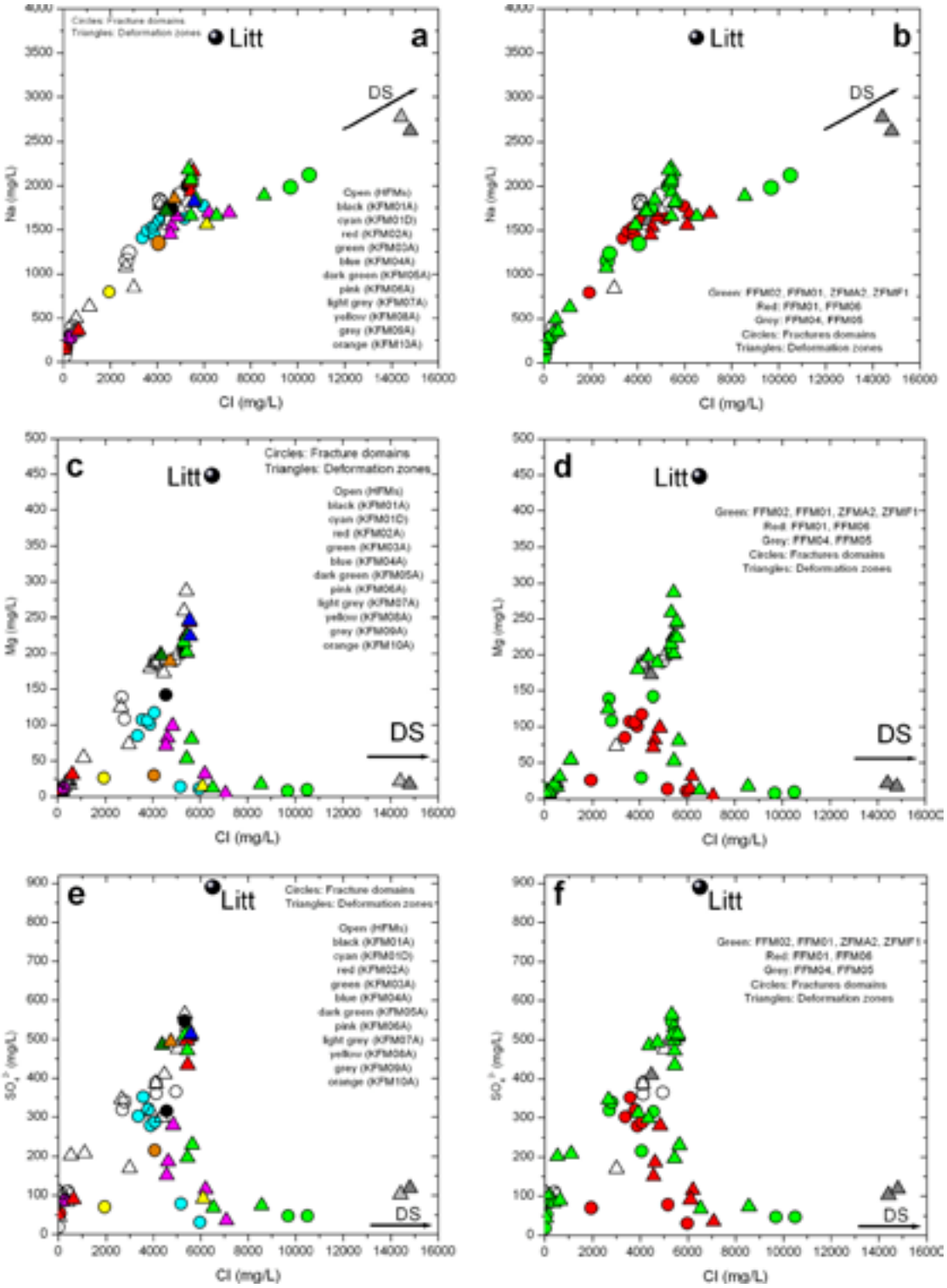

Figure 3-6. *Sodium (a and b), magnesium (c and d) and sulphate (e and f) vs chloride in the groundwaters from Forsmark area. Groundwater samples are coloured by boreholes (left panels) and by the structural domains (right panels) In both cases, triangles indicate deformation zones and circles, fracture domains. Litt and DS indicate the position of these end-members (Littorina and Deep Saline) in the plots; due to the fact that the chloride content in the Deep Saline water is close to 50,000 mg/L, the chemical values for this end-member are only indicated as an arrow orientated towards their position. The rest of the plots in the section follow the same structure.*

Sulphate deserves an additional comment as its behaviour is clearly different with respect to what has been found in Laxemar. While sulphate in Forsmark shows an initial increase with the maximum values when salinity is around 5,000–6,000 mg/L of Cl, and then there is a clear decrease towards zero (Figure 3-6e and f; similar to the behaviour in Olkiluoto), in Laxemar sulphate increases gradually as the salinity increases.

This contrasting behaviour must be related to the process controlling sulphate content in these waters. Forsmark groundwaters are undersaturated with respec to gypsum (Figure 3-7a and b) but they evolve towards equilibrium with it as chloride increases up to 6,000 mg/L. Then, the waters evolve towards a more undersaturated state and finally the deepest groundwaters from KFM03 and the more saline waters from outside the target area seem to evolve again to less undersaturated values. The same behaviour has been seen in Olkiluoto groundwaters. However, in Laxemar groundwaters the gypsum SI trend indicates a clear evolution towards equilibrium which is reached at chloride values of 10,000 mg/L and maintained even in the most saline waters.

This behaviour support the hypothesis that the main source of sulphate in the Forsmark groundwaters is the contribution of Littorina end-member, not being factible (as it is in the case of Laxemar) the participation of gypsum dissolution (which, in fact, has not been identified in the Forsmark fracture fillings).

For calcium (Figure 3-8a and b) the separation between the two trends (Littorina or Deep Saline) is not as clear as for the previous components. In this case the dominant trend is the one towards the saline end-member, perfectly reasonable as it is the only end-member with very high calcium contents. The positive correlation with increasing chloride content in the most saline groundwaters, indicates that mixing is the main process controlling the concentration of this element in these groundwaters.

In spite of the extent of reequilibrium with calcite affecting dissolved Ca (see below), the high Ca content of the mixed waters (coming from saline end members) obliterates the effects of mass transfer with respect to this mineral. This fact justifies the quasi-conservative behaviour of calcium, at least in waters with chloride contents higher than 5,000 mg/L. Simple theoretical simulations of mixing between a brine end member and a dilute water, with and without calcite equilibrium, have shown the negligible influence of reequilibrium on the final dissolved calcium contents.

The calcium trend towards Littorina is much less clear as calcium contents in the Littorina end-member are very low and its contribution in the mixture with pre-Littorina waters is comparatively negligible with respect to the calcium content already present in the pre-Littorina groundwaters.

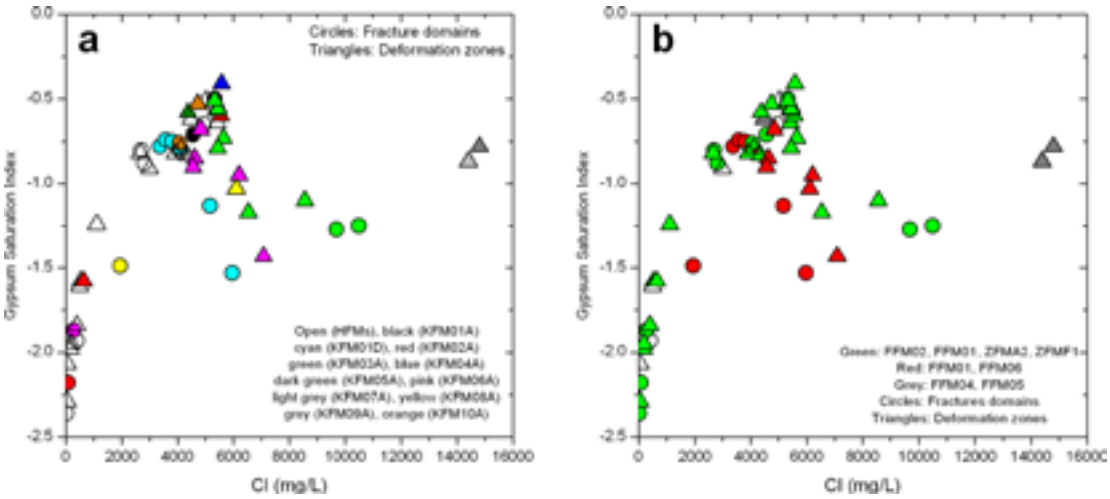

Figure 3-7. *Gypsum saturation index vs chloride in the groundwaters from Forsmark area. Groundwater samples are coloured by boreholes (a) and by the structural domains (b) In both cases, triangles indicate deformation zones and circles, fracture domains.*

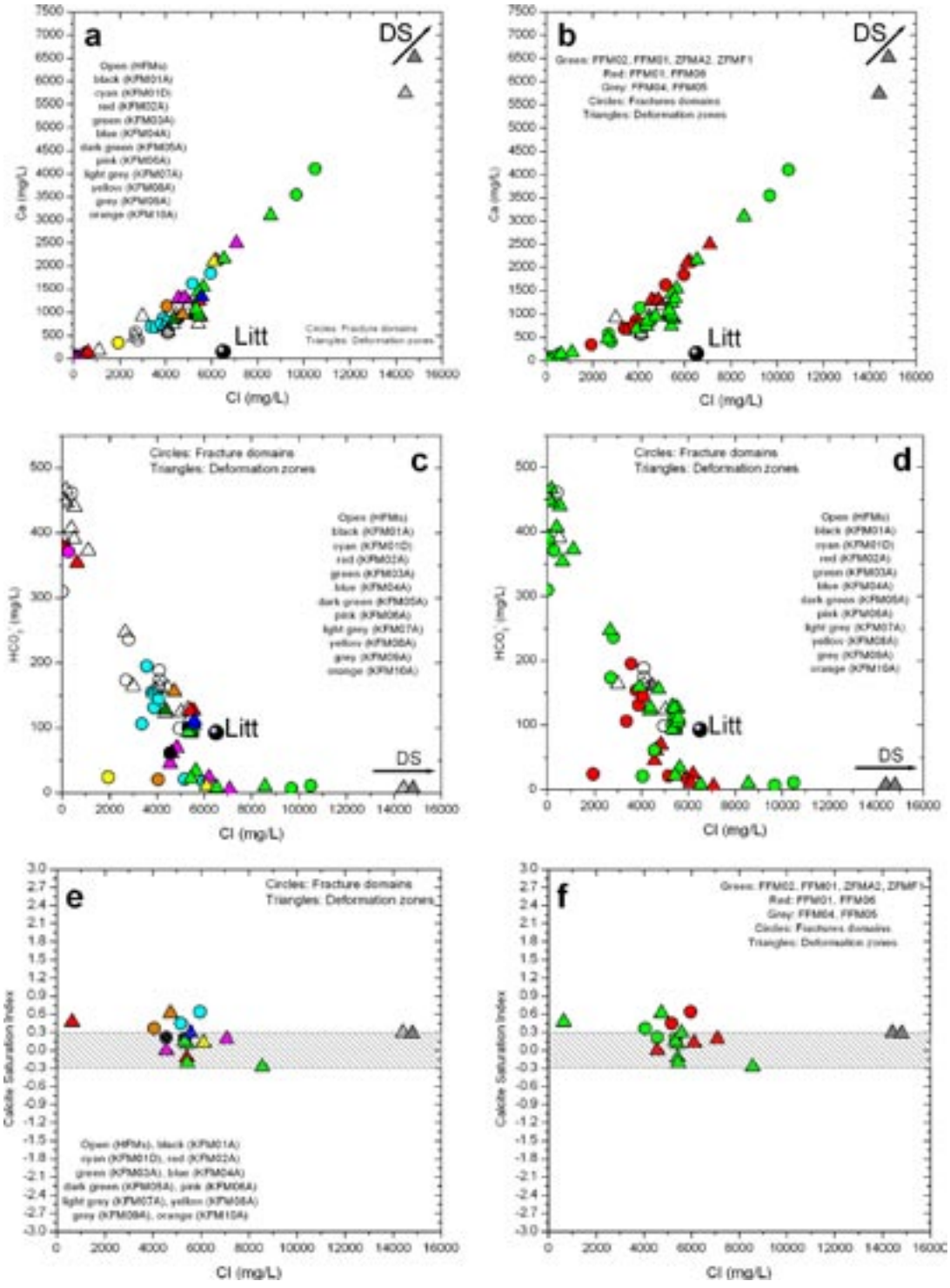

Figure 3-8. *Calcium (a and b), alkalinity (c and d) and calcite saturation index (e and f) vs chloride in the groundwaters from Forsmark area. Groundwater samples are coloured by boreholes (left panels) and by the structural domains (right panels) In both cases, triangles indicate deformation zones and circles, fracture domains. Litt and DS indicate the position of these end-members (Littorina and Deep Saline) in the plots; due to the fact that the chloride content in the Deep Saline water is close to 50,000 mg/L, the chemical values for this end-member are only indicated as an arrow orientated towards their position.*

Bicarbonate (alkalinity) is, together with chloride and sulphate, the third major anion in the system, and is the most abundant in the non-saline waters. Its concentration is high in the shallow groundwaters (Figure 3-8c and d) as a result of atmospheric and biogenic CO_2 influence and/or calcite dissolution (see Section 3.3). The alkalinity content reaches equilibrium (or over-saturation) with calcite in the fresh groundwaters and then decreases dramatically with depth as it is consumed by calcite precipitation, whereas calcium keeps increasing as a result of mixing.

Figure 3-8 panels e and f, show the calcite saturation index in the Forsmark waters. Only samples with pH values measured in the field have been plotted. Most of the brackish and saline groundwaters are in equilibrium with this mineral (inside the considered uncertainty range of ±0.3 SI units /e.g. Nordstrom and Ball 1989/, shadowed area in panels e and f of Figure 3-8), supporting the re-equilibrium processes after the mixing events. The generalized calcite equilibrium is the main control of the pH values in these waters.

The content of dissolved SiO_2 in groundwaters has a narrow range of variation for the saline groundwaters, indicative of a possible solubility control (Figure 3-9a and b). This range of silica contents enlarges at Cl ~ 5,500 mg/L, where waters show different silica contents for the same chloride concentration. Nevertheless, most groundwaters are in equilibrium conditions with respect to chalcedony (Figure 3-9c and d) within the usual uncertainty of ±0.2 SI units /e.g. Deutsch 1997/ for this mineral.

Therefore, the increase in dissolved SiO_2 by dissolution of silicates in surface waters and shallow groundwaters seems to evolve towards geochemical conditions where dissolved silica ir controlled by chalcedony solubility.

3.4.2 Distribution with depth

As has been already stated, chloride is one of the main components in these groundwaters and it is directly correlated with their salinity. The uppermost 100–150 m in the Forsmark area are represented in general by groundwaters from deformation zones (triangles). These groundwaters display a wide chemical variability (here with respect to chloride), mainly due to the presence of discharge waters or saline waters of marine origin.

However, below this shallow depths, Cl distribution with depth is slightly different depending on the zone (Figures 3-10a and b). Waters from FFM01 (Figure 3-10a) show a progresive increase of chloride with depth from –100 m down to –650 m, almost independently of representing fracture domains or defomation zones (circles and triangles). Then, waters from FFM04 and 5, outside the target area (boreholes KFM07A and 09A) show an important shift to higher values. This higher salinity is clearly associated with a higher proportion of the Deep Saline end-member (Figure 3-10c).

Waters from the other system (FFM02 and FFM03 and the gently diping deformation zones, Figure 3-10b) have a wide range of Cl contents at 100 m depth reaching values as high as 5,000 mg/L, then they show a range of constant Cl contents around this value from 200 to 600 m depth and then they increase progressively with depth but only up to 10,000 mg/L of Cl even at around 1,000 m depth. This trend is also consistent with the proportion of the deep saline end-member in these waters (Figure 3-10d) and more interesting, most of the groundwaters with a constant value of Cl around 5,500 mg/L are characterized by a high and relatively constant Littorina contribution (Figure 3-10f) which is not so important in the other system (Figure 3-10e).

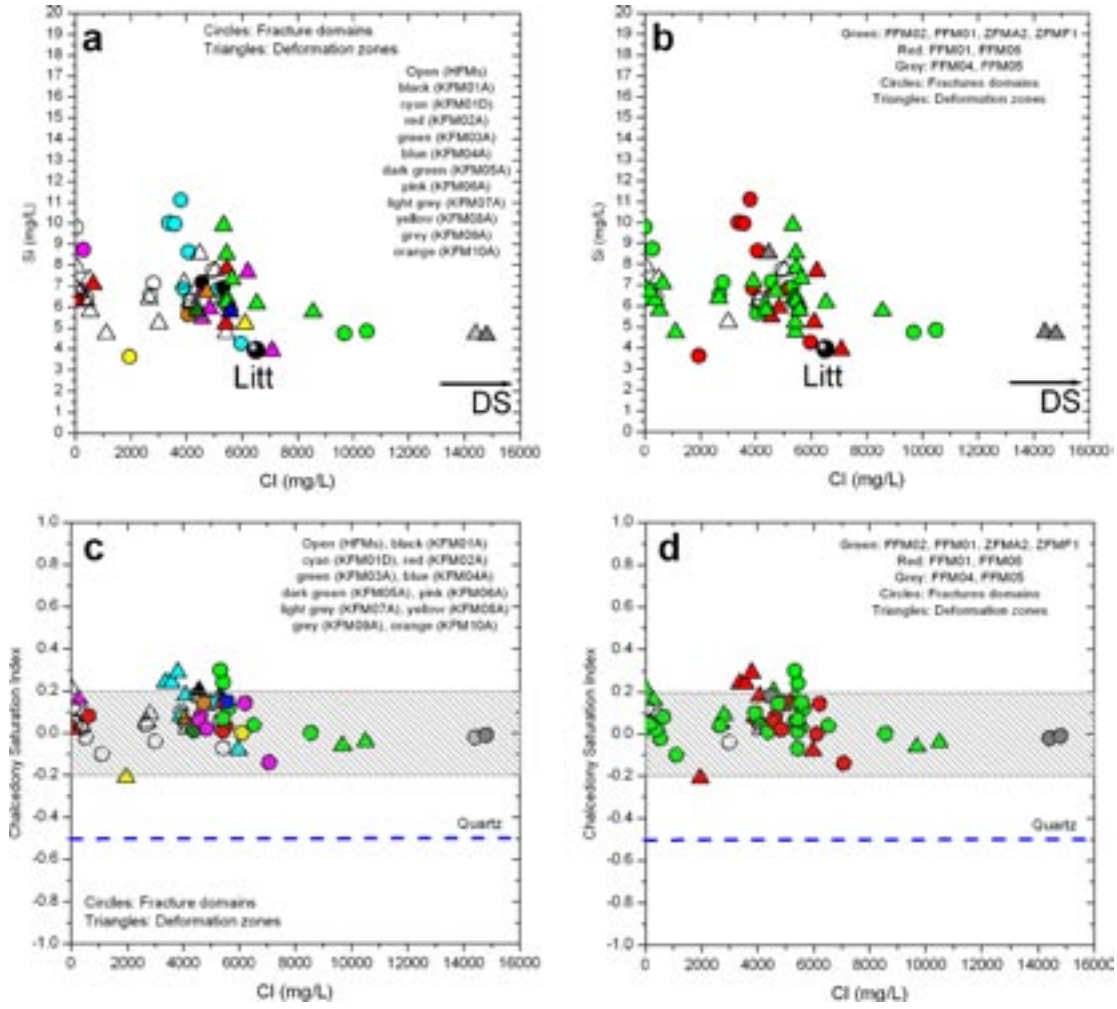

Figure 3-9. *Silicon (a and b) and chalcedony saturation index (c and d) vs chloride in the groundwaters from Forsmark area. Groundwater samples are coloured by boreholes (left panels) and by the structural domains (right panels) In both cases, triangles indicate deformation zones and circles, fracture domains. Litt and DS indicate the position of these end-members (Littorina and Deep Saline) in the plots; due to the fact that the chloride content in the Deep Saline water is close to 50,000 mg/L, the chemical values for this end-member are only indicated as an arrow orientated towards their position.*

Figure 3-11 shows the same kind of plots for calcium (panels a and b) and sodium (panels c and d). Comparing these plots with the ones for chloride a similar behaviour can be observed, mainly for calcium, that follows exactly the same trends as chloride in the two separated systems (panels a and b in Figures 3-11 and 3-10). Again, sodium shows a relatively constant concentration around 2,000 mg/L in the fracture domain FFM02 and FFM03 (Figure 3-11d), also associated to the high proportions of Littorina contributions down to 500 m depth. In the other system (fracture domain FFM01, Figure 3-11c) sodium also shows a more or less constant concentration but in this case it is around 1,500 mg/L as a consequence of a less marine contribution in the uppermost 300 m and a higher contribution of the saline end-member deeper down.

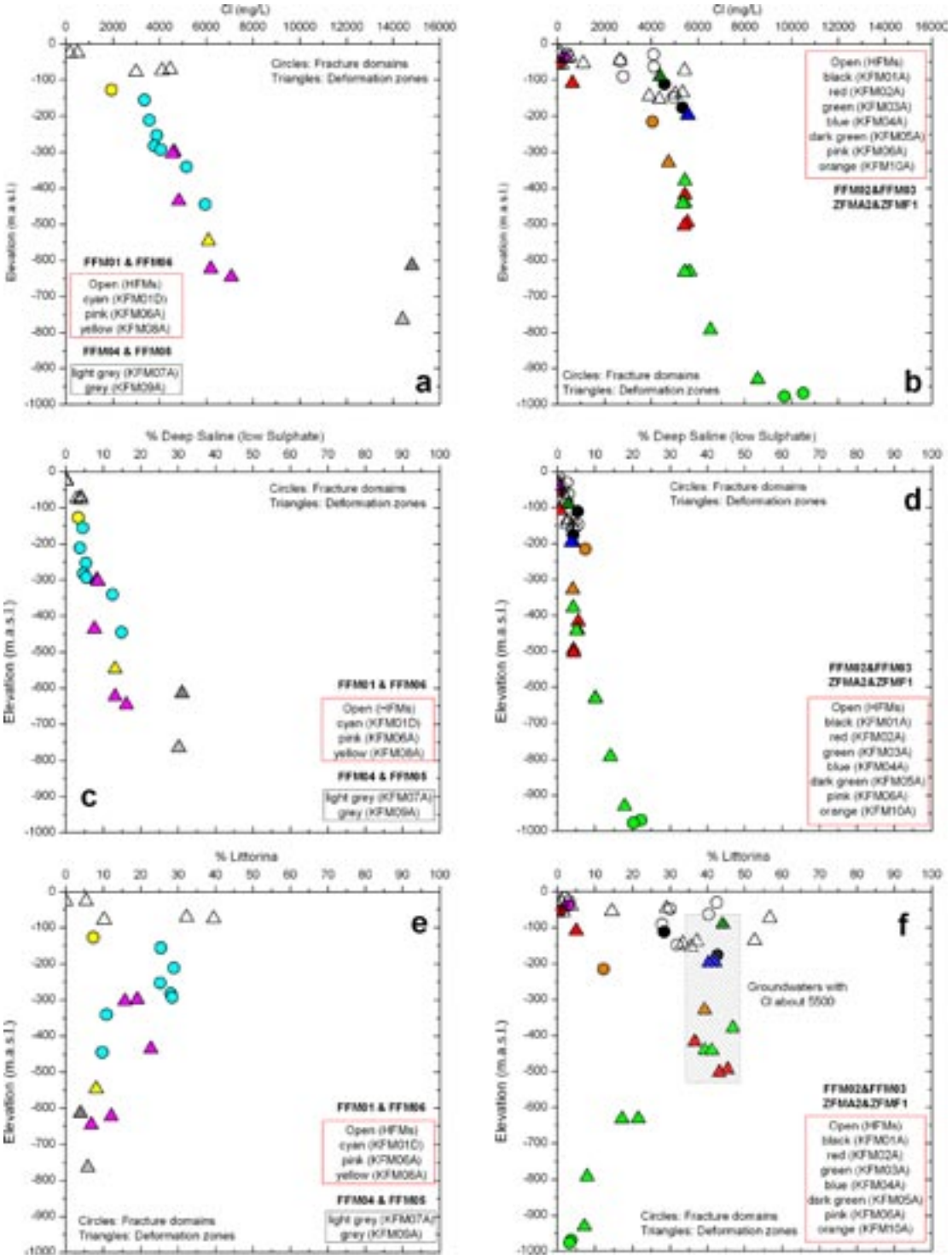

Figure 3-10. *Chloride distribution (a, b) and Deep Saline (c, d) and Littorina (e, f) mixing proportions with respect to depth in the two different systems at Forsmark. Left plots represent the waters sampled in the fracture domain zones (FFM01 and FFM06) including those samples from marginal areas to the target area (FFM04 and FFM05; in grey). Right plots represent waters samples in fracture domains FFM02 and FFM03, and samples taken from the gently dipping deformation zones. In both cases, triangles indicate deformation zones and circles, fracture domains. The rest of the plots in the section follow the same structure.*

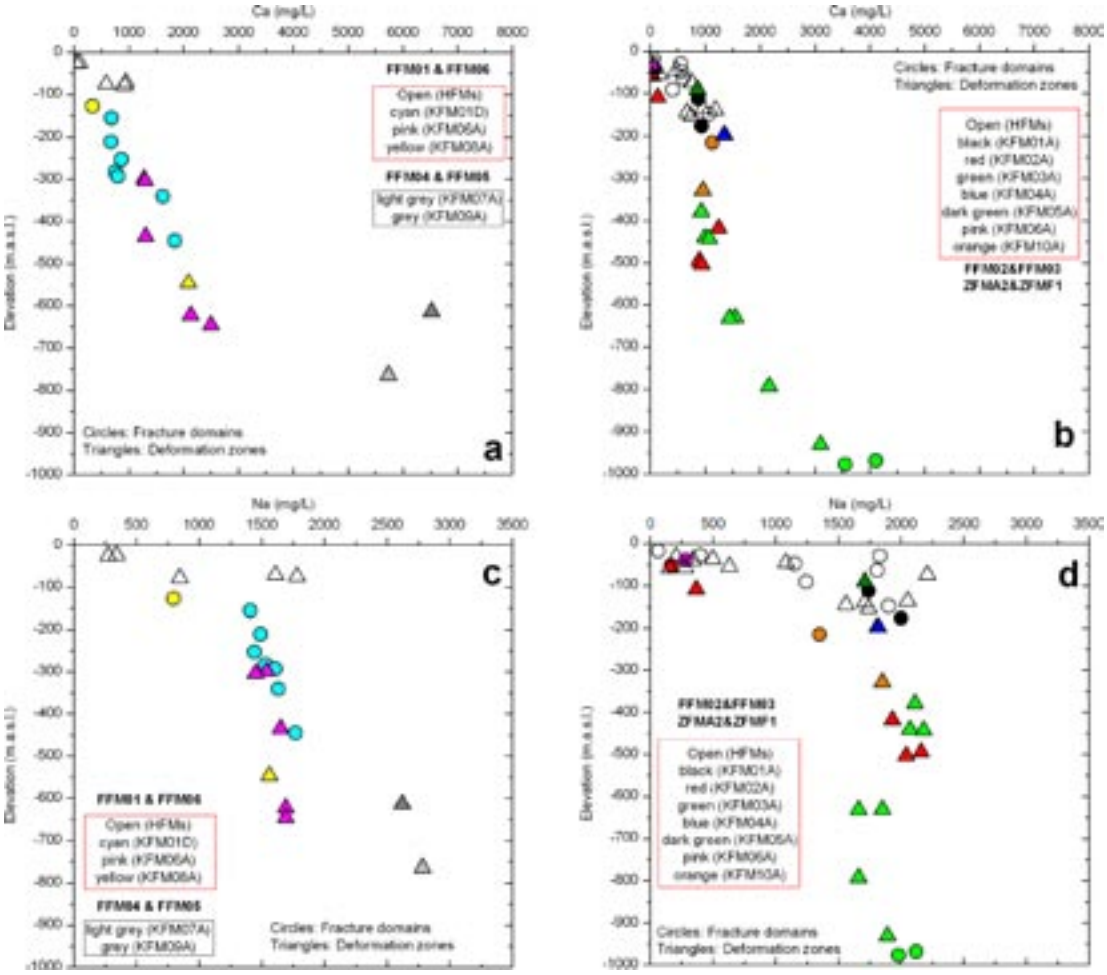

Figure 3-11. *Calcium and sodium distribution with respect to depth in the two different systems at Forsmark. Left plots represent the waters sampled in the fracture domain zones (FFM01 and FFM06) including those samples from marginal areas to the target area (FFM04 and FFM05; in grey). Right plots represent waters samples in fracture domains FFM02 and FFM03, and samples taken from the gently dipping deformation zones. In both cases, triangles indicate deformation zones and circles, fracture domains.*

Sulphate and magnesium have also a different behaviour between the two systems (Figures 3-12a and c versus b and d). Waters from FFM01 (Figure 3-12a and c) have lower sulphate and magnesium contents than waters from the other system (panels b and d) and they decrease progressively with depth reaching the lowest values in the deepest samples from the marginal zone (FFM04 and FFM05; grey samples).

Waters from the other system (FFM02 and FFM03 and the gently diping deformation zones, Figure 3-12b and d) display a very wide range of values in the first 150 m due to marine influence either recent (Baltic Sea) or old (Littorina relicts or discharge areas). Maximum sulphate and magnesium contents are found between 200 and 600 m depth and then decrease progressively with depth. Again, this behaviour is clearly the result of the Littorina influence (Figure 3-12f).

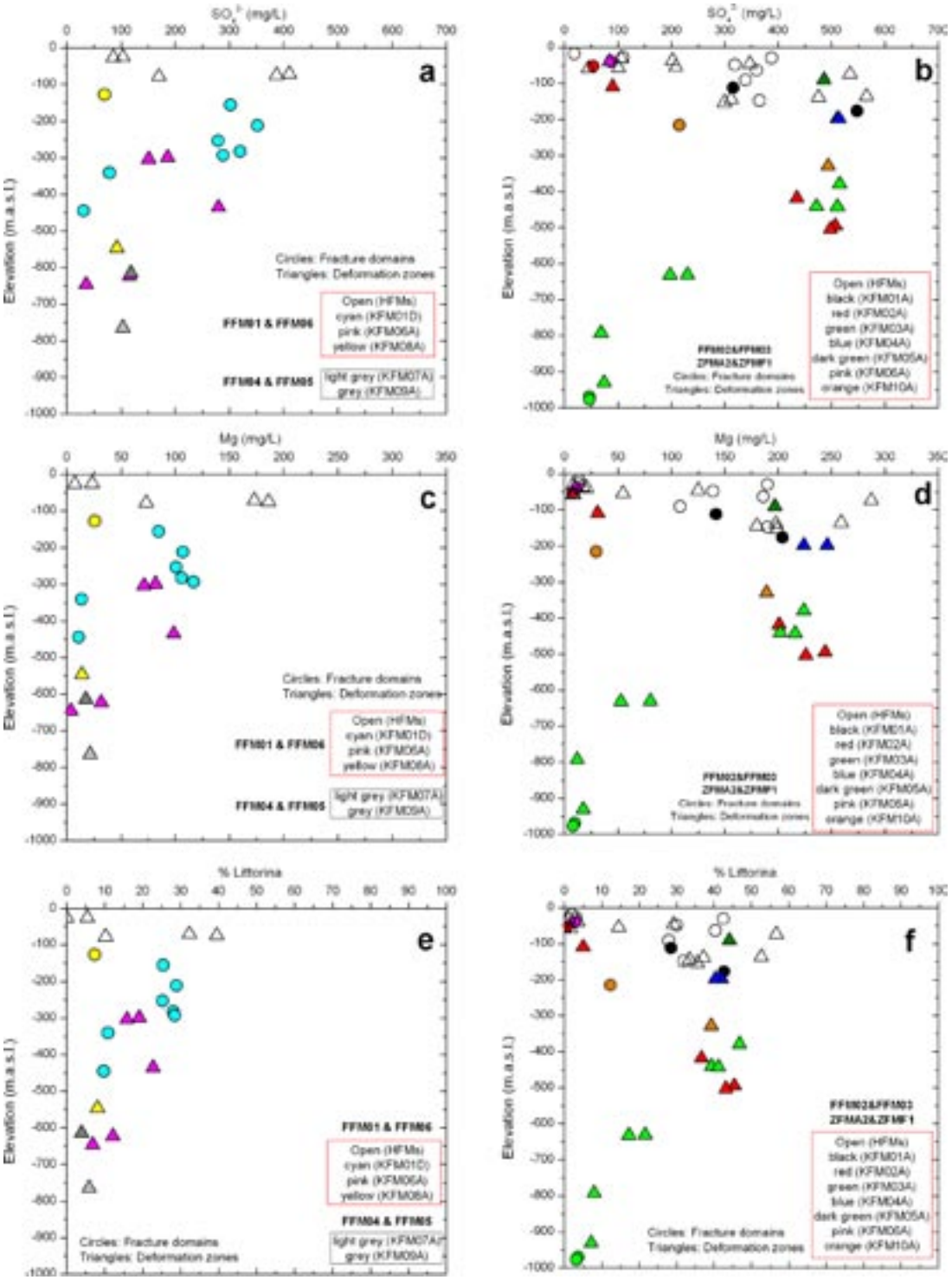

Figure 3-12. *Sulphate (a, b), magnesium (c, d) and Littorina mixing proportions (e, f) with respect to depth in the two different systems at Forsmark.*

Bicarbonate contents are highly variable in the first 150 m (Figure 3-13a and b) where the carbonate system is very active (see Section 3.3). Then concentrations decrease to very low values in both areas (Figure 3-13, panels a and b). However, bicarbonate is higher in most waters from FFM02, FFM03 and the gently diping deformation zones, than in the waters from the other system for the same depth, possibly also related to the higher Littorina contribution in these groundwaters . The lowest values are found in the deepest samples (700–800 m) from the marginal zone (FFM04 and 05, grey samples).

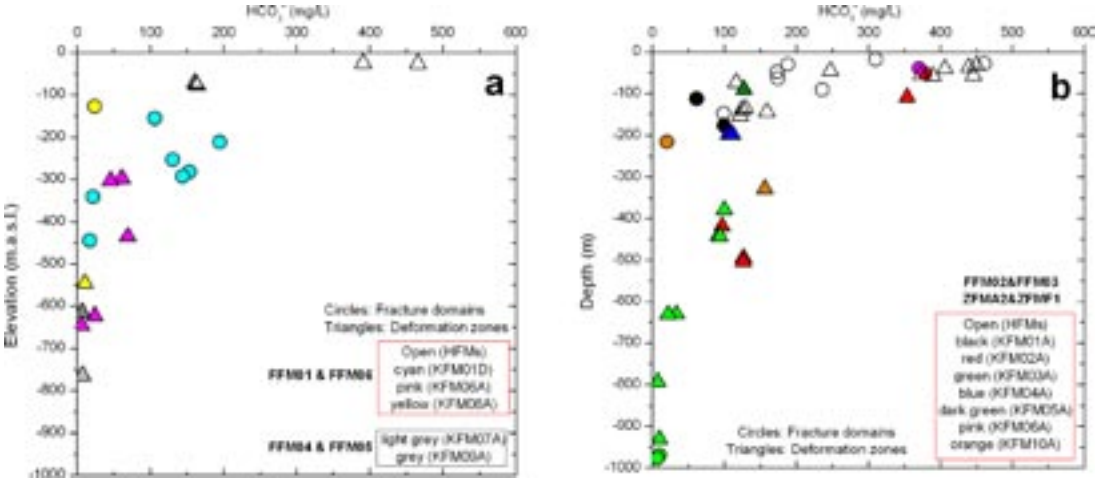

Figure 3-13. *Bicarbonate distribution with respect to depth in the two different areas at Forsmark.*

Directly related to this parameter are CO_2 partial pressure (pCO_2), pH and calcite saturation index. Their distribution is shown in Figure 3-14 (only samples with pH values measured in the field have been considered).

Except for one sample taken in KFM06A, the rest of the samples from FFM01, and even FFM04 and 5 (Figure 3-14a), have pH values between 8 and 8.5. As expected, pCO_2 in equilibrium with these waters decreases with depth (panel c), as CO_2 is consumed by water-rock interaction and/or decreased by mixing with saline waters with very low carbon content. Most groundwaters are in equilibrium with calcite.

Waters from the other system (Figure 3-14b) have lower pH values (around 7.5) and higher pCO_2 (panel d) although most of the waters are also in equilibrium with calcite (inside the uncertainty range of 0.3 SI units, /e.g. Nordstrom and Ball 1989/).

The high pCO_2 values in most of the waters taken from deformation zones in FFM02, 03 and gently diping deformation zones (higher than in the free atmosphere) may be associated with the influence of shallow groundwaters (recharge groundwaters with high CO_2) or with deeper groundwaters with high contents of $CO_{2(gas)}$ which could be related to biological activity. Figure 3-15 shows the good correlation found between these two parameters (calculated pCO_2 and measured $CO_{2(g)}$ contents) for the samples with enough data although more studies are needed on this subject.

3.4.3 Summary of the non-redox system in the deep groundwaters

Geochemical trends and modelling calculations in the Forsmark groundwaters point out that mixing processes represent the irreversible process which trigger the evolution of the system and are the main responible of some of their compositional characters. The presence of lineal trends in the evolution of non-conservative elements (Ca, Mg, Na, SO_4^{2-}, and even K, not shown in the plots) with respect to chloride indicate that the subsequent water-rock interaction processes have not been intensive enough to modify or mask these trends.

Spatially, the type and intensity of mixing processes affect differently the two structural systems defined at Forsmark: in the low transmissive part (FFM01) the effects of mixing processes with older waters (Deep Saline, Old-meteoric + Glacial) are the dominant while the influence of Littorina is more restricted; however, in the more transmissive system (FFM02 and FFM03), Littorina effects are much more important.

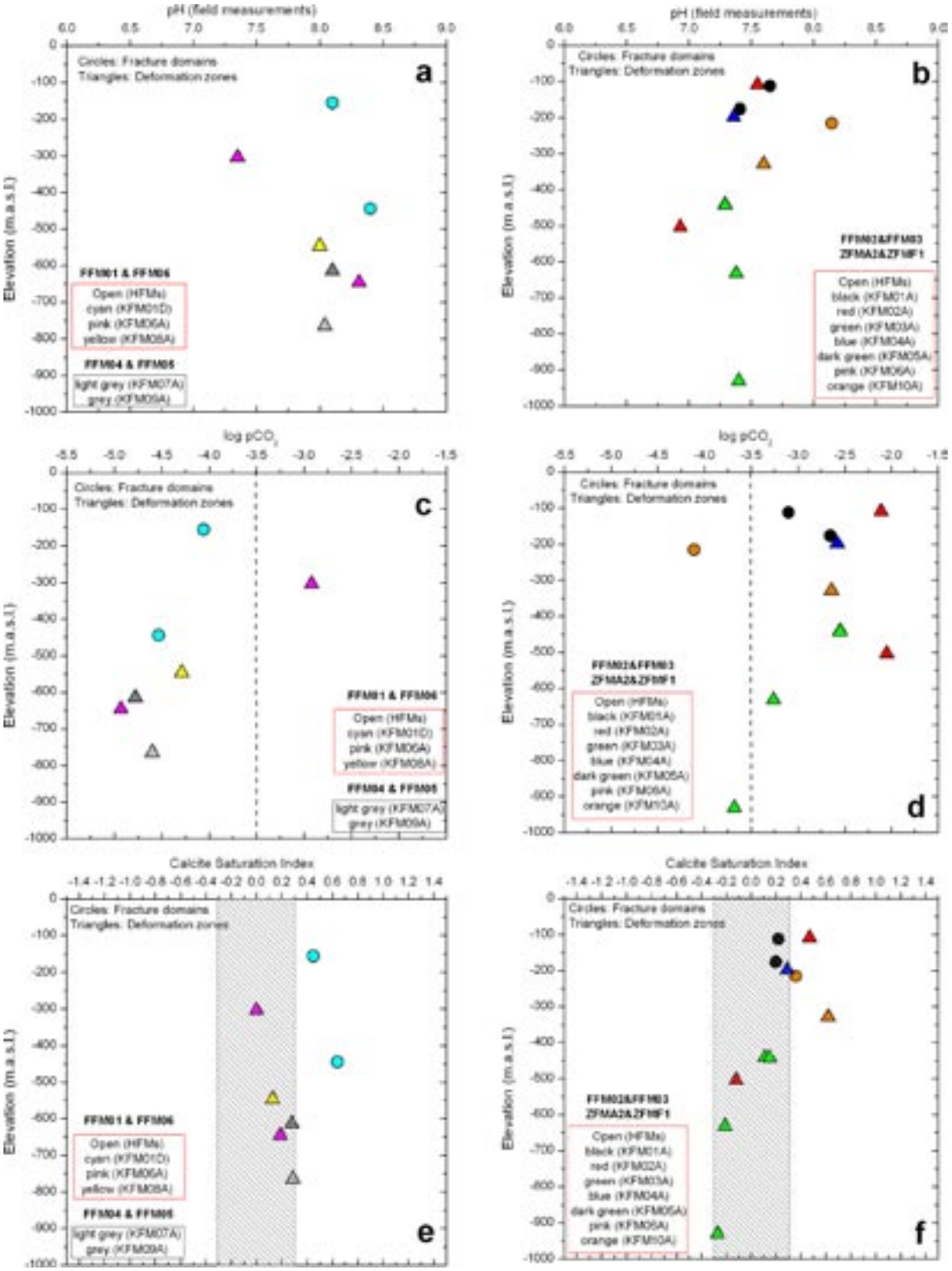

Figure 3-14. *pH (a, b), log pCO_2 (c, d), and calcite saturation indexes (e, f) with respect to depth in the two different areas at Forsmark.*

Littorina intrusion in this last system affects to pre-existing waters with lower chloride concentration but nor very different from the own marine intruding water. This fact would explain the variability in the content of elements such as sulphate of magnesium (characteristically enriched in the Littorina end-member) for a very narrow chloride content of around 5,500 mg/L. Moreover, Littorina percent distribution with depth is fairly homogeneous (35–50%) down to 550 m in this transmissive system. Considering a mean value of 43%, this circumstance would imply a contribution of this end-member to the chemistry of the already present groundwaters

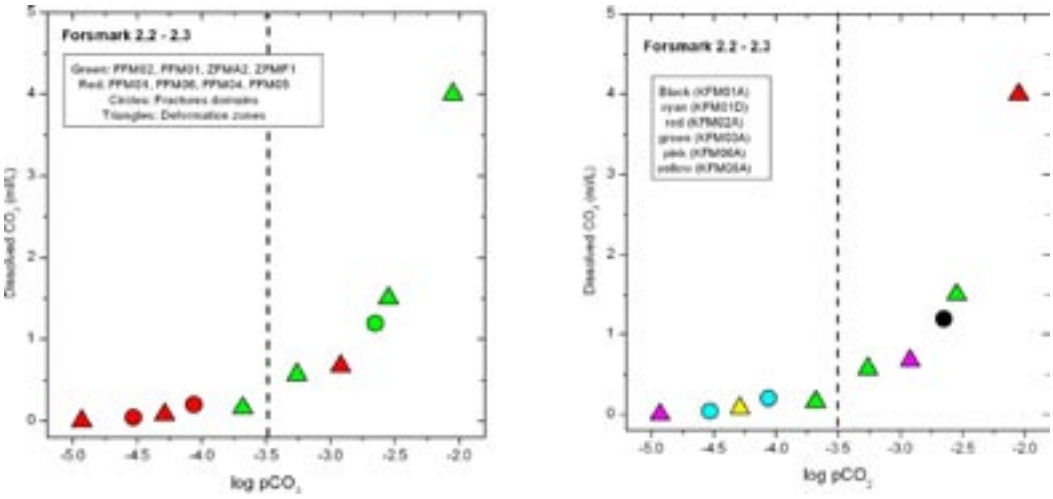

Figure 3-15. *Dissolved CO_2 versus calculated log pCO_2 in the Forsmark groundwaters. Left panel shows the values coloured by structural domains while they are coloured by borehole in the right panel.*

at these depths that would be 1,580 mg/L of sodium, almost 400 mg/L of sulphate and 193 mg/L of magnesium. These values fit very well with the contents found in the present groundwaters (around 2,000 mg/L Na, 500 mg/L SO_4^{2-} and 200 mg/L Mg) even not considering the contribution of the pre-Littorina groundwaters to the final mixture. These observations indicate that, in spite of being susceptible of chemical reactions (sulphate-reduction or cation exchange), the concentration of sodium, magnesium and sulphate in these waters appears to be mainly controlled by the proportions of the Littorina end-member.

Obviously, if mixing is the irreversible process, the induced disequilibrium must relax through water-rock interaction processes. Any mixing scenario produced by dilution or salinization will activate ionic-exchange processes (see Appendix C in this report) affecting the dissolved contents of Ca, Mg, Na or K. The effects of exchange processes will depend on the cation exchange capacity (CEC) of fracture fillings and up to now no definite CEC values are available. Reequilibrium processes with respect to calcite or chalcedony have also been identified controlling the pH and the dissolved silica contents, respectively, independently of the paleohydrogeological history of mixing. Finally, redox parameters in these groundwaters are totally conditioned by microbiological and water-rock interaction processes (see Section 3.5).

Therefore, the statement “mixing processes control some major characters of the groundwaters” does not mean that water-rock interaction has not influence in the system. It means that these hydrogeological systems evolve through a complex combination of mixing and water-rock interaction where the irreversible process of mixing is the crucial part.

As a summary, the uppermost 100–150 m in the Forsmark area are mainly represented by groundwaters from very transmissive deformation zones. These groundwaters display a wide chemical variability, mainly due to the presence of discharge waters or saline waters of marine origin (recent marine waters or old Littorina relicts). However, the very recent infiltrating waters are mainly controlled by weathering reactions and only in some cases by mixing with previous and more saline waters.

Below 200 m depth, in spite of the occurrence of chemical reactions affecting calcium, sodium, magnesium and sulphate (calcite equilibrium ionic exchange and sulphate reduction), their chemical contents are mainly controlled by mixing and their values are clearly related to the proportion of each end-member.

The mixing proportions are different in the two main systems differentiated in Forsmark: the waters from FFM01 (including the marginal waters from FFM04 and 5) and the waters from FFM02, 03 and the gently dipping deformation zones. Waters from the first system have a larger

contribution of Deep Saline waters at shallower depths. The same could be said for the influence of the cold-diluted component (Old meteoric-Glacial end-member). In the other system, groundwaters are characterized by a higher proportion of Littorina (almost double) and a larger penetration depth of this end-member (600 m instead of 300 m in the first system). This results in generally higher sulphate and magnesium contents in this second system.

Even though most of the major ions in groundwaters at the studied area are mainly determined by mixing processes, pH and Eh are controlled by the chemical reactions occurring there. The pH is mainly controlled by calcite dissolution-precipitation reactions and microbial activities, being of secondary importance to the influence of other common chemical processes, such as aluminosilicate dissolution-precipitation or cation exchange.

3.5 Redox system in the groundwaters

The redox system is one of the most complicated and discussed items in hydrogeochemistry and, therefore, it has been considered here that the only way to deal with it is to know, understand and interpret all the information related to it (hydrochemical, mineralogical and microbiological) as a whole. Therefore, this section integrates the results obtained from the potentiometrical Eh measurements, redox pair calculations, speciation-solubility calculations and microbiological analysis to identify the main controls of the redox state in groundwaters.

The potentiometric Eh measurement can have both technical and interpretative problems; however, SKB has developed (over the last 25 years) one of the best available methodologies for the measurement of this parameter /Auqué et al. 2008/ and its careful use is, at the very least, an extremely helpful information for the study of something as complex as the redox system. For instance, measured Eh values can be used to deduce the type of oxyhydroxide that may control these measured values (oxyhydroxides/Fe^{2+} are clearly electroactive redox pairs and this methodology has been successfully used in previous works; e.g. /Grenthe et al. 1992, Banwart 1999/). But, in any case, all the conclusions and interpretations of this chapter have been obtained independently of the Eh value, or have been tested and confirmed with other data or reasoning lines:

- all the speciation-solubility calculations and their corresponding conclusions with respect to sulphur and manganese have been obtained independently of the measured Eh value, or, in the case of uranium, they have been checked using the only available data for the homogeneous U(IV)-U(VI) redox pair; and
- as it has been stated above, using the available mineralogical and microbiological data.

Following the same criteria as in previous reports, here a detailed description and discussion of the redox system including the geochemical characterisation of iron, sulphur, uranium and manganese is presented.

3.5.1 Selection of redox data

Selection of representative Eh and pH values

The selection of the pH and Eh values for any specific borehole section has been based on a very careful analysis of the data delivered by SICADA. The whole selection procedure is described in Appendix A. Table 3-19 contains all the selected values for the subsequent discussion.

There are 19 sets of logs in the Forsmark area, corresponding to 19 different packed sections in 12 boreholes (KFM01A, 01B, 02A, 03A, 04A, 05A, 06A, 07A, 08A, 09A, 10A and 11A), ranging in depth from 110 to 950 m and covering different areas from the two systems differentiated in Forsmark. Twelve of them passed the initial selection criteria and nine were included in Group 1 (only three logs were included in Group 2, see Table 3-19).

Table 3-19. Eh values selected in the Forsmark area where SKB methodology has been used. DF: data freeze, only the new 2.2 and 2.3 data freezes are indicated, the rest of the samples correspond to 2.1 data freeze. Category: indicates the category of the sample (see Smellie and Tullborg, Appendix 1, this report). Depth correspond to the Elevation of the mid section. The pH and temperature values correspond to the values selected from Chemmac logs, down-hole or surface. See also Appendix A in this contribution. The pH data correspond to the field measurements except in the cases in "italics" which were determined in laboratory. The column called Group indicates the quality of the Eh value as it is reported in Appendix A.

Data freeze	Borehole	Sample No. #	Category	Depth (m)	Borehole lenght (m)	T	pH (field meas.)	pe	Eh value (mV)	Group
	KFM01A	4538	2	–111.75	110–120	6.91	7.65	–3.51	–195	1
	KFM01A	4724	2	–176.27	176–183	7.60	7.41	–3.37	–188	1
2.2	KFM01D	12316	2	–340.87	428–435	9.65	8.10	–4.69	–263	1
2.2	KFM01D	12343	1	–445.17	568–575	10.75	8.40	–4.61	–260	1
	KFM02A	8016	3	–503.34	509–516	11.40	6.93	–2.53	–143	1
	KFM03A	8284	2	–442.35	448–455	10.70	7.29	–3.12	–176	1
	KFM03A	8273	2	–631.91	639–642	13.10	7.38	–3.45	–196	2
	KFM03A	8281	3	–930.50	939–946	17.20	7.40	–4.25	–245	1
	KFM06A	8809	3	–301.99	353–360	8.94	7.35	–2.77	–155	1
2.3	KFM10A	12552	2	–214.77	298–305	8.56	8.15	–5.03	–281	2
2.3	KFM10A	12517	T3	–328.08	478–487	9.46	7.60	–4.60	–258	1
2.3	KFM11A	12728	5	–374.56	447–454	9.73	*7.38***	–3.33	–187	2

* This sample is from the same interval as the previous one (#12343) and corresponds to the time series.

** Only this value was measured in the laboratory.

Most of the retained Eh values agree very well with the recommended value suggested in the specific P-reports where the hydrochemical characterisation of each borehole is summarised /Wacker et al. 2003, 2004 abc, 2005 abc, Nilsson et al. 2006/. P-reports for KFM10A and KFM011A are not available yet and the Eh values have been selected by the UZ group. The Eh value selected for KFM010A at 328 m depth is −258 mV, in agreement with the data provided by SICADA; however, it must be used with caution. Exceedingly high Fe^{2+} concentrations were analysed over the whole measurement period (Table 3-20), suggesting drilling disturbances. It is not clear (until the P-report is available) if this problem has also affected Chemmac logs.

Selection of samples for redox modelling

As already advanced in previous SDM reports, one of the main problems affecting the available samples for the redox modelling is the high percentage of drilling water in most of them, lower than 10% but usually higher than 1% (the maximum recommended value; e.g. /Wacker et al. 2004 ab/. Small amounts of oxygen, incorporated with the drilling water or by direct contamination with air, can produce important changes in the redox system of the groundwaters, although they were not detectable during Chemmac logging (see Appendix A of this report).

In spite of the important efforts made by the Site Characterisation team, this problem has persisted during Forsmark 2.2 and 2.3 campaigns. As a consequence, the number of samples suitable for redox modelling is still small (Table 3-20). As a trade-off between quality and quantity, only *samples with less than 10% of drilling water* have been used (as in previous phases). This means accepting a level of uncertainty on the original redox characters of the system but, at least, this would enable to study whether the mentioned alterations have occurred and their possible effects on the undisturbed conditions. So, for this modelling task samples with less than 10% of drilling water and enough redox data were selected (Table 3-20), including good Eh and pH data from continuous loggings, analytical data for Fe^{2+}, U, S^{2-} and CH_4, and microbiological information.

Table 3-20. Important chemical, physicochemical and microbiological parameters in the selected samples for redox modelling at Forsmark. DF: data freeze, only the new 2.2 and 2.3 data freezes are indicated, the rest of the samples correspond to 2.1. Cat: indicates the category of the sample /Smellie et al. 2008/. Depth corresponds to the elevation of the mid part of the sampling interval. The pH data correspond to the field measurements except in the cases in "italics" which were determined in the laboratory. Ferrous iron, sulphide, uranium and manganese are expressed in mg/L; methane, in ml/L. $\delta^{34}S$ is expressed in ‰ CDT. IRB (iron reducing bacteria) and SRB (sulphate reducing bacteria) are expressed as MPN (most probable number) in cells/mL. The shadowed rows indicate the samples of time series corresponding to the selected sample just above them.

DF	KFM	Sample	Cat	Depth (m)	DW (%)	pH	Eh (mV)	Fe^{2+}	S^{2-}	CH_4	U ($x10^{-3}$)	Mn	$\delta^{34}S$ (‰CDT)	IRB	SRB
	01A	4538	2	–111.75	0.76	7.65	–195	0.953	0.014		1.5	0.691	25.5	4,000	1.2
	01A	4724	2	–176.27	4.80	7.41	–188	0.475		0.12	14.9	1.020	25.6	4.0	0.2
2.2	01D	12316	2	–340.87	3.40	8.10	–263	1.330	0.01	0.14	01.9	0.171	33.8	80.0	7.0
2.2	01D	12343[a]	1	–445.17	0.80	8.40	–260	0.763	0.010				24.0	100	13,000
2.2	01D	12354	T1	–445.17	0.90	8.40	–260	1.230	b.d.l.	4.60	0.8	0.113	24.7		
2.3	02A	12002	2	–417.80	2.56	*7.36*		1.360	0.058		25.9	1.840	22.5		
2.2	02A	12004	2	–494.97	3.41	*7.19*		2.260	0.066		122.0	2.070	21.9		
2.3	02A	12507[b]	T2	–494.97	6.64	*7.25*		1.970	0.167		143.0	2.330	26.6		
	02A	8016	3	–503.34	6.77	6.93	–143	1.840	0.01	0.04	88.6	2.160	24.9	4.0	1.4
	03A	8011[c]	2	–379.06	0.60	*7.37*		0.558	0.004			1.140			
	03A	8012	T2	–379.06	0.55	7.42		0.656			3.5	1.130	25.0		
	03A	8284	2	–442.35	0.40	7.29	–176	1.110	0.047	0.03		1.250	25.7	4.0	17
2.2	03A	12001	2	–631.10	5.70	*7.49*		1.060	0.701		45.2	0.510	25.1		
2.3	03A	12512	T2	–631.10	4.50	*7.43*		0.838	0.538		49.5	0.478	26.9		
	03A	8273	2	–631.91	4.35	7.38	–196	0.233		0.07	46.1	0.319	27.8	22	30
	03A	8281	3	–930.50	8.75	7.40	–245	0.208	0.058	0.06	0.7	0.114	27.3	–	500
2.2	03A	12005[d]	2	–969.14	0.70	*6.27*		1.360	0.838				29.1		
2.3	03A	12513	T2	–969.13	1.55	*7.11*		0.656	0.587		0.7	0.065	30.9		
	03A	8152	3	–977.67	3.85	*8.26*		0.026	0.033	0.05	0.4	0.009	29.6	<0.2	24
	04A	8267	3	–197.00	7.45	7.36		2.120			62.0	2.810	24.5		
	06A	8809	3	–301.99	7.70	7.35	–155	1.110		0.024	9.6	0.578	27.5	23	0.4
	06A	8785	2	–645.34	1.55	8.31		0.923	0.018	0.09		0.082	38.4	2.0	0.2
	07A	8843[e]	3	–759.72	0.60	8.04		0.262	0.062				22.8	–	<0.2
	07A	8879	T3	–759.72	0.35	8.04		0.162	0.134	0.04	0.2	0.127	30.2		
2.2	08A	12000	2	–546.42	5.05	8.00		0.726	0.012	0.03	6.4	0.191	29.1	500	500
2.2	09A	12243	2	–614.21	1.83	8.10		0.103	0.004		0.1	0.107	27.0		
2.3	10A	12552	2	–214.77	4.45	8.15	–281	1.430	0.027		0.1	0.186	25.2	500	500
2.3	10A	12517	T3	–328.08	3.55	7.60	–258[f]	15.40	0.065		5.6	1.190	24.0	1,600	2,800

[a] #12343 has not measured methane, therefore, sample #12354 (row below) has also been selected.

[b] #12507 has been selected apart from the previous one as it shows very high values for S^{2-} and U.

[c] #8011 has not measured uranium and then, sample #8012 has also been selected.

[d] #12005 has an anomalously low pH (e.g. calcite saturation index of –1.3, unreasonable and never found at these depths) and therefore, sample #12513 has also been selected.

[e] #8843 has not measured methane, therefore, sample #8879 has also been selected.

[f] This value must be used with caution (see text).

The selected samples (28 samples) cover a wide range of depths (from 110 to 950 m; Table 3-20) and belong to two different water types: brackish-saline groundwaters (Cl = 3,700–6,000 mg/L), distributed from 110 to 643 m; and the deepest and more saline groundwaters (from 760 to 1,000 m). All the samples selected here have been categorised as type 1, 2 or 3. But in some

cases, two samples have been chosen for one depth (the selected and another from the time series, shadowed rows in Table 3-20) when one of the important parameters was missed in the selected one or was very different from it.

3.5.2 General trends of redox data

Eh values in Forsmark range from −143 to −281 mV (Figure 3-16a to d). As is obvious from the plot, the number of Eh values is higher than in previous phases but still not enough to obtain definitive conclusions, specially in the fracture domain FFM01 (Figure 3-16c). Nevertheless some preliminary comments are worth including.

Panels a and b of Figure 3-16 show the selected samples ploted in an Eh-pH plot. Samples in panel a are represented by symbols (circles for fracture domains and triangles for deformation zones) and colours (different boreholes). Samples in panel b are also represented by symbols with the same meaning, and 2 colours indicating the system they belong to (see Section 3.1, 3.3, 3.4; /Smellie et al. 2008, Olofsson et al. 2007/): red represent groundwaters taken in fracture domains FFM01 and FFM06 (below deformation zone ZFMA2); and green symbols represent

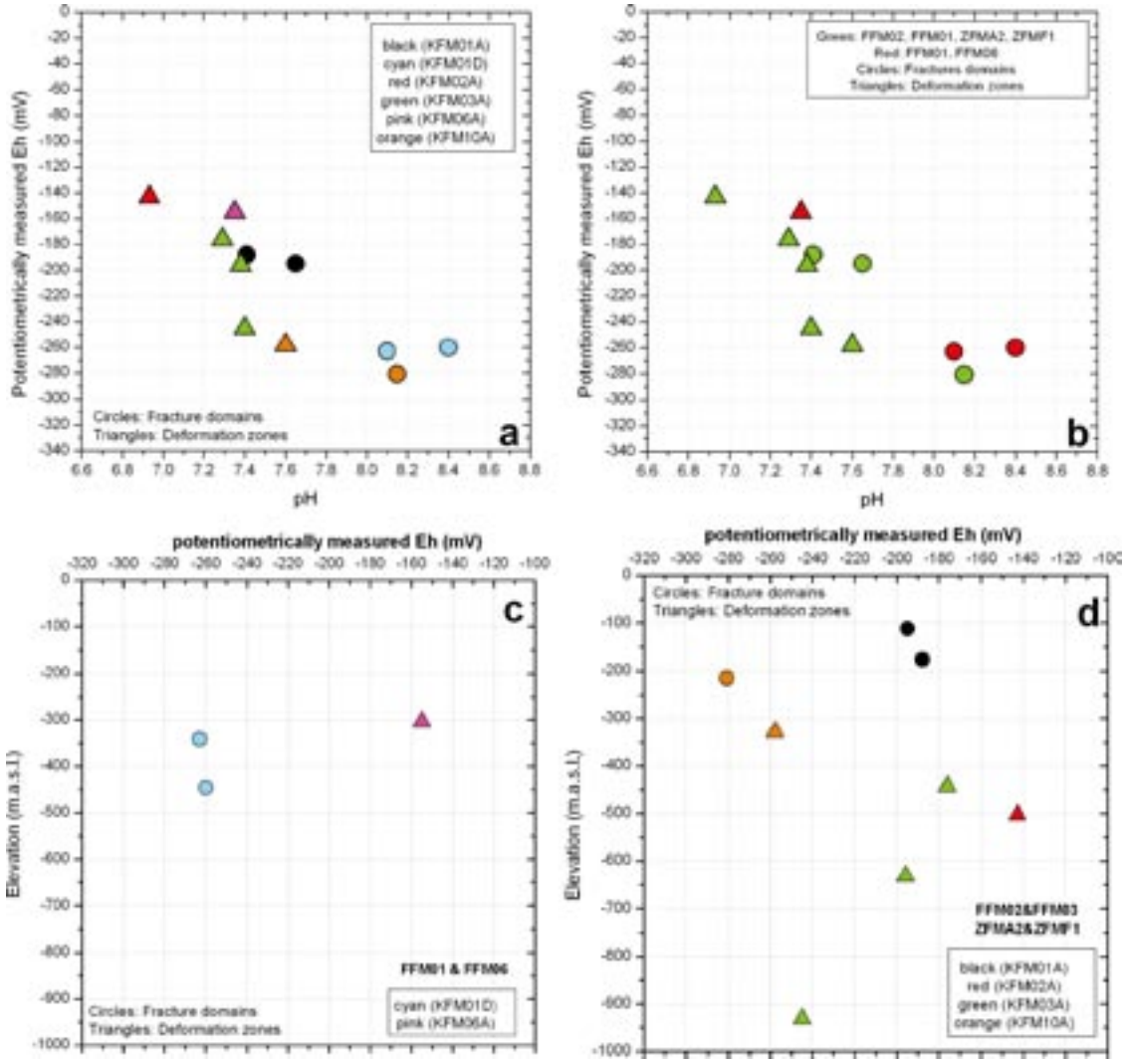

Figure 3-16. *pH-Eh (a and b) and Eh-depth plots (c and d) for the Forsmark area. Groundwater samples are coloured by boreholes (a) and by the structural domains (b); (c) represents only the waters sampled in the fracture domain FFM01; and (d) represents waters samples in fracture domains FFM02 and FFM03, and samples taken from the gently dipping deformation zones. In both cases, the samples are coloured by boreholes. Triangles indicate deformation zones and circles, fracture domains.*

groundwaters taken in FFM02, FFM03 and in the gently diping deformation zones. Panels c and d separate in two plots the samples from these two systems coloured by boreholes (as it was done in Section 3.4).

Eh-pH plots (panels a and b in Figure 3-16) show a general trend of decreasing Eh values as the pH increases, with the more reducing and alkaline waters in fracture domains FFM01 and FFM03 (circles in red and green) and the more oxidising and less alkaline waters in deformation zones (triangles). However, waters from fracture domains in borehole KFM01A (black circles) have Eh values closer to the waters from deformation zones, whereas waters from deformation zones in KFM03A and KFM10A (red and orange triangles, respectively) have Eh values similar to the ones observed in the fracture domain waters from KFM01D and KFM10A. All samples are located in a clearly reducing zone and most of them are in the range defined by /Drever 1997/ for groundwaters buffered by sulphate-reduction.

Panels c and d in Figure 3-16 show the distribution of Eh values with depth in the two differentiated systems. The highest Eh values (from −140 to −180 mV) are found in boreholes KFM02A, KFM06A and KFM03A between 300 and 500 m depth. Several samples from KFM01A and KFM03A range from −180 to −200 mV, both at shallower and deeper depths. Finally, the third group of samples with the lowest Eh values (<−240 mV) correspond to samples from KFM01D and KFM10A at the same depth interval (200 to 450 m depth) and to the deepest sample with potentiometrical values from KFM03A (930 m depth).

From these plots, it is clear that Eh measurements do not show any simple trend with depth in any of the two systems. The only clear trend is displayed by the samples from KFM03A (green) where Eh values decrease with depth from −180 mV to −250 mV. So, no distinct grouping can be seen in the plots as waters from the two systems can be found with the same Eh and pH ranges and at the same depths. The most reducing values are associated with a deep and saline water outside the target area (FFM03) and with two brackish waters (–200 to –500 m depth) at both sides of the ZFMA2. There are more saline waters sampled at the marginal part of the area (KFM07A and 09A) but no Chemmac logs are available.

The distribution of Eh with depth can also be seen in Figure 3-17, which is a simplified 3D picture of the site. There the sparseness and heterogeneous distribution of the data are obvious. This distribution with depth does not seem to clearly show the trend observed in other crystalline systems (e.g. in Palmottu, where a similar methodology for Eh measurements was used) and in most aquifers elsewhere, where a marked decrease of redox potential is observed as the residence time and depth of the waters increase /e.g. Drever 1997, Blomqvist et al. 2000/.

As already stated in Forsmark 2.1, this behaviour could be the result of a modification in the original redox state in some groundwaters (perturbation of the system; see below) but it can also be the consequence of the complex hydrological setting and paleohydrogeological evolution of the Forsmark area, with both sub-vertical and sub-horizontal hydraulic structures and the presence of pockets and lenses of old sea water more or less isolated in the bedrock. More data would be needed in order to better differentiate between these two possibilities.

Iron, manganese, sulphide and uranium concentrations do not show a clear trend of variation with the chloride concentrations, as already shown by the data from 2.1 data freeze. This is mainly due to the wide range of concentrations of these elements in Littorina-rich groundwaters with 5,500 mg/L of chloride, where also the maximum concentrations are found. Therefore, instead of plotting these elements against chloride, their distribution against depth in two plots is presented here following the same methodology as before: left plots show the waters from FFM01 and FFM04 and FFM05, and right plots show the waters from FFM02, FFM03 and the gently diping deformation zones. This is what is shown in Figure 3-18. The first interesting observation is the lack of a clear depth dependence and the second one is that the highest values (over one order of magnitude in most cases) are associated with the right plots, waters from the FFM02, FFM03 and gently dipping deformation zones.

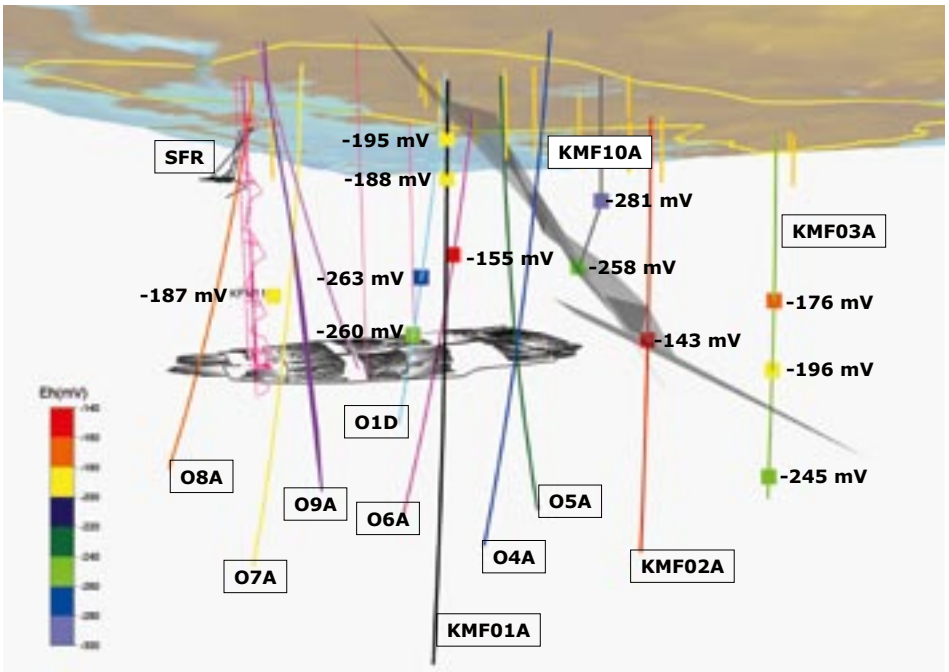

Figure 3-17. *3D plot of the site with the available Eh values superimposed on a simplified sketch of the system showing the position of the boreholes, the major gently dipping deformation zones ZFMA2 and ZFMF1, the schematic layout of the repository (horizontal grey structure) and the SFR.*

Fe^{2+} values below 200 m are always below 2 mg/L except for the suspiciously very high values in KFM10A at 328.08 m depth (section 478–487.5 m) with a range of concentrations from 7.4 to 15.4 mg/L (Figure 3-18b).

Manganese evolves with depth as expected in the system corresponding to FFM01 and the marginal waters (FFM04 and FFM05) with typically low values (< 0.5 mg/L, Figure 3-18c). The other system (plotted in panel d) have very high Mn contents not only in the shallow part of the system but also down to 500 m depth (atypical in granitic systems). These Mn-rich groundwaters show a very important Littorina signature (see Section 3.5.7).

Except for two samples in HFM19 at 150 m depth (with S^{2-} about 1.5 mg/L) S^{2-} contents from the surface down to 600 m depth are very low (even below detection limit) in both systems (Figure 3-18e and f) and slightly increase from there downwards (although only in borehole KFM03). It is interesting to notice the change in behaviour due to the introduction of the 2.2 and 2.3 samples, with the highest S^{2-} contents at 610 m depth (in a deformation zone) and at 969–982 m (in fracture domain) in KFM03A.

As for uranium, it has variable concentrations but usually high at depth between 100 and 650 m (up to 143 µg/L), again in waters with a high Littorina percentage associated with deformation zones in the system of FFM02 and FFM03 fracture domains (Figure 3-18h). Below this depth, U concentrations decrease drastically. In general high U values increase with time (re-sampling; see Section 3.5.6).

All these observations suggest that the behaviour of the redox parameters in the two systems at Forsmark is very different. Waters from FFM01, FFM06 and the marginal waters from FFM04 and FFM05, have very low contents independently of being associated to fracture domains or deformation zones, while waters from FFM02 and FFM03 have comparatively high concentrations. In this second system, between 500 and 600 m depth, an important change in the dominant species or the components that buffer the redox system occurs. This change coincides with the transition from brackish, high Littorina waters (Cl^- between 4,500 and 5,500 mg/l) to more saline groundwaters (Cl^- > 7,000 mg/l), which is an indication of the existence of groundwater layers with different hydrochemical characters and a different geochemical evolution.

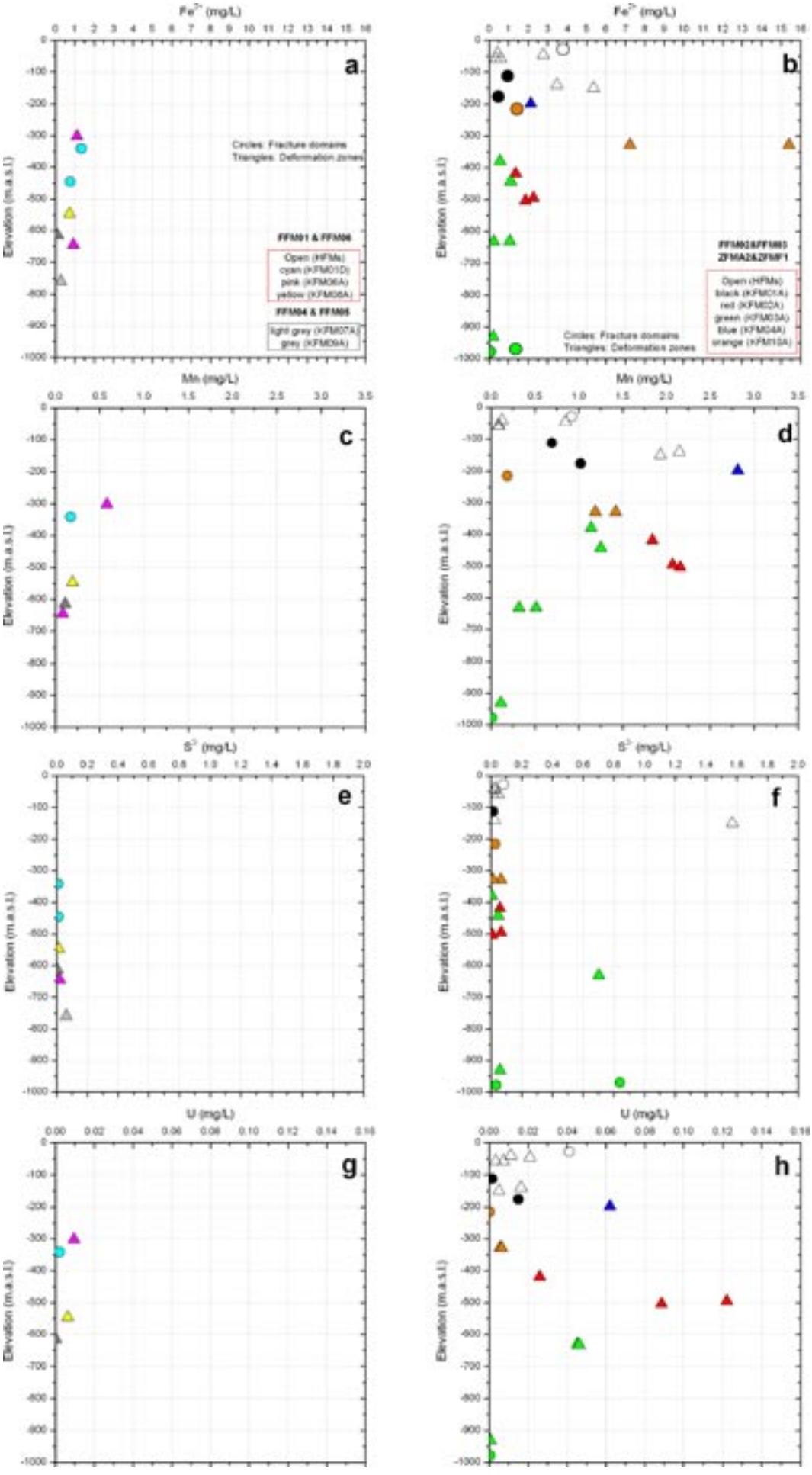
a
b
c
d
e
f
g
h
Fe2+ (mg/L)
Mn (mg/L)
S2- (mg/L)
U (mg/L)
Elevation (m.a.s.l.)
Circles: Fracture domains
Triangles: Deformation zones
FFM01 & FFM06
Open (HFMs)
cyan (KFM01D)
pink (KFM06A)
yellow (KFM06A)
FFM04 & FFM05
light grey (KFM07A)
grey (KFM09A)
FFM02&FFM03
ZFMA2&ZFMF1
Open (HFMs)
black (KFM01A)
red (KFM02A)
green (KFM03A)
blue (KFM04A)
orange (KFM10A)

Figure 3-18. *Redox elements distribution with depth in the Forsmark area groundwaters. Waters from categories 1, 2, 3 and 4 have bee plotted. Left plots represent the waters sampled in the fracture domain zones (FFM01 and FFM06) including those samples from marginal areas to the target area (FFM04 and FFM05; in grey). Right plots represent waters samples in fracture domains FFM02 and FFM03, and samples taken from the gently dipping deformation zones. In both cases, triangles indicate deformation zones and circles, fracture domains. (a) and (b) Ferrous iron; (c) and (d) Manganese; (e) and (f) Sulphide; and (g) and (h) Uranium.*

In the following sections the results from redox pair modelling are presented and their consequences to the iron and sulphur systems (including solubility calculation concerning iron-sulphide phases) discussed. The analysis of the uranium and manganese systems is presented separately, as each of them have interesting particularities important for a comprehensive understanding of the natural system and the perturbations that could have affected it.

3.5.3 Redox pair modelling

The redox pairs that have been analysed here are the same as in the previous phases /e.g. SKB, 2004c, 2005a, 2006a, 2007/: the dissolved SO_4^{2-}/HS^- and CO_2/CH_4 redox pairs, and the heterogeneous couples $Fe^{2+}/Fe(OH)_3$, $HS^-/S_{(c)}$, SO_4^{2-}/FeS_{am} and SO_4^{2-}/ pyrite. These are the redox pairs that, apparently, have performed better in similar systems elsewhere in the Scandinavian Shield (see /Gimeno et al. 2007/ and references therein).

PHREEQC and/or the thermodynamic data included in the WATEQ4F database have been used for the calculations, except in the case of the heterogeneous pair Fe^{2+}/ $Fe(OH)_3$ for which three different sets of log K values have been used for the solid (see /Gimeno et al. 2007/ for more details): (1) the set of values proposed by /Nordstrom et al. 1990/ corresponding to amorphous-microcrystalline hydrous ferric oxides, HFOs, or ferrihydrites (log K = 3 to 5); (2) the value derived from the calibration proposed by /Grenthe et al. 1992/ for a wide spectrum of Swedish groundwaters (log K= −1.1 for a crystalline phase such as hematite or goethite); and (3) the value of log K = 1.2 defined by /Banwart 1999/ using the same methodology as /Grenthe et al. 1992/ but working with groundwaters from the Äspö large-scale redox experiment (see /Gimeno et al. 2007 and Banwart 1999/ for more details). The redox potential corresponding to the Fe^{2+}/ $Fe(OH)_3$ heterogeneous redox pair has been obtained in all these calculations using the already mentioned equilibrium constants and the Fe^{2+} activity calculated with PHREEQC. Alternatively, this redox potential has also been calculated from the calibrate defined by /Grenthe et al. 1992/ and /Banwart 1999/ as a function of pH and the total concentration of Fe^{2+}. Results are summarised in Table 3-21 and Figure 3-19.

As already reported in /Gimeno et al. 2007/, the Eh values obtained with the $Fe^{2+}/Fe(OH)_3$ redox pair considering a microcrystalline $Fe(OH)_3$ are more oxidising than the measured ones, and they are not included in the table nor in the plots.

The Eh values calculated with the $Fe^{2+}/Fe(OH)_3$ redox pair and using the calibration by /Grenthe et al. 1992/ (or the corresponding equilibrium constant) are in good agreement with the Eh values measured in two deep samples from KFM03 (sample #8281 at 930.5 m depth and sample #8273 at 631.9 m depth; Table 3-21 and green samples in Figure 3-19, panel a). For the rest of the samples this calibration gives more reducing values than those measured. This lack of agreement is clearly seen in panel a of Figure 3-19.

On the contrary, the Eh calculated with the same redox pair and using the calibration proposed by /Banwart 1999/ (or the corresponding equilibrium constant) is in good agreement (Figure 3-19, panel b) with all measured values in brackish groundwaters except for the two deepest samples from borehole KFM03A (mainly the deepest, sample #8281; Table 3-21). This suggests that the redox state of the brackish and saline groundwaters can be controlled by different iron oxyhydroxides (or by iron oxyhydroxides with a different degree of crystallinity).

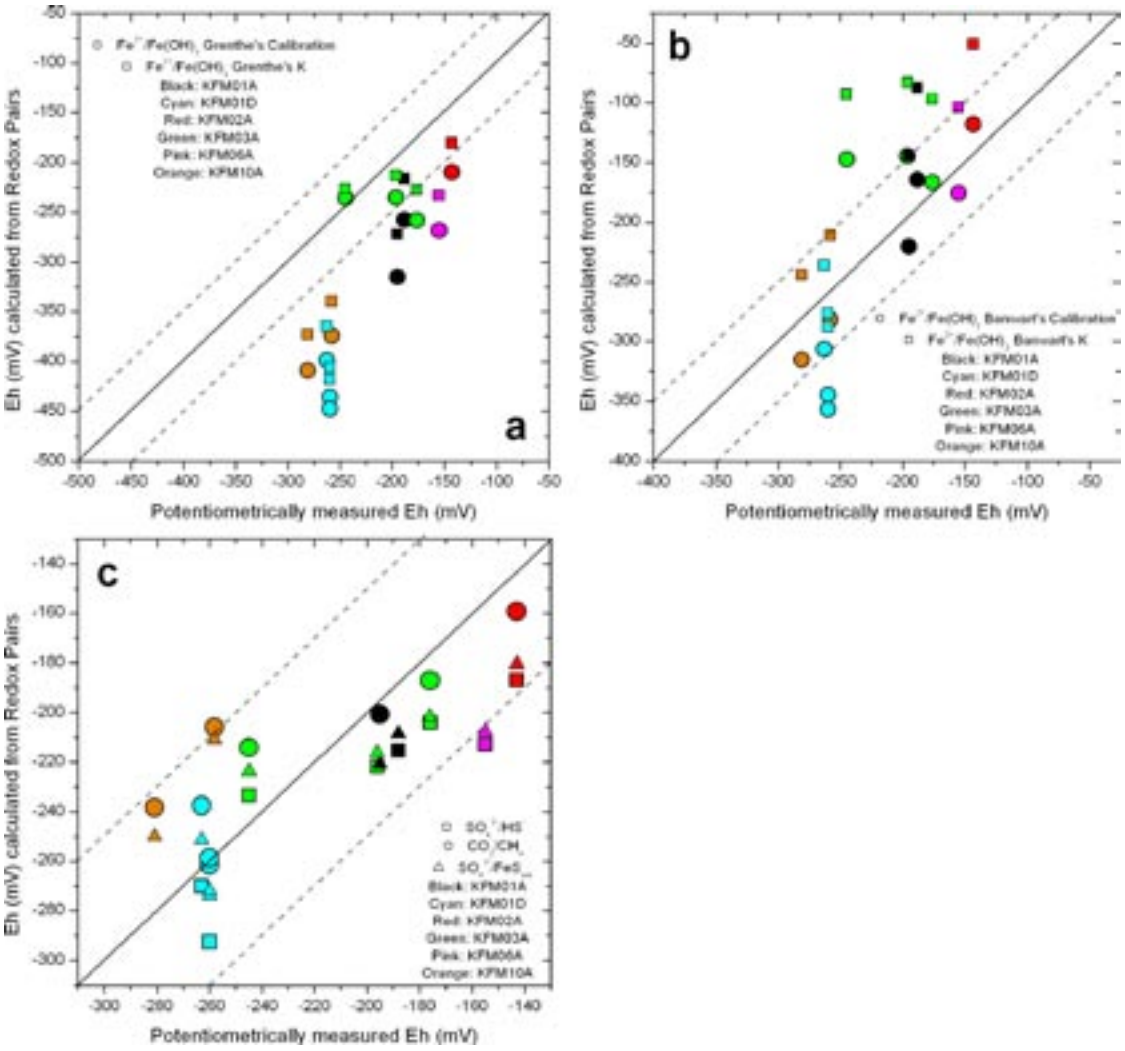

Figure 3-19. *Comparison of the Eh values potentiometrically measured with Chemmac and the Eh values calculated with the different redox pairs. (a) and (b) panels: $Fe^{2+}/Fe(OH)_3$, and (c) panel, SO_4^{2-}/HS^-, SO_4^{2-}/FeS_{am} and CO_2/CH_4. The dashed lines indicate the accepted range of Eh variability of ±50mV.*

Sulphur redox pairs show, in general, a good agreement with the potentiometrically measured Eh values (Table 3-21; Figure 3-19, panel c). The results obtained with the homogeneous SO_4^{2-}/HS^- pair and the heterogeneous SO_4^{2-}/FeS_{am} redox buffer agree very well with the measured ones (as it occurs in Laxemar; /SKB 2006d/), usually better than with the redox buffer SO_4^{2-}/pyrite. In more detail, the values calculated with this last pair show that:

a) the highest differences are in the most reducing waters (#12316, KFM01D; #12552 and #12517, KFM10A; and the deep sample from KFM03A) where this pair gives slightly more oxidising values (Table 3-21); and

b) the best agreement is associated with the less reducing and isolated brackish groundwaters (#8616, KFM02A; #8284, KFM03A; #8809, KFM06A; Table 3-21).

These differences can be interpreted mostly in the context of the presence or absence of recent activity of sulphate-reducing bacteria (SRB) in these parts of the system (see below).

The enormous advantage of using Eh values derived from a redox pair is that tentative Eh values for samples without measured data can be obtained. For example, for the saline samples outside the target area (grey triangles in both panels in Figure 3-20, corresponding to KFM07A and 09A) the results obtained indicate a progresive decrease of redox potential with depth from –200 mV to around –260 mV.

Table 3-21. Eh values for the selected samples in the Forsmark area. The potentiometrically measured values (column Chemmac) are shown for comparison with the values calculated with the different redox pairs. The redox potential corresponding to the Fe^{2+}/ $Fe(OH)_3$ heterogeneous redox pair has been obtained using the correspondient equilibrium constants and the Fe^{2+} activity calculated with PHREEQC (K eq in the heading). Alternatively, this redox potential has also been calculated from the calibrate defined by /Grenthe et al. 1992/ and /Banwart 1999/ as a function of pH and the total concentration of Fe^{2+} (Calibrat. in the heading).

DF	KFM	Sample	Category	Depth (m)	Cl mg/L	SO_4^{2+} mg/L	Fe^{2+} mg/L	S^{2-} mg/L	CH_4 ml/L	pH*	Eh								
											Chem-mac	SO_4/HS^-	SO_4/ Pyrite	SO_4/ FeS_{am}	CO_2/CH_4	$Fe^{2+}/Fe(OH)_3$ /Grenthe et al. 1992/		$Fe^{2+}/Fe(OH)_3$ /Banwart 1999/	
																K eq.	Calibrat	K eq.	Calibrat.
	01A	4538	2	–111.75	4,562.8	315.65	0.953	0.014		7.65	–195	–200.6	–184.0	–220.9		–272.0	–314.8	–144.0	–220.4
	01A	4724	2	–176.27	5,329.5	546.97	0.475		0.12	7.41	–188		–168.5	–208.5	–215.3	–216.0	–257.4	–87.5	–164.0
2.2	01D	12316	2	–340.87	5,160	78.60	1.330	0.01	0.14	8.10	–263	–237.5	–218.9	–251.5	–270.0	–365.0	–398.9	–236.0	–306.5
2.2	01D	12343	1	–445.17	5,960	31.10	0.763	0.010		8.40	–260	–261.46	–243.3	–273.9		–406.1	–435.9	–276.6	–344.8
2.2	01D	12354	T1	–445.17	5,800	38.30	1.230		4.60	8.40	–260	–258.7	–241.7	–271.8	–292.6	–418.0	–447.5	–288.0	–356.5
2.3	02A	12002	2	–417.80	5,440	435.00	1.360	0.058		7.36		–200.8	–168.6	–208.6		–259.0	–274.7	–127.0	–185.9
2.2	02A	12004	2	–494.97	5,540	434.00	2.260	0.066		7.19									
2.3	02A	12507	T2	–494.97	5,370	437.00	1.970	0.167		7.25		–196.7	–160.7	–201.1		–249.0	–265.2	–117.3	–176.2
	02A	8016	3	–503.34	5,410	498.00	1.840	0.01	0.04	6.93	–143	–159.3	–137.7	–180.4	–186.9	–180.5	–209.6	–51.0	–118.1
	03A	8011	2	–379.06	5,440	515.00	0.558			7.37		–192.5	–169.8	–210.6		–238.3	–260.8	–106.8	–171.7
	03A	8012	T2	–379.06	5,450	495.00	0.656			7.42			–173.3	–213.9		–257.0	–267.0	–121.0	–178.1
	03A	8284	2	–442.35	5,330	511.00	1.110	0.047	0.03	7.29	–176	–187.0	–161.4	–201.7	–203.9	–227.0	–257.9	–97.0	–166.3
2.2	03A	12001	2	–631.10	5,640	230.00	1.060	0.701		7.49		–219.0	–179.8	–218.7		–275.0	–290.7	–143.5	–202.2
2.3	03A	12512	T2	–631.10	5,700	216.00	0.838	0.538		7.43		–214.5	–176.5	–216.3		–259.0	–274.7	–128.0	–185.9
	03A	8273	2	–631.91	5,430	197.00	0.233		0.07	7.38	–196		–174.7	–216.2	–221.9	–213.0	–235.0	–83.0	–144.5
	03A	8281	3	–930.50	8,560	73.90	0.208	0.058	0.06	7.40	–245	–214.1	–182.2	–223.9	–233.5	–226.0	–235.7	–93.0	–147.3
2.2	03A	12005	2	–969.14	10,500	47.00	1.360	0.838		6.27		–143.22	–105.2	–153.1		–70.6	–91.1	60.9	0.9
2.3	03A	12513	T2	–969.13	10,400	44.80	0.656	0.587		7.11		–199.9	–161.6	–203.6		–196.0	–214.9	–65.0	–125.1
	03A	8152	3	–977.67	9,690	46.70	0.026	0.033	0.05	8.26		–264.7	–242.3	–279.2	–281.8	–314.0	–330.0	–182.0	–242.2

	04A	8267	3	–197.00	5,580	514.00	2.120			7.36			–161.3	–199.4		–233.0	–285.5	–106.0	–190.0
	06A	8809	3	–301.99	4,560	151.00	1.110		0.024	7.35	–155		–168.4	–207.5	–212.7	–233.0	–268.0	–104.0	–175.3
	06A	8785	2	–645.34	7,080	115.00	0.923	0.018	0.09	8.31		–215.0	–243.7	–279.0	–294.0	–333.0	–354.7	–202.0	–265.6
	07A	8843	3	–759.72	14,400	103.00	0.262	0.062		8.04		–249.7	–220.4	–256.3		–330.4	–349.5	–199.3	–261.3
	07A	8879	T3	–759.72	14,800	99.30	0.162	0.134	0.04	8.04		–252.2	–221.4	–257.9	–264.0	–318.0	–337.7	–187.0	–249.4
2.2	08A	12000	2	–546.42	6,100	91.50	0.726	0.012	0.03	8.00		–236.4	–214.7	–249.3	–260.0	–342.0	–367.3	–212.0	–277.1
2.2	09A	12243	2	–614.21	14,800	118.00	0.103	0.004		8.10		–242.6	–224.6	–261.1		–314.0	–336.8	–183.0	–247.5
2.3	10A	12552	2	–214.77	4,050	215.00	1.430	0.027		8.15	–281	–238.3	–217.7	–250.1		–373.0	–409.0	–244.0	–315.4
2.3	10A	12517	T3	–328.08	3,690	400.00	15.40	0.065		7.60	–258	–205.8	–176.8	–210.9		–340.0	–374.3	–211.0	–281.7

* pH values in italics were measured in laboratory. The rest of the values were taken in the field with Chemmac.

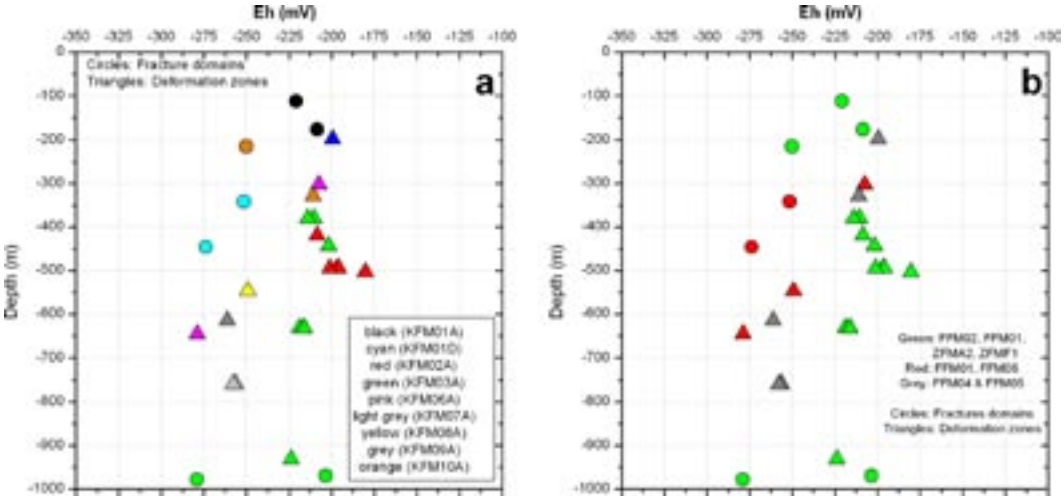

Figure 3-20. *Eh values calculated with the SO_4^{2-}/FeS_{am} redox pair with respect to depth. Groundwater samples are coloured by boreholes (a) and by the structural domains (b) In both cases, triangles indicate deformation zones and circles, fracture domains.*

Moreover, more than 80% of the waters from the "green" system (FFM02, FFM03 and gently dipping deformation zones) in different boreholes have a very narrow range in the calculated potentials (between –200 and –225 mV). This situation is mainly associated with the presence of brackish Littorina-rich groundwaters with a similar composition at different levels (between 100 and 630 m depth) and reinforces the observation of absence of a clear depth dependence of the calculated potential.

Finally, Eh values obtained with the non-electroactive pair CO_2/CH_4 are also in fairly good agreement with measured values (within a range of ± 50mV). In fact, the homogeneous sulphur and the methane redox pairs define a range of Eh in the middle of which the Eh value from the heterogeneous SO_4/FeS_{am} pair is always plotted (Figure 3-19 panel c).

The suphur and the CO_2/CH_4 redox pairs used here provide similar potentials (inside the uncertainty range usually accepted of ± 50mV). This is not strange at all as the redox windows for these redox pairs are very close, when not overlapping. It is a question merely related to the stoichiometry of the reactions and their equilibrium constants (see, for instance, /Kölling 2000/).

3.5.4 The iron system

The $Fe^{2+}/Fe(OH)_3$ heterogeneous redox pair is the most clearly electroactive and, therefore, one of the most feasible to control the Eh measurements in natural systems. However, the variability of the oxyhydroxides solubilities as a function of their particle size and specific surface area very much influences the obtained Eh value (for a review, see /Gimeno et al. 2007/). This relation has been successfully used in the literature on this subject /Grenthe et al. 1992, Banwart 1999, Trotignon et al. 2002/ to deduce the type of oxyhydroxide factible to control the measured Eh potentials.

This identification is important as the intrusion of oxygen in a reducing medium produces the formation of otherwise non-existing low crystalline phases, able to control the measured Eh. Identification of this situation is basic not only when interpreting Eh values but also when interpreting other characters related to the iron system, as will be shown below.

Integration of geochemical, mineralogical and microbiological data allow a more detailed analysis of the geochemical conditions where iron system dominates the redox characters of the Forsmark groundwaters.

Redox pair implications for the iron system

The redox potential measured in the deepest groundwaters in Forsmark (at 630 and 930 m depth in KFM03; FFM03 fracture domain) are fairly reducing and they seem to be in equilibrium with a clearly crystalline iron oxyhydroxide (in agreement with Grenthe's calibration) such as the ubiquitous hematite. This is coherent with the reducing character and long residence time of these groundwaters, where low crystallinity phases are not expected (/SKB 2004c/ and references therein). Therefore, they could be taken as the redox value in pristine conditions. The lack of measured Eh values in the more saline samples (KFM07A and KFM09A) prevent any additional comment.

The rest of the groundwaters show a very good agreement between their electrode potential measured values and the ones calculated with the calibration by /Banwart 1999/. This suggests that these Eh values could be controlled by the occurrence of an iron phase with an intermediate crystallinity, such as the one considered by /Banwart 1999/ in the Äspö large-scale redox experiment. This intermediate phase would be a recent low-crystallinity iron oxyhydroxide recrystallized from an amorphous one.

The presence of this intermediate iron oxyhydroxide with a higher solubility than a crystalline phase is only possible if there exists an oxidizing disturbance. There is no clear and systematic relationship between high contents of drilling water in these groundwater samples and the Eh control by intermediate-crystallinity oxyhydroxides. Therefore, the perturbation of the system could also be related to contamination with atmospheric air. However, independent of the mechanism, this perturbation seems to affect mostly the brackish groundwaters, which are also associated to deformation zones. This suggests that the original conditions of these waters and/or the lithological-hydrogeological system associated must have some characteristic that makes them more susceptible.

The occurrence of an oxyhydroxide of intermediate crystallinity would indicate that the system is still evolving and compensating the effects of the intrusion of oxygen. In fact, most of the Eh values are quite reducing, and it is expected that they will evolve towards even more reducing values as the low crystallinity oxyhydroxides re-crystallize. Fe-oxides were observed to precipitate during drilling in the KFM02A borehole (see comment 15) at 640 m depth and KOV01 at 620.3 m /Dideriksen et al. 2007/. The precipitated phases were identified mainly as fine grained (particle size less than 10 nm) amorphous or poorly crystalline phases (ferrihydrites), with some other more ordered structures in lower amounts[15].

Additionally, the presence of poorly-crystalline iron oxyhydroxides could be important in the interpretation of the available IRB (iron reducing bacteria) microbiological data. The use of ferric oxyhydroxides as TEAPs (terminal electron acceptor processes) by IRB depends on their crystallinity and surface area in such a way that the less crystalline phases (ferrihydrite and lepidocrocite) or the crystalline phases (goethite or hematite) with high surface area constitute the favourite primary source /Roden and Zachara 1996, Roden 2003, Bonneville et al. 2004, Pedersen et al. 2005/.

Therefore, the induced precipitation of poorly crystalline phases could enhance, at least, the observed IRB activity taking into account the opportunistic nature of the microorganisms. In spite of the fact that IRB are generally more abundant at shallow depths (<200 m in the studied sites from Sweden and Finland; /Pedersen, 2001/), high IRB populations have been found between 100 and 550 m depth in the Forsmark area in KFM01A at 111.75 m depth, KFM01D at 341 and 445 m depth, KFM08A at 546 m depth and KFM10A at 214 m and 328 m depth (Table 3-20).

[15] The presence of metallic iron and magnetite was also identified in that work as fine grained particles likely arising from the drilling equipment and its corrosion products. The presence of severe corrosion processes in the downhole equipment was indicated by /Wacker et al. 2004a/ in the KFM04A borehole and these processes could affect other boreholes due to the presence of Fennoskan HVDC (High Voltage Direct Current) cable in the vicinity of the Forsmark area /Nissen et al. 2005/. The existence of corrosion processes, already indicated by /Gimeno et al. 2007/, could also affect Eh measurements (e.g. through magnetite nanoparticles). This problem merits further research.

Iron concentrations, mineralogy and IRB activity

The highest iron concentrations in the Forsmark groundwaters are found in the upper 200 m (except for the suspicious values obtained in KFM10A at 328 m depth; Figure 3-18 and 3-21b). These high concentrations in the shallow groundwaters are indicative of an anoxic environment with effective reductive dissolution of Fe-silicates (e.g. Fe^{3+}-bearing clay minerals) or, more likely, of ferric oxyhydroxides.

Clay minerals and goethite are specially abundant in fracture fillings in the upper 100 m at Forsmark compared with the proportions found at greater depths. This is especially true for goethite, very rare at depth but frequent at these shallower levels (e.g. in the uppermost 20–40 m interval the amount of goethite can represent up to 25% of the total mineralogy; /Drake et al. 2006/). There are few detailed data on the properties of this mineral but the goethites studied by /Dideriksen et al. 2007/ are very fine grained, with particle sizes lower than 100 nm.

Reductive dissolution may proceed abiotically, but microbially-mediated reactions through dissimilatory iron reduction /e.g. Banwart 1999, Larsen et al. 2006/ play the pivotal role in Fe^{2+} mobilization. The presence of this microbial process seems to be confirmed by the available

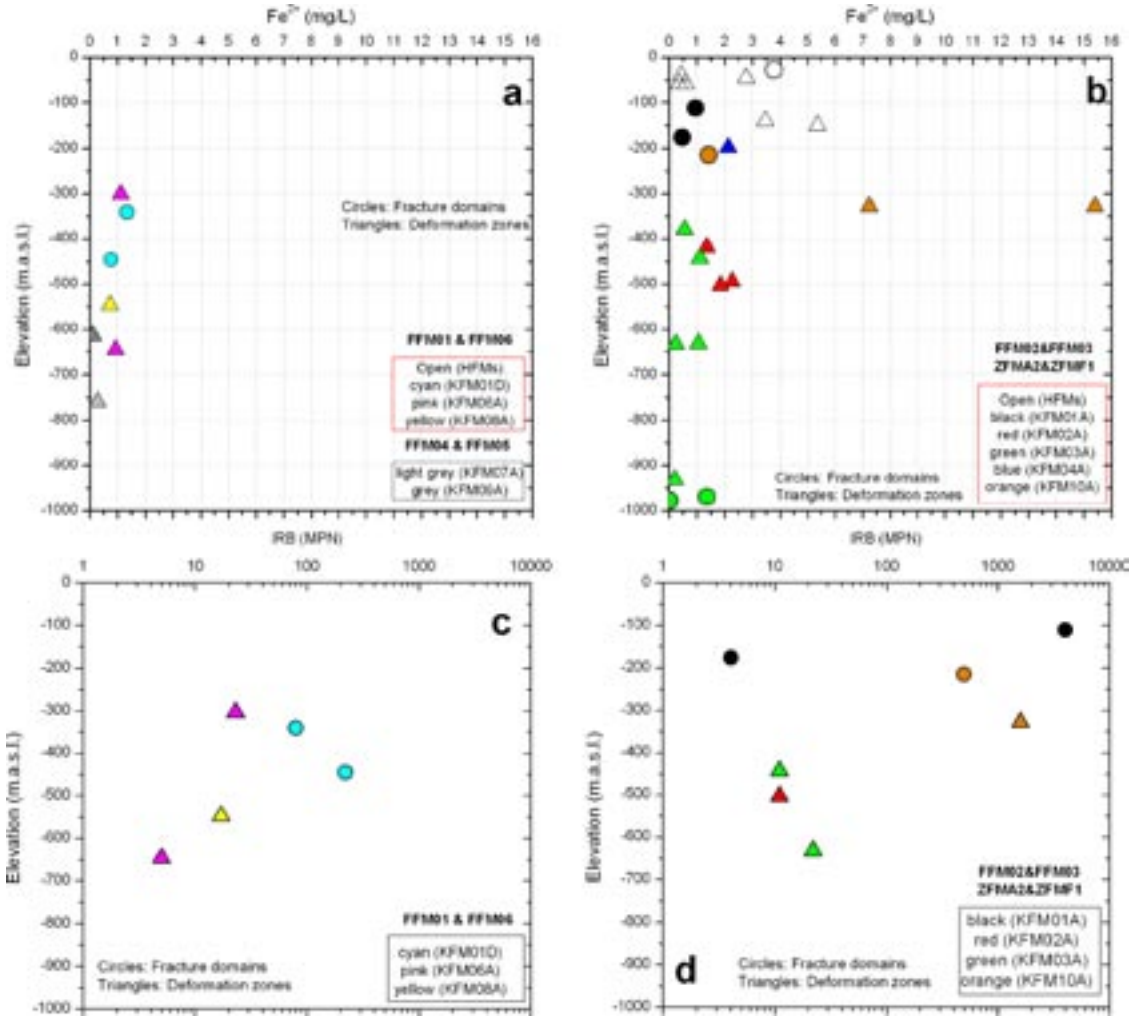

Figure 3-21. *Ferrous iron (a and b) and Most Probable Number of Iron Reducing Bacteria (c and d) distribution with depth in the Forsmark area groundwaters. Waters from categories 1, 2, 3 and 4 have been plotted. Left plots represent the waters sampled in the fracture domain zones (FFM01 and FFM06) including those samples from marginal areas to the target area (FFM04 and FFM05; in grey). Right plots represent waters samples in fracture domains FFM02 and FFM03, and samples taken from the gently dipping deformation zones. In both cases, triangles indicate deformation zones and circles, fracture domains.*

microbiological data from the shallow groundwaters (< 200 m depth). High amounts of IRB occur in KFM10A at 214 m depth (MPN = 500 cells/mL) and in KFM01A at 111.75 m depth (MPN = 4,000 cells/mL; Figure 3-21c and d; Table 3-20 and /Halbeck and Pedersen 2008/). Moreover, the mineralogy of fracture fillings in the this shallow zone (with high proportions of goethite) indicate the existence of adequate substrates for in situ IRB activity.

Whether IRB populations detected at deeper levels (in KFM01D at 341 and 445 m depth, KFM08A at 546 m depth and KFM10A at 328 m depth) represent "in situ" or induced activity needs to be further studied.

Discussion

Redox potentials measured in the deepest Forsmark groundwaters (at 630 and 930 m depth in KFM03A deformation zones in FFM03 fracture domain) are fairly reducing and they seem to be in equilibrium with crystalline hematite. This is coherent with the reducing character and long residence time of these groundwaters, where low crystallinity phases are not expected (/SKB 2004c/ and references therein). Therefore, they could be taken as the redox values in pristine conditions.

Except for these cases, the iron system seems to be clearly affected by drilling and sampling disturbances. Most Eh values in brackish groundwaters (at depths between110 and 646 m and associated to deformation zones) seem to be controlled by the occurrence of an iron phase with an intermediate crystallinity such as the one considered by /Banwart 1999/ in the Äspö large-scale redox experiment. This intermediate phase has to be a recent poorly crystalline iron oxyhydroxide recrystallized from an amorphous phase formed during a brief oxidizing period. Detailed mineralogical determinations in KFM02A borehole indicate the presence of fine grained amorphous and poorly crystalline phases induced by drilling, supporting the results obtained from redox pair calculations.

The occurrence of this oxyhydroxide of intermediate crystallinity would indicate that the system is still reacting and compensating for the effects of intrusion of oxygen from drilling. In fact, most of the Eh values are quite reducing, and it is expected they will evolve towards even more reducing values as the microcrystalline oxyhydroxides re-crystallize. Also, the presence of these poorly crystalline iron oxyhydroxides can enhance IRB activity, as they are the preferred substrate for these microorganisms, accelerating the evolution of the system towards a more reducing state.

Therefore, most measured Eh values do not correspond to the pristine conditions in the aquifer. But, even so, the careful measurement of Eh is still a very valuable aid to identify this type of disturbances and their impact on the system.

Independent of the problems and uncertainties related to the Eh measurements, integration of geochemical, mineralogical and microbiological data indicate the presence of a dominant post-oxic environment (according to the terminology proposed by /Berner 1981/) in the upper 200 m of bedrock at Forsmark. In this environment, the reductive dissolution of ferric oxyhydroxides by IRB seems to be the main control of the measured Fe^{2+} concentrations in the groundwaters. However, localized sulphidic environments can also occur in this shallow post-oxic zone (see below).

3.5.5 The sulphur system

As in previous SDM phases, results derived from the study of saturation states with respect to the more soluble iron monosulphides (amorphous and crystalline – or mackinawite–[16]) and the integration of these results with the available geochemical, mineralogical and microbiological data relative to the sulphur system are presented here.

[16] The term *"amorphous" FeS* is used here as equivalent to the more accurate terms of disordered mackinawite or nanoparticulate mackinwite /Wolthers et al. 2003, Rickard 2006/ and the term *mackinawite* as equivalent to ordered mackinawite or crystalline mackinawite.

Solubility calculations

Samples selected for solubility calculations are those with continuous loggings of temperature, pH and Eh. Several additional samples with analytical data of dissolved S^{2-} and Fe^{2+} and in situ pH value were also selected. The total number of samples is 14 (Table 3-20), all of them with a charge imbalance lower than 5% (calculated as described in /Gimeno et al. 2007/).

Saturation indices are shown in Figure 3-22. They indicate a clear undersaturation of most studied waters with respect to the amorphous monosulphide independently of the system. In the case of the fracture domains FFM01 and the maginal FFM04 and FFM05 (Figure 3-22a) this is true for all the samples. However mackinawite is in equilibrium in some waters with low sulphidic signature in brackish groundwaters (KFM01D at 445 m depth) and in saline groundwaters with higher sulphide contents (KFM07A at 759 m depth; Figure 3-22a).

In the other system (FFM02, FFM03 and gently dipping deformation zones; Figure 3-22b) waters are also undersaturated with respect to both mosulphides except for samples from KFM10A corresponding to data freeze 2.3 (and including the problematic sample at 328 m depth with exceedingly high Fe^{2+} contents).

Samples with the highest S^{2-}concentrations in cored boreholes (samples #12005 and #12513 at 969 m depth and samples #12001 and #12512 at 631 m depth; Table 3-21 and Figure 3-18e) and in percussion boreholes (samples in HFM19 at 140 m depth, with S^{2-} around 1.5 mg/L; Figure 3-18e) were not included in the original data set due to unreliable pH values (measured in the laboratory). To deal with this uncertainty, theoretical pH values have been calculated with PHREEQC by adding/substracting CO_2 until calcite equilibrium is reached. Under these conditions, saturation states with respect to amorphous monosulphides are between +0.1 and +0.4 at 969 m depth, between +0.03 and +0.16 at 631 m depth, and between +0.3 to + 0.4 at 150 m depth, not very different from the results obtained with the laboratory pH values. Therefore, as it would be expected from their $Fe^{2+}$and S^{2-} concentrations, these waters are in equilibrium with amorphous monosulphides. These saturation states are plotted with a different symbol in Figure 3-22 (stars).

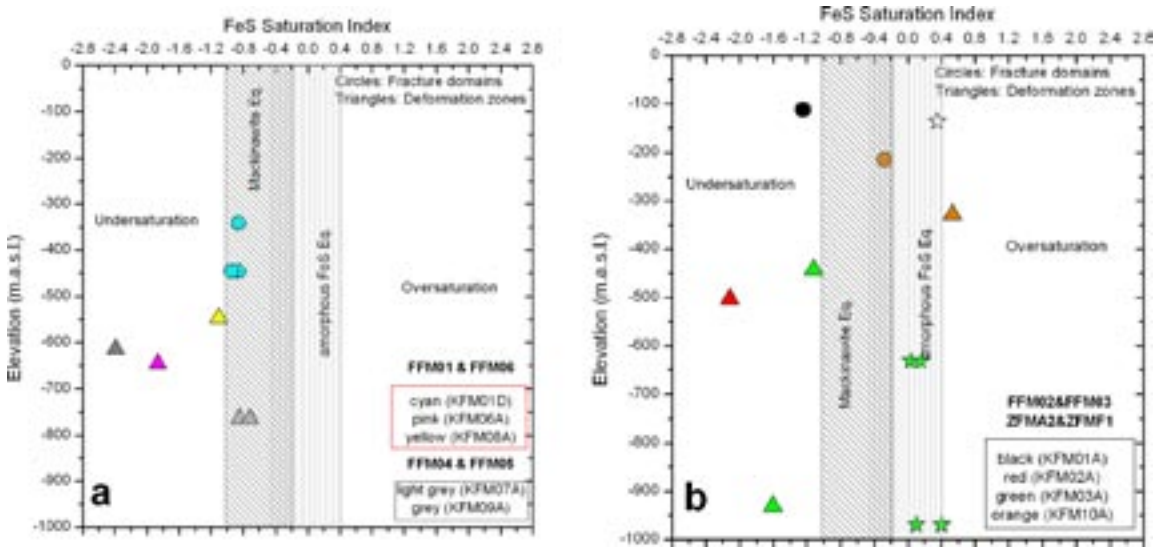

Figure 3-22. *Saturation indexes for ferrous iron monosulphide (FeS) in the Forsmark groundwaters as a function of depth. (a) values coloured by the borehole; and (b) values coloured by their location in the system. The shadow zones represent the SI=0 and the uncertainty range (±0.4 units) for the amorphous (light grey vertical lines) and the microcrystalline phase (dark grey inclined lines). Samples represented by stars correspond to those with pH in equilibrium with calcite (see text for explanations).*

Precipitation of iron monosulphides occurs in waters where SRB activity produces enough $S^{2-}$and there is Fe^{2+} available. As a result, dissolved sulphide contents decrease. However, if Fe^{2+} is not available, S^{2-} increases in solution and the monosulphides precipitation is inhibited in spite of the SRB activity.

The active precipitation of iron monosulphides seems to be much less important in Forsmark than in Laxemar, and it can be due to the absence of a source of iron, the alteration of the pristine conditions in the groundwater system, or to a lower SRB activity.

In this case there are abundant sources of iron in fracture fillings, mainly Fe-chlorites and hematite /Sandström et al. 2004, Sandström and Tullborg 2005/. In fact, iron concentrations in most Forsmark groundwaters are not particularly low and thus, iron availability is not a limiting factor.

Perturbations in the original sulphide content have been detected in re-sampled and monitoring sections from 400 to 1,000 m depth, showing that dissolved S^{2-} increases with time (a detailed study of this can be found in /Gimeno et al. 2007/). But these variations do not apreciably change the general picture.

Therefore, the frequent undersaturation with respect to the amorphous iron monosulphides must be related to a low activity, or absence, of SRB.

SRB activity and geochemistry in Forsmark groundwaters

The number of boreholes and borehole sections studied is already high and low amounts of SRB have been detected so far /Hallbeck and Pedersen 2008/. From fifteen investigated sections appreciable SRB activity (MPN>100) has been found in five of them at different depth (Figure 3-23). Waters from FFM01 have important SRB activity in KFM01D (445 m depth) and in KFM08A (550 m depth), and waters from the other system show high values in KFM03A (at depths around 630 and 930 m), and between 200 and 400 m depth in KFM10A (from 30 to 2,800 MPN of SRB; Table 3-20). So, in general, the detected sulphate-reduction activity is very restricted at present in Forsmark, although the number of detections has increased in the latest data freeze.

In most cases the agreement between geochemical and microbiological indicators of SRB activity is very good. In the fracture domains FFM02 and FFM03, the aforementioned high SRB activity is mostly associated with groundwaters in equilibrium with amorphous monosulphides. This association supports the occurrence of active monosulphide precipitation triggered by an important sulphate-reducing activity in brackish (at 214, 328 and 631 m depth) and saline groundwaters (at 969 m depth; Figure 3-23d).

The same agreement is found in waters undersaturated with respect to iron monosulphides: they have low concentrations of SRB (and other metabolic groups). These waters usually have an important Littorina contribution and correspond to more or less isolated pockets with a very low nutrients supply /Hallbeck 2007/.

In FFM01, groundwaters only reach mackinawite equilibrium in samples at 445 and 546 m depth (KFM01D and KFM08A boreholes; Figure 3-22a). This situation agrees with the highest SRB populations detected in these zones (Figure 3-23c). However, it is not clear why such amounts of SRB only promote mackinawite equilibrium.

$\delta^{34}S$ values (Table 3-20) range from 21.9 to 38.4‰, clearly higher than present values of the Baltic Sea at Forsmark (17.2 to 21.7‰). They can be indicative of SRB activity but not of the moment or the place in which it took place. For instance, the isotopic values in the accumulations of brackish Littorina-rich groundwaters likely reflect the occurrence of sulphate-reduction activity in the sea floor during the Littorina stage, and not a present activity.

The absence of recent monosulphide precipitation in the Littorina pockets is consistent with the results obtained from the SO_4^{2-}/FeS_{am} redox buffer, as the Eh values obtained with this buffer do not agree as well as SO_4^{2-}/pyrite, with the measured ones. The assumption here is that the precipitation occurred during Littorina infiltration through the marine sediments (see Section 2.1)

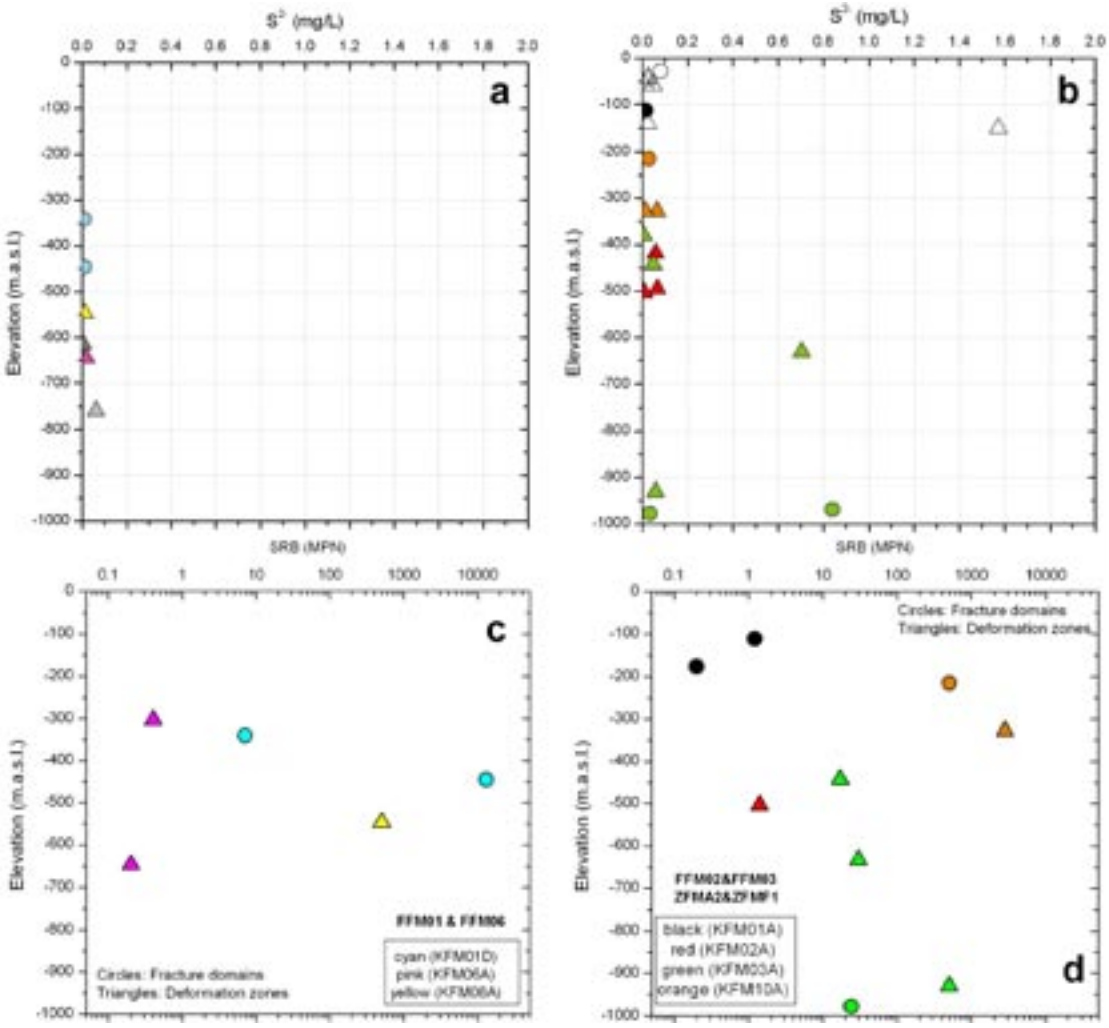

Figure 3-23. *Sulphide (a and b) and Most Probable Number of Sulphate Reducing Bacteria (c and d) distribution with depth in the Forsmark area groundwaters. Waters from categories 1, 2, 3 and 4 have been plotted. Left plots represent the waters sampled in the fracture domain zones (FFM01 and FFM06) including those samples from marginal areas to the target area (FFM04 and FFM05; in grey). Right plots represent waters samples in fracture domains FFM02 and FFM03, and samples taken from the gently dipping deformation zones. In both cases, triangles indicate deformation zones and circles, fracture domains.*

in such a way that once these waters were isolated from the hydraulic flow, they re-equilibrate with respect to more crystalline sulphides, pyrite for instance. This evolution justifies the good Eh results obtained with the SO_4^{2-}/pyrite buffer for these waters (Table 3-21) and could support the statement that the sulphur redox system is an effective buffer inherited from the Littorina period. The inheritance of the redox characters in the isolated Littorina-rich waters has also been identified in the manganese system.

Discussion

The number of groundwater samples with sulphidic character and in equilibrium with respect to iron monosulphides is lower in Forsmark than in Laxemar. From the data available up to now, the agreement between geochemical and microbiological indicators of SRB activity is very good. Both types of indicators show the active occurrence of SRB in brackish groundwaters at shallow depths, between 150 and 210 m depths, and in brackish or saline groundwaters at greater depths, between 631 m and 900–1,000 m in Forsmark, in agreement with the maximum depth of bacterial activity of this type in Laxemar /SKB 2006d/.

The same agreement is found for the brackish groundwaters at depths between 220 and 600 m; waters undersaturated with respect to iron monosulphides have very low concentrations of SRB. Most of the brackish groundwaters in this depth range are characterised by having an important Littorina proportion and they should correspond to more or less isolated pockets with a very low nutrients supply.

Available data suggest that the sulphur system plays an important role in the control of the redox character of the groundwaters from 200 m depth down. It controls sulphide and ferrous iron concentrations in waters through active precipitation of monosulphides (SRB activity) and seems to be responsible for some of the redox characteristics in the Littorina-rich groundwaters.

3.5.6 New data on the "uranium problem" in Forsmark groundwaters

The elevated dissolved uranium concentrations found in some Forsmark groundwaters between 200 and 650 m depth have aroused considerable interest owing to their potential environmental implications and effects on the safety case for a high-level radioactive waste repository.

The results presented by /Gimeno et al. 2007/ on the origin of these high uranium contents in some Forsmark groundwaters integrated all available data from Forsmark 2.1. Several problems were identified, mainly the small number of available groundwater samples with the necessary data (e.g. measured Eh values). To mitigate this limitation, several samples from the Forsmark 2.2 data freeze were also included in the study. Besides, in the case of samples without potentiometric Eh measurements, the SO_4^{2-}/S^{2-} redox potentials were used.

Some other key parameters were unavailable (or very scarce) in Forsmark 2.1. This was the case of the oxidation state of dissolved uranium in groundwaters, its association with colloidal phases, the nature of the U mineral phases in fracture fillings, and the U-series isotopes in fracture coatings and waters.

This document updates previous results (Forsmark 2.1) by using the new groundwater samples from 2.2 and 2.3 data freezes together with the additional information collected for colloids and isotopes. With respect to mineralogy, work done in the fracture fillings has failed to detect more uranium minerals (Tullborg pers. comm. 2007) apart from the ones found in KFM03A at 644 m depth /Sandström and Tullborg 2005/. Overall, the new groundwater data do not change the general picture (including the detected problems and conclusions).

Forsmark groundwaters with high uranium contents

Forsmark groundwaters with high uranium contents are located at depths between 180 and 631 m, with values between 14 and 122 µg/L U. As can be deduced from Table 3-22 and pointed out by /Gimeno et al. 2007/, these uranium contents (three first rows in Table 3-22) cannot be considered "anomalous" when compared with similar environments. Uranium concentrations above 10 µg/L are well within the usual range of values reported in many other parts of the Scandinavian Shield, and even the maximum values found in Forsmark are far below the highest values recorded in other sites (Table 3-22).

General characterization of high uranium groundwaters

The general geochemical features observed in the Forsmark groundwaters with high uranium concentrations (> 10 µg/L) were described in detail in /Gimeno et al. 2007/. Only a general summary will be provided here to facilitate the understanding of the subsequent geochemical calculations.

The first interesting character was already shown in Figure 3-18 (panels g and h) which is also presented here in Figure 3-24, and it is the main association of high uranium contents with waters from gently dipping deformation zones in fracture domain FFM03.

Table 3-22. Comparison of the high U-concentrations found in Forsmark and in other sites.

Area / Country	Depth (m)	Uranium concentration (µg/L) (range/mean value/ max. value)	Reference
Forsmark (Sweden)	180–632	14–122 / –/ –	This work
	700–1,000	– / –/ 1	This work
	Surface waters (lakes and streams)	– / –/ 40	This work
Laxemar (Sweden)	Surface waters	– / –/ 14	/SKB 2006a/
	200–1,000	– / –/ 1	
Stripa (Sweden)	< 60	– / –/ 90	/Nordstrom et al. 1985/
	300–450	– / –/ 35	
	> 600	– / –/ 10	
Sweden (328 drinking water samples)	–	– / 14.3/ 427	/Isam et al. 2002/
Aspö (Sweden)	Surface waters	– / –/ 8	/Smellie and Laarksoharju 1992/
Finsjön (Sweden)	70–400	– / –/ 16	/Smellie and Wikberg 1989/
Olkiluoto (Finland)	< 100	– / –/ 18	/Pitkänen et al. 2004/
	> 200	– / –/ 4	
Palmottu (Finland)	Surface waters	– / –/ 11	/Blomqvist et al. 2000/
	100–150	– / –/ 900	
	> 200	1–10 / –/ –	
Finland (7,000 drinking water samples)	–	– / 32/ 20,000	/Salonen and Huikuri 2002/
Finland (drinking water well)	–	– / –/ 14,900	/Asikainen and Kahlos 1979/
Norway (crystalline bedrock)	–	16–34 / –/ 750	/Frengstad et al. 2004/
	–	– / –/ 170	/Banks et al. 1995ab/
	–	– / –/ 2,000	/Reimann et al. 1996/
Lac du Bonnet batholith (Canada)	Near surface	– / 100–/ 1,000	/Gascoyne 1997, 2004/
	200–400	1–300 / –/ –	
	> 600	1–10 / –/ –	
Eye-Dashwa Lakes pluton (Canada)	–	– / –/ 50	/Gascoyne 1989,1997/

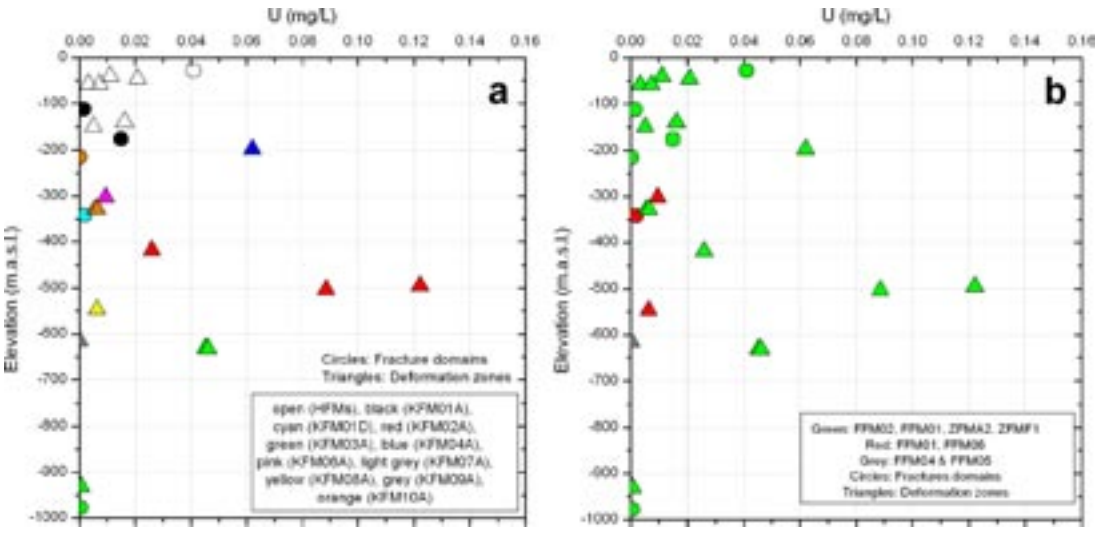

Figure 3-24. *Uranium contents with respect to depth. Groundwater samples are coloured by boreholes (a) and by the structural domains (b) In both cases, triangles indicate deformation zones and circles, fracture domains.*

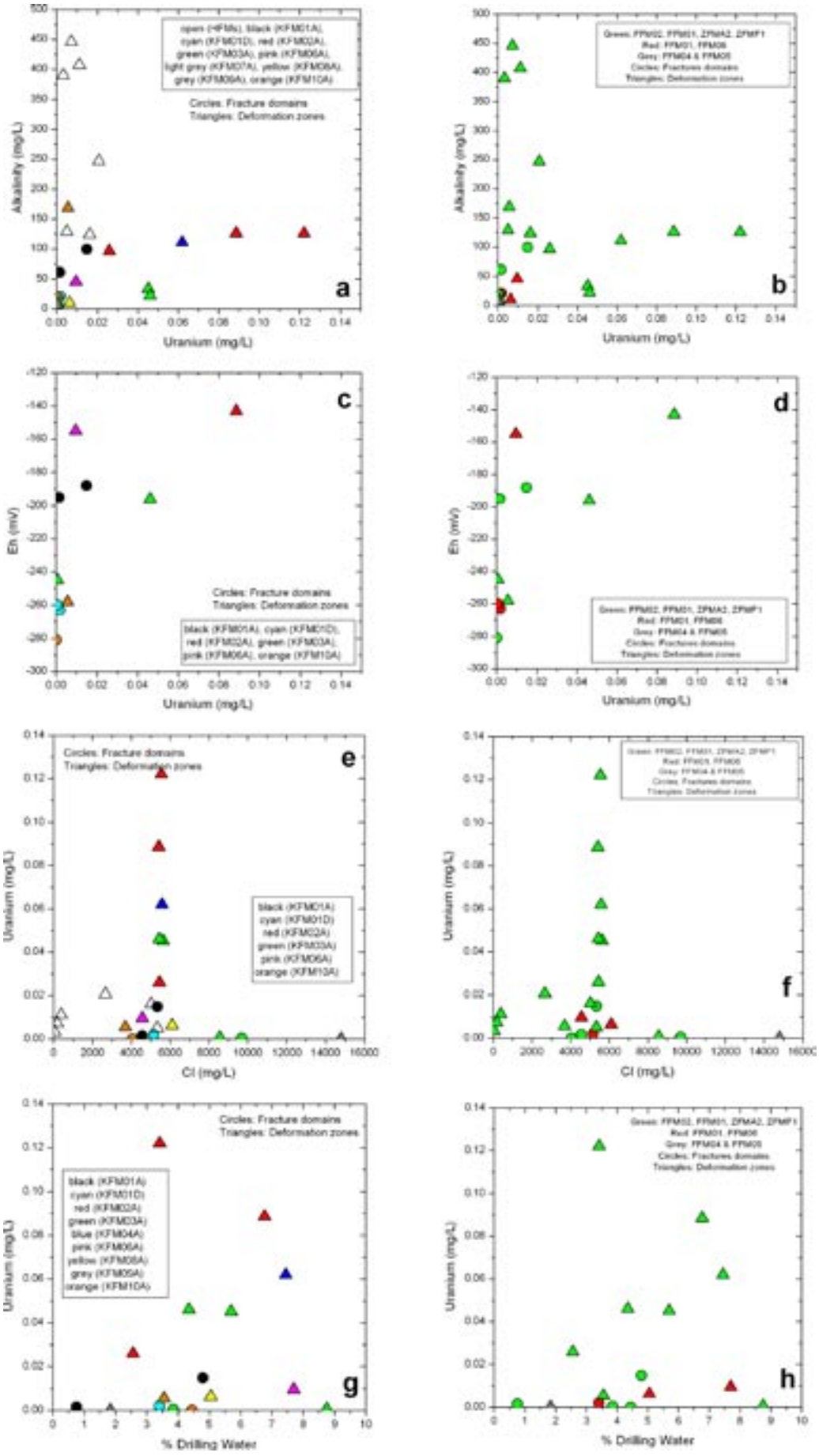
Alkalinity (mg/L)
Uranium (mg/L)
Circles: Fracture domains
Triangles: Deformation zones
a
b
Eh (mV)
c
d
Uranium (mg/L)
Cl (mg/L)
e
f
% Drilling Water
g
h

Figure 3-25. *Panels (a) and (b): Alkalinity vs uranium concentrations in Forsmark groundwaters. Panels (c) and (d) display U vs Eh in the Forsmark groundwaters. Panels (e) and (f) and (g) and (h) show the uranium contents vs chloride and percent of drilling water, respectively. Groundwater samples are coloured by boreholes (left plots) and by the structural domains (right panels) In both cases, triangles indicate deformation zones and circles, fracture domains.*

A thorough analysis of the main geochemical features of these waters has been performed to find the reasons of this behaviour. As a general trend, correlation of uranium and alkalinity in the Forsmark groundwaters (Figure 3-25, panels a and b) does not show the decrease of uranium concentration with the decrease of alkalinity that has been found in other systems (Stripa, Canada). However, the trend of increasing uranium with alkalinity is more clearly seen when only the range of alkalinity from 90 to 130 mg/l is considered. This correlation is caused by the combined effect of Eh (Figure 3-25, panels c and d) and alkalinity on uranium speciation. As detailed in /Gimeno et al. 2007/, under the mildly reducing conditions present in the Forsmark groundwaters with high uranium concentrations, the alkalinity increase leads to an increase in the carbonate species and their complexation with uranium which, in turn, enhances the dissolution of U solid phases and increase the dissolved uranium concentrations.

Although no clear correlation between Eh and uranium content can be established, groundwaters with high uranium contents tend to have less reducing Eh values than the rest of Forsmark groundwaters (Figure 3-25, panels c and d). As described in /Gimeno et al. 2007/, high uranium concentrations are correlated with an almost constant chloride concentration of 5,000–5,600 mg/L (Figure 3-25, panels e and f) in waters characterised by a high proportion of the Littorina end-member. No evidence of more saline groundwaters (>5,600 mg/L Cl) with high uranium contents has been found.

Moreover, waters with high uranium content also tend to have a medium to high drilling water content (around 7%), although the correlation between both variables is by no means perfect (Figure 3-25, panels g and h). Problems with the interpretation of the percentage of drilling water /Gimeno et al. 2007, Buckau 2007/ still remain in the newly delivered data. In fact, there are also waters with low uranium contents and a high percent of drilling water, which suggests that the possible perturbation produced by the presence of drilling water is only effective in those zones where uranium mineral phases are available to be mobilised /Gimeno et al. 2007/.

The different igneous rocks present in the Forsmark area have generally uranium concentrations around 4–5 ppm, in agreement with mean values reported for this element in granitic rocks /Reimann and Caritat 1998/ and similar to values in the Äspö subarea /Tullborg et al. 1991/ and in the Canadian shield granites /Gascoyne 1989/. However, the analysis performed in the fracture coatings of Forsmark show that uranium contents are almost always higher than in the bedrock (up to 2,200 ppm, /Sandström and Tullborg 2005/. These elevated U-levels found in some of the Forsmark fractures could be considered as anomalies indicative of the presence of uranium mineralisations or enrichments in the surfaces of the fracture fillings. In fact, /Sandström and Tullborg 2005/ have recently pointed out the occurrence of pitchblende in fracture fillings at 644 m depth in the KFM03A borehole, where waters with elevated uranium concentrations have been sampled.

Evaluation of new groundwater samples

Groundwaters with uranium concentrations higher than 10 µg/L have been found in five boreholes in Forsmark 2.1 (KFM01A, 02A, 03A, 04A, 06A) and in two further sections in Forsmark 2.2 (KFM06C and 09A; Table 3-23).

Table 3-23. Forsmark groundwaters with uranium concentrations higher than 10 µg/L and their location.

Borehole	Depth (m)	Fracture Domains and Deformation Zones		U (µg/L)	
				Data freeze 2.1	Data freeze 2.2–2.3
KFM01A	176.3	FFM02	Deformation Zone Waters	15–20	
KFM02A	417.8	ZFMA2		14–26	25.9–31.3
	495–503	ZFMF1		65–88.6	122–143
KFM03A	631	DZ in FFM03		45–59	45–50
KFM04A	200	ZFMA2		35–62	
KFM06A	298.5	FFM01	Fracture Domain Waters	9–11	24
KFM06C	434.8	FFM06			44.4
KFM09A	601.9	FFM06			85.9

New samples from four sections previously sampled during Forsmark data freeze 2.1 (in KFM02A, KFM03A and KFM06A) maintain their low or high U values, although several differences have been detected:

- KFM01A: the new samples taken at section 109–130 m (115.79 m depth) have as low uranium concentrations (2.6–3.8 µg/L) as the samples taken previously at similar depths (section 110.1–120.8 m, 111.75 m depth).
- KFM02A: the new samples at section 411–442 m (417.8 m depth) show higher uranium contents (26 – 30 µg/L) than samples taken previously at section 413.5–433.5 m (414.72 m depth) with 14 – 26 mg/L (Figure 3-26). The percentage of drilling water is similar in both sets (2–5%) but the new samples have higher Fe^{2+} and S^{2-} concentrations, and low but detectable tritium.

  At section 509–516.8 (503.34 m depth) high uranium contents were measured during 2003 (as high as 89 µg/L). Data freeze 2.2 and 2.3 show new samples taken at similar depth (section 490–518 m; 494.17 m depth) with higher uranium concentrations (122 to 143 µg/L; Figure 3-26) and increased S^{2-} concentrations. Drilling water contents were relatively constant during the different sampling periods (3–7%).
- KFM03A: the two new samples taken at section 969.5–994.5 m (969.14 m depth) have low uranium concentrations (0.3–0.7 µg/L) similar to those found at section 980–1,001 m (967.77 m depth) in the previous data freeze (0.2–0.4 µg/L U; see Figure 3-26, the three different green symbols fall one over the other). The percentage of drilling water in the new samples is lower (around 1%) and the Fe^{2+} and S^{2-} concentrations are significantly higher.

  New samples from the 2.2 and 2.3 data freezes at section 638.5–650 m have a slightly more saline character and higher Fe^{2+} and S^{2-} concentrations than groundwaters sampled at a similar depth included in the previous data freeze (section 639–646 m). However, they show similar high uranium values (around 45–60 µg/L), similar percentage of drilling water (4–6%), and undetectable tritium.
- KFM06A: new samples from Forsmark 2.3 at section 341–362 m (298.5 m depth; Sample #12399) have uranium concentrations as high as 24 µg/L, whereas contents in the previous 2.1 data freeze a similar sampled section (353.5–360.6, 301.9 m depth) were 9–11 µg/L (Figure 3-26). This increase in uranium contents coincides with an increase in Fe^{2+} and S^{2+} contents, and with low but detectable tritium (in 2.1 samples tritium was below the detection limit).

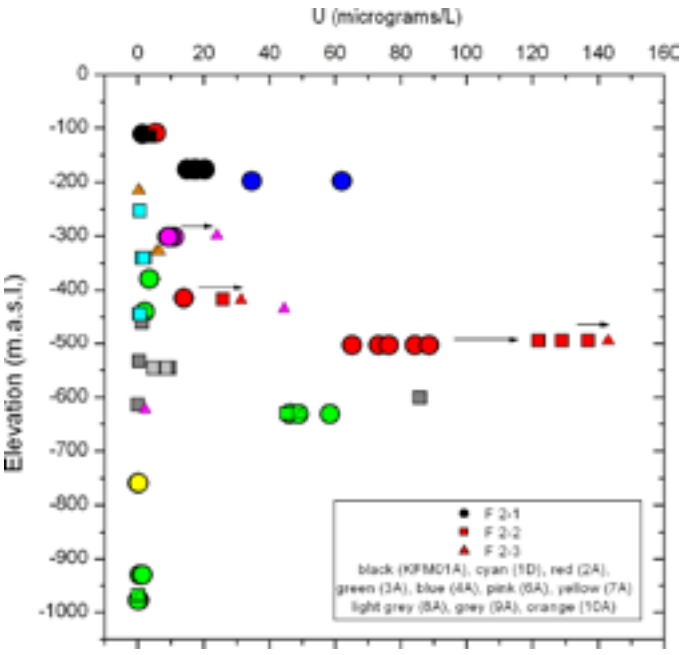

Figure 3-26. *Uranium distribution with depth in the different boreholes (different colours) showing the values obtained in the different data freezes (circle for 2.1, squares for 2.2 and triangles for 2.3). Arrows indicate the concentration trends with time (or data freezes)*

In summary, the evolution of dissolved uranium contents over time shows two trends: (a) low contents remain generaly low over time, and (b) high contents found in other sections usually increase slightly with time. This last trend is paralleled, in many cases, with the simultaneous increase in dissolved Fe^{2+} and S^{2-}. This correlation between uranium, Fe^{2+} and S^{2-} could be important as an increase in Fe^{2+} and S^{2-} would indicate a more reducing environment, in spite of which uranium concentrations increase. This observation could indicate that high dissolved uranium contents are, at least to some extent, an original characteristic of these waters in contact with uranium minerals, instead of being the exclusive result of an external perturbation of the redox state of the system due to drilling and sampling /Gimeno et al. 2007/.

With regard to the two new U-rich samples detected in Data freeze 2.2 and 2.3 for Forsmark (Table 3-23), there are some sampling drawbacks that cast doubt on their representativeness. In the case of sample #12216 (borehole KFM09A), it was taken by "tube sampling" /Nilsson 2006/ and it is also anomalous with respect to other elements (high contents of Fe and Si). Samples taken between packers in the same borehole a month later (three samples, #12241 to #12244) at a similar depth (614.21 m; borehole section 785.1– 792.24 m) have a similar composition for the major elements but the anomalously high values of Fe, Si and U have disappeared (Fe = 0.15 mg/L, Si = 4.5 mg/L, and very low uranium concentrations, about 0.1 µg/L); and without a dramatic decrease of the drilling waters content (1.8 to 2.33% vs 4.6% in the previous sampling). Therefore, the previously detected high-U content should probably be considered a sampling artifact. When the P-report become available this hypothesis will be checked as it would be very interesting to trace the origin of this temporal anomaly in the uranium content being the only case in which the anomaly has disappeared with time.

As for sample #12500 (borehole KFM06C), it also contains a *very high* percentage of drilling water (27.3%). Therefore, caution should be taken when using this sample in the context of the uranium question in Forsmark.

The number of new boreholes and sampled sections is not as high as it would be necessary to determine the spatial distribution of groundwaters with high uranium contents. However as it is indicated in Table 3-23, these waters are mainly associated to gently dipping deformation zones in FFM02 and FFM03. Only the samples from KFM06A, 06C and 09A are located in the

other system (fracture domains FFM01 and FFM04 and 05) and samples from KFM06C and 9A are, at least, problematic. In any case, groundwaters with high uranium contents seem to be spatially limited to, and associated with specific tectonic and paleohydrological features. The new samples from Forsmakr 2.2 and 2.3 data freezes do not contradict this hypothesis, already reported in /Gimeno et al. 2007/, for the origin of the high uranium contents in some of these groundwaters.

Uranium in colloids

Once the high *dissolved* uranium contents are identified, the second step is the study of uranium in the *colloidal* fraction. Data reported to date correspond to groundwaters with low dissolved uranium content (KFM01D, KFM06A, KFM07A, KFM08A; /Nilsson et al. 2006, Wacker et al. 2006ab, Berg et al. 2006/ and to groundwaters with the highest U content (KFM02A and KFM03A; /Berg and Nilsson 2006/). Although not published yet, there are also available data for KFM01D (section 568–575.1m) and KFM10A corresponding to data freeze 2.3. This information is summarized in Table 3-24.

Waters with low U values (KFM01D, KFM06A, KFM07A and KFM08A) have U associated with the <1,000 D or <5,000 D fractions. Fractions with higher molecular weights (that may imply the presence of a colloid phase in the groundwater) do not have uranium or it is in a very low concentration.

But most important, results obtained by /Berg and Nilsson 2006/ in high uranium groundwater samples at KFM02A and KFM03A (Table 3-24) show that U exists almost entirely associated with species with a molecular weight less than 1,000 D (g/mol), too small to be considered as colloids. Moreover, no detectable amounts of uranium particles or colloids are caught in the filters. The other analysed elements (Fe, Si, and Mn) are also carried as "truly" dissolved elements and only minor colloidal fractions of sulphur have been detected.

These results indicate that the occurrence of U-bearing colloids in the studied waters is very low and can not be the cause of the high concentrations found in some groundwaters.

Uranium redox pairs

The Eh value used by /Gimeno et al. 2007/ for the U speciation-solubility calculations is one of the main uncertainties in these calculations. The number of samples from packed sections with high uranium content (>10.0 µg/L) was only five and only four of them had potentiometric Eh measurements (Table 3-25). Several high-U samples from Forsmark data freezes 2.2 and 2.3 were also included in the report, but without Eh measurements. For these samples with no Eh measurement, the Eh value used for the uranium speciation-solubility calculations was obtained from the $Fe(OH)_3/Fe^{2+}$ and SO_4^{2-}/S^{2-} redox pairs.

The results from speciation-solubility calculations indicated that waters with elevated uranium contents belong to a particularly critical range of Eh and alkalinity values in which the U-carbonate species can drastically change in content, affecting the solubility of the uranium phases present in the system (such as uraninite or pitchblende) whose stability would be enhanced due to the reducing Eh values. Therefore, in these cases, uranium speciation and saturation indexes with respect to uranium minerals were totally dependent on the selected Eh value.

The only way to avoid this dependence is by having analytical contents of the different dissolved uranium oxidation states, mainly U(IV) and U(VI). In this way the speciation distribution for each oxidation state can be obtained from their analytical concentration without using the Eh data. This calculation keeps the possible redox disequilibrium between the two uranium forms and the rest of the redox pairs, or the disequilibrium with respect to the potentiometrically measured Eh. Then, an independent redox potential for the redox pair U(IV)/U(VI) can be obtained.

In spite of the limited number of samples where U(IV) and U(VI) have been analysed in the Forsmark groundwaters, they have been included in the speciation-solubility calculations to assess the magnitude of several uncertainties identified in the previous report /Gimeno et al. 2007/.

Table 3-24. Uranium contents in the different fractions filtered through different cut-offs in different sections (indicated as borehole lengths) from boreholes KFM01D, KFM02A, KFM03A, KFM06A, KFM07A, KFM08A and KFM10A. The dissolved uranium content (together with S^{2-} and Fe^{2+}) in one sample (of quality between 1 and 3) of each section, as well as the range of concentration found in the different sampling campaigns are also shown. Concentrations are expressed in µg/L except for S^{2-} and Fe^{2+}(mg/L). The values corresponding to the waters with high uranium content are highlighted in grey.

	KFM01D			KFM02A		KFM03A
	428.5–435.6	428.5–435.6	568–575.1	411–442	490–518	633.5–650
U in selected sample	1.94 (#12316)	0.799 (#12354)	0.8 (#12354)	26.6 (#12002)	122 (#12004)	45.2 (#12001)
U range in section	1.35–2.15	0.52–0.79	0.5–0.8	–	122–143	45.2–46.3
Not filtered				26.6±4.3	119±20	45.3±7.3
Filtrate 0.40 µm				25.9±4.1	122±20	44.8±7.2
Filtrate 0.05 µm				26.6±4.3	121±19	42.3±7.4
< 1,000 D	1.9±0.3	0.55±0.07	0.55	23.3±4.0	106±18	37.6±6.0
> 1,000 D				2.1±1.2	9.2±6.1	5.3±2.7
< 5,000 D	1.9±0.3	0.47± 0.06	0.47			
> 5,000 D	< 0.1	<0.01	bdl			
S^{2-}	bdl	bdl	bdl	0.058	0.066	0.701
Fe^{2+}	1.33	1.23	1.23	1.36	2.26	1.06
% Drill.	3.4	0.9	0.9	2.85	3.8	5.70

	KFM06A	KFM07A	KFM08A	KFM10A	
	(353.5–360.8)	(848–1,001)	(683.5–690.6)	(298–305)	(478–488)
U in selected sample	9.57 (#8809)	0.337 (#8843)	6.35 (#12000)	0.1 (#12552)	0.56 (#12517)
U range in section	8.15–11.0	0.184–0.337	4.86–9.67	0.1–0.4	5.6–6.5
Not filtered					
Filtrate 0.40 µm					
Filtrate 0.05 µm					
< 1,000 D	7.5±0.75	0.22±0.03	7.8 ± 0.8	0.104	5.2
> 1,000 D					
< 5,000 D	7.98±0.8	0.18±0.03	4.5±0.8[(a)] 6.9±1.0	0.1	5.41
> 5,000 D			0.9±0.5[(a)] 1.0±0.5	0.013	bdl
S^{2-}	bdl	0.062	0.012	0.027	0.065
Fe^{2+}	1.11	0.262	0.726	1.43	14.4
% Drill.	7.7	0.6	5.05	4.45	3.55

[(a)] Analyses performed in 2005-10-13 and 2005-10-27.

Table 3-25. General information of the samples with high uranium concentrations (>10.0 µg/L). Depth correspond to the Elevation of the mid section. Category: indicates thecategory of the sample /Smellie et al. 2008/. DW (%) indicates the percent of drilling water. The pH data correspond to the field measurements except in the cases in "italics" which were determined in laboratory. Ferrous iron, sulphide, and uranium are expressed in mg/L.

Data Freeze	KFM	Depth (m)	Sample	Category	DW (%)	pH	Eh (mV)	Fe^{2+}	S^{2-}	U ($x10^{-3}$)
2.1	01A	–176.3	4724	2	4.80	7.41	–188	0.475		14.9
2.3	02A	–417.8	12002	2	2.56	*7.36*		1.360	0.058	25.9
2.2		–495	12004	2	3.41	*7.19*		2.260	0.066	122.0
2.3		–503	12507[b]	T2	6.64	*7.25*		1.970	0.167	143.0
2.1			8016	3	6.77	6.93	–143	1.840	0.009	88.6
2.2	03A	–631	12001	2	5.70	*7.49*		1.060	0.701	45.2
2.3			12512	T2	4.50	*7.43*		0.838	0.538	49.5
2.1			8273	2	4.35	7.38	–196	0.233		46.1
2.1	04A	–197	8267	3	7.45	7.36		2.120		62.0
2.1	06A	–302	8809	3	7.70	7.35	–155	1.110		9.6

As far as the authors know, the only available uranium redox species data are the ones recently obtained by /Suksi and Salminen 2007/. They have determined the dissolved U(IV) and U(VI) contents in one of the samples with the highest uranium concentrations: sample #12323 (Table 3-26) from borehole KFM02A at 494.97 m depth (borehole section 490–518 m). Unfortunately the chemical analysis of this sample is not complete (e.g. there are no data of field pH, HCO_3^- or Cl). To perform the speciation-solubility calculations, the data obtained by /Suksi and Salminen 2007/ have been "assigned" to sample #12004 from the same section (Table 3-29) and which has similar compositional characteristics.

As displayed in Table 3-26, groundwater samples in this borehole section have uranium concentrations between 122 and 143 *µg/L* with amounts of drilling water between 3.05 and 6.64%. Total dissolved uranium concentration in sample #12323 was 129 *µg/L* and dissolved U(IV) contents in several sub-samples ranged between 1.4 and 4.7 *µg/L*, which represents 1.1 to 3.6% of the total dissolved uranium. From these data, U(VI) concentrations can be obtained by subtraction.

Speciation-solubility calculations

Speciation-solubility calculations have been performed using PHREEQC /Parkhurst and Appelo 1999/ and two different thermodynamic databases: SKB-TDB June 2005, /Duro et al. 2005/ and NAGRA (Nagra/PSI TDB 01/01; /Hummel et al. 2002/).

Table 3-26. Some parameters of interest for samples taken at KFM02A in section 490–518 m (at 494.97 m depth) where uranium oxidation states, U(IV)–U(VI) have been analysed.

Sample	Sampling date	% drilling water	pH	Fe^{2+} (mg/L)	S^{2-} (mg/L)	U (*µg/L*)
12004	2005/11/07	3.41	7.19	2.26	0.066	122
12311	2006/06/20	3.05	7.16	1.84	0.065	137
12323	2006/06/26	–	–	–	–	129
12507	2006/10/18	6.64	7.25	1.97	0.167	143

SKB-TDB derives directly from the NAGRA database (Nagra/PSI TDB 01/01) with modifications or extensions for elements of special interest for Performance Assessment. Thermodynamic data for species and minerals of the carbon, sulphur and silica systems are identical to the ones included in NAGRA which, in turn, come from the review performed by /Nordstrom et al. 1990/ for these systems and are also included in the WATEQ4F database /Ball and Nordstrom 2001/.

As shown in Table 3-27, the Eh values calculated from the U(IV)/U(VI) redox pair with the SKB and NAGRA databases are slightly different as a consequence of the different species and thermodynamic data considered for the reduced and oxidized uranium forms in each database. In any case, the discrepancy is smaller than 25 mV.

Unfortunately there are no Eh values from Chemmac for this section during the 2005–2006 sampling period to compare with the calculated results. Only Eh values calculated from different redox pairs can be compared and, as shown in Table 3-28 and Figure 3-27. Most of them are compatible but slightly higher than the values obtained from the U(IV)/U(VI) redox pair with SKB's TDB and using the two possible uranium (IV) concentrations (–136 to –152 mV).

However, potentiometric Eh logs were recorded at a similar depth (503.4 m, section 509–516.8 m borehole length) during 2003 (Forsmark data freeze 1.1) and a representative value of –143 mV was obtained for groundwater with a very similar composition (e.g. high uranium contents, around 70–90 *µg/L)* to those sampled at 495 m depth (section 490–518 m) during 2005–2006. This value is in very good agreement with the value obtained from the U(IV)/U(VI) redox pair with the SKB-TDB and it is close to the lower limit obtained with the NAGRA database (Table 3-27 and Figure 3-27). Although this result is based on only one determination of the U(IV)/U(VI) redox pair, it is very suggestive and consistent with the results obtained in Palmottu (Finland). In the Palmottu system, where redox conditions are less reducing (measured Eh from +70 to –110 mV), a good correspondence between measured and calculated Eh from the *electroactive* U(IV)/U(VI) redox pair was obtained /Ahonen et al. 1994, Bruno et al. 1996/. This correspondence reflects the equilibrium of these waters with a redox buffer in the systems represented by $UO_{2.33}$ /Ahonen et al. 1993, Bruno et al. 1996, Langmuir 1997, Blomqvist et al. 2000/.

Table 3-27. Redox potentials calculated from the U(IV)/U(VI) redox pair with the SKB and NAGRA databases and using the analytical data by /Suksi and Salminen 2007/.

U(IV) concentration/percentage	Eh (mV) SKB TDB	Eh (mV) NAGRA TDB
1.4 µg/L / 1.1%	–136	–112
4.7 µg/L /3.6%	–152	–128

Table 3-28. Eh values obtained for the groundwater samples taken in KFM02A at section 490–518 m (494.97 m depth). Results for the $Fe(OH)_3/Fe^{2+}$ redox pair are calculated from the oxyhydroxide solubility proposed by /Banwart 1999/ using both Fe^{2+} activities and Fe^{2+} analytical concentrations. The mean value is indicated for each sample. See also Figure 3-27 (range in green).

Sample	Sampling date	Eh (mV)				
		SO_4^{2+}/S^{2-}	SO_4^{2+}/Pyrite	SO_4^{2+}/FeS	$Fe(OH)_3/Fe^{2+}$	U^{4+}/U^{6+}
12004	2005/11/07	–189	–156	–197	–140 ± 30	–130± 20
12311	2006/06/20	–187	–147	–186	–140 ± 20	
12507	2006/10/18	–197	–161	–201	–147 ± 30	

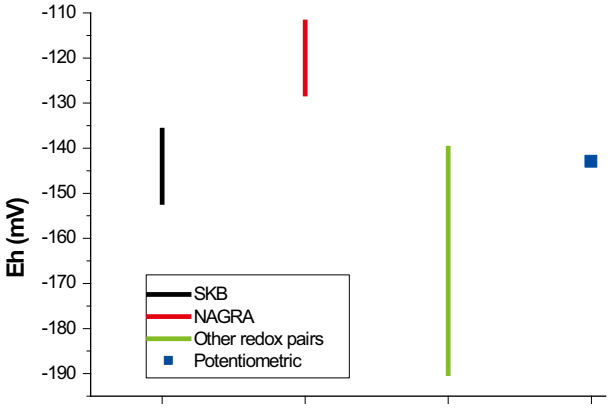

Figure 3-27. *Ranges of Eh calculated with different redox pairs compared with the potentiometrically measured. Black and Red lines indicate the values from the uranium redox pair calculated with the two different data-bases (SKB and NAGRA, respectively. Green line shows the range covered by other redox pairs (Table 3-28). The blue square represents the potentiometrically measured value.*

These new data on U(IV)-U(VI) concentrations, though limited, give the opportunity to compare and verify previous results on the uranium speciation and equilibrium states of these high uranium groundwaters based on the speciation-solubility calculations carried out by /Gimeno et al. 2007/.

Speciation results with the SKB and NAGRA databases for sample #12004, considering 3.6% U(IV) and using three different Eh values, are shown in Table 3-29. For the first two columns, an Eh value of −189 mV (calculated from the SO_4^{2+}/S^{2-} pair, as reported in /Gimeno et al. 2007/) was used in the speciation calculations. As it can be clearly seen, the calculated percentage for U(IV) is higher than the values determined analytically (last column). With the SKB-TDB there is a clear predominance of U(VI) species, which is in agreement with the analytical data. The NAGRA TDB predicts the opposite trend, i.e. a clear predominance of the U(IV) species.

When using the Eh values calculated from the U(IV)/U(VI) redox pair with the highest proportion of U(IV) (Eh = −152 mV with SKB-TDB and Eh = −128 mV with NAGRA), the results change dramatically (Table 3-29). When using SKB-TDB independently of the Eh value speciation results are very similar to the percentage found analytically. However, the results using NAGRA TDB only fit with the analytical value with the lower Eh (−128 mV). These findings indicate that the results obtained in uranium speciation calculations may vary noticeably depending on the thermodynamic database used.

Table 3-29. Distribution of U (IV), U (V) and U (VI) species (in percent) calculated from total dissolved uranium and different Eh values for sample 12004.

% Species	Eh = –189 mV (from SO_4^{2+}/S^{2-})		Eh = –152 mV (from U(IV)/U(VI) with SKB database)		Eh = –128 mV (from U(IV)/U(VI) with NAGRA database)		Analytical data (%)
	SKB	NAGRA	SKB	NAGRA	SKB	NAGRA	
% U (IV)	26.1	73.49	3.36	21.72	0.5	3.8	1.1 to 3.6
% U (VI)	70.5	24.64	95.23	76.5	98.9	95.34	96.49 to 98.9
% U (V)	3.36	1.86	1.4	1.78	0.5	0.83	–

These results are consistent with the high sensitivity of uranium speciation to small variations in Eh (and/or alkalinity) pointed out by /Gimeno et al. 2007/. Speciation calculations carried out by those authors using the WATEQ4F database /Ball and Nordstrom 2001/, the NAGRA database /Hummel et al. 2002/ and the SKB-TDB database /Duro et al. 2005/ indicated that uranium speciation was generally dominated by the U(IV)-hydroxide complexes ($U(OH)_4^0$) and the U(VI)-carbonate complexes (especially $UO_2(CO_3)_3^{4-}$). However, the relative proportions of dissolved species in each groundwater sample are quantitatively different depending on the database used (see Figure 3-28).

Even though uranium speciation is quantitatively affected by the species and thermodynamic values included in the different databases, all of them indicate *qualitatively* that the redox potential in these groundwaters is not low enough to prevent the formation of hexavalent carbonate uranium complexes. This complexation process could affect the total uranium contents in the waters depending on other parameters related to the carbonate system, such as pH or alkalinity. Moreover, it can be deduced that Forsmark groundwaters with high uranium contents belong to a particularly critical range of Eh values in which the U-speciation may change drastically. Although not developed here, the same conclusion can be stated for the range of alkalinity contents in these groundwaters (see /Gimeno et al. 2007/ for details).

Regarding the solubility calculations, the results obtained by /Gimeno et al. 2007/ indicated that the most likely phases that could be in an apparent equilibrium in the high-U Forsmark groundwaters are the amorphous phases $UO_{2.66}$, $UO_{2(am)}$ and $USiO_{4(am)}$. For $UO_{2.66}$, saturation indexes are stable around +1 and, therefore, they can be considered in equilibrium (taking into account an uncertainty range of ± 1 for the SI calculation). $UO_{2(am)}$ and $USiO_{4(am)}$ are apparently oversaturated (between +1.8 and +2.0 for $USiO_{4(am)}$, and between +2.5 and +3 for $UO_{2(am)}$).

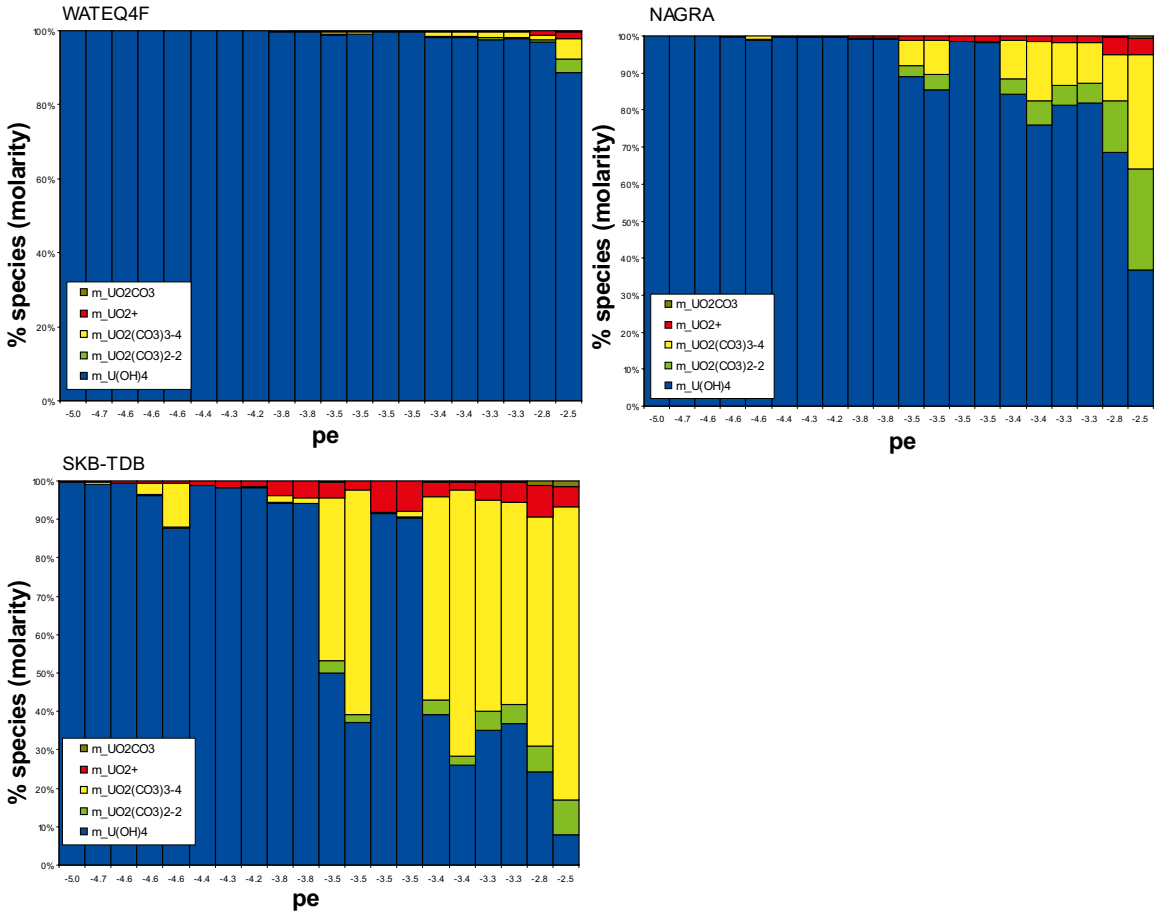

Figure 3-28. *Uranium speciation results with WATEQ4F (top and left), NAGRA (top and right) and SKB (bottom) thermodynamic databases.*

However, these phases could also be in equilibrium because the solubility of these phases seems to be slightly higher than the one considered in the TDBs used here. As explained in detail in /Gimeno et al. 2007/, the solubility values for the $UO_{2(am)}$ obtained from the Forsmark groundwaters were higher than any of the values included in the WATEQ4F, SKB and NAGRA thermodynamic databases, but very consistent with the solubility value proposed by /Rai et al. 1990/. In the case of amorphous coffinite ($USiO_{4(am)}$), SI results obtained with the SKB and NAGRA databases suggested that Forsmark groundwaters with the highest uranium contents could be in equilibrium with this phase if its solubility was two orders of magnitude higher than reported in the databases.

New calculations of saturation indexes with respect to $UO_{2.66}$, $UO_{2(am)}$ and $USiO_{4(am)}$ in the sample #12004 have been carried out in two different ways: (a) using the total dissolved uranium and an Eh value of –189 mV (from SO_4^{2-}/S^{2-} redox pair); and (b) using U(IV) and U(VI) concentrations (Table 3-30). In this second case, oversaturation decreases for the three mineral phases in all cases (different U(IV) concentration or different database).

The oversaturation state of $UO_{2(am)}$ and $USiO_{4(am)}$ also decreases when using a different Eh value. Nevertheless, the saturation indexes for $UO_{2(am)}$ are still high enough to be compatible with a higher solubility for this phase than the one included in the thermodynamic databases used here.

This verification exercise appears to confirm the common equilibrium situations previously identificated by /Gimeno et al. 2007/ with respect to uranium amorphous phases in this set of groundwaters with high but very variable dissolved uranium concentrations.

Therefore, the two key observations to justify the dissolved uranium concentration in Forsmark groundwaters are (1) the occurrence of amorphous U-phases in fracture fillings and (2) the mildly reducing Eh values, which allow for uranium-carbonate complexation.

The alteration of an originally more reducing environment due to the intrusion of oxygen or drilling water could be the cause of an increase in the degree of carbonate complexation, thus enhancing the dissolution of uranium phases and increasing the amount of dissolved uranium. Another possible cause has been suggested for the development of local oxidising conditions is related to the corrosion effects in the borehole equipment due to the presence of Fennoskan HVDC (High Voltage Direct Current) cable in the vicinity of the Forsmark area /Nissen et al. 2005/. Even assuming that the redox potential had been unaffected, variations in the carbonate system (alkalinity) due to the input of drilling waters could have significant effects in the mobilization of uranium from mineral phases.

The solubility of crystalline and amorphous UO_2 increases due to uranium-carbonate complexation, that is, depending on the pH, alkalinity or CO_2 partial pressure conditions /Bruno et al. 1997, Iwatsuki et al. 2004/. In the Forsmark groundwaters the range of alkalinity although narrow (22–125 mg/l), is in the specially critical range for the Eh measured in these waters.

Table 3-30. Saturation indexes for sample 12004 using total dissolved uranium and Eh =–189 mV (from SO_4^{2-}/S^{2-} redox pair) and using U(IV)-U(VI) concentrations. Calculations with U(IV)-U(VI) contents have been performed for the range of U(IV) concentrations analysed by /Suksi and Salminen 2007/. Results from SKB and NAGRA databases are compared.

	SI using U_{Tot} and Eh = –189 mV		SI using U(IV) and U(VI) concentrations U (IV)= 1.4 *µg/L*		U(IV) = 4.7 *µg/L*	
	SKB	NAGRA	SKB	NAGRA	SKB	NAGRA
$UO_{2(am)}$	+2.66	+2.6	1.30	+0.8	+1.83	+1.32
$USiO_{4(am)}$	+2.02	+1.95	0.67	+0.15	+1.19	+0.67
$UO_{2.66}$	+1.15	–	–0.21	–	+0.32	–

The increase in alkalinity produces a very important increase in the carbonate species, enhancing the dissolution of U solid phases, increasing the dissolved uranium concentrations and thus justifying the observed correlation between dissolved uranium and alkalinity in the groundwaters of Forsmark /Gimeno et al. 2007/.

Some data on the uranium disequilibrium series

Some data on $^{234}U/^{238}U$ activity ratios (AR) in groundwaters are available /Suksi and Salminen 2007/ and results on the studies of uranium natural decay series in fracture lining materials in Forsmark can be seen in /Smellie et al. 2008/. /Suksi and Salminen 2007/ have determined the AR values for the dissolved U(IV) and U(VI) in groundwaters from KFM02A at section 491–515 m (490–518 m in data freeze 2.3). The results indicate that both uranium oxidation states have the same $^{234}U/^{238}U$ activity ratio (AR around 2), suggesting that U(IV) and U(VI) represent the same U inventory. From this observation, /Suksi and Salminen 2007/ propose two possible origins for the dissolved uranium in these groundwaters:

1) oxidised U(VI) has been antropogenically introduced into the reducing groundwater environment and it has been partially reduced to U(IV) or
2) an in situ U(IV) mineral with AR around 2 has been oxidized resulting in the observed uranium dissolved species.

Discussion

Results obtained from the U(IV)/U(VI) redox pair in the high uranium groundwaters from Forsmark are too scarce (only one!) to reach a definite conclusion. But the calculated redox potential is in the same range than the one obtained using significant redox pairs and buffers in this system. It is also very similar to the Eh previously measured in the same sampled section. Moreover, it is consistent with the findings obtained in the Palmottu system /Ahonen et al. 1994, Bruno et al. 1996/.

In Forsmark, the presence of uranium mineral phases has also been detected and speciation-solubility calculations indicate an equilibrium with respect to amorphous phases ($UO_{2(am)}$ or $UO_{2.66}$). Under these conditions, the U(IV)/U(VI) redox pair can act as a mediator in the control of the measured redox potential. But, more importantly, this situation would indicate that uranium mineral phases can participate in the redox control of the system, buffering the perturbation of the pristine conditions by drilling and/or sampling. Therefore, this subject merits further attention.

In any case, the results obtained with the U(IV)/U(VI) data in speciation-solubility calculations do not change at all the conclusions previously obtained by /Gimeno et al. 2007/. The main implication of the obtained results is that these waters will not be able (from a thermodynamic point of view) to dissolve a hypothetical spent fuel in contact with them. These waters are in equilibrium with uranium amorphous phases and therefore they are also strongly oversaturated with respect to crystalline uraninite or to the spent fuel material. That is, the uranium mobility in some Forsmark groundwaters is controlled by phases more soluble than crystalline uraninite or spent fuel.

The original conditions of some of the Forsmark groundwaters (mainly the redox state) seem to have been modified by drilling operations, drilling waters and/or by the external input of oxygen. The extent of the induced alteration is difficult to quantify but, as already stated, the solubility of these amorphous phases is very sensitive to small variations in pH, Eh and in the carbonate system. Therefore, the elevated uranium concentrations found in some waters could have been magnified with respect to unaltered conditions. In any case, these high uranium concentrations seem to be constrained by equilibrium conditions with respect to amorphous phases, which can be a relevant aspect for the performance assessment.

3.5.7 Manganese in Forsmark groundwaters

Newly available data on manganese in the Forsmark groundwaters do not change any of the observations and conclusions addressed in Forsmark 2.1 /Gimeno et al. 2007/. Here, a summary of that work and the final results found when including the new data from data freezes 2.2 and 2.3 is presented.

Manganese concentrations in surface waters, near-surface groundwaters and deep groundwaters in the Forsmark area vary from very low (below detection limit) to 3 mg/l. In terms of their location in the area, as shown in Figure 3-29, there is a clear difference between the contents and distribution of this element in the two main systems: very high manganese values associated with the deformation zones from FFM02 and FFM03, and lower values evolving towards very low values in the deformation zones from FFM01 and from the marginal areas of FFM04 and FFM05.

There is a good correlation between Mn and Fe^{2+} in groundwaters (Figure 3-30, panels a and b), which could be an indication of their control by iron-manganese phases (oxyhydroxides, clays), or the operation of surface processes between dissolved manganese and iron oxyhydroxides as it is suggested by the decrease of manganese concentrations with increasing pH (Figure 3-30, panels e and f; /Gimeno et al. 2007/).

With respect to other redox elements or parameters (S^{2-}, uranium, Eh), dissolved Mn does not show clear correlations; only in the case of uranium a weak positive correlation can be inferred (Figure 3-30, panels c and d).

As already said, the highest values are found in groundwaters with chloride contents around 5,500 mg/L. Deeper and more saline groundwaters have lower manganese concentrations (<0.5 mg/L; Figure 3-31a and b). There is also no clear correlation between Mn and Ca except that the higher manganese values are associated to the lowest calcium contents (Figure 3-31, panels c and d).

On the other hand, Mn does show a positive correlation with respect to alkalinity (Figure 3-31, panels e and f): Mn and alkalinity increase together until this last parameter reaches values around 100 mg/L (brackish groundwaters). The known negative trend between alkalinity and depth (or chlorine), typical of these granitic systems, and the very low Mn contents in the more saline waters, strengthen the Mn-alkalinity correlation in the 0–100 mg/l alkalinity range. But this correlation could also be partially conditioned by the activity of Mn reducing bacteria (MRB) that produce Mn^{2+} but also HCO_3^- (due to the oxidation of organic matter). However, there seems to be no generalised MRB activity (or without enough intensity) in Forsmark groundwaters to justify this relationship.

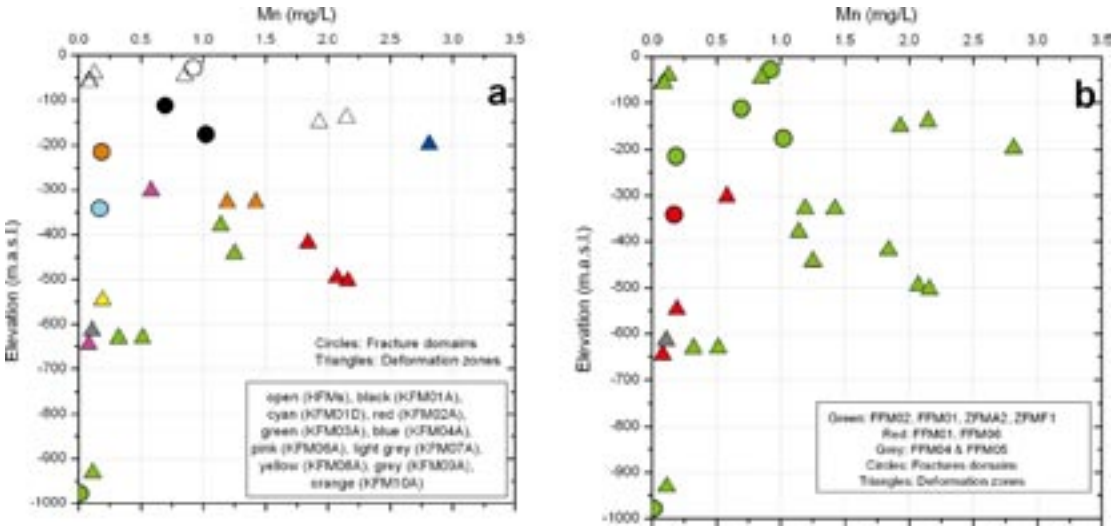

Figure 3-29. *Distribution of Manganese with respect to depth. Groundwater samples are coloured by boreholes (a) and by the structural domains (b) In both cases, triangles indicate deformation zones and circles, fracture domains.*

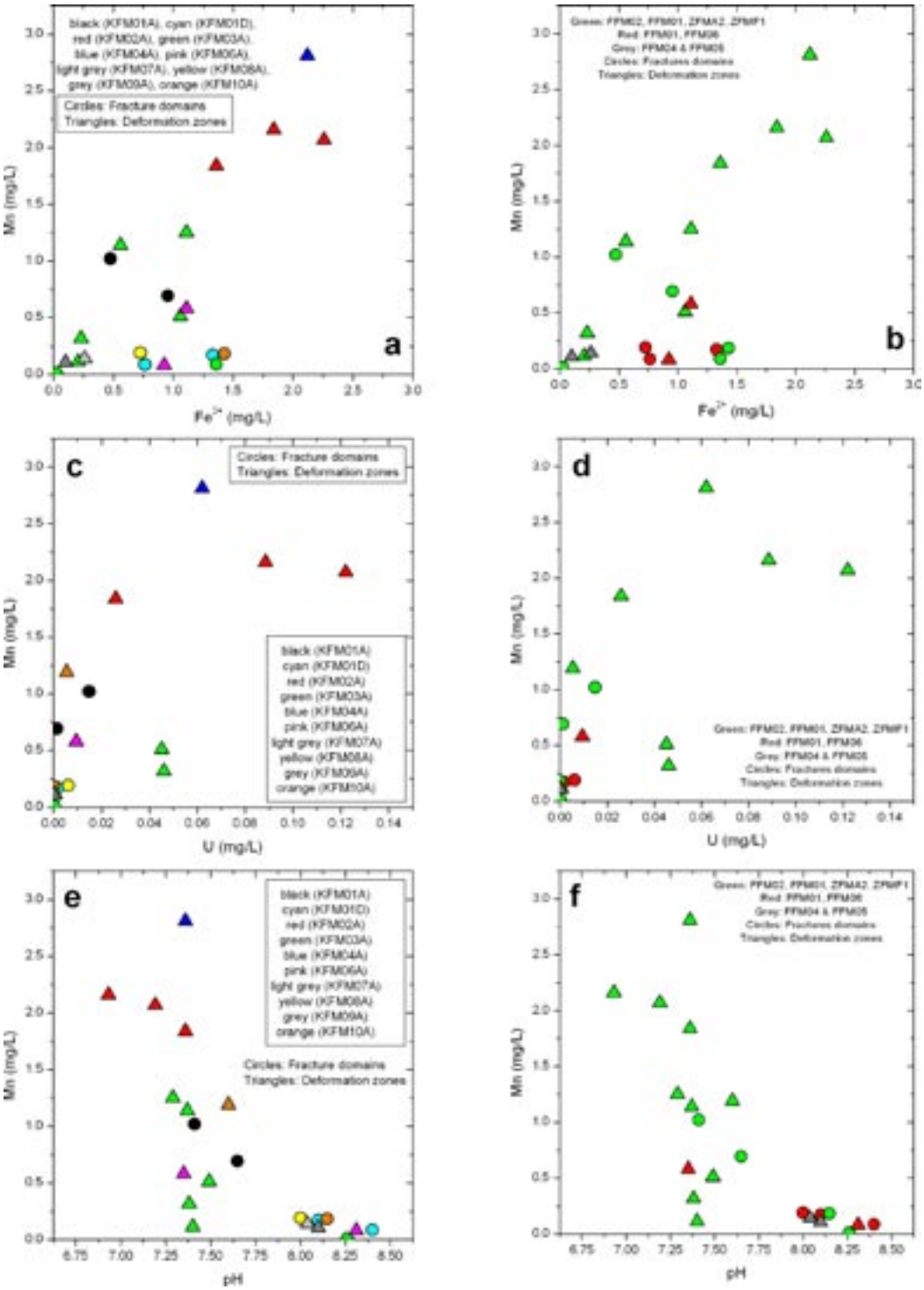

Figure 3-30. *Manganese contents in Forsmark groundwaters with respect to different parameters. (a) and (b) Ferrous iron concentration; (c) and (d) Uranium content and (e) and (f) pH.Groundwater samples are coloured by boreholes (left panels) and by the structural domains (right panels) In both cases, triangles indicate deformation zones and circles, fracture domains.*

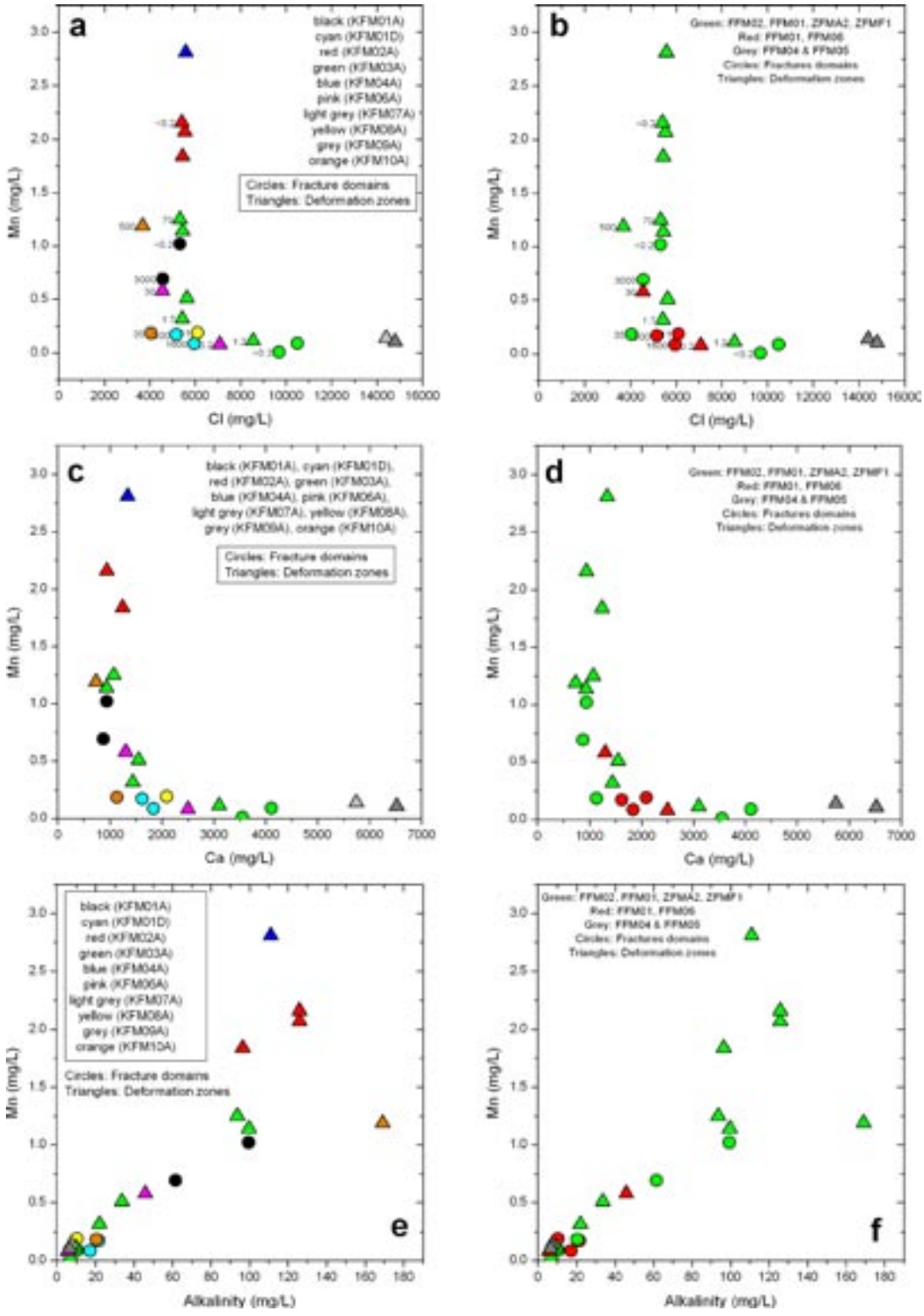

Figure 3-31. *Manganese contents in Forsmark groundwaters with respect to the contents of chloride (a, b), calcium (c and d) and alkalinity (e and f). The sampleswith available microbiological data (MPN of MRB) are indicated with a number besides the point.*

As a general rule, microbiological studies carried out in Forsmark (Hallbeck and Pedersen 2008) have detected a low activity of MRB except in some recent samples (Figure 3-32). In the deeper and more saline waters the absence of MRB is consistent with the low measured Mn^{2+} contents. MRB activity can influence Mn^{2+} concentrations in some shallow groundwaters (<200 m depth) but it seems to have no effect on the variable and usually high Mn concentrations in most brackish groundwaters where there is neither general correlation between dissolved Mn and MRB abundances (Figure 3-31) nor between MRB and rhodochrosite saturation states (Figure 3-33).

Speciation-solubility calculations have been performed with PHREEQC /Parkhurst and Appelo 1999/ and the WATEQ4F database /Ball and Nordstrom 2001/. Results indicate strong undersaturation states for all Mn oxides and oxyhydroxides included in the database. The only Mn mineral that reaches equilibrium in the studied groundwaters is rhodochrosite ($MnCO_3$; Figure 3-33), considering a SI uncertainty range of ±0.5[17].

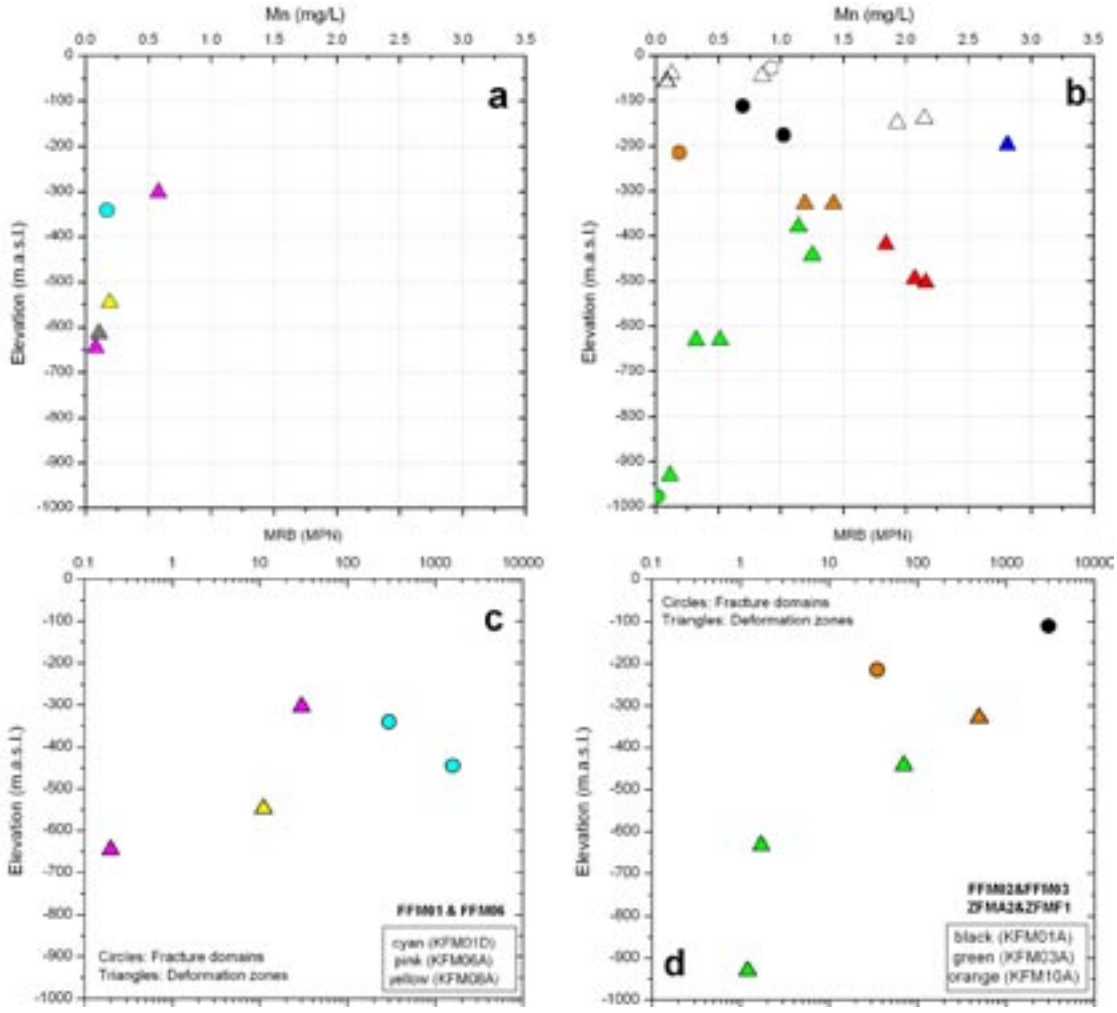

Figure 3-32. *Distribution of most probable number (MPN) of manganese reducing bacteria (MRB) with depth in Forsmark groundwaters. (a) waters sampled in the fracture domain zones (FFM01 and FFM06) including those samples from marginal areas to the target area (FFM04 and FFM05; in grey). (b) waters sampled in fracture domains FFM02 and FFM03, and samples taken from the gently dipping deformation zones. In both cases, triangles indicate deformation zones and circles, fracture domains.*

[17] The solubility value of rhodochrosite used in the calculations is the one included in WATEQ4F database /Ball and Nordstrom 2001/, log K = –11.13. This value is very similar to the more recent values proposed by /Jensen et al. 2002/. The uncertainty range has been fixed in a 5% of the log K value.

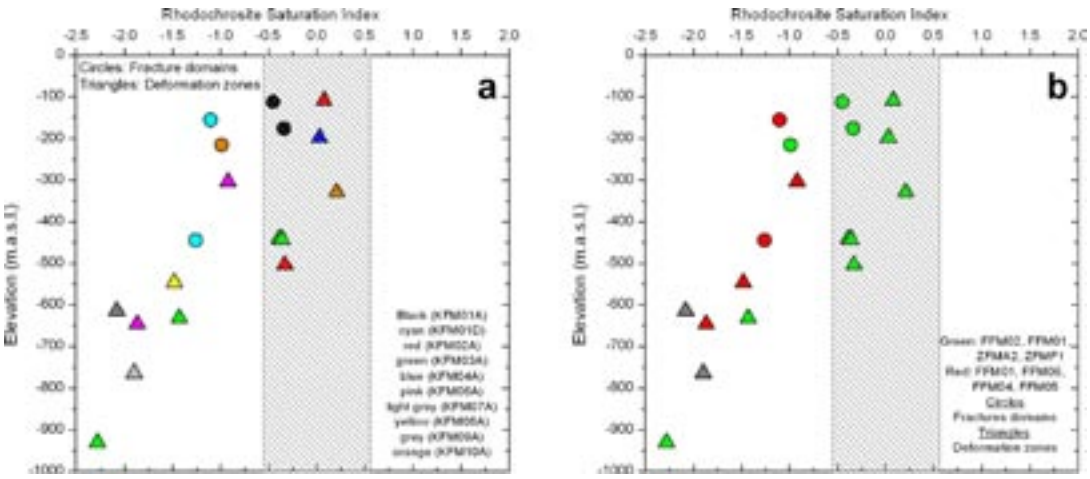

Figure 3-33. *Rhodochrosite saturation index with respect to depth in Forsmark groundwaters. Left panel shows the samples coloured by the borehole code, and right panel shows their location in different areas.*

Equilibrium with rhodochrosite is reached by the waters from the system of FFM02 and FFM03 and the gently dipping deformation zones (Figure 3-33b), down to 500 m. In contrast, groundwaters from the other system (FFM01 and marginal fracture domains FFM04 and FFM05; red and grey symbol, respectively) are all clearly undersaturated with respect to this mineral as expected for most granitic groundwaters. Therefore, waters from the first system have special features conditioning also the manganese behaviour, the most obvious being their high proportions of Littorina waters /Gimeno et al. 2007/.

As thoroughly described in /Gimeno et al. 2007/ precipitation of rhodochrosite has long been described in very different environments but its direct control on dissolved Mn has not been described in any granitic groundwater system. To overcome this deficiency, speciation-solubility calculations with groundwater samples from other sites located in the Scandinavian Shield (Laxemar, Olkiluoto and Palmottu) were carried out. The aim was to find out whether or not equilibrium with rhodochrosite was common in their deep and old groundwaters. The results proved that only those groundwaters with a high proportion of Littorina reached equilibrium with this mineral /Gimeno et al. 2007/.

All evidences suggest a clear link between equilibrium with rhodochrosite and high proportions of Littorina in the groundwaters. Figure 3-34 shows the relationship between manganese contents and rhodochrosite saturation indices with respect to Littorina proportion as calculated by M3. As it is clear from the plots, groundwaters with high Mn contents and in equilibrium with respect to rhodochrosite have Littorina proportions higher than 20% (panels a to d). These waters are associated with the waters from deformation zones in fracture domains FFM02 and FFM03 (green dots) between 50 to 500 m depth.

The reason why this clear correlation with Littorina exists was extensively explained in the previous report /Gimeno et al. 2007/. It is related to the diagenetic history of the marine sediments in the Littorina sea. In the Baltic Sea, Mn-carbonate formation has taken place for the last 7,000 yr (Littorina stage) related to the periodic renewal of deep waters by inflows of North Atlantic surface waters. This scenario of periodic authigenesis of rhodochrosite justifies the intrusion of marine waters with high (and variable) concentrations of dissolved Mn^{2+} into the groundwater system. During the mixing event of marine waters with the original groundwaters occupying the hydrological system under reducing conditions, the high Mn contents would act as a signature of their origin only in those situations where the proportion of marine water was high. When the proportion of Littorina was small, the undersaturation state with respect to rhodochrosite, typical of the original groundwaters, would prevail.

In summary, it seems that the proportion of Littorina in the groundwater is the key factor to understand equilibrium with rhodochrosite.

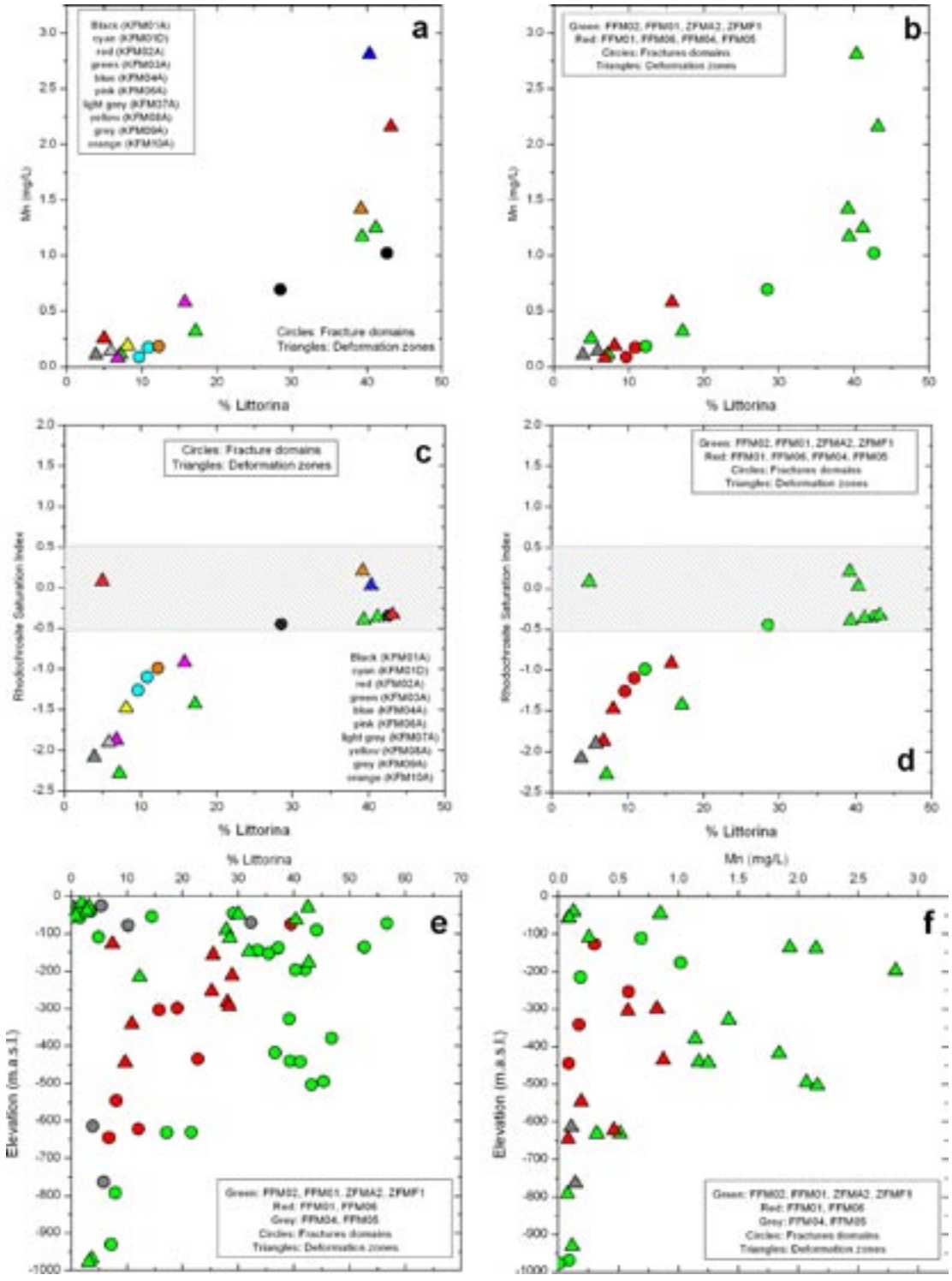

Figure 3-34. *Manganese contents (a, b) and rhodochrosite saturation indices (c, d) in Forsmark groundwaters with respect to the Littorina proportion. The general distribution of Littorina proportion and manganese contents are shown in panels (e) and (f).*

The anthropogenic perturbations of the system (oxygen intrusion, high drilling water proportion, etc), already mentioned in previous sections, could have introduced modifications in the concentration of dissolved Mn^{2+}. But, if this is indeed the case, they have not been strong enough to alter the equilibrium state with respect to rhodochrosite, a state that seems to be "natural" in other groundwater systems (Olkiluoto, etc) with high proportions of Littorina that have not undergone anthropogenic perturbations.

3.5.8 Summary of the redox modelling

The inclusion of new data from the 2.2 and 2.3 data freezes does not change the main conclusions already stated by /Gimeno et al. 2007/ on the redox processes in the Forsmark groundwaters.

The number of samples with representative and complete data for the analysis of the redox system (Eh values, Fe^{2+}, S^{2-}, Mn, U, microbial and mineralogical data) have been increased with respect to the previous evaluation, especially in the number of Eh determinations.

The analysis performed in this work has confirmed that sampling (or drilling-induced) problems previously reported in Forsmark may have altered the original redox conditions of the hydrochemical system. These sampling problems seem to affect some of the new available redox data (e.g. those of KFM10A borehole) in data freezes 2.2–2.3 (although the P-reports for the new boreholes are not available yet).

The ***general features of redox parameters*** are similar to the ones defined by /Gimeno et al. 2007/. Eh values range from −143 to −281 mV and their distribution with depth is very heterogeneous. Therefore, Eh values do not clearly show the observed trend in other crystalline systems and in most aquifers elsewhere, where a marked decrease of redox potential is observed as the residence time and depth of the waters increase /e,g, Drever 1997/.

As already stated in Forsmark stage 2.1, this behaviour could be the result of a modification in the original redox state in some groundwaters but it could also be the consequence of the complex hydrological setting and paleohydrogeological evolution of the Forsmark area, with both sub-vertical and sub-horizontal hydraulic structures and the presence of pockets and lenses of old sea-water in the bedrock.

Iron, manganese, sulphide and uranium concentrations do not show a clear depth dependence, although the highest values and variability are generally associated with the higher transmisive deformation zones in fracture domains FFM02 and FFM03 where all water types over pale-hydrogeological history can interact more easily, at least down to 600 m depth.

Fe^{2+} shows variable but high concentrations in the shallower levels (< 200 m depth) and high concentrations of Mn are found down to 600 m, mainly associated to Littorina-rich groundwaters. S^{2-} contents from are locally high in some shallow groundwaters and 200 to 600 m depth are very low or below detection limit and increase from there downwards. The highest S^{2-} contents are found at 650 m and near 1,000 m depth, clearly associated to SRB activity. Uranium shows variable concentrations but usually high (up to 0.122 mg/L) at depth between 100 and 650 m, again in those waters with a high Littorina percentage. In deeper waters U concentrations decrease drastically.

All these observations suggest that there is a depth range, between 500 and 600 m, where an important change in the dominant species or in the components that buffer the redox system occurs. This change coincides with the transition from brackish groundwaters (Cl^- between 4,500 and 5,500 mg/L) to more saline groundwaters (Cl^- > 7,000 mg/L), which is an indication of the existence of groundwater layers with different hydrochemical characters and different geochemical evolution.

In the target area (FFM01), less transmisive and when mostly “old” groundwaters are found, iron, sulphide, manganese and uranium concentrations are rather homogeneous and low.

The iron system is the most clearly affected by drilling and sampling disturbances. Most of the Eh values determined in brackish groundwaters (at depths between 110 and 646 m) seem to be controlled by the occurrence of an iron phase with an intermediate crystallinity, like that considered by /Banwart 1999/ in the Äspö large-scale redox experiment. This intermediate phase would be a recent microcrystalline iron oxyhydroxide recrystallized from an amorphous one.

The presence of this intermediate iron oxyhydroxide with higher solubility than a truly crystalline phase is possible in these brackish groundwaters if a brief oxidizing disturbance has taken place. Recent and detailed mineralogical determinations in KFM02A borehole indicate

the presence of fine grained amorphous-poorly crystalline phases (including some other more ordered structures; e.g. goethite) induced by drilling, supporting the results obtained from redox pair calculations.

This situation has not been detected in the deeper saline groundwaters. The redox potential measured in the deepest groundwaters in Forsmark is one of the most reducing in the system, and it is in agreement with the value obtained with the calibration by /Grenthe et al. 1992/. This would indicate that the Eh value of these groundwaters is undisturbed and appears to be controlled by a clearly crystalline iron oxyhydroxide such as hematite. This is coherent with the reducing character and long residence time of these groundwaters, where low crystallinity phases are not expected (/SKB 2004c/ and references therein).

The sulphur system seems to be especially important for the general understanding of the redox processes in Forsmark groundwaters. Perturbations in the original sulphide content can be deduced from the increases observed with time in most of re-sampled and monitored sections. The increases in S^{2-} concentrations in the brackish groundwaters shallower than 600 m depth are more restricted. The more clear increases are found in saline groundwaters, which clearly indicates the sulphidic character of these deep waters (between 640 and 1,000 m depth). This observation is in agreement with the available microbiological data at these depths (high SRB values at almost 1,000 m depth).

Precipitation of "amorphous" monosulphides and, therefore, recent and intense SRB activity occurs only locally (mainly associated with deformation zones). In the groundwaters between 220 m and 600 m dissolved sulphide contents are low due to localized precipitation of monosulphides in Fe^{2+} rich environments and, mainly, to limited recent SRB activity in Littorina-rich groundwaters.

Although the present SRB activity seems to be more restricted than in the Laxemar zone, the sulphur system also plays a fundamental role in the redox characters of the Forsmark groundwaters. It could even be extended to the more or less isolated Littorina-rich groundwaters, where the SRB would have been active during the Littorina stage.

With respect to ***the uranium system*****,** the simplest explanation of the available data indicates that the origin of the high dissolved uranium contents detected in the Forsmark brackish groundwaters associated to the deformation zones, are related to local U anomalies or mineralisations in contact with these groundwaters. Limited mineralogical data seem to confirm this point.

Speciation-solubility calculations support this conclusion and indicate that the high uranium contents are the result of two factors: (a) the control exerted by an amorphous (and very soluble) uranium phase present in the system, and (b) the weakly reducing Eh values which may allow uranium complexation and reequilibrium depending on Eh and dissolved carbonate.

High-U waters in Forsmark have a range of uranium concentrations that span one order of magnitude. This variation could be easily justified by equilibrium situations under slightly different conditions. Within the Eh and alkalinity ranges that characterise Forsmark waters, uranium speciation is very sensitive to minor modifications in these parameters because they affect the extent of uranium carbonate complexation and, therefore, the solubility of the solids.

This last point is important considering the possible modification of the natural conditions undergone by these waters. The alteration of an originally more reducing environment and/or the increase of dissolved carbonate (e.g. by mixing with drilling waters) could have been the cause of the increase of uranium-carbonate complexation enhancing the dissolution of uranium phases and increasing the contents of dissolved uranium with respect to the originally present in the system.

With respect to the ***manganese system***, low Mn contents and undersaturation with respect to rhodochrosite in deep (>700 m) saline Forsmark groundwaters are a very common situation, as also observed in many other granitic groundwater systems. However, brackish groundwaters with an important Littorina contribution have high Mn concentrations and reach equilibrium with respect to rhodochrosite. This is very common in other granitic systems in the

Scandinavian Shield unless the Littorina proportion happens to be in the same range. This suggests that the high Mn content and the equilibrium with rhodochrosite in brackish groundwaters are characters imposed by the superficial marine environment prevailing during the Littorina stage. The observation of this signature in Forsmark groundwaters has been probably favoured by the isolated character (pockets) of the analysed samples and by the lack of bacterial activity.

The number of available data for the study of the redox processes at Forsmark is not as high as it would be necessary, more considering the sampling problems and the own complexity of the hydrological system. However, even with the existing uncertainties, a conceptual model on the general performance of the redox processes at Forsmark, which integrates all the information about them, is presented in Section 4.

3.6 The effect of the extended 2.3 data freeze on groundwater modelling

This section presents the new data delivered from SICADA after the 2.3 data freeze (2007/10/17) as what has been called the "extended 2.3 data freeze". The new data set for groundwaters include new data from already sampled boreholes (HFM01, 02, 03, 04, 05, 06, 08, 09, 10, 13, 14, 15, 16, 19, 20, 21, 22, 27, 32, 33, 36; KFM01A, 1B, 1D, 2A, 2B, 3A, 4A, 6A, 6C, 7A, 8A, 10A) and new samples and new data from new boreholes (KFM08D, 11A, 12A). The total set of samples separated by boreholes and indicating the corresponding depths are indicated in Table 3-31.

The whole set of new samples has been evaluated by /Smellie et al. 2008/ and, after an exhaustive analysis of the data quality, an assignment to different categories was made. After that, the samples labelled as categories 1, 2, 3 and 4 were used to check the effects of the new information on the groundwater model proposed above and based on the Forsmark 2.3 data freeze.

Figures 3-35 to 3-38 display the distribution of the main chemical parameters with depth including the new samples from the extended 2.3 data freeze (plotted as stars as their specific location in deformation zones or fracture domains have not been defined yet) in order to see how they fit with the general picture already drawn with the previous data. These plots represent the samples coloured by boreholes (left panels) and by their location in the different systems (right panels).

In general they show the same trends and are included in the same range of values as the set of samples from Forsmark 2.3 data freeze. Therefore, their inclusion in the conceptual model does not add or modify any of the previous conclusions.

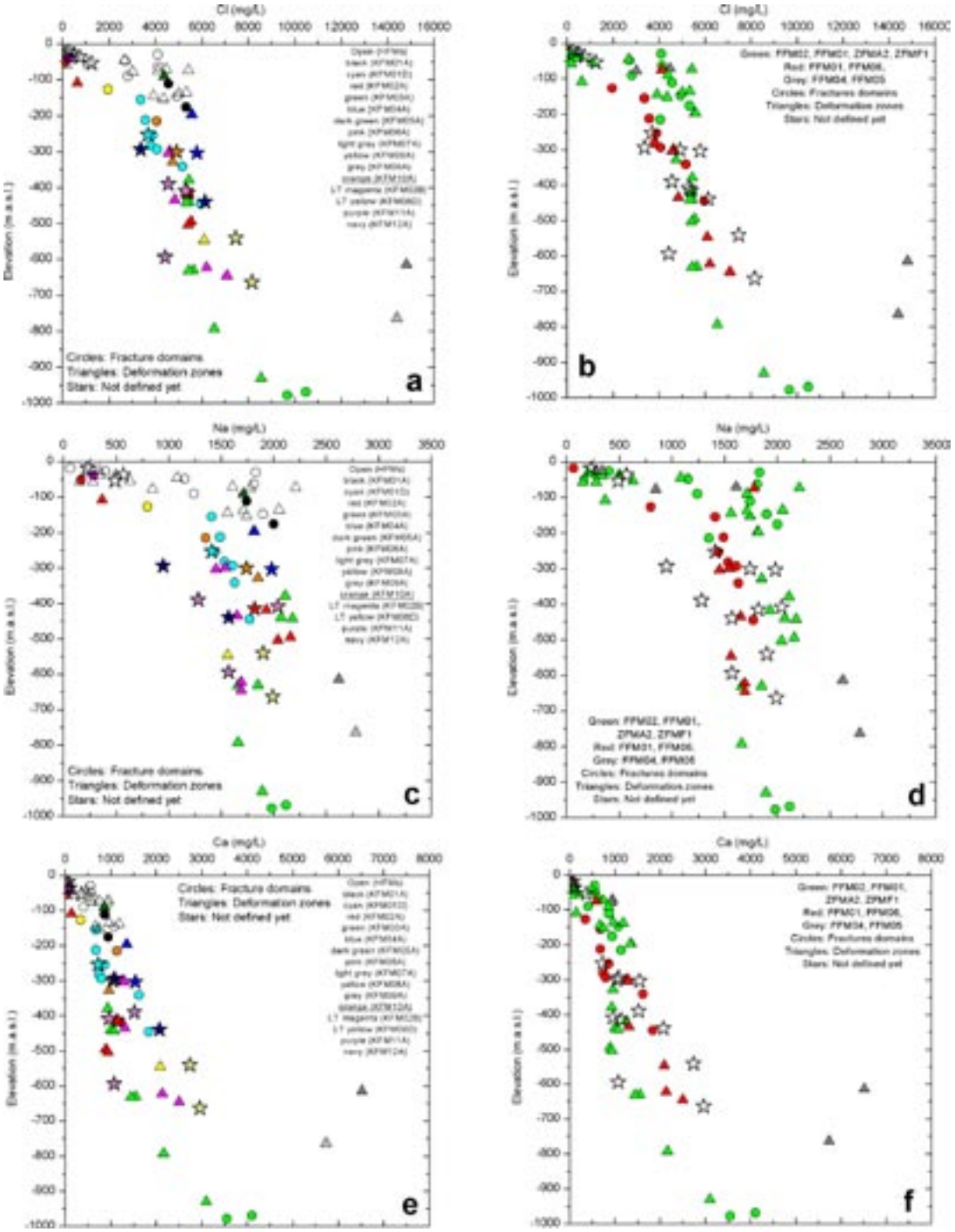

Figure 3-35. *Chloride (a, b), sodium (c, d) and calcium (e, f) distribution with respect to depth in the two different systems at Forsmark. Left panels show the samples coloured by the borehole code, and right panel shows their location in different areas. In both cases, triangles indicate deformation zones and circles, fracture domains. The rest of the plots in the section follow the same structure.*

Table 3-31. Number of new samples from the ”extended” 2.3 data freeze.

	Number of new samples	Sampling Depths				
HFM	68					
KFM01A	8	–115.79	–176.26			
KFM01B	1	–36.60				
KFM01D	2	–252.53	–343.03			
KFM02A	13	–108.85	–414.81	–417.80	–494.97	–503.47
KFM02B	3	–407.79				
KFM03A	12	–379.06	–440.79	–631.10	–969.13	
KFM04A	5	–196.86	–302.75			
KFM06A	9	–298.54	–303.24	–622.78	–645.95	
KFM06C	2	–434.84	–527.04			
KFM07A	6	–318.12	–763.62			
KFM08A	3	–27.94	–134.31	–238.03		
KFM08D	16	–540.63	–664.06			
KFM10A	6	–214.77	–299.83	–301.28	–328.08	
KFM11A	12	–389.7	–593.7			
KFM12A	6	–293.6	–439.2			

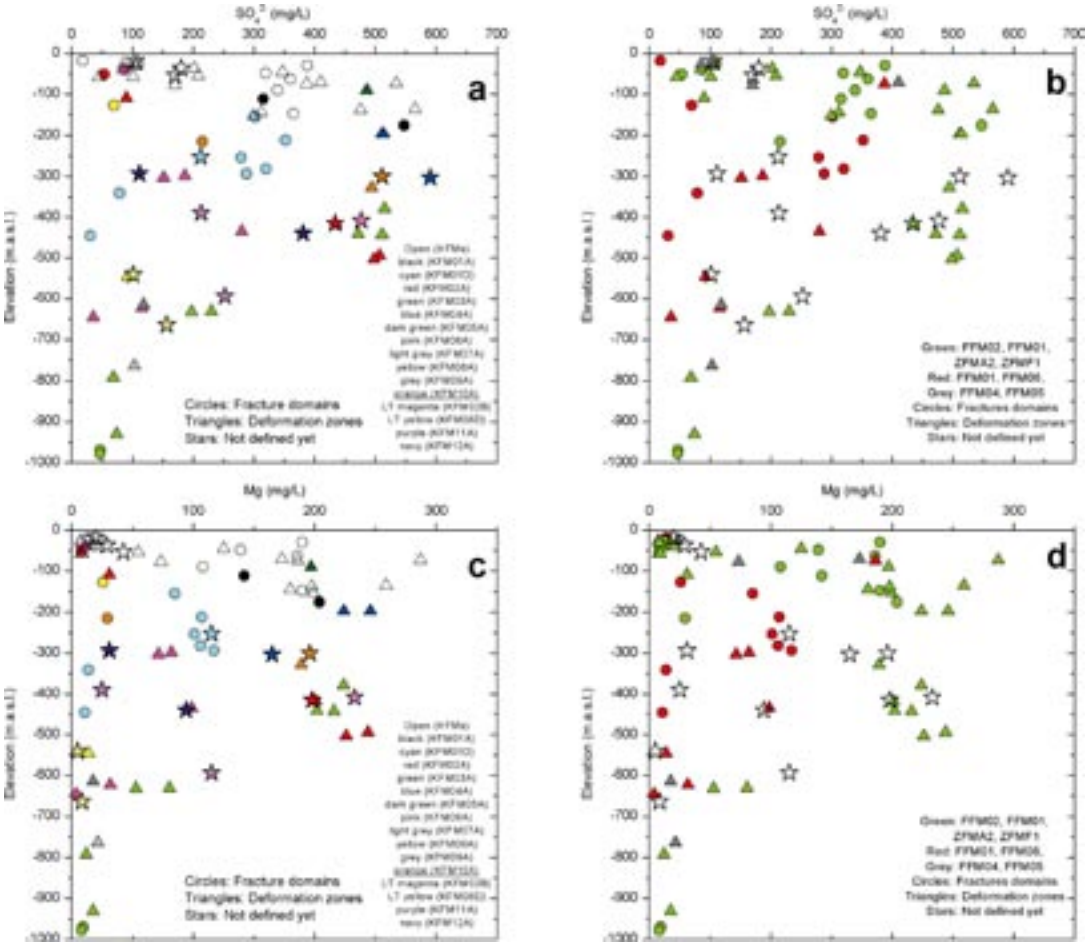

Figure 3-36. *Sulphate (a, b) and magnesium (c, d) distribution with respect to depth in the two different systems at Forsmark. Left panels show the samples coloured by the borehole code, and right panel shows their location in different areas. In both cases, triangles indicate deformation zones and circles, fracture domains.*

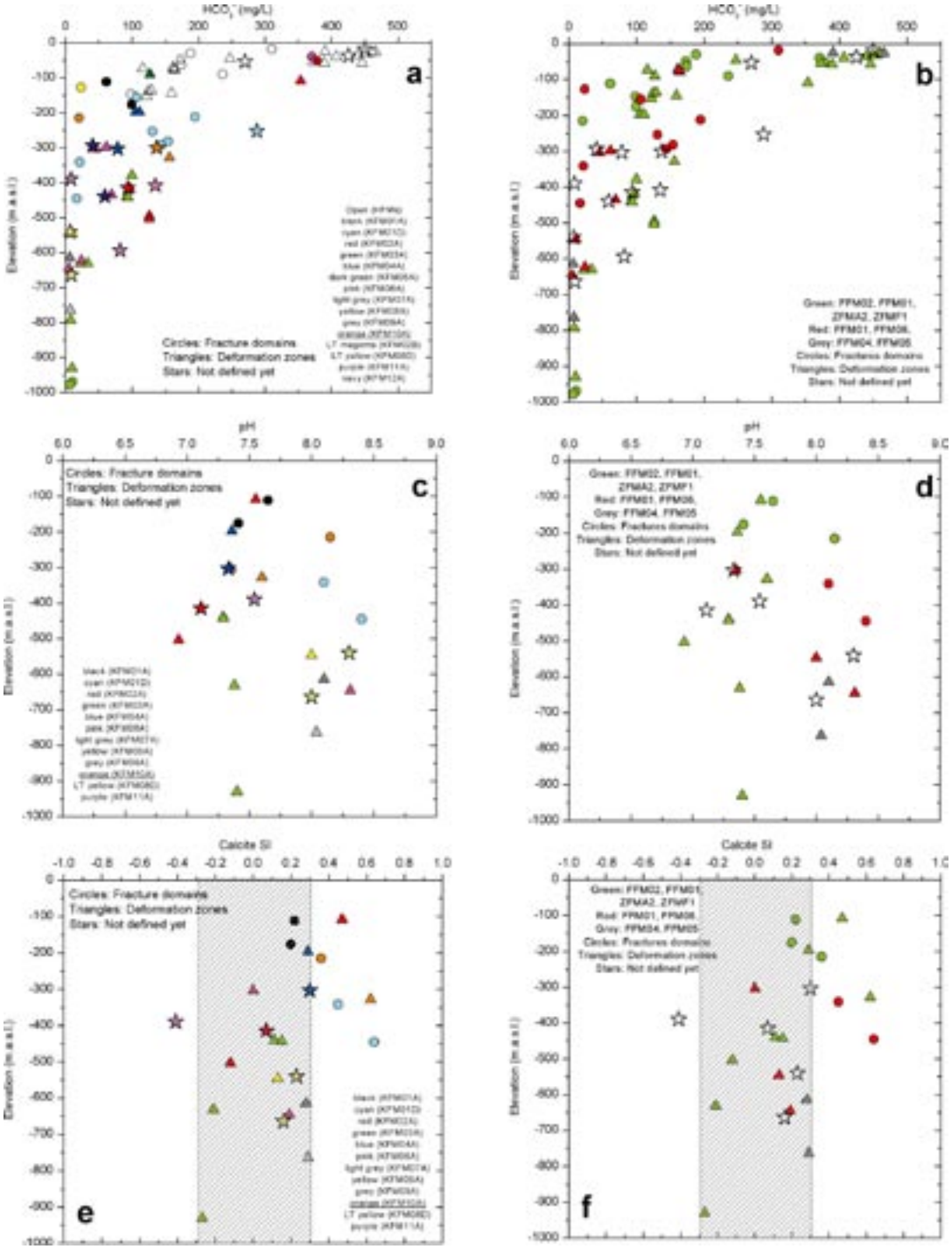

Figure 3-37. *Bicarbonate (a, b), pH (c, d) and calcite saturation index (e, f)distribution with respect to depth in the two different systems at Forsmark. Left panels show the samples coloured by the borehole code, and right panel shows their location in different areas. In both cases, triangles indicate deformation zones and circles, fracture domains.*

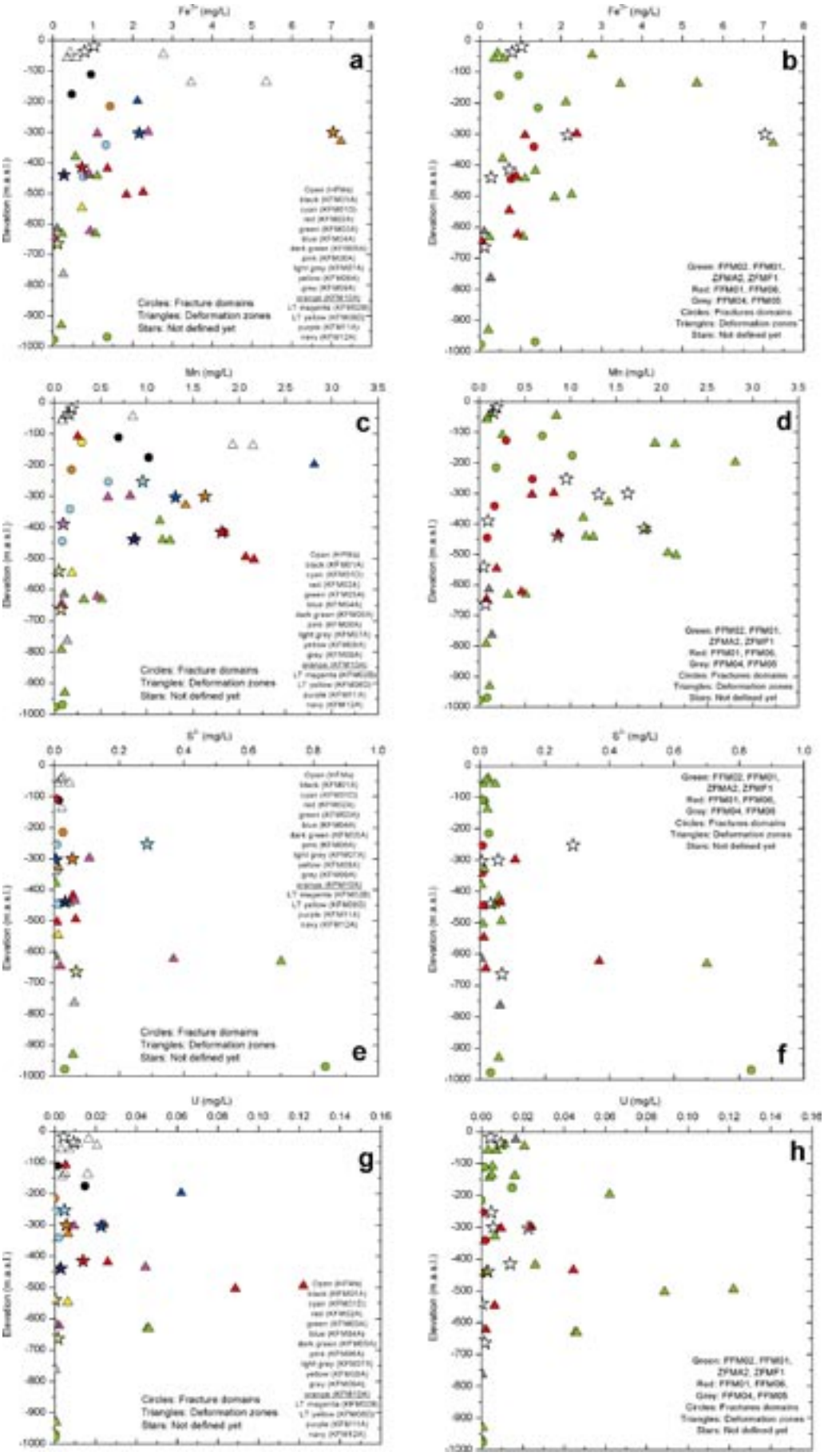

Figure 3-38. *Ferrous iron (a, b), manganese (c, d), sulphide (e, f) and uranium (g, h) distribution with respect to depth in the two different systems at Forsmark. Left panels show the samples coloured by the borehole code, and right panel shows their location in different areas. In both cases, triangles indicate deformation zones and circles, fracture domains.*

4 Overall conceptual model for groundwater evolution

4.1 Temporal evolution of mixing

Our conceptual model is based on the observation that in the hygrogeochemical system at Forsmark there is no simple binary mixture between the different types of waters but a more complicated one, with at least five different end-members involved. These possible end-members are: (1) a deep saline groundwater, (2) an old meteoric water, (3) a glacial melt-water, (4) a Littorina Sea water, and (5) a recently altered meteoric water. The chemical characteristics of each end-member water have been reviewed in Section 2.1, and the existence of an old meteoric component has been confirmed in Section 2.3.

Taking into account the geological and climatic evolution in the Scandinavian Shield, a model for the temporal evolution of mixing has been constructed. This model consists of the following five stages:

- A deep saline groundwater is formed in the crystalline bedrock (covered by several kilometres of sediments) over hundreds of millions of years mainly by water-rock interaction /Smellie et al. 2008/. This is the *Deep Saline end-member*. Subsequent erosion reduced this sedimentary cover until, in the Late Tertiary, the present bedrock was exposed once again /Lidmar-Bergström 1996/ resulting in a progressive dilution of the brine in the upper 1,000 m (or more) of the bedrock and the consequent salinity gradient with depth.
- During the last three million years, a succession of glacial and interglacial periods has triggered the alternating or simultaneous input into the upper part of the crystalline basement of glacial melt-waters and meteoric waters. Because of the complex and rapid change of climatic conditions, these two end-member waters (*the Glacial and the Old Altered Meteoric*) never appear as pure end-member waters. As indicated by the isotopic signatures (mainly $\delta^{18}O$) of the groundwater samples, the binary mixtures of these two end-members have a maximum glacial contribution of 50%.
- Any of the dilute glacial and meteoric waters (or their mixtures) formed during the previous stage can mix, if pushed downwards by gravity or forced by the weight of glaciers, with the saline groundwaters that occupy most parts of the deeper basement. These mixing events would generate a rather steep salinity gradient in the groundwater system, with diluted waters in the upper part, brackish waters in the middle, and saline waters in the lower part.
- 9,500 year ago, after the last glacial period, a brackish sea (*the Littorina Sea*) was established in what is today the Baltic Sea. The Forsmark area was under the waters of this sea for 9,500 years and, as a consequence, Littorina Sea waters percolated down into the basement. Because of the salinity gradient already present in the basement, Littorina waters could penetrate down only until encountering groundwaters with similar salinity (a chlorine content of around 5,500 mg/L).
- After the Forsmark area emerged from the Littorina Sea as a result of post-glacial rebound and uplift less than 1,000 years ago, modern meteoric waters started to penetrate into the upper part of the groundwater system. These waters became the *Recent Altered Meteoric end-member* after reacting with the soil and overburden materials, and mixed with the Littorina and pre-Littorina groundwaters. The composition of this Recent Altered Meteoric end-member is thought to be very similar to the Old Meteoric one.

This temporal model of mixing explains the vast majority of the groundwater compositions found not only in the Forsmark area, but also in the Laxemar and Olkiluoto areas. This strengthens the confidence in the proposed mixing history.

Finally, as /Smellie et al. 2008/ indicate, the above description is valid for areas in the Forsmark bedrock where first Holocene glacial meltwater and then later Littorina Sea water have been introduced; the brackish sea water has only been able to intrude (by density turnover) were fresh water (mainly glacial) had previously filled the fractures. Therefore two different systems have developed in the Forsmark area:

- The higher transmissive deformation zones and the more fractured domains (FFM03 and parts of FFM01/02), where all water types (Saline, Old Meteoric ± Old Glacial + Saline, Holocene glacial, Littorina and present altered Meteoric) can be found to have interacted to various degrees, and
- The target area (FFM01), where at least parts of the aquifer have been isolated and therefore only Saline and Old Meteoric ± Old Glacial + Saline groundwaters can be identified.

This two different systems show slightly (but important) different chemical characters and geochemical processes which will be shown in the following Section.

4.2 General conceptual model

In this section, a general description of the main characteristics and processes controlling the hydrogeochemical evolution with depth in the Forsmark groundwater system is presented.

The hydrochemical characteristics and evolution of the **Near surface waters** (up to 20 m depth) is mainly determined by weathering reactions and especially affected by the presence of limestones. The biogenic CO_2 input (derived from decay of organic matter and root respiration) and the associated weathering of carbonates control the pH and the concentrations of Ca and HCO_3^- in the near-surface environment.

Current seasonal variability of CO_2 input produces variable but high calcium and bicarbonate contents in the Forsmark near-surface waters: up to 240 mg/L Ca and 150 to 900 mg/L HCO_3^-. These high concentrations are due to the extensive presence of limestones in the overburden, a feature very uncommon in Swedish soils.

Shallow dilute groundwaters (from 20 to 100–200 m depth) do not show the same variability and high HCO_3^- or Ca contents as the near-surface groundwaters. Therefore, most near-surface groundwaters are isolated and not hydraulically connected to the shallow groundwater systems. Only waters with short residence time in the overburden (fast paths), and therefore, more diluted, are effectively recharging the shallow hydrological systems. If the biological activity becomes more restricted in the future (e.g. during glaciations) reactions will mainly proceed inorganically and recharge waters will probably be even more dilute.

The uppermost 150–200 m in the Forsmark area are represented by groundwaters in deformation zones. These groundwaters display a wide chemical variability, mainly due to the presence of discharge waters or saline waters of marine origin (recent or old Littorina relicts). However, the very recent infiltrating waters are mainly controlled by water-rock interaction processes and only in some cases by mixing with previous and more saline waters.

In the **Deep groundwater system** (below 200 m depth) the major chemical contents are mainly controlled by mixing and their values depend on the proportion of each end-member. The mixing proportions are different in the two main systems: the more transmissive zone in fracture domains FFM02 and FFM03, and the more isolated system represented by fracture domain FFM01.

Waters from the more transmissive system are characterized by a higher proportion of Littorina (almost double) than waters from the other more isolated zones (FFM01) and by a larger penetration depth of Littorina waters (600 m in deformation zone waters from FFM03 and 300 m in FFM01). This results in contents generally higher of sulphate, magnesium and manganese in the transmissive area than in the isolated zones of the target area (FFM01).

However, waters from the target area have a larger contribution of old waters Deep Saline and Glacial at shallower depths.

Even though the compositional characteristics of the deep saline groundwaters in the studied area are mainly determined by mixing processes, pH and Eh are controlled by chemical reactions. pH is mainly controlled by calcite dissolution-precipitation reactions and of secondary importance is the influence of other common chemical processes, such as aluminosilicate dissolution-precipitation or cation exchange.

With regard to the **redox processes and parameters in the shallow and deep groundwater systems**, the inclusion of new data from 2.2 and 2.3 data freezes, does not change the main conclusions already stated by /Gimeno et al. 2007/ on the redox processes and their problems in the Forsmark groundwaters.

Although more detailed studies are necessary to complete the redox characterisation of the shallow groundwater system, tentative calculations allow inferring the existence of a generalised anoxic state with possible episodic inputs of oxidising waters. However, these oxidising episodes have not been intense enough to exhaust the reducing capacity of fracture filling minerals (such as Fe-II chlorite or pyrite) still present in the shallow system /Drake et al. 2006/. For calculation purposes in the Forsmark shallow system, the use of the heterogeneous pair $Fe(OH)_3/Fe^{2+}$ seems to produce consistent Eh values.

Three parts with different redox evolution as a function of depth can be differentiated. As a general trend, the precipitation of Fe(II)-monosulphide plays a linking role between the iron and sulphur redox systems.

In the uppermost part of the system (**< 200 m depth**) Fe^{2+} dissolved contents are high and represent post-oxic environments in which IRB activity seems to be dominant. Locally sulphidic environments with high contents of dissolved sulphide, active precipitation of amorphous monosulphide and, therefore, important SRB activity, can also be found.

Most of the groundwaters sampled **between 200 and 600 m** seem to be associated with the presence of pockets or lenses with an important Littorina contribution. The presence of these pockets represents a discontinuity in the normal evolution of the system with depth.

In this middle part, Fe^{2+} dissolved contents are generally lower than in the shallow groundwater system. The iron system at these depths seems to be disturbed, as suggested by the occurrence of amorphous iron oxyhydroxides now evolving towards more crystalline phases. Most of the Eh values determined in brackish groundwaters (at depths between 110 and 646 m) seem to be controlled by the occurrence of these intermediate crystalline phases.

Dissolved sulphide concentrations at those depths are systematically low (<0.3 mg/L) and locally controlled by the precipitation of amorphous Fe(II)-monosulphides linked to the activity of SRB in brackish groundwaters. However, the metabolic activity of microorganisms in most of these waters is very limited and some of their redox characters (Mn concentrations, sulphide buffering) seem to be mainly inherited or influenced by the Littorina intrusion stage.

Dissolved uranium concentrations in these groundwaters are generally high, probably associated with the presence of uranium amorphous phases in the fracture fillings.

From 600 m depth down, dissolved sulphide concentrations are the highest found in the system. This is consistent with the occurrence of SRB and with the active precipitation of Fe(II)-monosulphides. The iron system seems to be limited by crystalline oxyhydroxides (mainly hematite) reflecting the pristine conditions of the geochemical system. This is coherent with the reducing character and long residence time of these groundwaters, where low crystallinity phases are not expected.

5 References

Ahonen L, Ervanne H, Ruskeeniemi T, Jaakkola T, Blomqvist R, 1993. Uranium mineral-groundwater equilibration at the Palmottu natural analogue study site, Finland. Mat. Res. Soc. symp. proc., 294, 497–504.

Ahonen L, Ervanne H, Jaakkola T, Blomqvist R, 1994. Redox chemistry in uranium-rich groundwater of Palmottu uranium deposit, Finland. Radiochimica Acta, 66/67, 115–121.

Alvi K, Winterhalter B, 2001. Authigenic mineralisation in the temporally anoxic Gotland Deep, the Baltic Sea. Baltica, 14, 74–83.

Appelo C A J, Postma D, 2005. Geochemistry, Groundwater & Pollution. Balkema, Rotterdam, The Netherlands, 2nd edition, 649 p.

Asikainen M, Kahlos H, 1979. Anomalously high concentrations of uranium, radium and radon in water from drilled wells in the Helsinki region. Geochim. Cosmochim. Acta, 43, 1681–1686.

Auqué L F, Gimeno M J, Gómez J, Puigdoménech I, Smellie J, Tullborg E-L, 2006. Groundwater chemistry around a repository for spent nuclear fuel over a glacial cycle Evaluation for SR-Can. SKB TR-06-31, Svensk Kärnbränslehantering AB, 123 pp.

Auqué L F, Gimeno M J, Gómez J, Nilsson A-C, 2008. Potentiometrically measured Eh in groundwaters from the Scandinavian Shield. Applied Geochemistry, 23, 1820–1833.

Ball J W, Nordstrom D K, 2001. User's manual for WATEQ4F, with revised thermodynamic data base and test cases for calculating speciation of major, trace, and redox elements in natural waters. U.S. Geological Survey, Open File Report 91–183, USA.

Banks D, Reimann C, Røyset O, Skarphagen H, Sæther O M, 1995a. Natural concentrations of major and trace elements in some Norwegian bedrock groundwaters. Applied Geochemistry, 10, 1–16.

Banks D, Røyset O, Strand T, Skarphagen H, 1995b. Radioelement (U, Th, Rn) concentrations in Norwegian bedrock groundwaters. Environmental Geology, 25, 165–180.

Banwart S A, 1999. Reduction of iron (III) minerals by natural organic matter in groundwater. Geochim. Cosmochim. Acta, 63, 2919–2928.

Bath A H, Jackson C P, 2002. Äspö Hard Rock Laboratory: Task Force on modelling of groundwater flow and transport of solutes. Review of Task 5. (International Progress Report SKB IPR-03-10), Svensk Kärnbränslehantering AB.

Bath A H, 2005. Geochemical Investigations of Groundwater Stability. SKI Report 2006: 12, 83 p.

Berg C, Nilsson A-N, 2006. Forsmark site investigation. Hydrochemical monitoring of percussion- and core drilled boreholes. Results from sampling and analyses during 2005. SKB P-06-57, Svensk Kärnbränslehantering AB, 46 p.

Berg C, Bergelin A, Wacker P, Nilsson A-N, 2006. Forsmark site investigation. Hydrochemical characterization in borehole KFM08A. Results from the investigated section at 683.5–690.6 (690.8) m. SKB P-06-63, Svensk Kärnbränslehantering AB, 81 p.

Berner R A, 1981. New geochemical classification of sedimentary environments. J. Sedim. Petrol. 51, 359–365.

Blomqvist R, Ruskeeniemi T, Kaija J, Ahonen L, Paananen M, Smellie J, Grundfelt G, Pedersen K, Bruno J, Pérez del Villar L, Cera E, Rasilainen K, Pitkänen P, Suksi J, Bonneville S, Van Cappellen P, Behrends T, 2004. Microbial reduction of iron (III) oxyhydroxides: effects of mineral solubility and availability. Chem. Geol., 212, 255–268.

Bottomley D J, Gascoyne M, Kamineni D C, 1990. Geochemistry, age, and origin of groundwater in a mafic Pluton, East Bull Lake, Ontario, Canada. Geochim. Cosmochim. Acta, 54, 933–1008.

Bottomley D J, Gregoire D, Raven K G, 1994. Saline groundwaters and brines in the Canadian Shield: geochemical and istotopic evidence for a residual evaporite brine component. Geochim. Cosmochim. Acta, 58, 1483–1498.

Bottomley D J, Katz A, Chan L H, Starinsky A, Douglas M, Clark I D, Raven K G, 1999. The origin and evolution of Canadian Shield brines: evaporation or freezing of seawater? New lithium isotope and geochemical evidence from the Slave craton. Chem. Geol., 155, 295–320.

Brenner W W, 2005. Holocene environmental history of the Gotland Basin (Baltic Sea). A micropalaeontological model. Palaeogeography, Palaeoclimatology, Palaeoecology, 220, 227–241.

Bruno J, Cera E, Duro L, Ahonen L, 1996. Deep gropndwater redox reactions in the Palmottu uranium deposit: the role of uranium and iron in these precesses. Posiva-96-24, 26 p.

Bruno J, Cera E, de Pablo J, Duro L, Jordana S, Savage D, 1997. Determination of radionuclide solubility limits to be used in SR 97.Uncertainties associated to calculated solubilities. SKB TR-97-33, Svensk Kärnbränslehantering AB, 184 p.

Buckau G, 2007. High Uranium issue. In: SKB (2007), Hydrogeochemical evaluation of the Forsmark site, modelling stage 2.1-issue report. SKB R-06-69, Svensk Kärnbränslehantering AB. (Appendix 7).

Burke I T, Kemp A E S, 2002. Microfabric analysis of Mn-carbonate laminae deposition and Mn-sulfide formation in the Gotland Deep, Baltic Sea. Geochim Cosmochim. Acta, 66, 1589–1600.

Böttcher M, Lepland A, 2000. Biogeochemisrty of sulfur in a sedemnt core from the west-central Baltic Sea: evidence freom stable isotopes and pyrite textures. Journal of Marine Systems, 25, 299–312.

Carman R, Rahm L, 1997. Early diagenesis and chemical characteristics of interstitial waters and sediements in the deep depostion bottoms of the Baltic Proper. Journal of Sea Research, 37, 25–47.

Carrera J, Vazquez-Sune E, Castillo O, Sanchez-Vila X, 2004. A methodology to compute mixing ratios with uncertain end-members. Water Res. Res., 40, W12101.

Casanova J, Read D, Frape S, 2000. The Palmottu Natural Analogue Project. Phase II: transport of radionuclides in a natural flow system. European Commission, Final Report, Phase II, EUR-19611, 171 p.

Casanova J, Négrel P, Blomqvist R, 2005. Boron isotope fractionation in groundwaters as an indicator of past permafrost conditions in the fractured crystalline bedrock of the fennoscandian shield. Water Research, 39, 362–370.

Clark I, Fritz P, 1997. Environmental isotopes in hydrogeology. CRC Press LLC, 328 p.

Culkin F, Cox R A, 1966. Sodium, potassium, magnesium, calcium and strontium in sea water. Deep-Sea Res., 13, 789–804.

Degueldre C, 1994. Colloid properties in groundwaters from crystalline formations. NAGRA Technical Report 92-05. Nagra, Wettingen, Suiza, 96 p.

Degueldre C, Grauer R, Laube A, 1996. Colloid properties in grantic groundwater systems. II. Stability and transport study. Applied Geochemistry, 11, 697–710.

Deutsch W J, 1997. Groundwater geochemistry. Fundamentals and applications to contamination. Lewis Publishers, New York, 221 pp.

Dideriksen K, Christiansen B C, Baker J A, Frandsen C, Balic-Zunic T, Tullborg E, Mørup S, Stipp S L S, 2007. Fe-oxide fracture fillings as a palæo-redox indicator: Structure, crystal form and Fe isotope composition. Chemical Geology, 244, 330–343.

Donner J, Kankainen T, Karhu J A, 1994. Radiocarbon ages and stable isotope composition of Holocene shells in Finland. In T. Andrén (ed), Proceedings of the Conference The Baltic – past, present and future. Stockholm March 14–16, 1994. Stockholm University. Quaternaria, A:7, 31–38.

Douglas M, Clark I D, Raven K, Bottomley D, 2000. Groundwater mixing dynamics at a Canadian Shield mine. Journal of Hydrology, 235, 88–103.

Drake H, Sandström B, Tullborg E-L, 2006. Mineralogy and geochemistry of rocks and fracture fillings from Forsmark and Oskarshamn: Compilation of data for SR-Can. SKB R-06-109, Svensk Kärnbränslehantering AB, 105 p.

Drever J I, 1997. The Geochemistry of Natural Waters: Surface and Groundwater Environments. 3rd ed., Prentice Hall, New York, USA, 436 p.

Duro L, Grivé M, Cera E, Doménech C, Bruno J, 2005. Update of a thermodynamic database for radionuclides to assist solubility limits alculation for PA. ENVIROS, Spain, 165 p.

Follin S, Johansson P-O, Hartley L, Holton D, McCarthy R, Roberts D, 2007. Updated strategy and test of new concepts for groundwater flow modelling in Forsmark in preparation of site descriptive modelling stage 2.2. SKB R-07-20, Svensk Kärnbränslehantering AB, 100 p.

Follin S, Stephens M B, Laaksoharju M, Nilsson A-C, Smellie J A T, Tullborg E-L, 2008. Modelling the evolution of hydrochemical conditions in the Fennoscandian Shield during Holocene time using multidisciplinary information. Applied Geochemistry 23: 2004–2020.

Frape S K, Fritz P, McNutt R H, 1984. Water –rock interaction and chemistry of groundwaters from the Canadian Shield. Geochim. Cosmochim. Acta, 48, 1617–1627.

Frape S K, Fritz P, 1987. Geochemical trends for groundwaters from the Canadian Shield. In: P. Fritz and S.K. Frape (eds.), Saline Water and Gases in Crystalline rocks. Geol. Assoc. Can. Spec. Pap., 33, pp. 19– 38.

Frape S K, Blyth A, Blomqvist R, McNutt R H, Gascoyne M, 2005. Deep fluids in the continents: II. Cryslalline Rocks. In: J.I. Drever (ed.). Surfaqce and ground water, weathering, and solis. Treatise on Geochemistry, vol 5. pp. 541–580. Elsevier.

Frengstad B, Kjersti A, Skrede M, Banks D, Reidar Krog J, Siewers U, 2004. The chemistry of Norwegian groundwaters: III. The distribution of trace elements in 476 crystalline bedrock groundwaters, as analysed by ICP-MS techniques. The Science of the Total Environment, 246, 21–40.

Frölich K, Grabczak J, Rozansky K, 1988. Deuterium and oxygen-18 in the Baltic Sea. Chem. Geol., 72, 77–83.

Gascoyne M, 1989. High levels of uranium and radium in groundwaters at Canada's Underground Laboratory, Lac du Bonnet, Manitoba, Canada. Applied Geochemistry, 4, 577–591.

Gascoyne M, 1997. Evolution of redox conditions and groundwater composition in recharge-discharge environments on the Canadian Shield. Hydrogeology Journal, 5, 4–18.

Gascoyne M, 1999. Long-term maintenance of reducing conditions in a spent fuel nuclear fuel repository. A re-examination of critical factors. SKB R-99-41, Svensk Kärnbränslehantering AB, 56 p.

Gascoyne M, 2004. Hydrogeochemistry, groundwater ages and sources of salts in a granitic batholith on the Canadian Shield, southeastern Manitoba. Applied Geochemistry, 19, 519–560.

Gimeno M, Auqué L F, Gómez J, 2004. Mass balance modelling. Contribution to the model version 1.2. In: SKB (2004), Hydrogeochemical evaluation for Simpevarp model version 1.2. Preliminary site description on the Simpevarp area. SKB R-04-74, Svensk Kärnbränslehantering AB, 463 p.

Gimeno M, Auqué L F, Gómez J, 2005. PHREEQC modelling. Contribution to the model version 1.2. In: SKB (2005), Hydrogeochemical evaluation. Preliminary site description. Forsmark area, version 1.2. SKB R-05-17, Svensk Kärnbränslehantering AB, 403 p.

Gimeno M, Auqué L F, Gómez J, 2007. Water-rock interaction modelling issues. In: SKB (2007), Hydrogeochemical evaluation of the Forsmark site, modelling stage 2.1-issue report. SKB R-06-69, Svensk Kärnbränslehantering AB. (Appendix 3).

Gingele F X, Kasten S, 1994. Solid-phase manganese in Southeast Atlantic sediments: implications for the paleoenvironment. Mar. Geol., 121, 317–332.

Glynn P D, Voss C I, 1999. SITE-94. Geochemical characterization of Simpevarp ground waters near the Äspö Hard Rock laboratory. SKI Report 96-29, SKI, Stockholm, Sweden, 210 p.

Gómez J B, Laaksharju M, Skårman E, Gurban I, 2006. M3 version 3.0: Concepts, methods, and mathematical formulation. SKB TR-06-27, Svensk Kärnbränslehantering AB.

Grenthe I, Stumm W, Laaksoharju M, Nilsson A C, Wikberg P, 1992. Redox potentials and redox reactions in deep groundwater systems. Chem. Geol., 98, 131–150.

Guha J, Kanwar R, 1987. Vug brines fluid inclusions: a key to the understanding of secondary gold enrichment processes and the evolution of deep brines in the Canadian Shield. In: P. Fritz and S. K. Frape (eds.), Saline water and gases in crystalline rocks. Geol. Assoc. Can. Spec. Pap., 33, pp. 95– 101.

Guimerá J, Duro L, Jordana S, Bruno J, 1999. Effects of ice melting and redox front migration in fractured reocks of low permeability. SKB TR-99-19, Svensk Kärnbränslehantering AB, 86 p.

Gustafsson B, 2004. Millenial changes of the Baltic Sea salinity. Studies of the sensitivity of the salinity to climate change. SKB TR-04-12, Svensk Kärnbränslehantering AB, 42 p.

Hallbeck L, 2007. Microbial, gas and colloid issues. In: SKB (2007) Hydrogeochemical evaluation of the Forsmark site, modelling stage 2.1-issue report. SKB R-06-69, Svensk Kärnbränslehantering AB. (Appendix 2).

Hallbeck L, Pedersen K, 2008. Explorative analysis of microbes, colloids and gases. SDM-Site Forsmark. SKB R-08-85, Svensk Kärnbränslehantering AB.

Heiser U, Neumann T, Scholten J, Stüben D, 2001. Recycling of manganese from anoxic sediments in stagnant basins by seawater inflow: a study of surface sediments from the Gotland basin, Baltic Sea. Marine Geology, 177, 151–166.

Hummel W, Berner U, Curti E, Pearson F J, Thoenen T, 2002. Nagra/PSI Chemical Thermodynamic Data Base 01/01. Nagra Technical Report NTB 02-16, Nagra, Wettingen, Switzerland.

Isam Salih M M, Pettersson H B L, Lund E, 2002. Uranium and thorium series radionuclides in drinking water from drilled bedrock wells: correlation to geology and bedrock radioactivity and dose estimation. Radiation Protection Dosimetry, 102, 249–258.

Iwatsuki T, Arthur R, Ita K, Metcalfe R, 2004. Solubility constraints on uranium concentrations in groundwaters of the Tono uranium deposit, Japan. Radiochim. Acta, 92, 789–796.

Jacobson R L, Usdowski E, 1975. Geochemical controls on a calcite precipitating spring. Contrib. Mineral. Petrol., 51, 65–74.

Jakobsen R, Postma D, 1989. Formation and solid solution behavior of Ca-rhodochrosite in marine muds of the Baltic deeps. Geochim. Cosmochim. Acta 53, 2639–2648.

Jensen D L, Boddum J K, Tjell J C, Christensen T H, 2002. The solubility of rhodochrosite (MnCO3) and siderite (FeCO3) in anaerobic aquatic environments. Applied Geochemistry, 17, 503–511.

Kankainen T, 1986. Loviisa power station final disposal of reactor waste. On the age and origin of groundwater from the rapakivi granite on the island of Hästholmen. YJT-86-29, Nuclear Waste Commission of Finnish Power Companies, Finland.

Kelly W C, Rye R O, Livnat A, 1986. Saline minewaters of the Keweenaw Peninsula, Northern Michigan: their nature, origin, and relation to similar deep waters in Precambrian crystalline rocks of the Canadian Shield. Am. J. Sci., 286, 281– 308.

Kloppmann W, Girard J P, Negrel P, 2002. Exotic stable isotope compositions of saline waters and brines from the crystalline basement. Chem. Geol., 184, 49–70.

Kulik D, Kersten M, Heiser U, Neumann T, 2000. Application of Gibbs energy minimization to model early-diagenetic solid-solution aqueous-solution equilibria involving authigenic rhodochrosites in anoxic Baltic Sea sediments. Aquatic Geochemistry, 6, 147–199.

Kunzendorf H, Larsen B, 2002. A 200–300 year cyclicity in sediment deposition in the Gotland Basin, Baltic Sea, as deduced from geochemical evidence. Applied Geochemistry, 17, 29–38.

Kölling M, 2000. Comparison of different methods for redox potential determination in natural waters. In:L. Schüring, H.D. Schulz, W.R. Fischer, J. Böttcher and W.H.M. Duijnisveld (eds.), Redox. Fundamentals, processes and applications. Springer. Chapter 4, 42–54.

Laaksoharju M, Wallin B, (Ed) 1997. Evolution of the groundwater chemistry at the Äspö Hard Rock Laboratory. Proceedings of the second Äspö International Geochemistry Workshop, Äspö, Sweden, June 6–7, 1995. SKB 97-04, Svensk Kärnbränslehantering AB.

Laaksoharju M, Tullborg E-L, Wikberg P, Wallin B, Smellie J, 1999. Hydrogeochemical conditions and evolution at the Äspö HRL, Sweden. Applied Geochemistry, 14, 835–859.

Laaksoharju M, Gimeno M, Auqué L F, Gómez J, Smellie J, Tullborg E V, Gurban I, 2004. Hydrogepchemical evaluation of the Forsmark site, model version 1.1. SKB R-04-05, Svensk Kärnbränslehantering AB, 342 p.

Langmuir D, 1997. Aqueous environmental geochemistry. Prentice Hall, 600 p.

Larsen O, Postma D, Jakobsen R, 2006. The reactivity of iron oxides towards reductive dissolution with ascorbic acid in a shallow sandy aquifer (Rømø, Denmark). Geochim. et Cosmochim. Acta, 70, 4827–4835.

Lepland A, Stevens R L, 1998. Manganese authigenesis in the Landsort Deep, Baltic Sea. Marine Geology, 151, 1–25.

Lidmar-Bergström K, 1996. Long term morphotectonic evolution in Sweden. Geomorphology, 16, 33–59.

Li Y-H, Bischoff J, Mathieu G, 1969. The migration of manganese in the Artic Basin sediments. Earth Planet. Sci. Lett. 7, 265–270.

Louvat D, Michelot J L, Aranyossy J F, 1997. Salinity origin and residence time of the Äspö groundwater system. In: M. Laaksoharju and B. Wallin (eds.), Evolution of the groundwater chemistry at the Äspö Hard Rock Laboratory. Proceedings of the second Äspö International Geochemistry Workshop, Äspö, Sweden, June 6–7, 1995. SKB, 97-04, Svensk Kärnbränslehantering AB.

Louvat D, Michelot J L, Aranyossy J F, 1999. Origin and residence time of salinity in the Äspö groundwater system. Applied Geochemistry, 14, 917–925.

Lundin L, Lode E, Stendahl J, Melkerud P-A, Björkvald L, Thorstensson A, 2004. Soils and site types in the Forsmark area. SKB R-04-08, Svensk Kärnbränslehantering AB, 102 p.

Lundin L, Lode E, Stendahl J, Björkvald L, Hansson J, 2005. Oskarshamn site investigation. Soils and site types in the Oskarshamn area. SKB R-05-15, Svensk Kärnbränslehantering AB, 96 p.

Luukkonen, 2001. Groundwater mixing and geochemical reactions. An inverse-modelling approach. In: A. Luukkonen and E. Kattilakoski (Eds.), Äspö Hard Rock Laboratory. Groundwater flow, mixing and geochemical reactions at Äspö HRL. Task 5. Äspö Task Force on groundwater flow and transport of solutes. Progress Report SKB IPR-02-41, Svensk Kärnbränslehantering AB.

NAGRA, 1994. Kritallin-I safety assessment Report. Nagra Technical Report NTB 93-22E, Nagra, Wettingen, Switzerland.

Négrel P, Casanova J, 2005. Comparison of the Sr isotopic signatures in brines of The Canadian and Fennoscandian shields. Applied Geochemistry, 20, 749–766.

Neumann T, Heiser U, Leosson M A, Kersten M, 2002. Early diagenetic processes during Mn-carbonate formation: evidence from the isotopic composition of authigenic Ca-rhodochrosites of the Baltic Sea. Geochim. Cosmochim. Acta, 66, 867–879.

Nilsson K, 2006. Forsmark site investigation. Hydrochemical logging in KFM09A. SKB P-06-95, Svensk Kärnbränslehantering AB.

Nilsson K, Bergelin A, 2006. Forsmark site investigation. Complete hydrochemical characterisation in KFM09A. Results from the investigated section at 785.1–792.2 m. SKB P-06-217, Svensk Kärnbränslehantering AB.

Nilsson K, Bergelin A, Nilsson A-N, 2006. Forsmark site investigation. Hydrochemical characterization in borehole KFM01D. Results from seven investigated borehole sections: 194.0–195.0 m, 268.8–264.8 m, 314.5–319.5 m, 354.9–355.9 m, 369.0–370.0 m, 428.5–435.6 m, 568.0–575.1 m. SKB P-06-227, Svensk Kärnbränslehantering AB, 56 p.

Nissen J, Gustafsson J, Sandström R, Wallin L, Taxén C, 2005. Forsmark site investigation. Some corrosion observations and electrical measurements at drill sites DS4, DS7 and DS8. SKB P-05-265, Svensk Kärnbränslehantering AB, 43 p.

Nordstrom D K, Andrwes J N, Carlsson L, Fontes J C, Fritz P, Moser H, Olsson T, 1985. Hydrogeological and hidrochemical investigations in boreholes. Final report of the Pase I geochemical investigations of the Stripa groundwaters. Stripa Project Technical Report 85-06, Svensk Kärnbränslehantering AB.

Nordstrom D K, Ball J W, 1989. Mineral saturation states in natural waters and their sensitivity to thermodynamic and analytical errors. Sci. Geol. Bull., 42 (4), 269–280.

Nordstrom D K, Plummer L N, Langmuir D, Busenberg E, May H M, Jones B F, Parkhurst D, 1990. Revised chemical equilibrium data for major water-mineral reactions and their limitations. In: Melchior, D.C. and Basset, R.L. (Eds.) Chemical Modeling of Aqueous Systems II. ACS Symp. Ser. pp. 398–413.

Olofsson I, Simeonov A, Stephens M, Follin S, Nilsson A-C, Röshoff K, Lindberg U, Lanaro F, Fredriksson A, Persson L, 2007. Site descriptive modelling Forsmark, stage 2.2. A fracture domain concept as a basis for the statistical modelling of fractures and minor deformation zones, and interdisciplinary coordination. SKB R-07-15, Svensk Kärnbränslehantering AB, 261 pp.

Parkhurst D L, Appelo C A J, 1999. User's Guide to PHREEQC (Version 2), a computer program for speciation, batch-reaction, one-dimensional transport, and inverse geochemical calculations. Water Resources Research Investigations Report 99-4259, 312 p.

Pedersen K, 2001. Diversity and activity of microorganisms in deep igneous rock aquifers of the Fennoscandian Shield. In: J.K. Fredrickson and M. Fletcher (eds.), Subsurface microbiology and biogeochemistry. Wiley-Liss Inc., New York. pp. 97–139.

Pedersen H, Postma D, Kakobsen R, Larsen O, 2005. Fast transformation of iron oxyhydrosxides by the catalytic action of aqueous Fe(II). Geochim. Cosmochim. Acta, 16, 3967–3977.

Piker L, Schmaljohann R, Imhoff J F, 1998. Dissimilatory sulfate reduction and methane production in Gotland Deep sediments (Baltic Sea) during a transition period from oxic to anoxic bottom water (1993–1996). Aquatic Microbial Ecology, 14, 183–193.

Pitkänen P, Luukkonen A, Ruotsalainen P, Leino-Forsman H, Vuorinen U, 1999. Geochemical modelling of groundwater evolution and residence time at the Olkiluoto site. Posiva report 98-10, 184 p.

Pitkänen P, Partamies S, Luukkonen A, 2004. Hydrogeochemical interpretation of baseline groundwater conditions at the Olkiluoto site. Posiva report 2003-07, 159 p.

Plummer L N, Prestemon E C, Parkhurst D L, 1994. An interactive code (NETPATH) for modelling NET geochemical reactions along a flow PATH-version 2.0. (Report USGS 95-4169), USGS, USA.

Puigdomenech I, 2001. Hydrochemical stability of groundwaters surrounding a spent nuclear fuel repository in a 100,000 year perspective. SKB TR-01-28, Svensk Kärnbränslehantering AB, 83 p.

Rai D, Felmy A R, Ryan J L, 1990. Uranium(IV) hydrolysis constants and solubility product of UO2·xH2O(am). Inorg. Chem., 29, 7852–7865.

Reimann C, Hall G E M, Siewers U, 1996. Radon, fluoride and 62 elements as determined by ICP-MS in 145 Norwegian hard rock groundwater samples. Sci. Total Environ., 192, 1–19.

Reimann C, Caritat P, 1998. Chemical elements in the environment. Spriger-Verlag, 398 p.

Rickard D, 2006. The solubility of FeS. Geochim. Cosmochim. Acta,70, 5779–5789.

Roden E E, Zachara J M, 1996. Microbial reduction of crystalline iron (III) oxides: influence of oxide surface area and potential cell growth. Environ. Sci. Technol., 30, 1618–1628.

Roden E E, 2003. Fe(III) oxide reactivity toward biological vs chemical reduction. Environ. Sci. Technol., 37, 1319–1324.

Salonen L, Huikuri P, 2002. Elevated Levels of Uranium Series Radionuclides in Private Water Supplies in Finland. Proceedings of the 5th International Conference on High Levels of Natural Radiation and Radon Areas. Munich, Germany on Sep 4–7, 2000. BfS Schriften. Strahlenhygine. High Levels of Natural Radiation and Radon Areas: Radiation Dose and Health Effects. Volume II: General Exposure Assessment, 24, 28–30.

Sandström B, Savolainen M, Tullborg E L, 2004. Forsmark site investigation. Fracture mineralogy. Results from fracture minerals and wall rock alteration in boreholes KFM01A, KFM02A, KFM03A and KFM03B. SKB P-04-149, Svensk Kärnbränslehantering AB, 93 p.

Sandström B, Tullborg E V, 2005. Forsmark site investigation. Fracture mineralogy. Results from fracture minerals and wall rock alteration in boreholes KFM01B, FM04A,KFM05A and KFM06A. SKB P-05-197, Svensk Kärnbränslehantering AB, 151 p.

Sjöberg E L, Georgala D, Rickard D T, 1984. Origin of interstitial water compostions in postglacial clays (Northeastern Sweden). Chemical Geology, 42, 147–158.

SKB, 2004a. Hydrogeochemical evaluation of the Simpevarp area, model version 1.1. SKB R-04-16, Svensk Kärnbränslehantering AB, 398 p.

SKB, 2004b. Hydrogeochemical evaluation of the Forsmark site, model version 1.1. SKB R-04-05, Svensk Kärnbränslehantering AB, 342 p.

SKB, 2004c. Hydrogeochemical evaluation for Simpevarp model version 1.2. Preliminary site description of the Simpevarp area. SKB-R-04-74, Svensk Kärnbränslehantering AB, 463 p.

SKB, 2005a. Hydrogeochemical evaluation Preliminary site description. Forsmark area, version 1.2. SKB R-05-17, Svensk Kärnbränslehantering AB, 403 p.

SKB, 2005b. Preliminary site description. Forsmark area – version 1.2. SKB R-05-18, Svensk Kärnbränslehantering AB, 752 p.

SKB, 2006a. Hydrogeochemical evaluation. Preliminary site description Laxemar subarea – version 1.2. SKB R-06-12, Svensk Kärnbränslehantering AB, 435 pp.

SKB, 2006b. Preliminary site description. Laxemar stage 2.1. Feedback for completion of the site investigation including input from safety assessment and repository engineering. SKB R-06-110, Svensk Kärnbränslehantering AB, 122 p.

SKB, 2006c. Site descriptive modelling. Forsmark stage 2.1. Feedback for completion of the site investigation including input from safety assessment and repository engineering. SKB R-06-38, Svensk Kärnbränslehantering AB, 444 p.

SKB, 2006d. Hydrogeochemical evaluation. Preliminary site description Laxemar subarea – version 2.1. SKB R-06-70, Svensk Kärnbränslehantering AB, 337 pp.

SKB, 2007. Hydrogeochemical evaluation of the Forsmark site, modelling stage 2.1-issue report. SKB R-06-69, Svensk Kärnbränslehantering AB.(Appendix 3).

Smellie J A T, Wikberg P, 1989. Hydrochemical investigations at Finnsjön. SKB TR-89-19, Svensk Kärnbränslehantering AB.

Smellie J A T, Laaksoharju M, 1992. The Äspö Hard Rock Laboratory: Final evaluation of the hydrogeochemical pre-investigations in relation to existing geologic and hydraulic conditions. SKB TR 92-31, Svensk Kärnbränslehantering AB, 239 p.

Smellie J A T, Laaksoharju M, Wikberg P, 1995. Äspö, SE Sweden: a natural groundwater flow model derived from hydrogeochemical observations. J. Hydrol., 172, 147–169.

Smellie J A T, Tullborg E V, 2005. Explorative analysis and expert judgement of major components and isotopes. Contribution to the model version 1.2 In: Hydrogeochemical evaluation. Preliminary site description. Forsmark area. Version 1.2. SKB R-05-17, Svensk Kärnbränslehantering AB, 403 p.

Smellie J, Tullborg E V, Waber N, 2006. Explorative analysis and expert judgement of major components and isotopes. Contribution to the model version 2.1. In: SKB (2006), Hydrogeochemical evaluation. Preliminary site description. Laxemar subarea, version 2.1. SKB R-06-70, Svensk Kärnbränslehantering AB, 337 p.

Smellie J, Tullborg E–L, Nilsson A, 2008. Explorative analysis and expert judgement of major components and isotopes. SKB R-08-84 SDM Site Forsmark, Svensk Kärnbränslehantering AB.

Sohlenius G, Emeis K-C, Andrén E, Andrén T, Kholy A, 2001. Development of anoxia during the Holocene fresh-brackish water transition in the Baltic Sea. Marine Geology, 177, 221–242.

Starinsky A, Katz A, 2003. The formation of natural cryogenic brines. Geochim. Cosmochim. Acta, 67, 1475–1484.

Suess E, 1978. Mineral phases formed in anoxic sediments by microbial decomposition of organic matter. Geochim. Cosmochim. Acta, 43, 339–352.

Suksi J, Salminen S, 2007. Forsmark site investigation. Study of U oxidation sates in groundwater with high U concentrations. SKB P-07-54, Svensk Kärnbränslehantering AB, 19 p.

Taylor K C, Alley R B, Fiacco R J, Grootes P M, Lamorey G W, Mayewski P A, Spencer M J, 1992. Ice core dating and chemistry by direct-current electrical conductivity. Journal of Glaciology, 38, 325–332.

Thompson J, Higgs N C, Jarvis I, Hydes D J, Colley S, Wilson T R S, 1986. The behaviour of manganese in Atlantic carbonate sediments. Geochim. Cosmochim. Acta, 50, 1807–1818.

Thury M, Gautschi A, Mazurek M, Müller W H, Naef H, Pearson F J, Vomvoris S, Wilson W, 1994. Geology and Hydrology of the crystalline basement of Northern Switzerland. Synthesis of regional investigations 198–1993 within the Nagra Radiactive Waste Disposal Program. Nagra, Technical Report 93-01.

Trotignon L, Michaud V, Lartigue J E, Ambrosi J P, Eisenlohr L, Griffault L, de Combarieu M, Daumas S, 2002. Laboratory simulation of an oxidizing perturbation in a deep granite environment. /Geochim. Cosmochim. Acta, *66*/, 2583–2601.

Tröjbom M, Söderbäck B, 2006. Chemical characteristics of surface systems in the Forsmark area. Visualisation and statistical evaluation of data from shallow groundwater, precipitation, and regolith. SKB R-06-19, Svensk Kärnbränslehantering AB, 164 p.

Tröjbom M, Söderbäck B, Tullborg E-L, Johansson P-O, 2007. Evaluation of the hydrochemistry in the Forsmark area with focus on the surface system. SKB R-07-55, Svensk Kärnbränslehantering AB.

Tullborg E L, Larson S A, 1984. δ18O and δ13C fro limestones, calcite fissure fillings and calcite precipitates from Sweden. GFF, 106, 127–130.

Tullborg E L, Wallin B, Landström O, 1991. Hydrogeochemical studies of fracture minerals from water conducting fractures and deep groundwaters at Äspö. SKB Progress Report 25-90-01, Svensk Kärnbränslehantering AB.

Tullborg E L, 1997. How do we recognize remants of glacial water in bedrock?. In: L. King-Clayton, N. Chapman, L.O. Ericsson and F. Kautsky (eds.), Glaciation and hidrogeology. Workshop on the impact of climate change and glaciations on rock stresses, groundwater flow and hydrochemistry. Past, present and future. SKI Report 97:13.

Vieno T, Nordman H, 1999. Safety assessment of spent fuel disposal in Hästholmen, Kivetty, Olkiluoto and Romuvara. TILA-99. Posiva 99-07, 253 p.

Wacker P, Bergelin A, Nilsson A C, 2003. Forsmark site investigation. Complete hydrochemical characterisation in KFM01A. Results from two investigated sections: 110.1–120.8 and 176.8–183.9 m. SKB P-03-94, Svensk Kärnbränslehantering AB, 82 pp.

Wacker P, Bergelin A, Berg C, Nilsson A C, 2004a. Forsmark site investigation. Hydrochemical characterisation in KFM04A. Results from two investigated borehole sections: 230.0–237.6 and 354.0–361.1 m. SKB P-04-109, Svensk Kärnbränslehantering AB, 60 pp.

Wacker P, Bergelin A, Berg C, Nilsson A C, 2004b. Forsmark site investigation. Hydrochemical characterisation in KFM03A. Results from six investigated borehole sections: 386.0–391.0 m, 448.9–453.0 m, 448.5–455.6 m, 639–646.1 m, 939.5–946.6, 980–1,001.2 m. SKB P-04-108, Svensk Kärnbränslehantering AB, 125 pp.

Wacker P, Bergelin A, Nilsson A C, 2004c. Forsmark site investigation. Hydrochemical characterisation in KFM02A. Results from three investigated borehole sections: 106.5–126.5, 413.5–433.5 m and 509.0–516.1 m. SKB P-04-70, Svensk Kärnbränslehantering AB, 97 pp.

Wacker P, Berg C, Nilsson A C, 2005a. Forsmark site investigation. Chemical characterisation in borehole KFM06A. Results from the investigated sections at 353.5–360.6 and 768.0–775.1 m. SKB P-05-178, Svensk Kärnbränslehantering AB, 56 pp.

Wacker P, Berg C, Nilsson A C, 2005b. Forsmark site investigation. Chemical characterisation in borehole KFM07A. Results from the investigated section at 848.0–1,001.55 m. SKB P-05-170, Svensk Kärnbränslehantering AB, 45 pp.

Wacker P, Berg C, Bergelin A, Nilsson A C, 2005c. Forsmark site investigation. Hydrochemical characterisation in KFM05A. Results from an investigated section at 712.6–722.0 m. SKB P-05-79, Svensk Kärnbränslehantering AB, 59 pp.

Wallin B, 1995. Paleohydrological implications in the Baltic area and its relation to the groundwater at Äspö, south-eastern Sweden. A literature study. SKB TR-95-06, Svensk Kärnbränslehantering AB, 68 p.

Wallin B, Peterman Z, 1999. Calcite fracture fillings as indicators of paleohydrology at Laxemar at the Äspö Hard Rock Laboratory, southern Sweden. Applied Geochemistry, 14, 953-962.

Westman P, Sohlenius G, 1999. Diatom stratigraphy in five offshore sediment cores from the northwestern Baltic proper implying large scale circulation changes during the last 8,500 years. Journal of Paleolimnology, 22, 53–69.

Westman P, Wastegård S, Schoning K, Gustafsson B, Omstedt A, 1999. Salinity change in the Baltic Sea during the last 8,500 years: evidence, causes and models. SKB TR-99-38, Svensk Kärnbränslehantering AB, 52 p.

Wolthers M, van der Gaast S J, Rickard D, 2003. The structure of disordered mackinawite. American Mineralogist, 88, 2007–20015.

Appendix A

Review of the Chemmac logs in the Forsmark area

A.1 Introduction and motivation of this report

This appendix can be considered as an *explanation document* about the values of redox potentials selected for modelling in the ChemNet group. The need of this document has been motivated by the questions arosen from the INSITE group after their review of the previous SDM (Site Descriptive Modelling) phases both, in Laxemar and Forsmark areas. Most of these questions were about some disagreements between Eh (sometimes also pH) values used in the different SDM phases. This document presents the final Eh and pH values selected by the group of the University of Zaragoza for modelling purposes explaining, when necessary, the differences with the values suggested or reported by other authors.

Forsmark studies started when the SDM phases did and therefore the only available data are the ones compiled since then (2003). Moreover, in this case there are P-reports on all the Chemmac[18] analysis performed in the site. This means that in all the cases, the University of Zaragoza has have the opportunity of comparing its own evaluation with the one reported in the P-reports.

Physicochemical data from the Forsmark area, as compiled and supplied by SKB's geodatabase SICADA, have a different number of working Eh electrodes (from one to five) in the examined sections and the logging time is also rather variable**.** This facts clearly demonstrate the technical difficulties associated with the determination of Eh in groundwaters even with the sophisticated SKB methodology.

When the analysis of these values was started, a decission was taken of re-evaluating all the available continuous logs from the Forsmark (and Laxemar) area in order to select a high-quality Eh and pH subset based on a common and well defined set of criteria. The aim of this exercise is to create an Eh database as complete as possible which can be used for geochemical modelling. For a more detailed description of the SKB methodology and the problems associated with the potentiometrically measured Eh, see /Auqué et al. 2007, submitted/.

The selection of an Eh value for an specific borehole section must be based on a very careful analysis of the results obtained with the three different electrodes (Au, Pt and C) both at depth and at the surface, the logging time, the pH, the conductivity, and the dissolved oxygen values. The basic requirement is that the measured potential correspond to the equilibrium potential and this fact can only be demonstrated if the different electrodes give coincident results. Ideally, the values selected as representative should only be those obtained simultaneously by all the used electrodes within a small Eh range (±50 mV) over a long period of time. However this criterion is excessively restrictive as there can be undesirable effects selectively affecting one electrode or the other, or technical problems affecting one of the two measurement cells (downhole or at the surface) that can reduce the number of active electrodes (/Auqué et al. 2007/ submitted).

Taking into account all these issues, the following selection criteria were applied:

- logs longer than a week (logging times of selected representative values are between 13 and 68 days);
- logs with stable and coincident readings (in a range smaller than 50 mV) by several electrodes in the long term; and
- logs with simultaneous and stabilized pH values (in order to minimize the uncertainty associated with the pH).

[18] The Chemmac measurement facilities include a communication system, measurement application and flow-through cells with electrodes and sensors at the surface (surface Chemmac) and downhole (borehole Chemmac; eg. /Wacker et al. 2003/).

The sets of Eh logs that fulfilled these criteria were then checked for the quality of the redox values and two groups of representative Eh values depending on the number of electrodes giving coincident readings were defined:

- Group 1 Eh values: stable and coincident readings in, at least, three electrodes, two of them at depth.
- Group 2 Eh values: stable and coincident readings in two electrodes, at depth or at the surface.

This grouping reflects the difference, in quantity and quality, of the information used to define the representative Eh value. Group 1 includes Eh values with the most complete information and based on readings at depth, which are, in principle, more reliable. Group 2 includes good quality values but limited in reliability by frequently interrupted logs, different recording times for each electrode, or other technical difficulties.

This selection guarantees the quality of the data for any modelling purposes. All selected Eh values have been included in the work table for ChemNet clearly indicating that they have been selected by the UZ group. However a separate table (also available in the Project Place) has been prepared containing all the physicochemical values (laboratory and field measurements when available), just in case someone else has his own criteria and prefer to use other values.

A.2 Selected values of Eh and pH

A.2.1 Introduction

The availability of in situ measured Eh and pH is fundamental for any geochemical calculation, mainly involving redox modeling. Therefore, all the information available in the P-reports have been carefully reviewed and some modifications with respect to the P-reports selections have been made.

After 2.2 datafreeze (October 2006) there are 18 sets of logs in the Forsmark area corresponding to 18 different packered sections in 10 boreholes (KFM01A, 01D, 02A, 03A, 04A, 05A, 06A, 07A, 08A and 09A), ranging in depth from 110 to 950 m.

With respect to Eh, nine of them passed the initial selection criteria and eight of these nine were included in Group 1 (only one log was included in Group 2, see Table A-1). These Eh values have associated simultaneous and stabilized pH values also obtained with Chemmac.

Most of the kept and eliminated Eh and pH values agree very well with the recommendations suggested in the specific P-reports where the hydrochemical characterisation of each borehole is summarised /Wacker et al. 2003, 2004abc, 2005abc, Berg et al. 2006, Nilsson and Bergelin 2006, Nilsson et al. 2006/. The Eh values not considered as representative here correspond to the borehole sections in red in Table A-1. Moreover, four sections without a representative Eh value have stable and representative pH values. An explanation of the reasons for the rejection or acceptation of these values follows.

When analytical data are available, redox pair calculations have been performed and the calculated Eh values are also shown in Tables A-2 and A-3. Note that some of the samples without measurements or not representative Eh values, show the Eh calculated with this methodology (Table A-3).

Table A-1. Eh values selected for the 2.3 phase in Forsmark area where SKB methodology has been used. Except the value corresponding to KFM03 between 639 and 642 m borehole section, (which has been considered a Group 2 value, in bold and italics), the rest of the values are Group 1 values. The pH values also correspond to the values selected from Chemmac loggs, down-hole or surface, considering logs longer than a week and with stable and coincident readings. The borehole sections indicated in red do not have a representative Eh value, either because there were no measurements (NM), or because they do not fulfil our criteria (NS). The information about the fracture domains based on /Olofsson et al. 2007/ is also included).

Borehole	Borehole length (m)	Depth (elevation secmid, m)	Fracture Domains and Deformation Zones	Sample representative for the section	Values selected for modelling by UZ	
					Eh (mV)	pH
KFM01A	110–120	–112	FFM02	4538	–195	7.65
	176–183	–176	FFM02	4724	–188	7.41
KFM01D	428–435	–341	FFM01	12316	–263	8.1
	568–575	–445	FFM01	12354	–260	8.4
KFM02A	413–433	–417	ZFMA2	8272	NM	7.11
	509–516	–503	ZFMF1	8016	–143	6.93
KFM03A	386–391	–379	ZFMA4	8012	NM	7.42
	448–455	–442	ZFMA7	8284	–176	7.29
	639–646	–632	ZFMB1	8273	–196	7.38
	939–946	–931	FFM03	8281	–245	7.40
	980–1,000	–978	FFM03	8152	NS	8.26 (lab)
KFM04A	354–361	–197	ZFMA2	8267	NS	7.36
KFM05A	712–722		(FFM01?)		NS	
KFM06A	353–360	–302	FFM01	8809	–155	7.35
	768–775	–645	FFM06	8785	NS	8.31
KFM07A	848–1,001	–760	FFM05	8879	NS	8.04
KFM08A	683–690	–546	FFM01	12000	NS	8.0
KFM09A	785–792	–614	FFM04	12243	NS	8.1

NM: no Eh measurements.

NS: Eh no selected.

Table A-2. Important chemical and physicochemical parameters for the samples selected for redox modelling in the Forsmark area. Grey rows indicate samples with less than 1% of drilling water. The borehole sections indicated in red do not have a representative Eh value, either because there were no measurements, or because they do not fulfil our criteria.

Borehole KFM	Sample	Borehole Section	Depth (elev. secmid)	pH	Eh (mV)	Cl (mg/L)	Alk (mg/L)	SO_4^{2-} (mg/L)	Fe^{2+} (mg/L)	S^{2-} (mg/L)	U(x10^{-3}) (mg/L)	CH_4 (ml/L)	% Drilling water
01A	4538	110–120	–112	7.65	–195	4,562.8	61.0	315.6	0.953	0.014	1.51	–	0.76
	4724	176–183	–173	7.41	–188	5,329.5	99.0	547.0	0.475	bdl	14.9	0.12	4.80
01D	12316	428–435	–341	8.1	–263	5,160	21.5	76.8	1.33	bdl	1.94	–	3.40
	12354	568–575	–445	8.4	–260	5,800	20	38.3	1.23	bdl	0.799	4.6	0.9
02A	8272	413–433	–415	7.11		5,380	93.4	434	0.727	bdl	13.9	–	2.18
	8016	509–516	–503	6.93	–143	5,410	126.0	498.0	1.84	bdl	88.6	0.04	6.77
03A	8012	386–391	–379	7.42		5,450.0	101.0	495.0	0.656	bdl	3.49	–	0.55
	8284[1]	448–455	–442	7.29	–176	5,330.0	93.7	511.0	1.1	0.047	2.21[2]	0.03	0.4
	8273	639–646	–632	7.38	–196	5,430	22.0	197	0.223	bdl	46.1	0.07	4.35
	8281	939–946	–931	7.4	–245	8,560	9.9	73.9	0.208	0.058	0.699	0.06	8.75
	8152	980–1,000	–978	8.26(lab)		9,690	6.92	46.7	0.026	0.033	0.445	0.05	3.85
04A	8267	354–361	–197	7.36		5,580	111.0	514.0	2.12	bdl	62.0	–	7.45
06A	8809	353–360	–302	7.35	–155	4,560.0	45.7	151.0	1.11	bdl[3]	9.57	–	7.7
	8785	768–775	–645	8.31		7,080	5.72	35.5	0.051	0.018	–	0.09	1.55
07A	8879[4]	848–1,001	–760	8.04		14,800	6.19	99.3	0.162	0.134	0.184	0.04	0.35
08A	12000	683–690	–546	8.0		6,100	10.4	91.5	0.726	0.012	6.35	0.03	5.05
09A	12243	785–792	–614	8.10		14,800	6.67	118.0	0.103	bdl	0.0535	–	1.83

[1] Sample selected as representative for this section is #8017. However, the sample used here (#8284) have more “redox” data and was taken during the Chemmac measurements.

[2] This value has been taken from sample #8017 from this section.

[3] The value of 0.002, corresponding to sample #8808 from the same section, has been used for modelling.

[4] Sample selected as representative for this section is #8843. However, the sample used here (#8879) have CH_4 data and lower drilling water content.

Table A-3. Important chemical and physicochemical parameters for the samples selected for redox modelling in the Forsmark area, and calculated Eh values using the redox pairs. Grey rows indicate samples with less than 1% of drilling water. The borehole sections indicated in red do not have a representative Eh value, either because there were no measurements, or because they do not fulfil our criteria.

Bh KFM	Sample	Borehole Section	Depth (elev. secmid)	pH	Fe^{2+} (mg/L)	S^{2-} (mg/L)	U(x10^{-3}) (mg/L)	CH_4 (ml/l)	Eh measured Chemmac (mV)	Eh calculated with redox pairs (mV)				
										SO_4^{2-}/HS^-[1]	CO_2/CH_4	SO_4^{2-}/Pyrite[2]	SO_4^{2-}/FeS_{ppt}[3]	Fe(OH)3/ Fe^{2+} Grenthe[4]
01A	4538	110–120	–112	7.65	0.953	0.014	1.51	–	-195	-200	--	–195	–235	–272
	4724	176–183	–173	7.41	0.475	bdl	14.9	0.12	–188		–217	–178	–221	–215
01D	12316	428–435	–341	8.1	1.33	bdl	1.94	–	–263					–365
	12354	568–575	–445	8.4	1.23	bdl	0.799	4.6	–260		–303			–418
02A	8272	413–433	–415	7.11	0.727	bdl	13.9	–						–245
	8016	509–516	–503	6.93	1.84	bdl	88.6	0.04	–143		–183.5	–149	–193	–163
03A	8012	386–391	–379	7.42	0.656	bdl	3.49	–						–213
	8284[4]	448–455	–442	7.29	1.1	0.047	2.21[5]	0.03	–176	–187	–212	–170	–212	–227
	8273	639–646	–632	7.38	0.223	bdl	46.1	0.07	–196		–229	–181	–225	–213
	8281	939–946	–931	7.4	0.208	0.058	0.699	0.06	–245	–214	–241	–187	–229	–226
	8152	980–1,000	–978	8.26(lab)	0.026	0.033	0.445	0.05		–265	–293			–314
04A	8267	354–361	–197	7.36	2.12	bdl	62.0	–				–173	–213	–235
06A	8809	353–360	–302	7.35	1.11	bdl[6]	9.57	–	–155					–233
	8785	768–775	–645	8.31	0.051	0.018	–	0.09			–294	–253	–290	–333
07A	8879[7]	848–1,001	–760	8.04	0.162	0.134	0.184	0.04		–252	–277	–229	–267	–319
08A	12000	683–690	–546	8.0	0.726	0.012	6.35	0.03		–236	–266			–342
09A	12243	785–792	–614	8.10	0.103	bdl	0.0535	–						–324

[1] Thermodynamic data taken from WATEQ4F database (in PHREEQC).

[2] Calculated with the stability constant reported in /Gimeno et al. 2007/ for $FeS_{ppt.}$.

[3] These values have been calculated using the Fe^{2+} activity calculated with PHREEQC. Then the equilibrium constant deduced by /Grenthe et al 1992/ (not their calibration) is used.

[4] Sample selected as representative for this section is #8017. However, the sample used here (#8284) have more “redox” data and was taken during the Chemmac measurements.

[5] This value has been taken from sample #8017 from this section.

[6] The value of 0.002, corrresponding to sample #8808 from the same section, has been used for modelling.

[7] Sample selected as representative for this section is #8843. However, the sample used here (#8879) have CH_4 data and lower drilling water content.

A.2.2 Eh and pH values selected for redox modelling

KFM01A at 110–120 m borehole length (112 m depth FFM02)

The values proposed in the P-report and accepted by the University of Zaragoza (as they fulfil the selection criteria) are: pH = 7.65 and Eh = –195 mV (Figures A-1 and A-2).

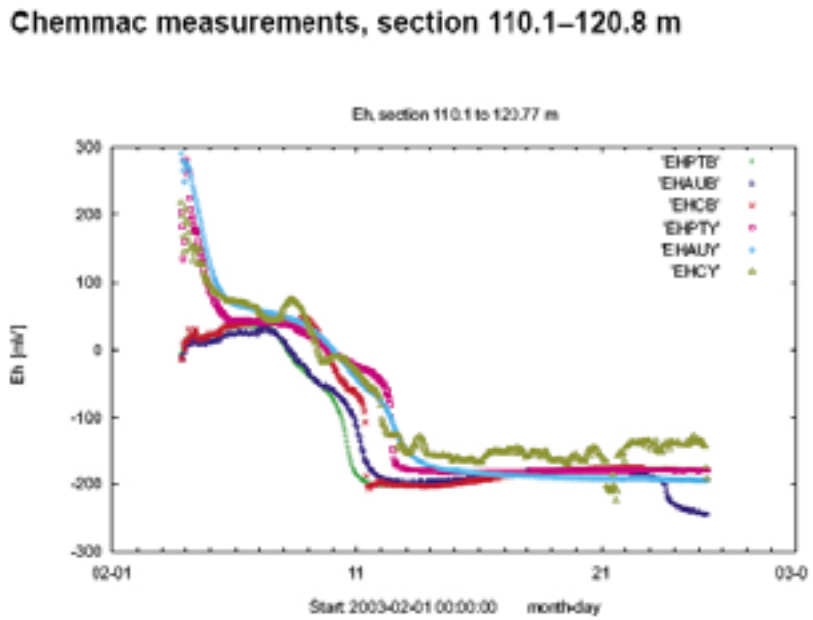

Figure A-1. *Redox potental measurements (Eh))in KFM01A (section 110–120 m) by platinum, gold and glassy carbon electrodes in the borehole section (EHPTB, EHAUB and EHCB) and at the surface (EHPTY, EHAUY and EHCY). The glassy carbon electrode at the surface shows a noisy signal due to an erroneous amplifier. (This plot and the figure caption is a copy of Figure A4-1 in /Wacker et al. 2003/ Appendix 4).*

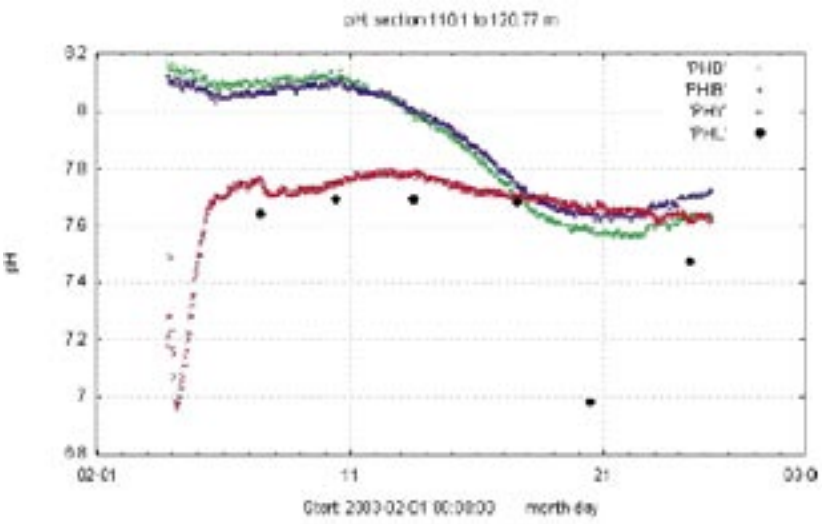

Figure A-2. *Measurements of pH in KFM01A (section 110–120 m) by two glass electrodes in the borehole section (PHB and PHIB) and one glass electrode at the surface (PHY). The laboratory pH in each collected sample (PHL) is given for comparison. (This plot and the figure caption is a copy of Figure A4-2 in /Wacker et al. 2003/, Appendix 4).*

KFM01A at 176–183 m borehole length (173 m depth; FFM02)

The values proposed in the P-report and accepted by the University of Zaragoza (as they fulfil the selection criteria) are: pH = 7.41 and Eh = –188 mV (Figures A-3 and A-4).

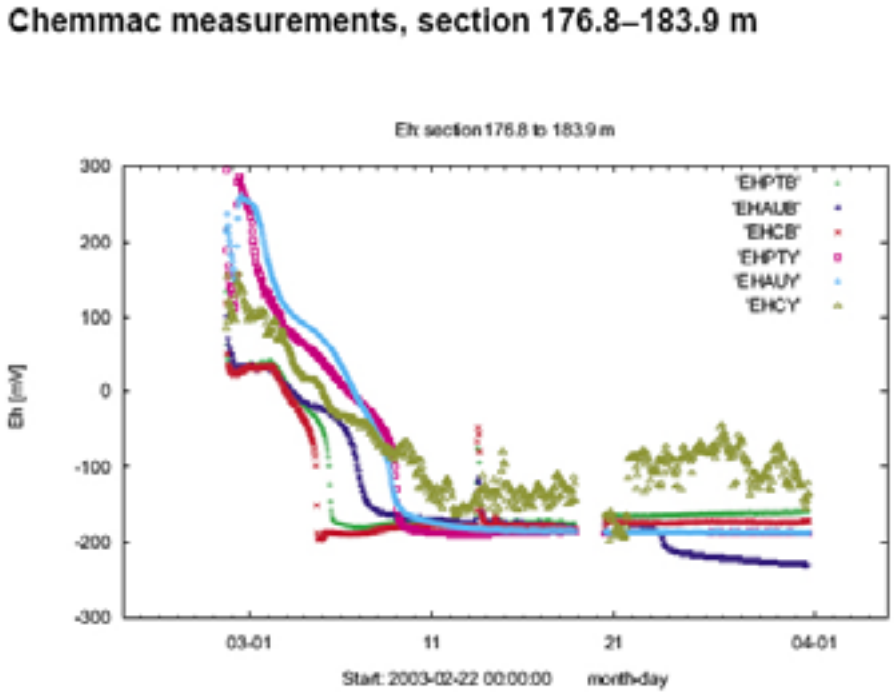

Figure A-3. *Redox potental measurements (Eh))in KFM01A (section 176–193 m) by platinum, gold and glassy carbon electrodes in the borehole section (EHPTB, EHAUB and EHCB) and at the surface (EHPTY, EHAUY and EHCY). The glassy carbon electrode at the surface shows a noisy signal due to an erroneous amplifier. (This plot and the figure caption is a copy of Figure A5-1 in /Wacker et al. 2003/ Appendix 5).*

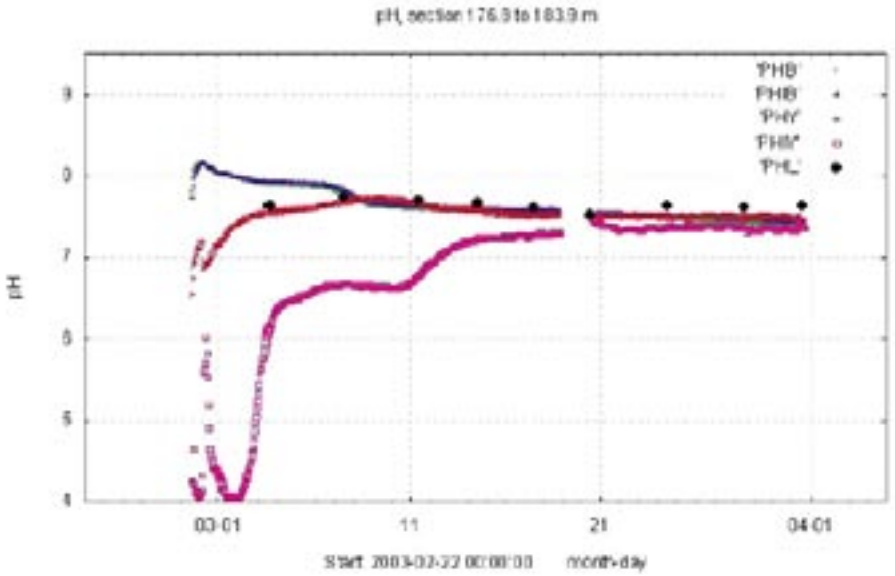

Figure A-4. *Measurements of pH) in KFM01A (section 176–193 m) by two glass electrodes in the borehole section (PHB and PHIB) and two glass electrodes at the surface (PHY and PHIY). The laboratory pH in each collected sample (PHL) is given for comparison. (This plot and the figure caption is a copy of Figure A5-2 in /Wacker et al. 2003/ Appendix 5).*

KFM01D at 428–435 m borehole length (341 m depth, FFM01)

The values proposed in the P-report and accepted by the University of Zaragoza (as they fulfil the selection criteria) are: pH = 8.1 and Eh = –263 mV (Figures A-5 and A-6).

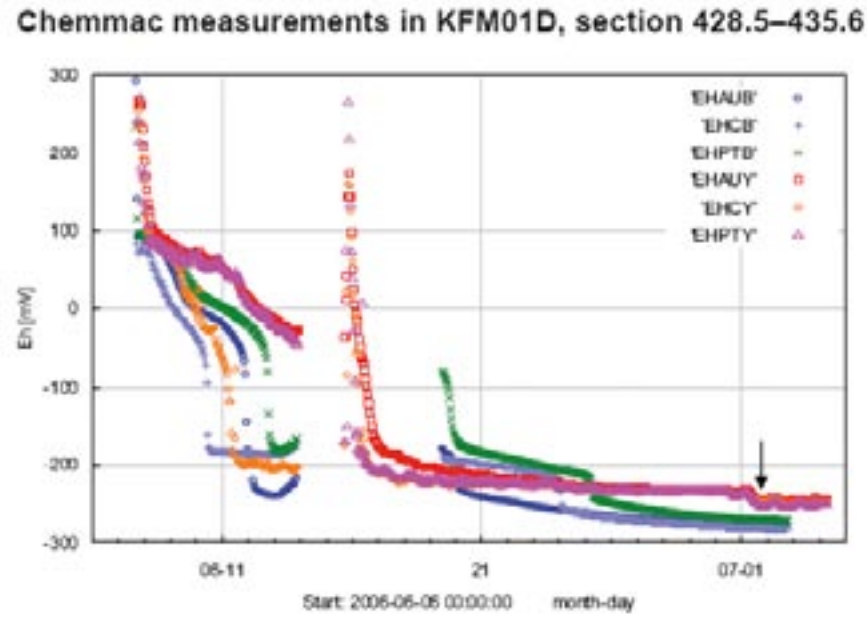

Figure A-5. *Redox potential measurements (Eh) in KFM01D (section 428–435 m) by gold, glassy carbon and platinum electrodes in the borehole section (EHAUB, EHCB and EHPTB) and at the surface by gold, glassy carbon and platinum (EHAUY, EHCY and EHPTY). The arrow shows the chosen representative Eh values for the borehole section. (This plot and the figure caption is a copy of Figure A8-1 in /Nilsson et al. 2006/ Appendix 8).*

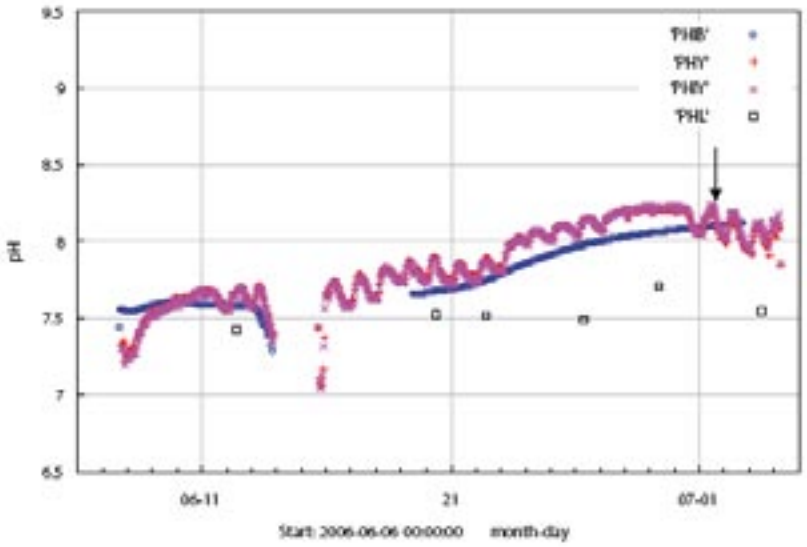

Figure A-6. *Measurements of pH in KFM01D (section 428–435 m) by two glass electrodes in the borehole section (PHB and PHIB) and two glass electrodes at the surface (PHY and PHIY). The laboratory pH in each collected sample (PHL) is given for comparison. The arrow shows the chosen representative pH values for the borehole section. (This plot and the figure caption is a copy of Figure A8-2 in /Nilsson et al. 2006/ Appendix 8).*

KFM01D at 568–575 m borehole length (445 m depth, FFM01)

The values proposed in the P-report and accepted by the University of Zaragoza (as they fulfil the selection criteria) are: pH = 8.4 and Eh = –260 mV (Figures A-7 and A-8).

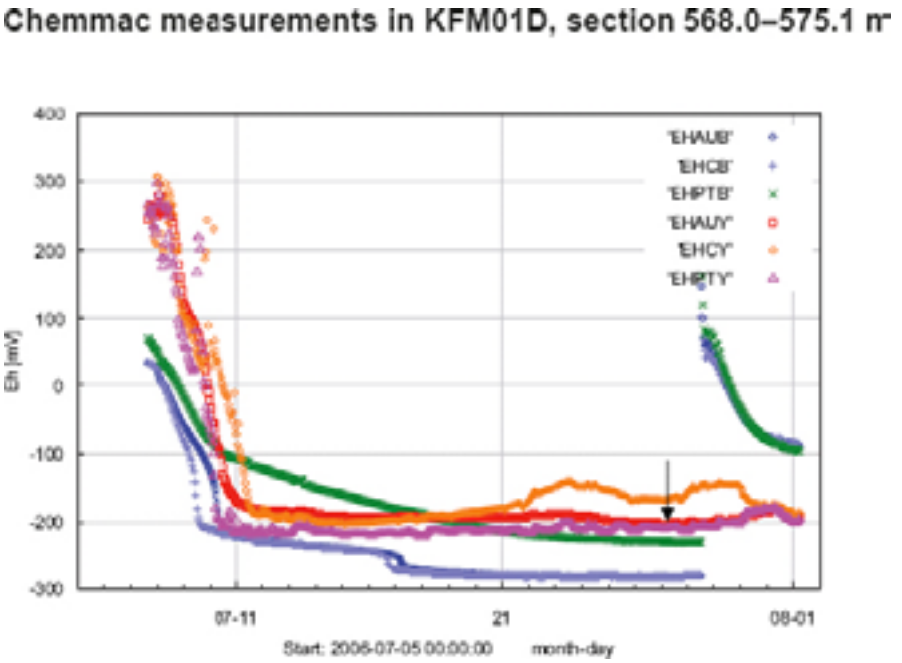

Figure A-7. *Redox potential measurements (Eh) in KFM01D (section 568–575 m) by gold, glassy carbon and platinum electrodes in the borehole section (EHAUB, EHCB and EHPTB) and at the surface by gold, glassy carbon and platinum (EHAUY, EHCY and EHPTY). The arrow shows the chosen representative Eh values for the borehole section. (This plot and the figure caption is a copy of Figure A9-1 in /Nilsson et al. 2006/ Appendix 9).*

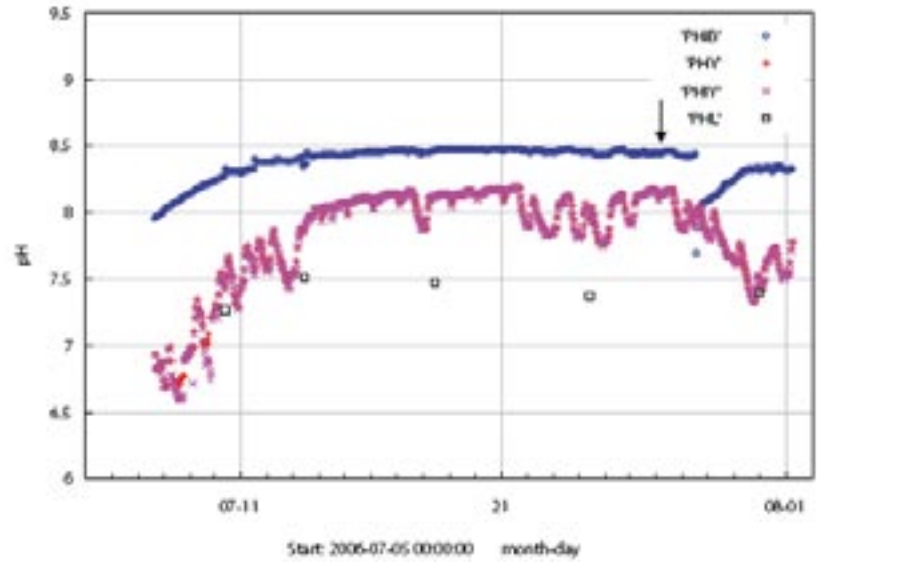

Figure A-8. *Measurements of pH in KFM01D (section 568–575 m) by two glass electrodes in the borehole section (PHB and PHIB) andtwo glass electrodes at the surface (PHY and PHIY). The laboratory pH in each collected sample (PHL) is given for comparison. The arrow shows the chosen representative pH values for the borehole section. (This plot and the figure caption is a copy of Figure A9-2 in /Nilsson et al. 2006/ Appendix 9).*

KFM02A at 413.5–433.5m borehole length (417 m depth; ZFMA2)

This section does not show Eh measurements, but the pH values are perfectly good for modelling. The selected value is pH = 7.11 and it has been included in the table in spite of it was not included in the SICADA delivery of 2.2 datafreeze (it was included in the 2.1). The pH measured in laboratory is 7.37 (red dots in Figure A-9).

KFM02A at 509–516 m borehole length (503 m depth, ZFMF1)

The Eh value proposed in the P-report and accepted by the University of Zaragoza (as the readings fulfil the selection criteria) is Eh = –143 mV (Figure A-10).

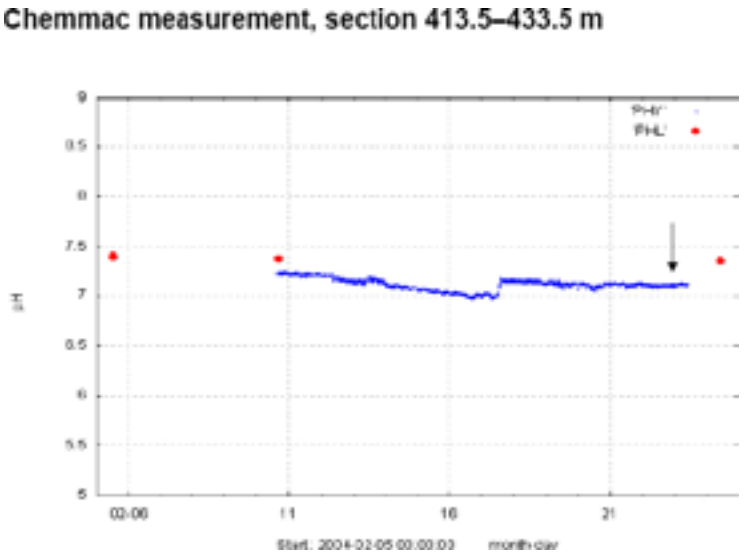

Figure A-9. *Measurements of pH in KFM02A (section 413–433 m)by a glass electrodes at the surface (PHY). The laboratory pH in each collected sample (PHL) is given for comparison. The arrow shows the chosen representative pH value for the borehole section. (This plot and the figure caption is a copy of Figure A6-1 in /Wacker et al. 2004a/, Appendix 6).*

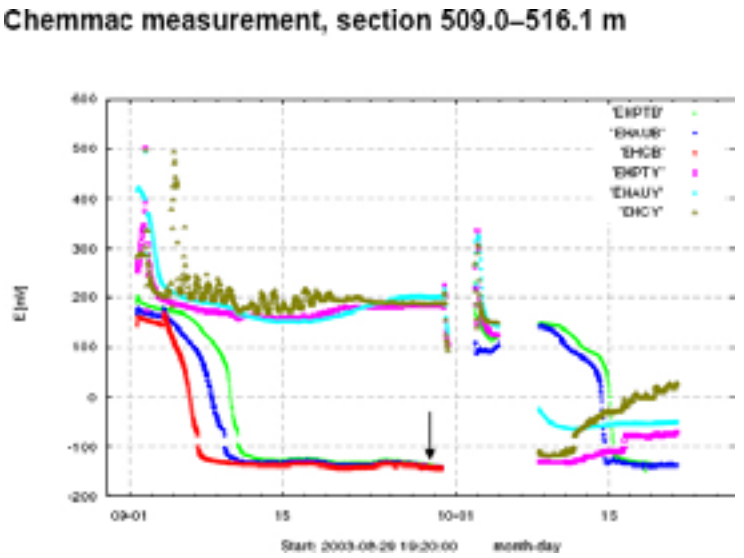

Figure A-10. *Redox potential measurements (Eh) in KFM02A (section 509–516 m) by platinum, gold and glassy carbon electrodes in the borehole section (EHPTB, EHAUB and EHCB) and at the surface (EHPTY, EHAUY and EHCY). The arrow shows the chosen representative Eh values for the borehole section. (This plot and the figure caption is a copy of Figure A7-1 in /Wacker et al. 2004a/ Appendix 7).*

However, a comment with respect to pH is needed here. The pH readings corresponding to the first stabilization of Eh electrodes seem to indicate a pH = 6.87 (although with some caution) just before measurements were stopped. Then, pH is around 7 in the following logs. So, a value of pH = 6.93 as more representative (Figure A-11) is suggested.

KFM03A at 386–391 m (379 m depth; ZFMA4)

This section do not have Eh measurements, but the rest of the parameters have been measured. The pH value for this section (pH =7.42) has been included in the table in spite of it has not been included in the SICADA delivery of 2.2 datafreeze (as it happens for KFM02 at 413–433 m, both were included in the 2.1). The pH measured in laboratory is 7.30 (red dots in Figure A-12).

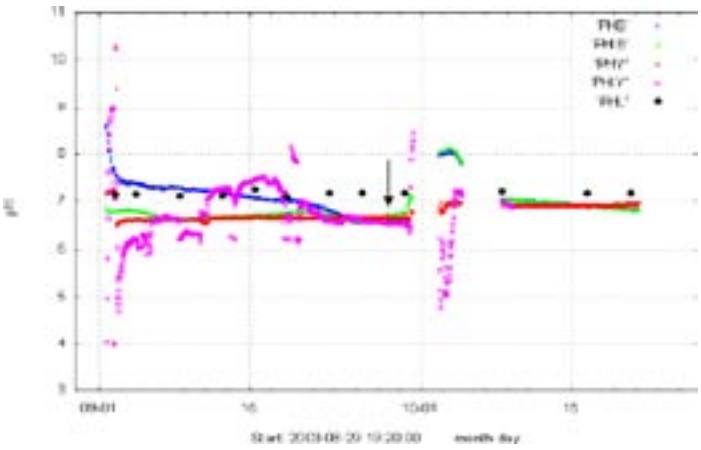

Figure A-11. *Measurements of pH in KFM02A (section 509–516 m) by two glass electrodes in the borehole section (PHB and PHIB) and two glass electrode at the surface (PHY and PHIY). The laboratory pH in each collected sample (PHL) is given for comparison. The arrows show the chosen representative pH values for the borehole section). (This plot and the figure caption is a copy of Figure A7-2 in /Wacker et al. 2004a/ Appendix 7).*

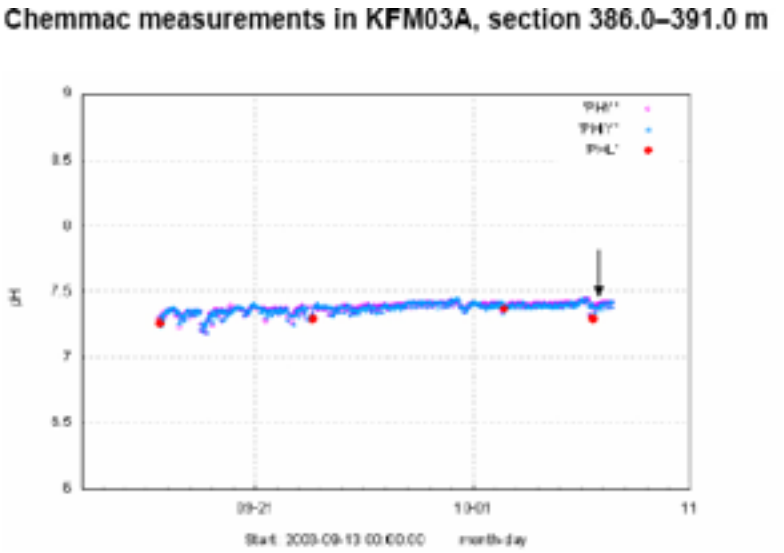

Figure A-12. *Measurements of pH in KFM03A (section 386–391 m) by two glass electrodes at the surface (PHY and PHIY). The laboratory pH in each collected sample (PHL) is given for comparison. The arrow shows the chosen representative pH values for the borehole section. (This plot and the figure caption is a copy of Figure A5-1 in /Wacker et al. 2004b/ Appendix 5).*

KFM03A at 448–455 m borehole length (442 m depth; ZFMA7)

The values proposed in the P-report and accepted by the University of Zaragoza (as they fulfil the selection criteria) are: pH = 7.29 and Eh = –176 mV (Figures A-13 and A-14).

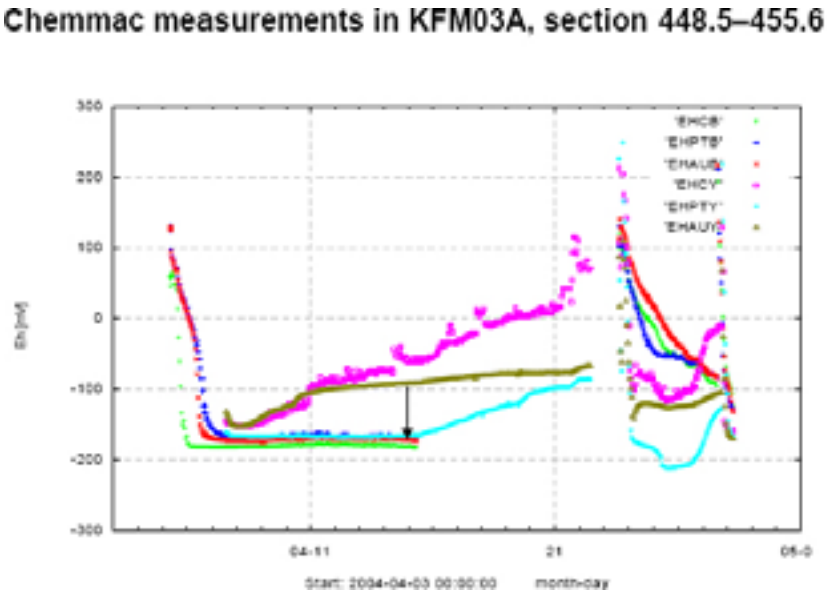

Figure A-13. *Redox potential measurements (Eh) in KFM03A (section 448–455 m)by platinum, gold and glassy carbon electrodes in the borehole section (EHPTB, EHAUB and EHCB) and at the surface (EHPTY,EHAUY and EHCY). The arrow shows the chosen representative Eh values for the borehole section. (This plot and the figure caption is a copy of Figure A7-1 in /Wacker et al. 2004b/ Appendix 7).*

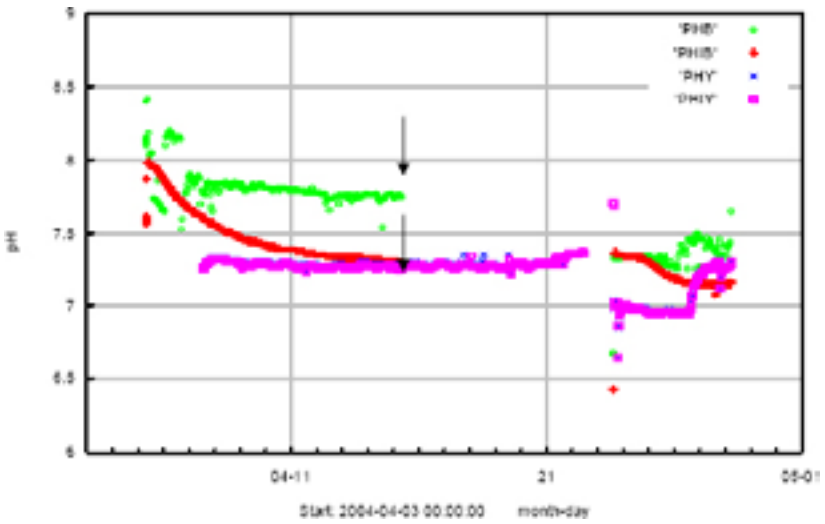

Figure A-14. *Measurements of pH in KFM03A (section 448–455 m) by two glass electrodes in the borehole section (PHB and PHIB) and two glass electrodes at the surface (PHY and PHIY). The arrow shows the chosen representative pH values for the borehole section. (This plot and the figure caption is a copy of Figure A7-2 in /Wacker et al. 2004b/ Appendix 7).*

KFM03A at 639–646 m borehole length (632 m depth; FFM03–ZFMB1)

The Eh value proposed in the P-report and accepted by the University of Zaragoza (as the readings fulfil the selection criteria) is Eh = –196 mV, the only value considered as Group 2 (Figure A-15). The reason for this is that the three borehole electrodes do not reach a stable value.

The pH value in the borehole is 7.38 and the value at surface is 7.48. This last value is more stable (Figure A-16) and therefore it was selected for the datafreeze 2.1. In the SICADA delivery of Forsmark 2.2 the value reported is 7.38 and this last one has been kept.

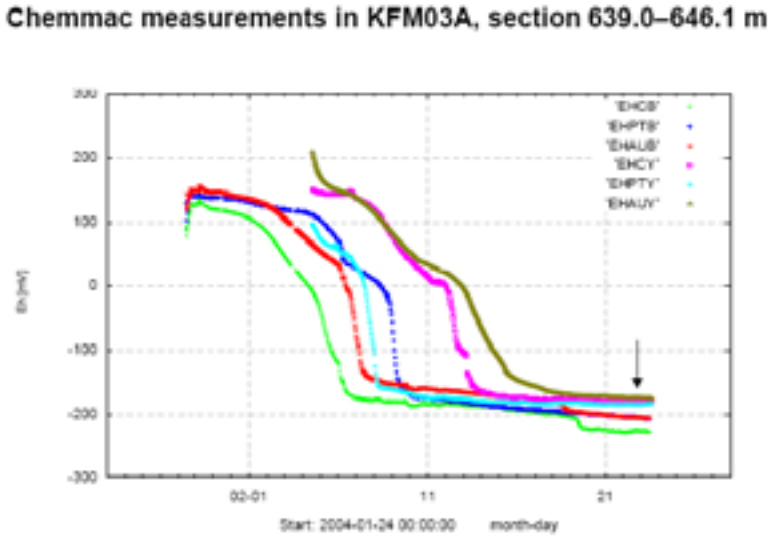

Figure A-15. *Redox potental measurements (Eh) in KFM03A (section 639–646 m) by platinum, gold and glassy carbon electrodes in the borehole section (EHPTB, EHAUB and EHCB) and at the surface (EHPTY, EHAUY and EHCY). The arrow shows the chosen representative Eh values for the borehole section. (This plot and the figure caption is a copy of Figure A8-1 in /Wacker et al. 2004b/ Appendix 8).*

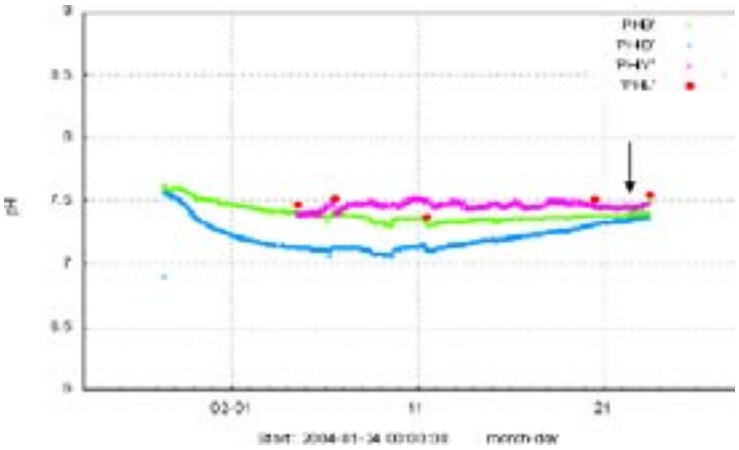

Figure A-16. *Measurements of pH in KFM03A (section 639–646 m)by two glass electrodes in the borehole section (PHB andPHIB) and one glass electrode at the surface (PHIY). The responses from PHY was not stable and was therefore rejected. The laboratory pH in each collected sample (PHL) is given for comparison. The arrow shows the chosen representative pH values for the borehole section. (This plot and the figure caption is a copy of Figure A8-2 in /Wacker et al. 2004b/ Appendix 8).*

KFM03A at 939–946 m borehole length (931 m depth; FFM03)

The values proposed in the P-report and accepted by the University of Zaragoza (as they fulfil the selection criteria) are: pH = 7.40 and Eh = –245 mV (Figures A-17 and A-18).

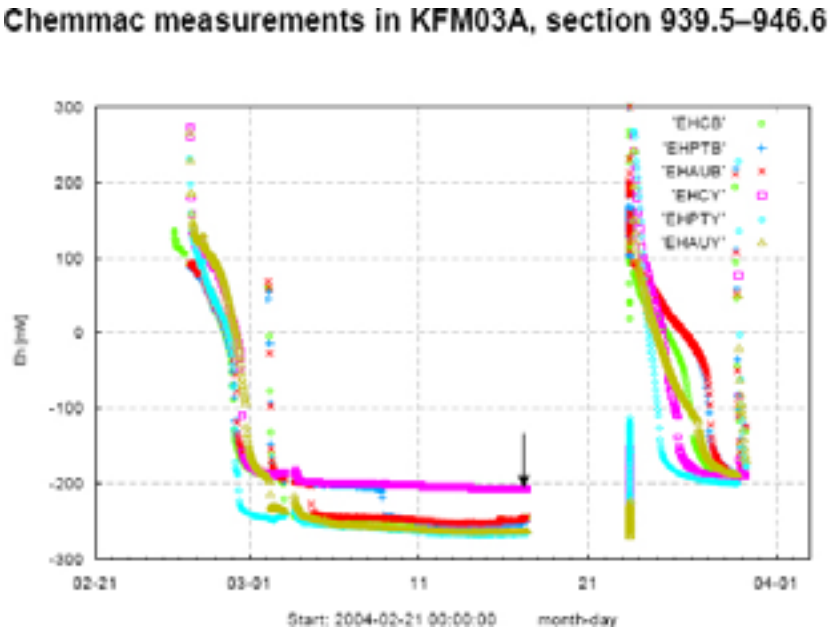

Figure A-17. *Redox potential measurements (Eh) in KFM03A (section 939–946 m) by platinum, gold and glassy carbon electrodes in the borehole section (EHPTB, EHAUB and EHCB) and at the surface (EHPTY, EHAUY and EHCY). The arrow shows the chosen representative Eh values for the borehole section. (This plot and the figure caption is a copy of Figure A9-1 in /Wacker et al. 2004b/ Appendix 9).*

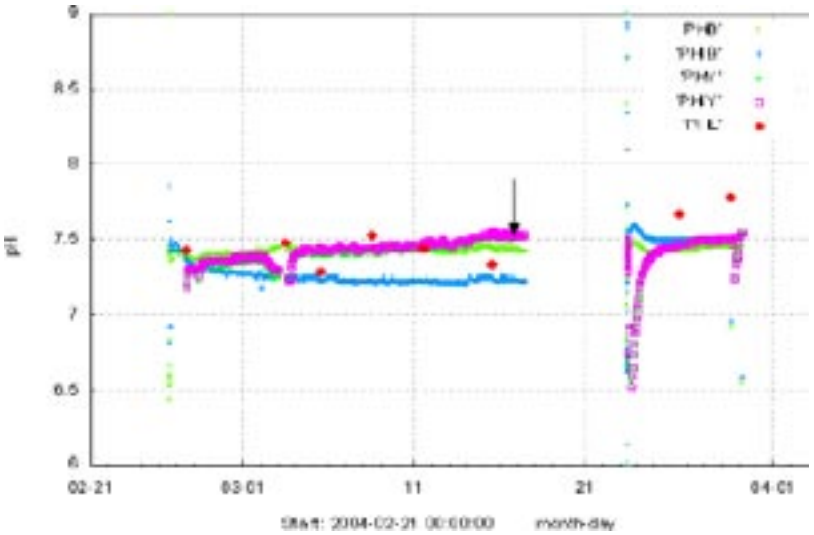

Figure A.-18. *Measurements of pH in KFM03A (section 939–946 m) by two glass electrodes in the borehole section (PHB and PHIB) and one glass electrode at the surface (PHIY). The laboratory pH in each collected sample (PHL) is given for comparison. The arrow shows the chosen representative pH values for the borehole section. (This plot and the figure caption is a copy of Figure A9-2 in /Wacker et al. 2004b/ Appendix 9).*

KFM06A at 353–360 m borehole length (302 m depth; FFM01)

The values proposed in the P-report and accepted by the University of Zaragoza (as they fulfil the selection criteria) are: pH = 7.35 and Eh = –155 mV (Figures A-19 and A-20).

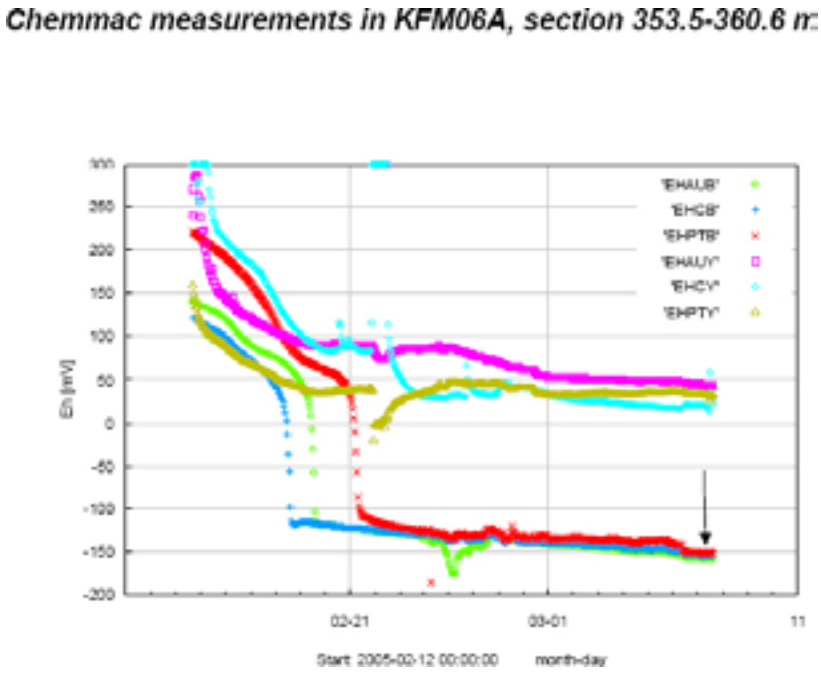

Figure A-19. *Redox potential measurements (Eh) in KFM06A (section 353–360 m) by platinum, gold and glassy carbon electrodes in the borehole section (EHPTB, EHAUB and EHCB) and at the surface (EHPTY, EHAUY and EHCY). The arrow shows the chosen representative Eh values for the borehole section. (This plot and the figure caption is a copy of Figure A6-1 in /Wacker et al. 2005c/ Appendix 6).*

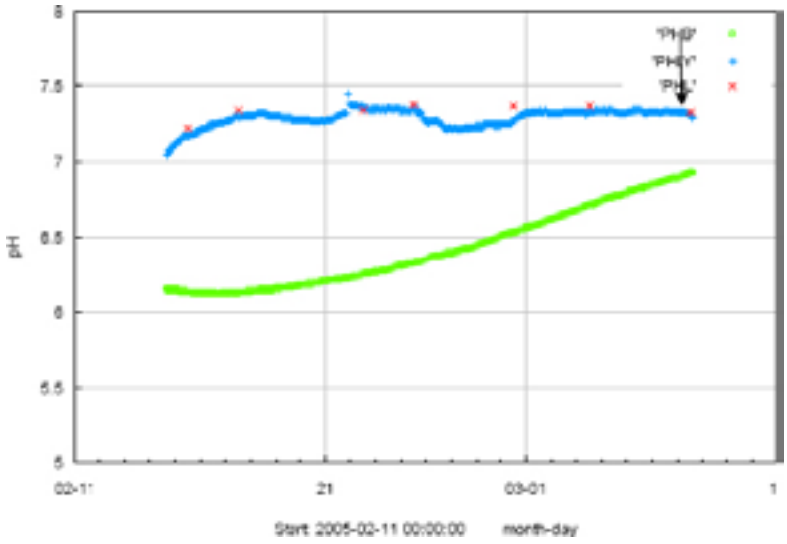

Figure A-20. *Measurements of pH in KFM06A (section 353–360 m) by two glass electrodes in the borehole section (PHB and PHIB) and two glass electrodes at the surface (PHY and PHIY). The laboratory pH in each collected sample (PHL) is given for comparison. The arrow shows the chosen representative pH values for the borehole section. (This plot and the figure caption is a copy of Figure A6-2 in /Wacker et al. 2005c/ Appendix 6).*

A.2.3 Eh values rejected for redox modelling

KFM03A at 980–1,000.2 m borehole length (978 m depth; FFM03)

There is no recommended Eh value in the P-report /Wacker et al. 2004b/ and none has been included here. The measurements are rejected because redox electrodes did not reach stable and agreeing values (Figure A-21). However, a value of –130 mV was considered in the review of /Bath 2007/ probably due to the fact that in spite of not considering a representative Eh, the P-report indicates that value with an arrow, as it can be seen in Figure A-21 and its caption.

The pH value recommended in the P-report is 8 (see Figure A-22) and it was the value used in Forsmark 2.1 phase modelling. This value corresponds to the surface electrode measurements and, as it also happens with the borehole electrodes, the reading is not stabilized at all. The lab pH of the representative sample in this section is 8.26 and this value has been used to analyse its influence on the redox modelling results obtained in Forsmark 2.1 (made with a pH of 8). The results indicate that differences are negligible, e.g. redox potential values obtained from the different redox pairs are in the range of +/−11 mV with respect to the old values. It is suggested to use this lab-pH in the modelling.

KFM04A at 354–361.13 m borehole length

There is no recommended Eh value in the P-report /Wacker et al. 2004c/ and none has been included here. The measurements are rejected because redox electrodes did not reach agreeing values (Figure A-23) and also severe corrosion was discovered in this borehole when the equipment was lifted to the ground surface /Wacker et al. 2004c/. However, a value of +100 mV was considered in the review of /Bath 2007/, probably due to the fact that two electrodes give the same reading. Here this value is not considered good at all.

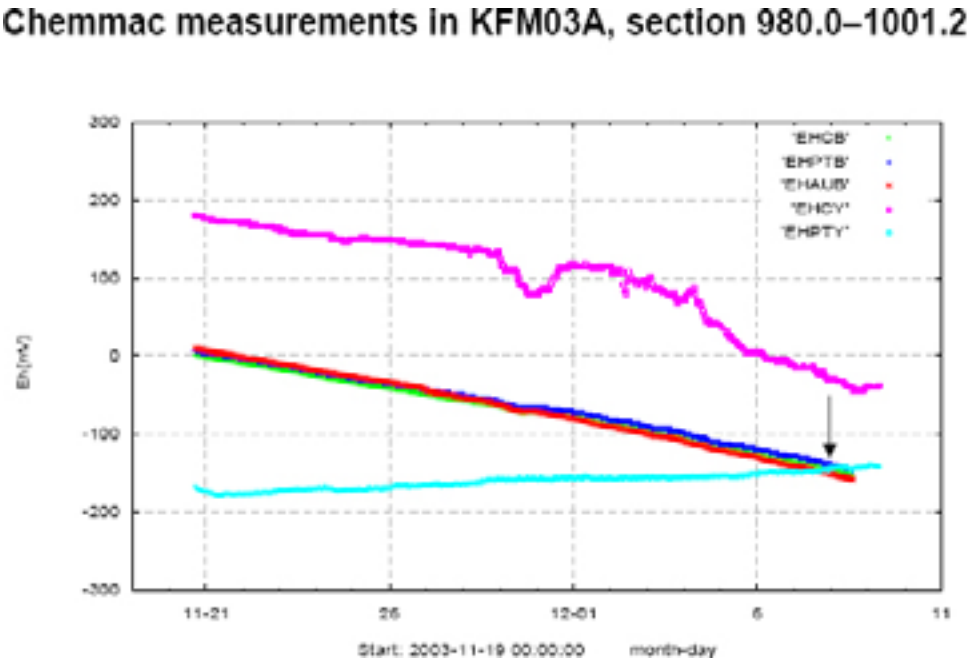

Figure A-21. *Redox potential measurements (Eh) in KFM03A (section 980–1,001 m) by platinum, gold and glassy carbon electrodes in the borehole section (EHPTB, EHAUB and EHCB) and at the surface (EHPTY and EHCY). EHAUY was omitted due to non-stable results. The arrow shows the chosen representative Eh values for the borehole section. (This plot and the figure caption is a copy of Figure A10-1 in /Wacker et al. 2004b/ Appendix 10).*

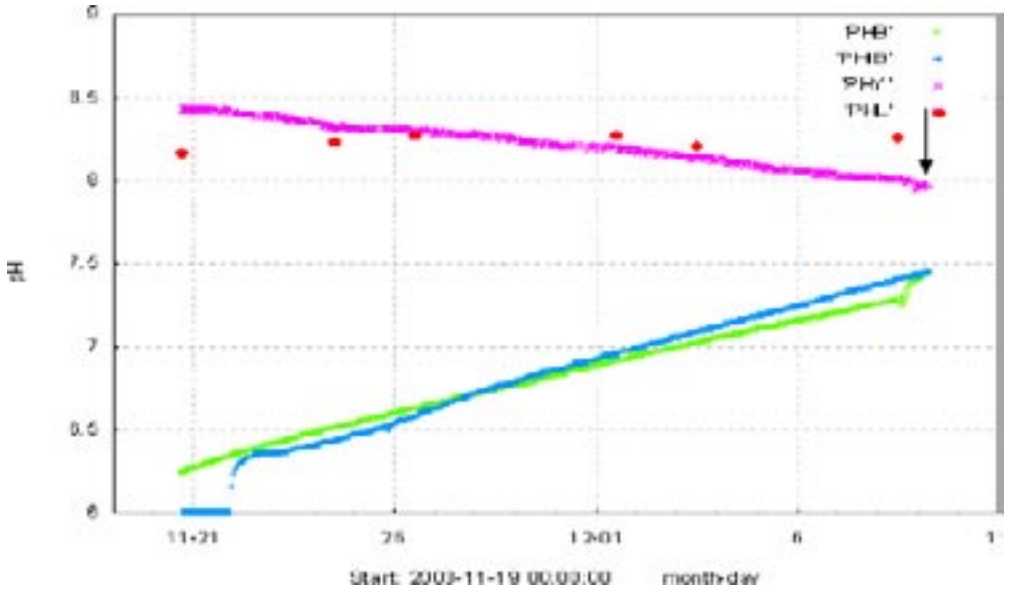

Figure A-22. *Measurements of pH in KFM03A (section 980–1,001 m) by two glass electrodes in the borehole section (PHB and PHIB) and one glass electrodes at the surface (PHY). The results from PHIY was not stable and was therefore omitted. The laboratory pH in each collected sample (PHL) is given for comparison. The arrow shows the chosen representative pH values for the borehole section. (This plot and the figure caption is a copy of Figure A10-2 in /Wacker et al. 2004b/ Appendix 10).*

Chemmac measurements (Eh, pH, electric conductivity, dissolved oxygen and temperature), section 354.0-361.1 m

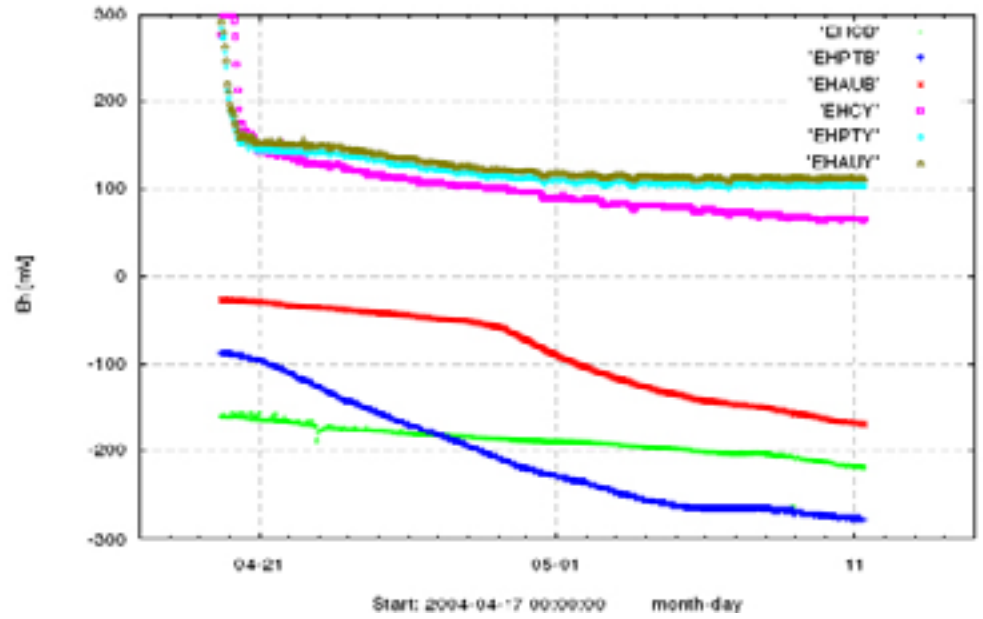

Figure A-23. *Redox potential measurements (Eh) in KFM04A (section 354–361 m) by platinum, gold and glassy carbon electrodes in the borehole section (EHPTB, EHAUB and EHCB) and at the surface (EHPTY, EHAUY and EHCY). (This plot and the figure caption is a copy of Figure A6-1 in /Wacker et al. 2004c/ Appendix 6).*

With respect to pH, considering the readings shown in Figure A-24, there is a fairly stable measurement at surface around pH=7.36. This value has not been included in the SICADA delivery of Forsmark 2.2. The pH measured in laboratory is 7.16.

KFM05A at 712.5–722 m borehole length

An Eh value of −274 mV was delivered by SICADA in Datafreeze 2.1. This value has been rejected by the University of Zaragoza because, although redox logs appear to indicate stable and reducing potential (Figure A-25), the collected water samples and measurements at this section are not regarded as representative due to the problems indicated in the P-report (mainly that water from above the upper packer intruded into the test section; /Wacker et al. 2005a/). This fact was explicitly warned in the column "water type" (as "GW, not representative") of the table delivered for datafreeze 2.1. In any case, the samples corresponding to this section have disappear from the data in datafreeze 2.2.

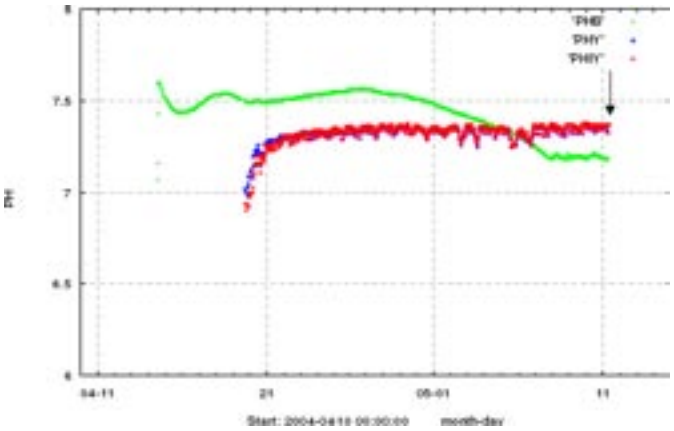

Figure A-24. *Measurements of pH in KFM04A (section 354–361 m) by a glass electrode in the borehole section (PHB) and two glass electrodes at the surface (PHY and PHIY). PHIB was omitted due to scattered values. The arrow shows the chosen representative pH values for the borehole section. (This plot and the figure caption is a copy of Figure A6-2 in /Wacker et al. 2004c/ Appendix 6).*

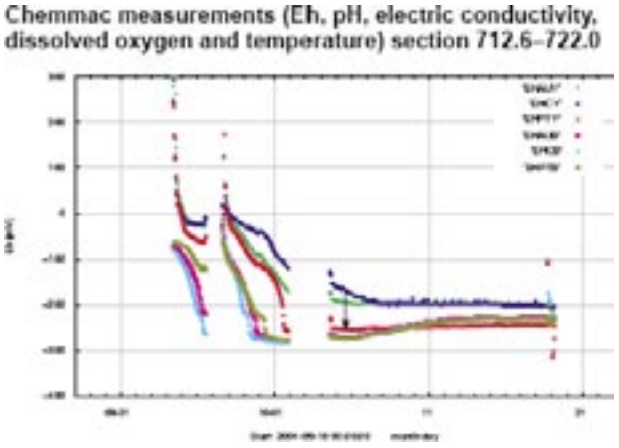

Figure A-25. *Redox potential (Eh) in KFM05A (section 712–722 m) measurements by platinum, gold and glassy carbon electrodes in the borehole section (EHPTB, EHAUB and EHCB) and at the surface (EHPTY, EHAUY and EHCY). The arrow shows the chosen representative Eh values for the borehole section. (This plot and the figure caption is a copy of Figure A6-1 in /Wacker et al. 2005a/ Appendix 6).*

With respect to pH the different electrodes do not reach an agreement (Figure A-26) and although a value of 7.5 is indicated in the P-report, the reasons expressed above made use to reject this value.

KFM06A at 768–775.12 m borehole length (645 m depth; FFM06–ZFMNE0725)

An Eh value of −200 mV was delivered by SICADA. It is considered acceptable in the corresponding P-report /Wacker et al. 2005c/. However, here this value is considered fairly uncertain but, if used, it should be done with caution. Electrodes readings are very different in depth and at surface. The proposed values in the P-report correspond to the borehole electrodes: one of them (Pt) shows values more than 50 mV higher than the other two; and the other two (Au and C) show coincident but not stable values (Figure A-27). The pH value selected has been 8.31 (Figure A-28).

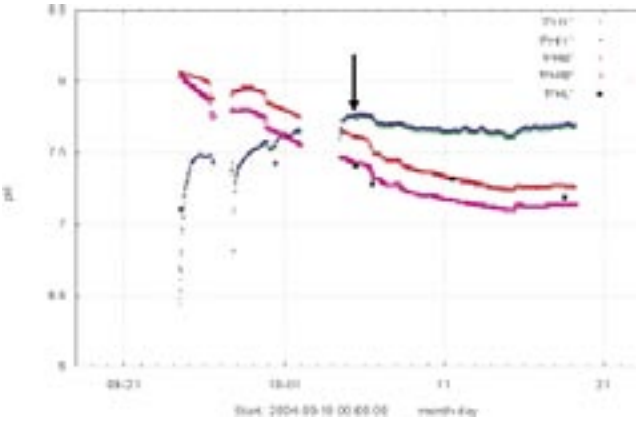

Figure A-26. *Measurements of pH in KFM05A (section 712–722 m) by two glass electrodes in the borehole section (PHB and PHIB) and two glass electrodes at the surface (PHY and PHIY). The laboratory pH in each collected sample (PHL) is given for comparison. The arrow shows the chosen representative pH values for the borehole section. (This plot and the figure caption is a copy of Figure A6-2 in /Wacker et al. 2005a/ Appendix 6).*

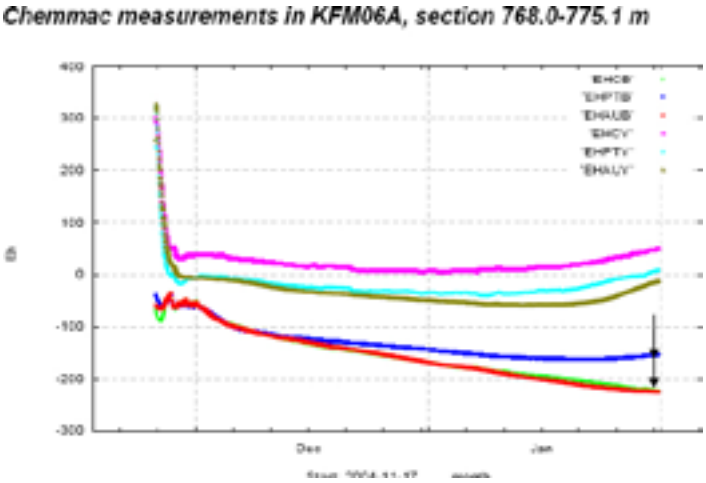

Figure A-27. *Redox potential measurements (Eh) in KFM06A (section 768–775 m) by platinum, gold and glassy carbon electrodes in the borehole section (EHPTB, EHAUB and EHCB) and at the surface (EHPTY, EHAUY and EHCY). The arrows show the chosen representative Eh values for the borehole section. (This plot and the figure caption is a copy of Figure A7-1 in /Wacker et al. 2005c/ Appendix 7).*

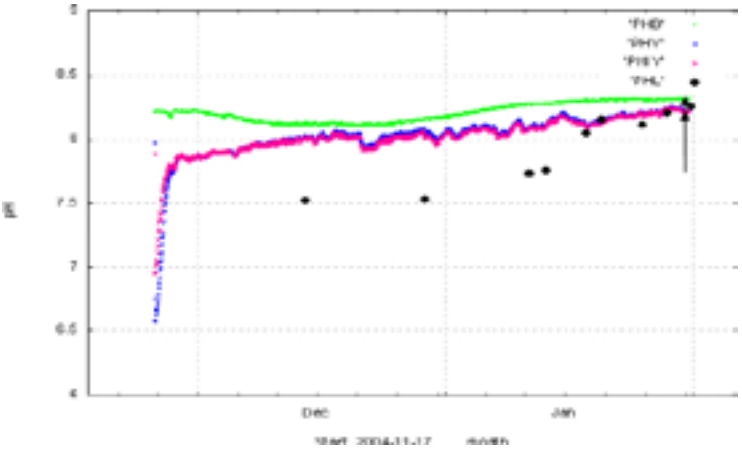

Figure A-28. *Measurements of pH in KFM06A (section 768–775 m)by two glass electrodes in the borehole section (PHB and PHIB) and two glass electrodes at the surface (PHY and PHIY). The laboratory pH in each collected sample (PHL) is given for comparison. The arrows show the chosen representative pH values for the borehole section. (This plot and the figure caption is a copy of Figure A7-2 in /Wacker et al. 2005c/ Appendix 7).*

KFM07A at 848–1,001.55 m borehole length (760 m depth; FFM05 ZFMNNW0100–ZFMB8)

An Eh value of +9 mV was delivered by SICADA (Figure A-29). This value was rejected by the University of Zaragoza because of its totally anomalous character. None of the chemical characteristics of the groundwaters in this section (saline groundwaters with Cl=14,000 mg/L, without tritium, noticeable amount of S^{2-} and CH_4, absence of dissolved oxygen, etc) is consistent with an oxidant value for Eh. Moreover, there is not a similar and reliable oxidant Eh value in groundwaters of similar composition and depth neither in Laxemar nor in the rest of the Fennoscandian Shield. The probable reason for this value could be the effect of up-coning associated to heavy pumping during and after drilling indicated in the P-Report /Wacker et al. 2005b/.

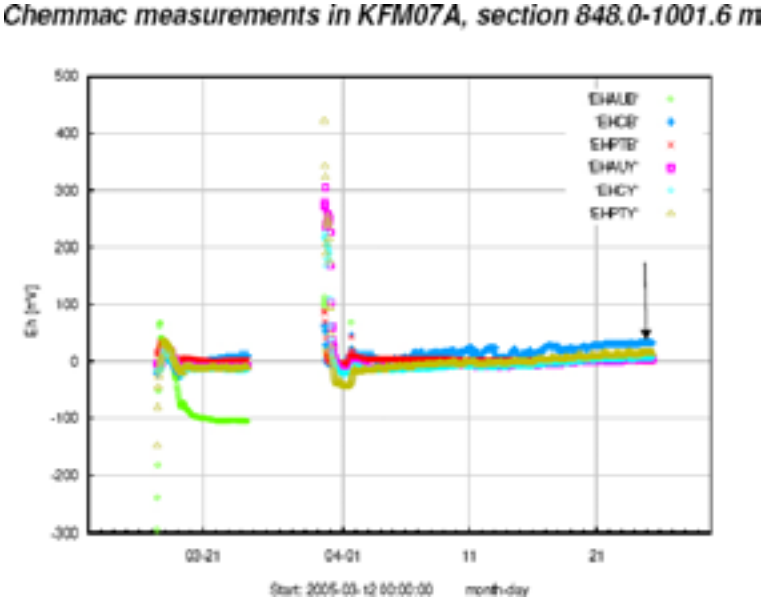

Figure A-29. *Redox potential measurements (Eh) in KFM07A (section 848–1,001 m) by gold, glassy carbon and platinum electrodes in the borehole section (EHAUB, EHCB and EHPTB) and at the surface (EHAUY, EHCY and EHPTY). The arrow shows the chosen representative Eh values for the borehole section. (This plot and the figure caption is a copy of Figure A6-1 in /Wacker et al. 2005b/ Appendix 6).*

With respect to the pH readings, a fairly stable and coincident value around 8.04 is shown by two electrodes (surface and borehole; Figure A-30). This value has been included in the Table as a representative pH.

KFM08A at 683.5–690.64 m borehole length (546 m depth; FFM01)

An Eh value of –209 mV was delivered by SICADA but it has been rejected by the University of Zaragoza. The readings do not fulfill the criteria (Figure A-31) and the value selected in SICADA and indicated in the P-report plot, is only for one electrode. The value is still kept in the Table for ChemNet (not in the table summarized here) but it is considered fairly uncertain and, if used, it should be done with caution.

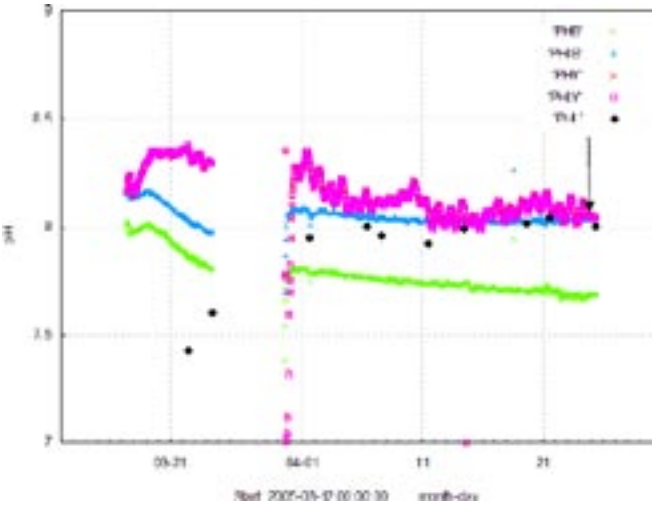

Figure A-30. *Measurements of pH in KFM07A (section 848–1,001 m) by two glass electrodes in the borehole section (PHB and PHIB) and two glass electrodes at the surface (PHY and PHIY). The laboratory pH in each collected sample (PHL) is given for comparison. The arrow shows the chosen representative pH values. (This plot and the figure caption is a copy of Figure A6-2 in /Wacker et al. 2005b/ Appendix 6).*

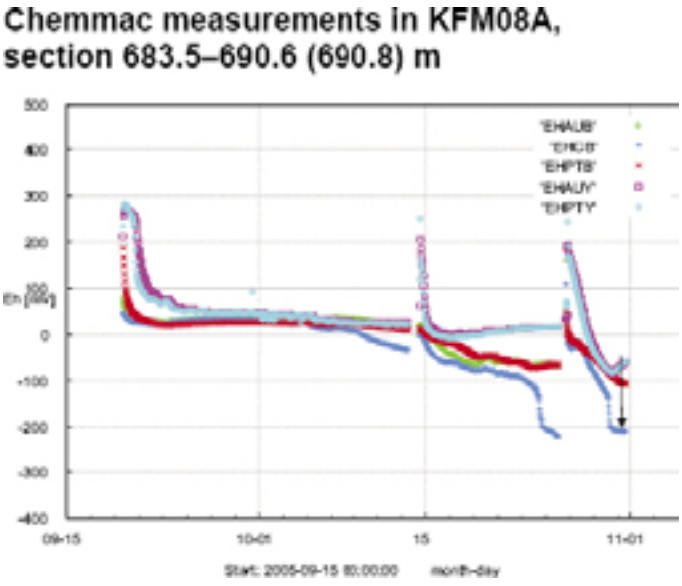

Figure A-31. *Redox potential measurements (Eh) in KFM08A (section 683–690 m) by gold, glassy carbon and platinum electrodes in the borehole section (EHAUB, EHCB and EHPTB) and at the surface by gold and platinum (EHAUY and EHPTY). The arrow shows the chosen representative Eh value for the borehole section. (This plot and the figure caption is a copy of Figure A8-1 in /Bergelin et al. 2006/ Appendix 8).*

The pH value selected for this section is 8.0 (Figure A-32).

KFM09A at 785.1–792.24 m borehole length (614 m depth; FFM04)

An Eh value of –229 mV is considered in the P-report as highly uncertain as it is based on only one electrode (Figure A-33). Therefore it was not delivered by SICADA. This value is also mentioned in the review of /Bath 2007/. The pH selected for modelling us 8.1 (Figure A-34).

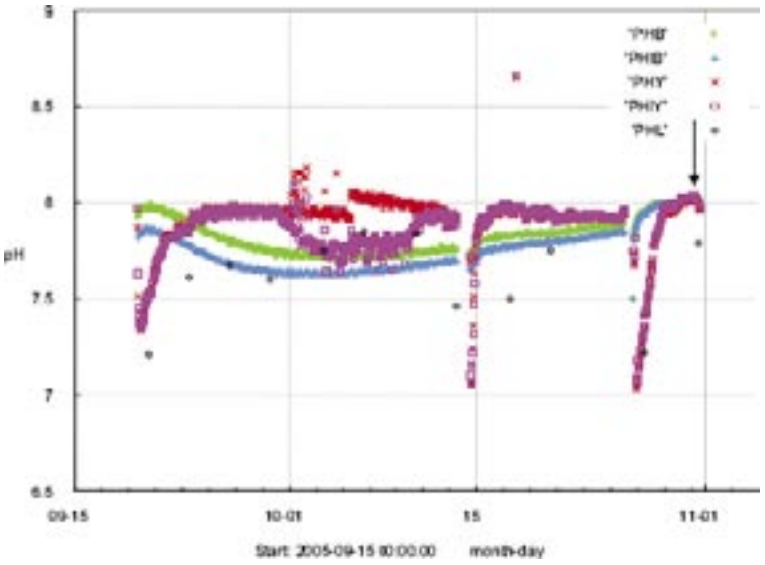

Figure A-32. *Measurements of pH in KFM08A (section 683–690 m) by two glass electrodes in the borehole section (PHB and PHIB) and two glass electrodes at the surface (PHY and PHIY). The laboratory pH in each collected sample (PHL) is given for comparison. The arrow shows the chosen representative pH values for the borehole section. (This plot and the figure caption is a copy of Figure A8-2 in /Bergelin et al. 2006/ Appendix 8).*

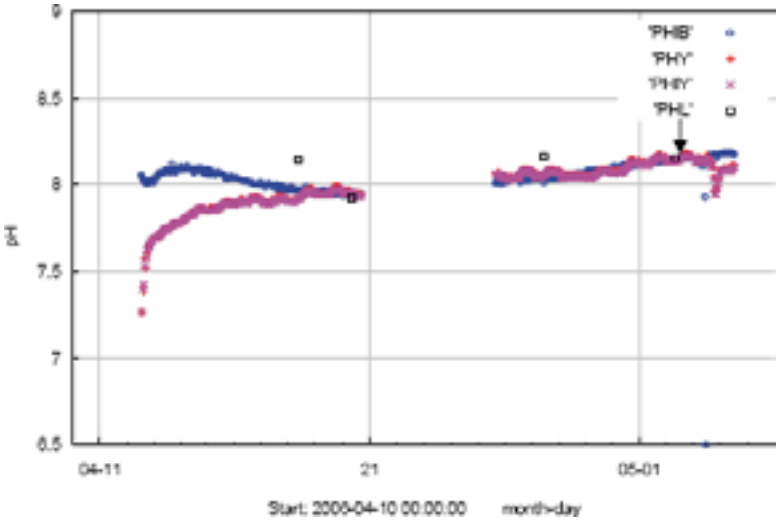

Figure A-33. *Redox potential measurements (Eh) in KFM09A (section 785–792 m) by gold, glassy carbon and platinum electrodes in the borehole section (EHAUB, EHCB and EHPTB) and at the surface (EHAUY and EHPTY). The results from the surface glassy carbon electrode were omitted because of noisy values. The arrows show the chosen representative Eh– values for the borehole section. (This plot and the figure caption is a copy of Figure A5-1 in /Nilsson and Bergelin 2006/ Appendix 5).*

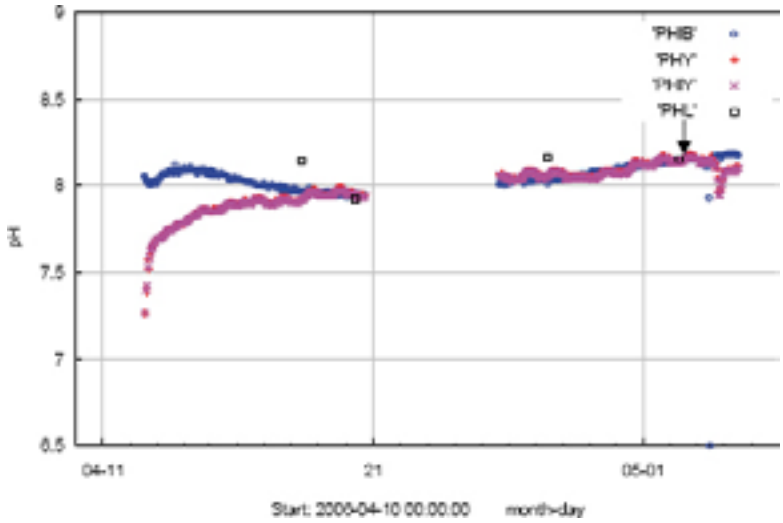

Figure A-34. *Measurements of pH in KFM09A (section 785–792 m)by one glass electrode in the borehole section (PH1B) and two glass electrodes at the surface (PHY and PHIY). The results from one glass electrode in the borehole section were omitted because of unstable values in the latter part of the investigation. The laboratory pH in each collected sample (PHL) is given for comparison. The arrow shows the chosen representative pH values for the borehole section. (This plot and the figure caption is a copy of Figure A5-2 in /Nilsson and Bergelin 2006/ Appendix 5).*

A.3 New values from Forsmark 2.3 data freeze

The new Chemmac values delivered from SICADA for the 2.3 data freeze are included in this separated section as they have not been checked with the values proposed in the P-reports as they are not available at the time this report has been done. So, only the analysis performed by the UZ group indicating the values selected and rejected and reasons for that is presented here.

The new samples with Chemmac data are the following:

- KFM10A: 478–487 m and 298–305 m Borehole section.
- KFM11A: 447–454 m Borehole section

KFM10A at 478–487.49 m borehole length (328.08 m depth; ZFMA2)

There are loggings for the three electrodes at depth (left in Figure A-35) and for two at the surface (right in Figure A-35). The three of them are very stable over time at around –258 mV in the borehole, and the two available at surface show also similar stable values for several days, although slightly lower (but always <50 mV). Therefore, these values are very good ones and satisfy perfectly the criteria adopted by us for their selection as Group 1 values in the modelling work in ChemNet for the SDM.

The pH values here were fairly stable with the four electrodes used (two at surface and two at depth) and almost coincident. Therefore, a field pH value of 7.6 has been selected for modelling.

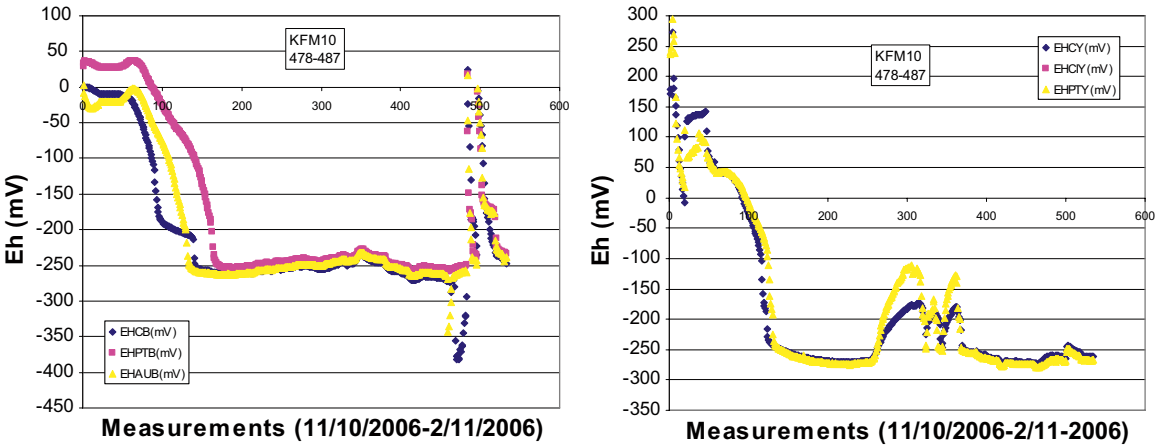

Figure A-35. *(a) Redox potential measurements (Eh) in KFM10A (section 478–487.49 m) by glassy carbon, platinum, and gold electrodes at depth (Ehcb, Ehptb and Ehaub; left) and by platinum and carbon at the surface (Ehpty and Ehcy; right) X axis indicates de number of measurements, and the title the time interval. This is the same for the rest of the plots in this section.*

KFM10A at 298–305.14 m borehole length (214.77 m depth; FFM03)

For this section there are also loggings for the three electrodes at depth (left in Figure A-36) and for two at the surface (right in Figure A-36). However, in contrast with the previous case, the three electrodes at depth do not show very stable values over time. They are the two electrodes at surface the ones that show fairly stable and coincident values for several days, even with several interruptions in between, at around –281 mV. Therefore, these data have been considered good enough to be included in the modelling purposes as Group 2 values.

There were also measurements with four pH electrodes and they are very stable and coincident at around 8.15, in spite of the interruptions in the measurements. Therefore, a field pH value of 8.15 has been selected for modelling.

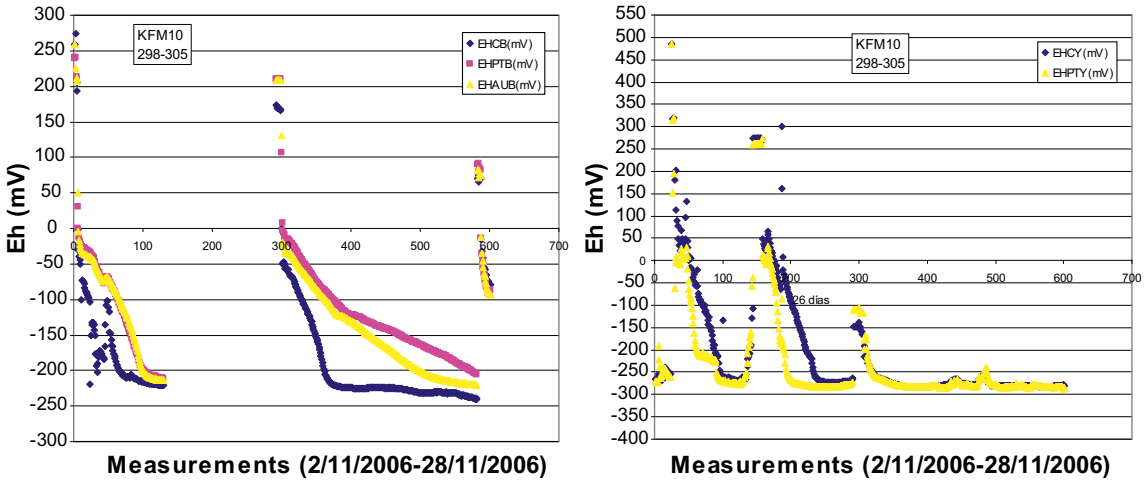

Figure A-36. *(a) Redox potential measurements (Eh) in KFM10A (section 298–305.14 m) by glassy carbon, platinum, and gold electrodes at depth (Ehcb, Ehptb and Ehaub; left) and by platinum and carbon at the surface (Ehpty and Ehcy; right) X axis indicates de number of measurements, and the title he time interval. This is the same for the rest of the plots in this section.*

KFM11A at 447.5–454.64 m borehole length (398.68 m depth)

For this section there are also loggings for the three electrodes at depth (left in Figure A-37) and for two at the surface (right in Figure A-37). In this case, two of the three electrodes at depth (gold and platinum) show very stable values at the end of the measurement period, at around –187 mV. The two electrodes at surface show always positive values, very unstable and non coincident. Therefore, these data have also been considered good enough to be included in the modelling purposes as Group 2 values.

In this case, in spite of the four electrodes measurements, none of them show stabilised values and therefore no selection of pH for modelling has been made.

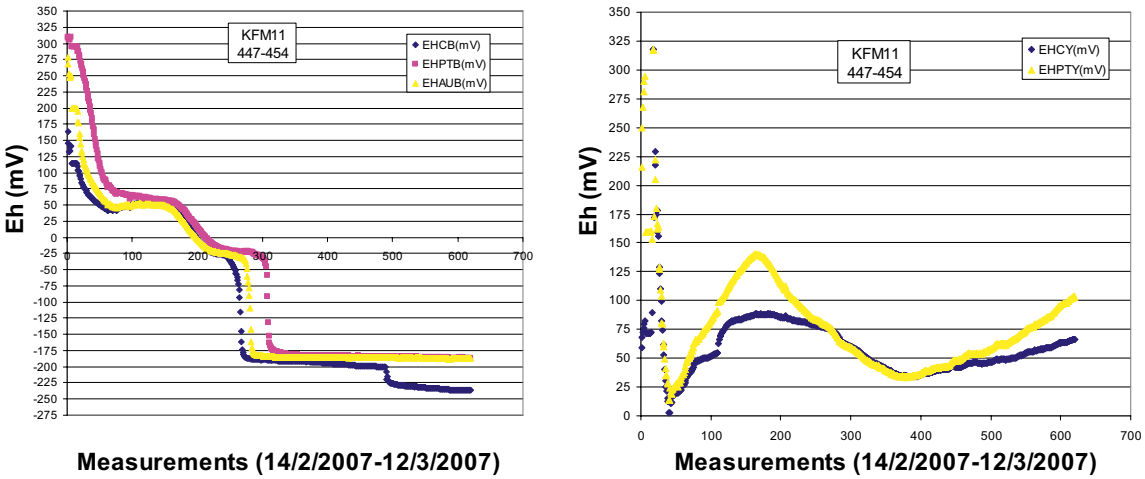

Figure A-37. *(a) Redox potential measurements (Eh) in KFM11A (section 447.5–454.64 m) by glassy carbon, platinum, and gold electrodes at depth (Ehcb, Ehptb and Ehaub; left) and by platinum and carbon at the surface (Ehpty and Ehcy; right) X axis indicates de number of measurements, and the title the time interval. This is the same for the rest of the plots in this section.*

Appendix B

Groundwater composition at repository depth

B.1 Introduction

This section summarizes (and extends) some of the SR-Can modelling results /Auqué et al. 2006/ on the present distribution of some important geochemical parameters in the system. The reason for using these results is that they have been obtained using a very interesting procedure which combines hydrogeological results obtained with CONNECTFLOW by /Hartley et al. 2006/ with a mixing and reaction-path simulation using PHREEQC. This coupling provides the theoretical but detailed compositional characters of the groundwaters on a rock volume (constituted by a grid with around one million points) that represents the whole regional area of Forsmark down to 2.3 km depth.

The hydrological results (*based on the site descriptive model, SDM, version 1.2*) contain mixing proportions of four component waters (a deep saline groundwater, a glacial melt-water, an old marine water, and an altered meteoric water) at every node of the 3D regional model domain. The geochemical calculations include both chemical mixing and equilibrium reactions with selected minerals: calcite, chalcedony and an Fe(III) oxyhydroxide (hematite with the equilibrium constant calculated by /Grente et al. 1992/). For most calculations the WATEQ4F thermodynamic database have been used as supplied with the PHREEQC code with the few modifications described in /Auqué et al. 2006/. In a few cases the "un-coupled" database (with suppressed redox equilibrium for the SO_4^{2-}/HS^- and HCO_3^-/CH_4 redox couples) has been used to test the effects on redox-sensitive elements (/see Auqué et al. 2006/ for more detailed information on the procedure and the calculations).

The compositional results obtained for 2020 AD (equivalent to the present conditions) have came to be in very good agreement with the data from the site[19] except for the most diluted samples which correspond to the upper 100 m of the rock volume /Auqué et al. 2006/. The advantage of these results is that they fill the entire volume, in contrast with the sparseness of the real samples, located only in the available borehole sections within the repository candidate volume.

In this appendix the modelled distribution of key geochemical parameters at the repository depth are presented in order to evaluate SKB´s groundwater suitability criteria and to obtain a preliminary view on the spatial hydrochemical variability.

B.2 Modelled distribution of important geochemical parameters in groundwaters at repository depth

Considering the main Safety functions from SR-Can, the results concerning the carbonate system (including Ca and alkalinity concentrations together with pH and calcite mass transfers), the potassium content, the salinity (TDS) and the redox system (iron and sulphide concentrations and Eh values) are presented here.

The way in which these results are presented follows the same graphical scheme for all geochemical parameters, with two different kinds of plots. The first type of plot consists of a 3D block with horizontal and vertical cross sections colour-coded with respect to the present-day values of each geochemical parameter as obtained from the SR-can calculations. The vertical scale is exaggerated six times to display the system more clearly, from the surface to 1,000 m depth. The horizontal plane is at 400 m depth, the repository layout being also shown in that plane, and the vertical plane is drawn perpendicular to the coast. The top surface shows the topography with the land areas in shades of brown and the Baltic Sea in shades of blue. The second type of plots are frequency histograms showing the variability of each geochemical parameter on the horizontal plane at repository depth (400 m).

[19] The predicted results reproduce the main chemical trends defined by the present data in the full compositional space, covering the observed chemical variability /Auqué et al. 2006/.

B.2.1 Salinity (TDS)

The landscape in Forsmark is a relatively flat peneplain that dips gently towards the east (that is, the coast). The whole area is located below the highest shoreline that occurred during the latest deglaciation and today's landscape is strongly influenced by the ongoing shoreline displacement of c. 6 mm per year. The higher salinity found in the eastern part of the site is partly related to the contribution of a modern Baltic marine water signature /Smellie and Tullborg 2005/ and to the presence of discharge zones of brackish groundwaters (or trapped remnants of these old waters). As was already stated in Section 3.3, this fact explains the very high TDS and Ca concentrations (almost 5,000 mg/L Cl and 900 mg/L Ca) found in many shallow groundwaters from Forsmark, mainly close to the coast (Figure B-1).

In general meteoric water (low TDS) is present in the uppermost c. 200 m of the bedrock. At depths between 200 and 800 m, the salinity remains fairly constant and then at depths between 800 and 1,000 m, the salinity increases to higher values (even higher than the highest value shown in the legend). However, in the north-western part of the system (outside the candidate area) the dilute groundwaters (<500 mg/L) reach important depths, even below the repository depth plane. This deep input of meteoric waters is also seen in the SE limit of the candidate area.

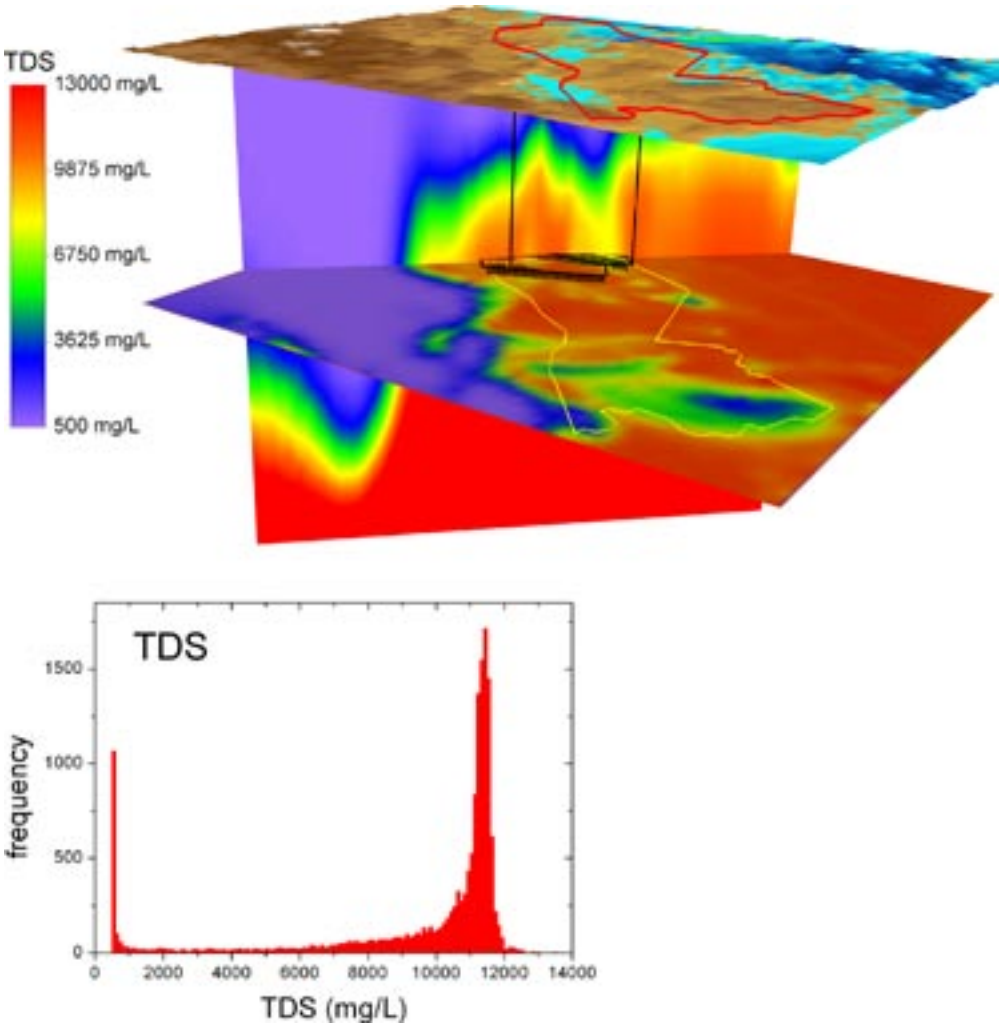

Figure B-1. *Calculated TDS at the Forsmark site. Upper panel: Horizontal and vertical cross sections colour-coded with respect to the TDS content. Left panel: Frequency histogram showing the concentration variability on a horizontal plane at repository depth (400 m) as shown in the figure above.*

Looking at the frequency histogram showing the variability at the repository depth two main groups of values are shown, one dilute (500 mg/L, out of the repository zone in the candidate area; Figure B-1) and the other brackish (11.5 g/L), clearly below the corresponding safety limit for the buffer, which is around 100 g/L (1.7 M).

B.2.2 Calcium

Calcium concentrations at Forsmark (Figure B-2) increase with depth but quicker towards the coast (NW-SE direction). In fact the influence of the meteoric waters is higher in the NW part of the system as it can be seen by the deeper input of dilute waters (already evident in the TDS plot). In general this plot shows a high variability of concentrations at repository depth. But looking at the frequency histogram of Ca concentrations at repository depth (Figure B-2) all the values are higher than 1 mM, and the maximum frequency is around 3.5 mM, clearly above the safety limit.

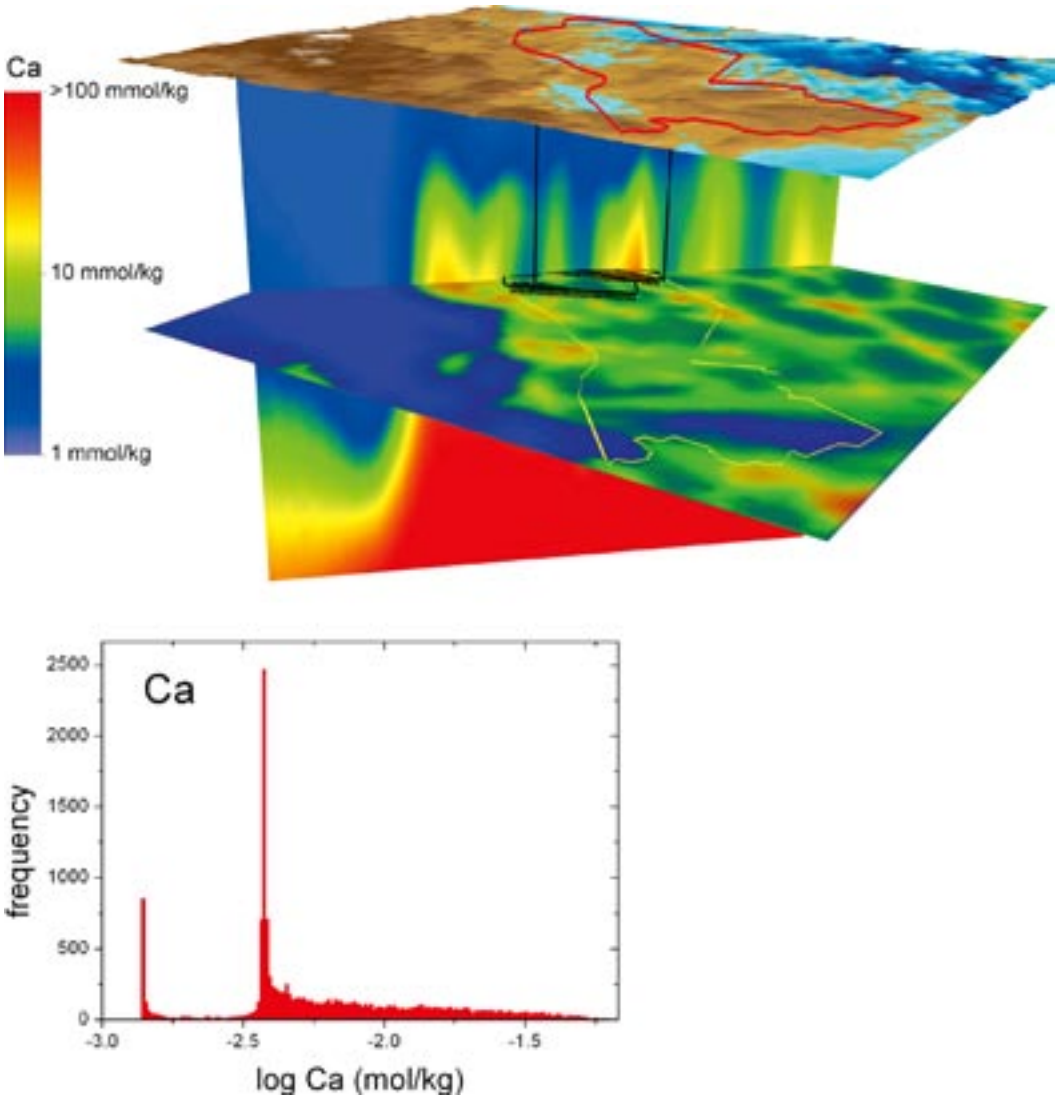

Figure B-2. *Calculated Ca contents at the Forsmark site. Upper picture: Horizontal and vertical cross sections colour-coded with respect to the present-day concentration of calcium (in logarithmic scale). Left panel: Frequency histogram showing the concentration variability (in log scale) on a horizontal plane at repository depth (400 m) as shown in the figure above. See the introduction for more explanations.*

B.2.3 pH and bicarbonate

For pH and bicarbonate, the mixing and reaction calculations are dominated by the precipitation and the dissolution of calcite (which is imposed in the model). The results are summarised in Figure B-3. The figure shows a distribution of bicarbonate very similar to the one shown by calcium (Figure B-2) but with the opposite depth-dependence: instead of increasing, it clearly decreases with depth. Values around 1.8 mM are common at the repository depth, as the frequency histogram shows.

pH also shows a slight increase with depth but with a narrower range of variability (7.4 to 7.9) from the surface to below the repository depth. In fact, the frequency histogram at repository depth points to this two values as the more frequent at that depth. Only deeper groundwaters have pH higher than 8, corresponding to that of the Deep Saline end-member. However, although in general pH values in the north-western part of the system show also the effect of a deeper input of meteoric waters, there is a N-S oriented vertical lens just outside the candidate area with the lowest pH values (6.75 to 7.25; blue colours in the medium panel of Figure B-3).

In the upper parts of the modelled domain meteoric waters dominate; they are relatively acid (pH < 7.4) and have high bicarbonate and CO_2 content (not displayed here). These meteoric waters are slightly undersaturated with respect to calcite (imposed by the model) and this mineral will therefore dissolve, as it is present in fracture fillings (Figure B-4). As a result, pH and Ca increase. Deeper down, waters have already reached equilibrium with calcite and when they mix with deeper Ca-rich groundwaters calcite precipitates due to over-saturation. The calculated amount of dissolved and precipitated calcite (mass transfer) for present-day conditions is shown in Figure B-4. Mass transfers are quite small, in absolute value less than 2×10^{-4} mol per litre of groundwater (see the frequency histogram)[20].

B.2.4 Potassium

Potassium concentrations are generally low in the groundwaters sampled at Forsmark and two main processes have been proposed to explain these low values: solubility control by sericite /Nordstrom et al. 1989/ and cation-exchange. None of them have been considered in SR-Can calculations; however, even if the exact mechanism is not known, all available groundwater data indicate that the increased infiltration of meteoric waters will not increase the present concentration of potassium (see Appendix C, dilution scenarios).

Potassium concentrations calculated in “only mixing” simulations are below 4 mM for the whole 3D area and lower than 3 mM for the slice at the repository depth (see frequency histogram, Figure B-5) which fits with the safety criterion “the lower the better” to avoid illitisation of the buffer.

B.2.5 Redox system

A fundamental requirement in the safety issues is that of reducing conditions. A necessary condition is the absence of dissolved oxygen, because any evidence of its presence would indicate oxidising conditions. The presence of reducing agents that react quickly with O_2, such as Fe(II) and sulphide, is sufficient to indicate reducing conditions. SR-Can results with respect to three parameters, the redox potential (pe or Eh), and the contents of Fe^{2+} and S^{2-} are summarised here. As it is the case for potassium, there are no quantitative requirements for these three parameters, only “the lower, the better”.

[20] The mass transfer values must be treated with caution. They are calculated from the prescribed mixing proportions for the four end members and re-equilibrium with calcite. In the real system mixing events are developed in successive steps with re-equilibrium stages between them. The effects of these simultaneous or successive mixing processes over the non-lineal behaviour of calcite saturation index must be explored.

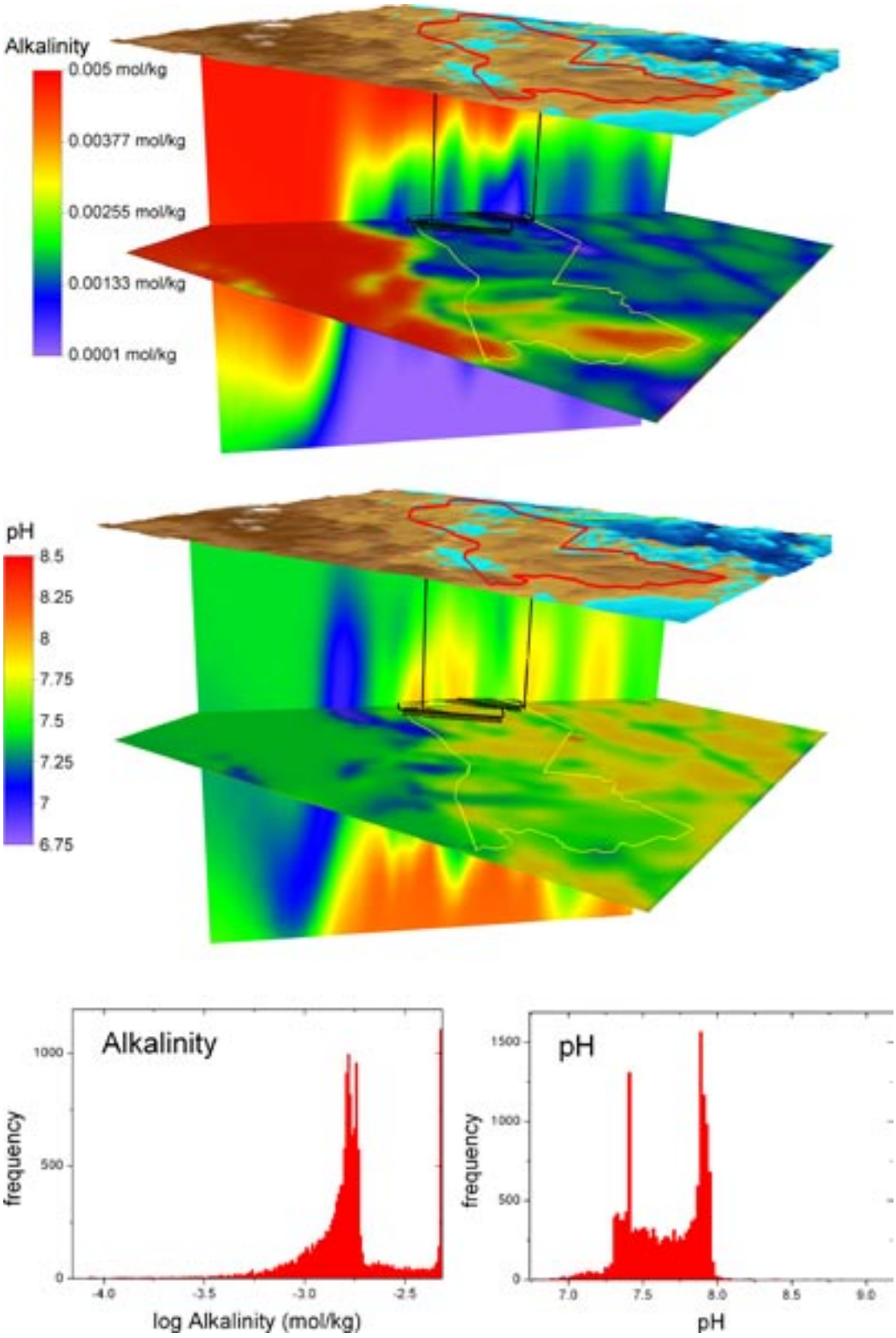

Figure B-3. *Calculated Alkalinity concentration (upper panel) and pH (medium panel) at the Forsmark site. The frequency histograms for both parameters are also shown in the lower part of the plot.*

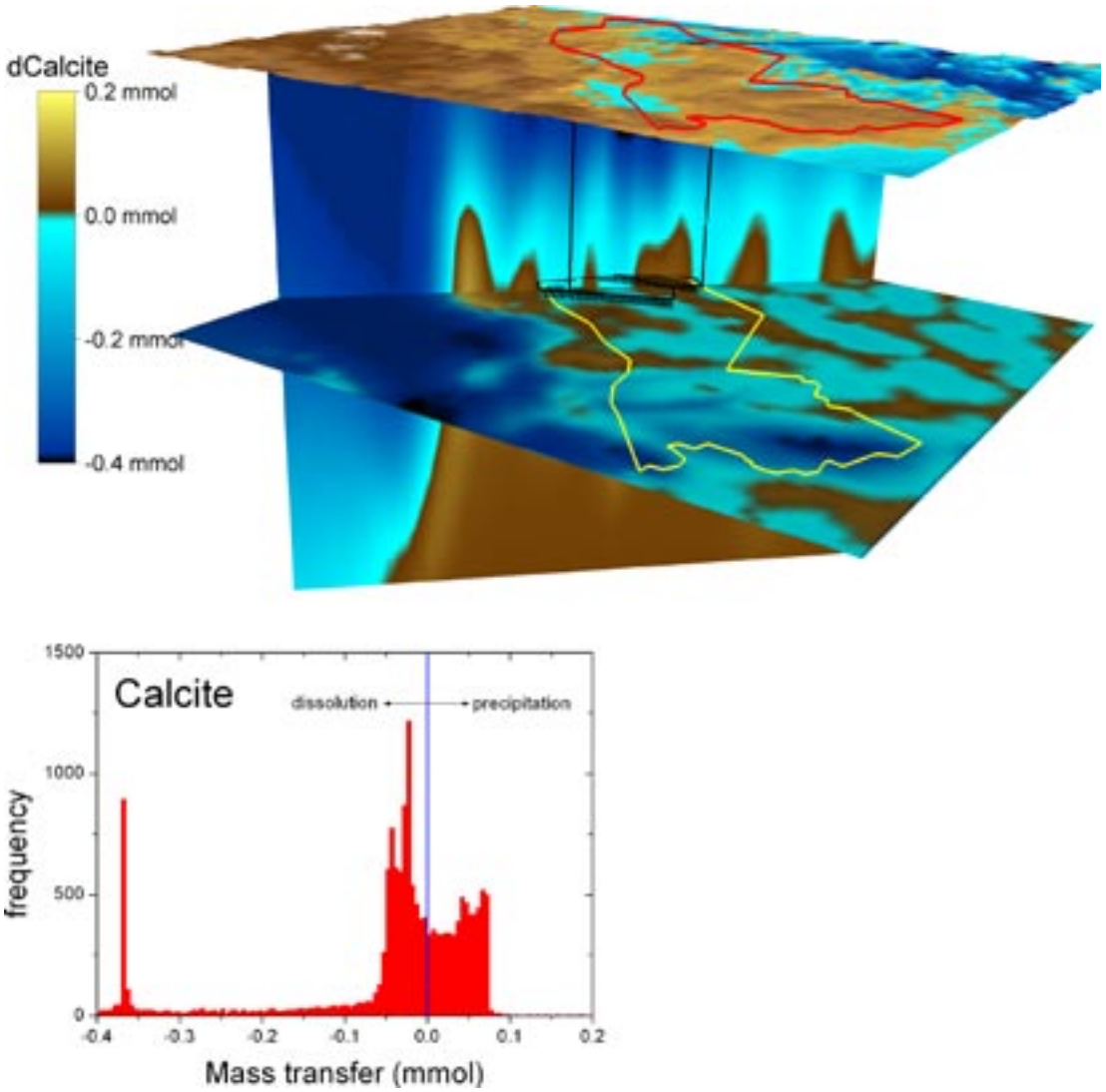

Figure B-4. *Calculated amounts of dissolved and precipitated calcite (mass transfer) for present-day conditions at Forsmark site. Upper panel: Horizontal and vertical cross sections colour-coded. Left panel: Frequency histogram of the mass transfer variability on a horizontal plane at repository depth (400 m) as shown in the figure above.*

SR-Can calculations include equilibrium with the iron(III) oxy-hydroxide ($Fe(OH)_{3(hematite\_Grenthe)}$) proposed by /Grenthe et al. 1992/ or an alternative model including equilibrium with recently precipitated (amorphous) iron(II) sulphide $FeS_{(ppt)}$ instead. When imposing equilibrium with an iron oxyhydroxide, two alternative options were also evaluated allowing or not redox equilibrium between sulphate and sulphide (referred as "coupled" and "un-coupled" database in /Auqué et al. 2006/, respectively). Results coming from the three different alternatives are shown here only when very different results have been observed.

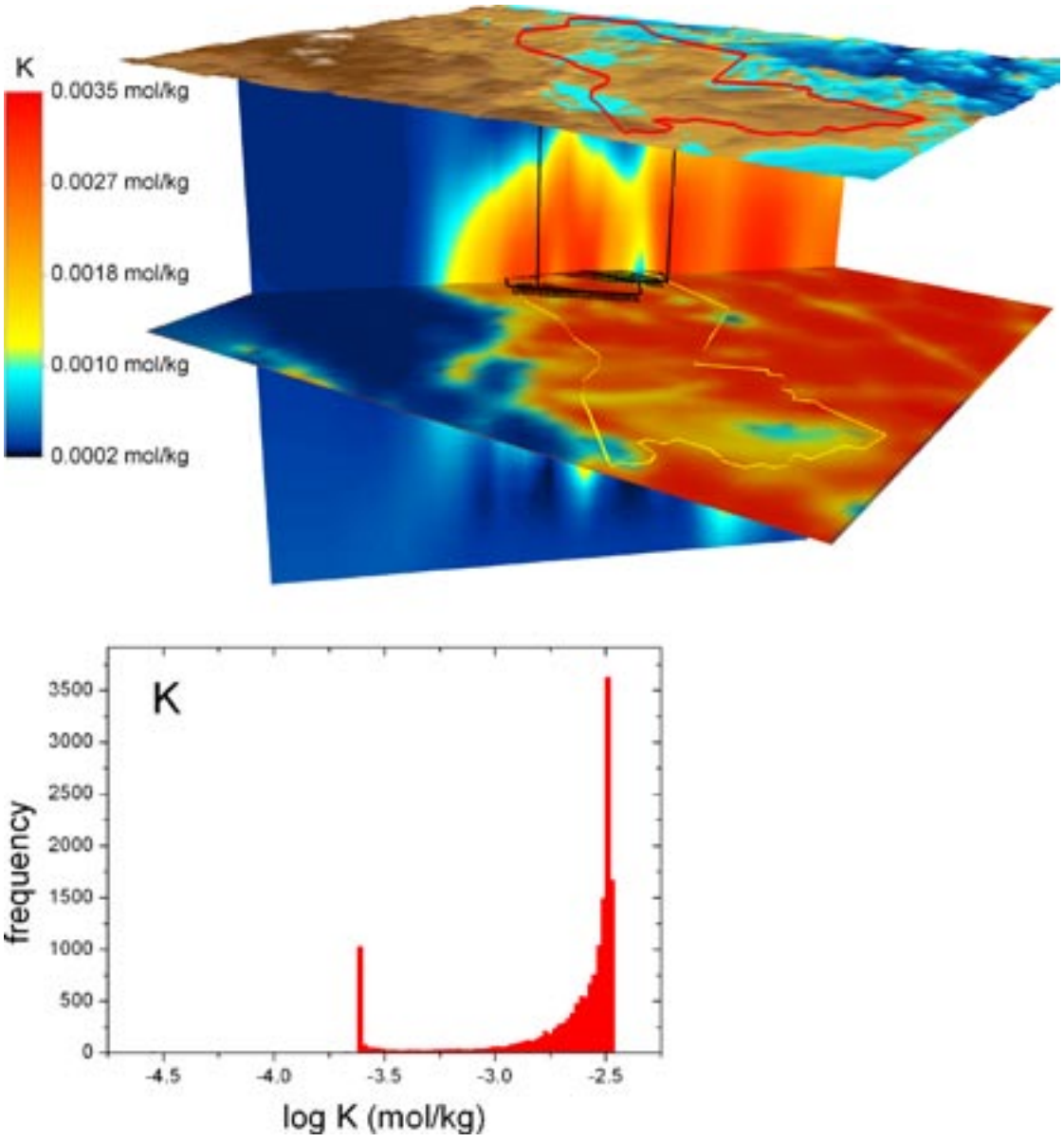

Figure B-5. *Calculate potassium concentration at the Forsmark site. Upper panel: Horizontal and vertical cross sections colour-coded with respect to the concentration of potassium. Left panel: Frequency histogram showing the concentration variability on a horizontal plane at repository depth (400 m) as shown in the figure above.*

pe

The first interesting observation in Figure B-6 is that, in spite of a very similar distribution of values, the values themselves are quite different depending on the mineral phase considered to be in equilibrium (iron oxyhidroxides in the upper panels and FeS in the lower left panel) and, mainly, whether redox equilibrium between sulphate and sulphide is allowed or not (differences between the left and right upper panels).

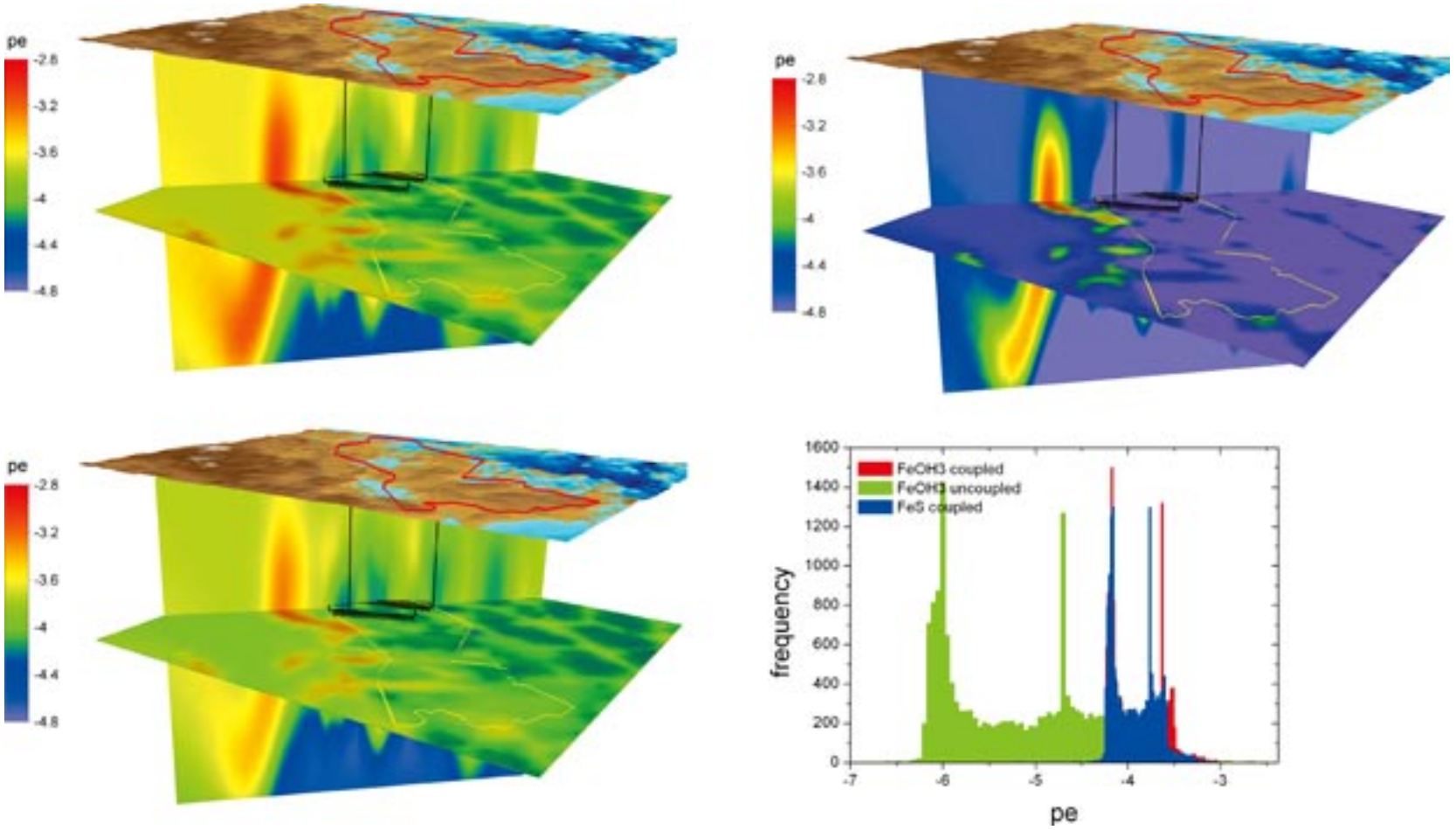

Figure B-6. *Calculated redox potential (pe) at the Forsmark site. Upper panels show the results using the iron oxyhydroxide for the mineral equilibrium calculations allowing (left) or not (right) the equilibrium between sulphate and sulphide. Lower left panel shows the results of equilibrating the waters with FeS with the same coupled data base as the plot just above. Lower right panel: Frequency histogram showing the pe variability on a horizontal plane at repository depth (400 m) as shown in the other panels.*

The highest calculated pe values are obtained assuming equilibrium with either $Fe(OH)_{3(hematite\_Grenthe)}$ or $FeS_{(ppt)}$ and using the "coupled" database. Both distributions are very similar although the highest pe values are found equilibrating with the iron oxyhydroxide (see also the red and blue frequency histograms in the lower left panel).

The lowest pe values (and therefore more desirable from a safety point of view) are those obtained when the redox potential is controlled by the $Fe(OH)_3/Fe^{2+}$ couple, in particular at pH > 7.5 (see Figure B-3), for the "un-coupled" database (green frequency histogram).

Because of the correlation between calculated redox potentials and pH, the pe distribution pattern is very similar to the one observed for pH (Figure B-3), with the areas with lower pH, which are a consequence of calcite precipitation, corresponding to areas with the highest calculated Eh. The presence of the deep meteoric input in the NW part of the system, and the lens-shaped volume of low pH values, is clearly seen in all the pe plots, indicating a less reducing environment.

Iron and sulphide

The sulphur and the iron systems are the two main redox systems identified in previous studies and operating in the Swedish groundwaters.

The concentration of Fe^{2+} is regulated by a complicated set of reactions including the slow dissolution of Fe^{2+} silicates, the precipitation of Fe^{2+} sulphides, and the redox reactions (including the activity of iron reducing bacteria). The concentrations of ferric iron are in general negligible in granitic groundwaters, as the oxy-hydroxides of Fe(III) are quite insoluble and they precipitate quickly. Moreover, the work by /Grenthe et al. 1992/ indicate that measured Eh in different Swedish groundwaters are controlled by equilibrium situations with a crystalline Fe(III) oxyhydroxide. So, the equilibrium with this phase was assumed for the reaction modelling.

Maximum sulphide concentrations measured in the Forsmark groundwaters are lower than 0.9 mg/L and they are usually below the detection limit. Under oxidising conditions sulphide is quickly oxidised to sulphate and, under reducing conditions, dissolved Fe^{2+} is normally present and the maximum sulphide concentrations are regulated by the precipitation of Fe(II) sulphide. So, equilibrium with this phase was assumed for the reaction modelling.

The results for the two redox-sensitive groundwater components analysed here, total dissolved iron and sulphide, are illustrated in Figures B-7 and B-8. As in the case of the redox potential, they also show a large variation of Fe^{2+} and S^{2-} values (10^{-7} to $10^{-4.5}$ for ferrous iron, and $10^{-6.5}$ to $10^{-4.5}$ for sulphide). This large variation probably reflects the effect of several processes on components that have low concentrations: small changes have a large impact on the final concentration. Microbial processes in particular are expected to greatly influence the concentrations of both.

The lowest Fe^{2+} values are obtained when equilibrating with the iron phase, mainly when redox equilibrium between sulphate and sulphide is allowed (Figure B-7, upper right panel; see also the frequency histogram). These values are lower than the ones measured at the site which is probably due to the fact that this model is the most conservative in giving the highest Eh values and the lowest reducing capacity, i.e., lowest Fe(II) content. Then, the highest ferrous iron values are found when equilibrating with the monosulphide or with the iron oxyhydroxide but allowing equilibrium between sulphate and sulphide (see frequency histogram).

With respect to sulphide, the results obtained assuming equilibrium with Fe(III) oxy-hydroxides give a broad range of calculated sulphide concentrations (Figure B-8 upper panel). Equilibrium with FeS(ppt) gives a narrow range but with higher values than those from the other model and covering the maximum concentrations analysed in the present-day groundwaters at Forsmark (with a value of $10^{-4.5}$ M).

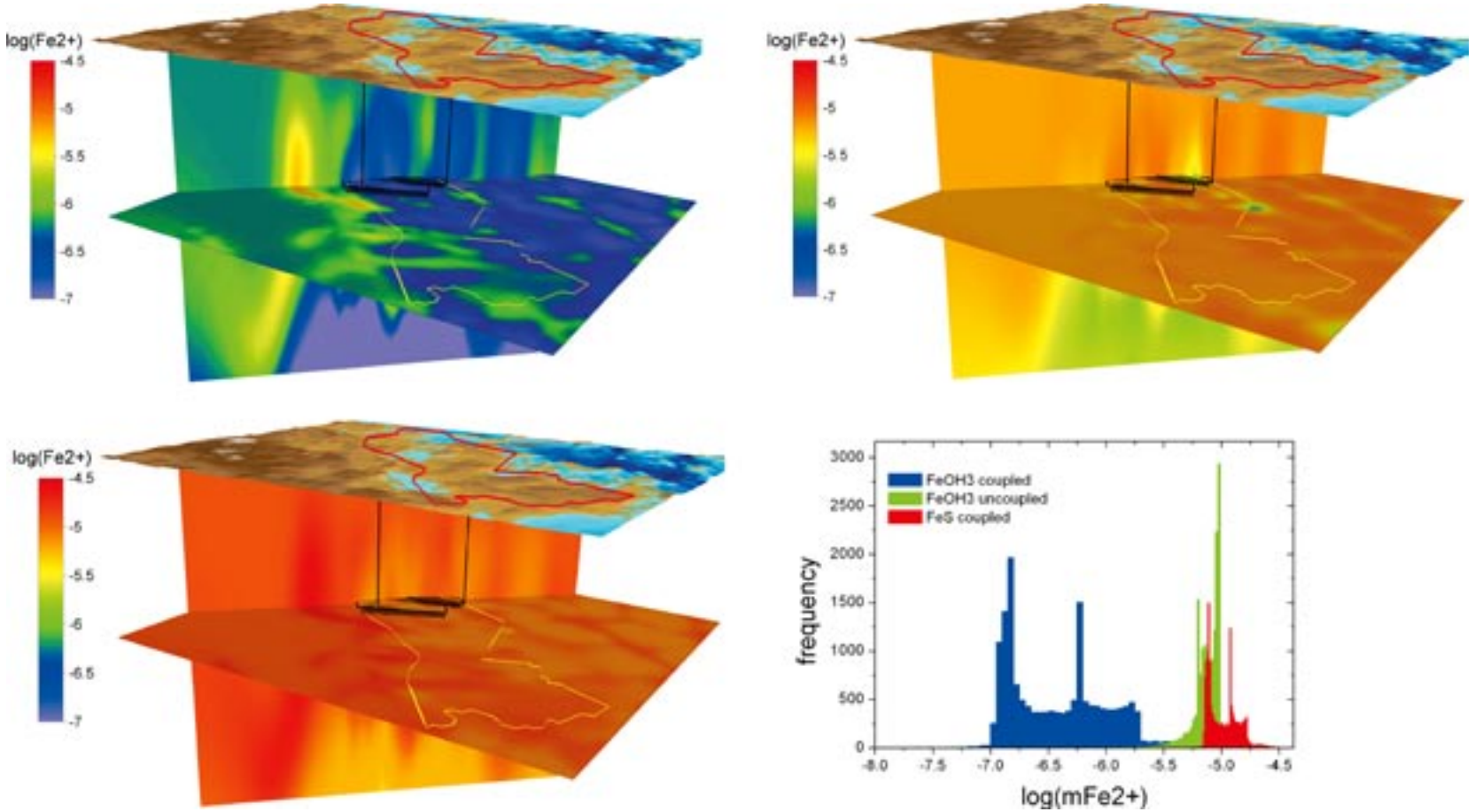

Figure B-7. *Calculated Fe^{2} contents at the Forsmark site. Upper panels show the results using the iron oxyhydroxide for the mineral equilibrium calculations allowing (left) or not (right) the equilibrium between sulphate and sulphide. Lower left panel shows the results of equilibrating the waters with FeS with the same coupled data base as the plot just above. Lower right panel: Frequency histogram showing the Fe^{2+} variability on a horizontal plane at repository depth (400 m) as shown in the other panels.*

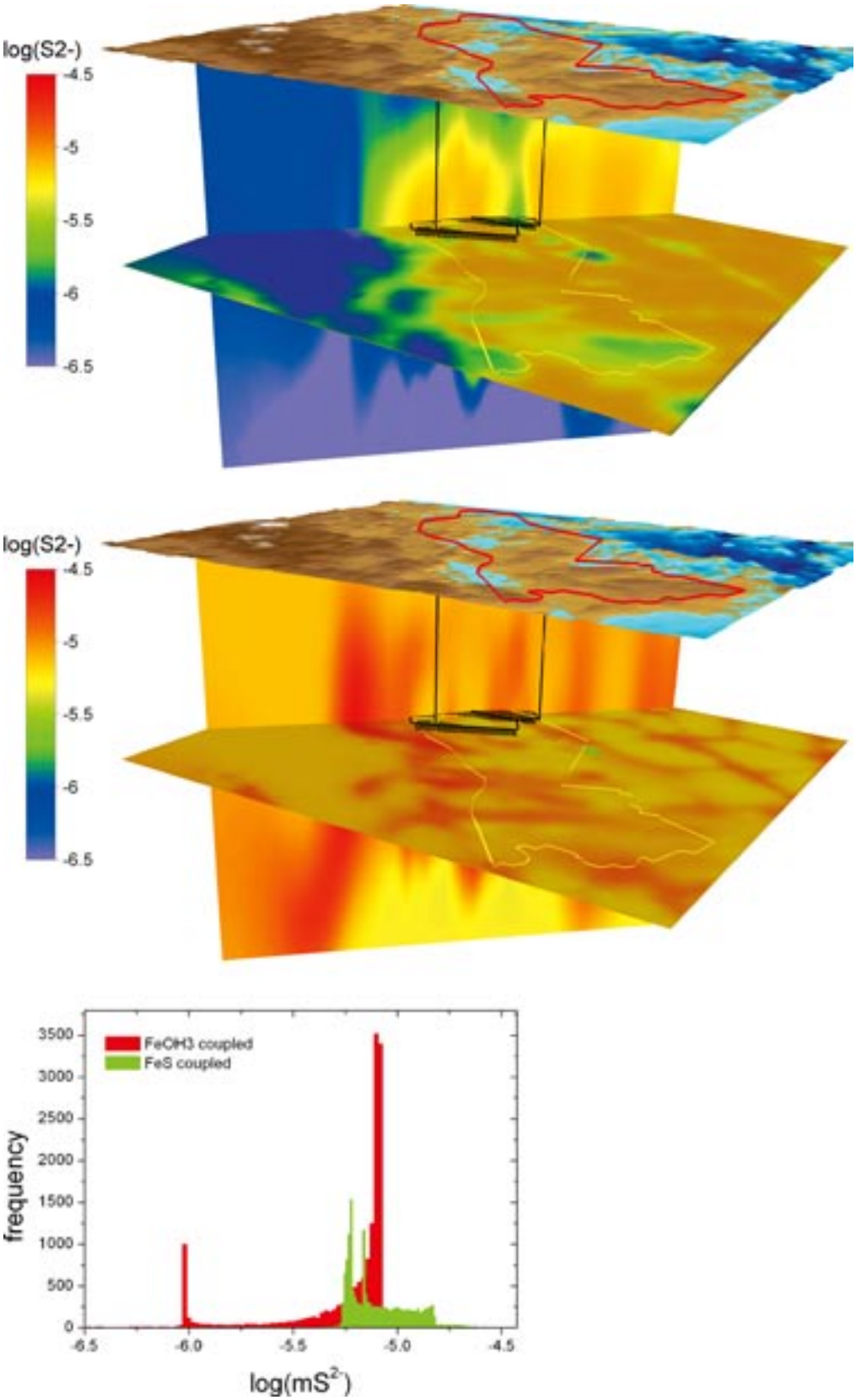

Figure B-8. *Upper and medium panels: Horizontal and vertical cross sections colour-coded with respect to the concentration of dissolved sulphide (in logarithmic scale). The horizontal plane is at 400 m depth and the vertical plane is perpendicular to the coast. The differences between the upper and the middle plots are the results of equilibrating the waters with $Fe(OH)_3$ or with FeS, respectively Left panel: Frequency histogram showing the concentration variability on a horizontal plane at repository depth (400 m) as shown in the figure above.*

Discussion

Among the variables required to define the geochemistry of groundwaters, the redox potential (Eh or pe) has been difficult to characterize and to model. Often disequilibrium among the different dissolved redox pairs is found in natural waters /Lindberg and Runnells 1984, Stefansson et al. 2005/ and an overall Eh value for a groundwater is often impossible to assign /Thorstenson 1984, Nordstrom and Munoz 1985, Langmuir 1997/. On the other hand, concentrations of redox elements are mainly dependent on the microbiological and mineralogical reactions and less on the mixing processes occurring in the studied system. In modelling terms, these concentrations will be very sensible to the equilibrium assumptions used in the simulations.

The different "redox alternatives" used in the simulations essentially pretend to obtain "indicative" Eh values and a range of predicted Fe^{2+} and S^{2-} concentrations to compare with the available data.

Assuming equilibrium with the crystalline $Fe(OH)_{3(hematite\_Grenthe)}$ and using the uncoupled database (redox equilibrium between sulphate and sulphide in solution is not allowed), the obtained redox potentials are more reducing (usually lower than –270 mV) than those measured in the system, and the predicted iron concentrations are lower than 0.6 mg/L.

If redox equilibrium between sulphate and sulphide in solution is allowed, the predicted Eh values are between –210 and –260 mV, Fe^{2+} concentrations are lower than 0.1 mg/L and S^{2-} concentrations lower than 0.2 mg/L. If the redox system is controlled by the equilibrium with amorphous monosulphides (therefore, assuming the existence of SRB activity in the system) the predicted Eh values are between –205 to –240 mV, Fe^{2+} concentrations vary from 0.3 to 1 mg/L, and S^{2-} from 0.06 to 0.5 mg/L. From these results two main conclusions can be extracted:

- Allowing or not homogeneous redox equilibrium (e.g. equilibrium between dissolved sulphate and sulphide) has important consequences in the predicted Eh values. The importance of these effects in the measured Eh values must be explored.
- The predicted ranges in Eh values and Fe^{2+} and S^{2-} concentrations are in general agreement with those measured in the system. The most significant differences are some notably higher Fe^{2+} concentrations and measured Eh values in the range from –140 to –200 mV. None of the simulated values cover this interval, indirectly supporting the existence of perturbations in the pristine conditions during drilling and sampling.

Finally, it must be taken into account that all the indicated results correspond to simulations where a single redox equilibrium is imposed on the whole system. In the real system, all redox buffers can be working in different parts depending on mineralogical and microbiological peculiarities. But, even so, the total chemical variability in the redox parameters seems to be reasonably covered by the considered equilibrium assumptions.

B.3 Conclusions

As part of the SR-Can assessment hydrogeological results obtained by /Hartley et al. 2006/ with CONNECTFLOW were coupled with a mixing and reaction-path simulation using PHREEQC on a rock volume that represent the whole regional area of Forsmark. Results of this coupling for the present situation can be used to address the conceptual 3-dimensional variability in the hydrochemical data derived from the present integrated knowledge on the system.

All key chemical suitability parameters for groundwaters have been considered in this section, mainly at the repository level. The modelled salinity, pH, Ca, HCO_3^- K and redox values are variable and heterogeneously distributed at the repository depth but all of them fulfil SKB's safety criteria even in the extrapolated results for unexplored volumes of the candidate area.

The total chemical variability observed in the system is covered by the predicted results and the 3D spatial distribution patterns of TDS, Ca, HCO_3^- and K concentrations are in qualitative agreement with the hydrochemical traits presently known in the system. This is not strange

as the hydrogeological site model /Follin et al. 2005, Hartley et al. 2005/ was calibrated by comparing the calculated mixing proportions, salinities and $\delta^{18}O$ values with the corresponding data measured at the site as well as with the mixing proportions calculated with the M3 code /Laaksoharju et al. 1999, Gómez et al. 2006/.

But the model also shows the existence of a high degree of complexity in the detailed distribution patterns of these parameters, with lenses, digits, etc in the 3D domain. And most important, some of these distribution patterns (e.g. for pH and Eh) only arise from the coupling with geochemistry as they are mainly controlled by reactions and not by mixing.

Obviously, this modelled spatial variability must not be confused with the "field" variability, represented by the present, more limited available hidrochemical data, some of which were used to calibrate the hydrogeological models. The results presented here are only a model, but it is the first integrated hydrological and geochemical model for the state of the system at present.

The coupled approach used here integrates very different types of data, assumptions and uncertainties from different disciplines in an unique view that allows addressing their final consequences on the spatial hydrochemical variability. Moreover, they predict geochemical values in unexplored volumes of the system, providing the opportunity to empirically verify these predicted results.

On the other hand, for the next site descriptive modelling (SDM version 2.2), an update strategy and new concepts for groundwater flow modelling has been prepared /Follin et al. 2007/. Using the same coupled approach with these future hydrological results and comparing the new model with the one presented here, it could be possible to verify which data, assumptions or extrapolations are more critical to the final results and re-evaluate them. This iterative approach should be tried.

Appendix C

Concentration and dilution scenarios in Forsmark evolution and SKB suitability criteria

C.1 Introduction

C.1.1 Motivation and objectives

From the Consolidated Review Issues (CRI) in the INSITE/SIERG document, the UZ group was asked to evaluate SKB´s groundwater suitability criteria during dilution/concentration processes at the repository depth. The main objective was to estimate, using present hydrochemical data, how much disturbance can be allowed for groundwaters at repository depth and still meet SKB´s suitability criteria.One of the issues specifically related to dilution/concentration processes is the variation in the salinity of the resulting groundwaters. The salinity of the groundwater in contact with the repository should be neither too high nor too low. Moreover, the concentration of divalent cations must be higher than 1 mmol/L to minimize negative impacts on the buffer and backfill materials.

As dilution/concentration processes are tightly related to the paleohydrochemical and future hydrochemical evolution of the sites (through inputs of different saline/dilute waters in the system), these suitability criteria were already evaluated in the context of SR-Can by /Auqué et al. 2006/, mainly during the evolution of the temperate period in the next glacial cycle. The main results of that study are summarized here and some of them are expanded with new modelling results or field data.

Although dilution/concentration scenarios are related to mixing between two different groundwaters, water-rock interaction is always superimposed and, in specific circumstances (when one end-member is dominant), it is even the sole controller of the groundwater geochemical evolution. Among other chemical reactions, cation exchange processes (important reactions in dilution/concentration scenarios) have been studied in especial detail, as they were not included in the earlier geochemical modelling performed by /Auqué et al. 2006/.

The studied dilution/concentration scenarios are those identified and/or modelled in the context of SR-Can assessment. Two possible concentration scenarios have been examined: (1) upconing of saline groundwaters, and (2) input of freeze-out brines. Also, two possible dilution scenarios have been considered: (1) meteoric dilution and, (2) glacial melt-water dilution.

C.1.2 Groundwater requirements from a KBS-3 repository

The primary safety function of the KBS concept is to completely isolate the spent nuclear fuel within copper canisters over the entire period assessed, which is one million years in SR-Can. If a canister is damaged, the secondary safety function is to retard any releases from the canisters. The main chemical characteristics necessary to fulfil these two requirements (isolation and retardation) are detailed below.

Reducing conditions is a fundamental requirement related to the absence of dissolved oxygen that could lead to the corrosion of the canister. Furthermore, should a canister be penetrated, reducing conditions would be essential to ensure a low dissolution rate of the fuel matrix, to maintain low solubilities of some radioelements and, for some others, to favour sorption in buffer, backfill and host rock.

Salinity (ionic strength) must be neither too high nor too low. Groundwaters of high ionic strengths would have a negative impact on the buffer and backfill properties, in particular on the backfill swelling pressure and hydraulic conductivity.

The upper limit of tolerable ionic strength is however highly dependent on the material properties of these components and since, in particular for the backfill, alternative materials are to be evaluated in the assessment, no specific criterion is given in SR-Can /SKB 2006a/. In general, ionic strengths corresponding to NaCl concentrations of approximately 70 g/L (1.2 M NaCl) are a safe upper limit for maintaining backfill properties, whereas the corresponding limit for the buffer is around 100 g/L (1.7 M). These safe numbers can be used as reference until specific criteria will be proposed.

On the other hand, salinity must be high enough to allow that total concentration of divalent cations exceeds 1 mM ($\sum [M^{2+}] \geq 10^{-3}$ M) in order to avoid chemical erosion of buffer. This condition is also required to maintain ***low natural colloid concentrations*** (and to avoid transport of radionuclides mediated by colloids) as the stability of colloids is largely decreased if the concentration of divalent cations exceeds 1 mM.

pH values between 4 and 11 to assure buffer and backfill stability and to exclude chloride corrosion of the canister if low pH values appear in combination with high chloride concentrations (in these conditions, [Cl] < 3 M is also desirable).

Low groundwater concentrations of other detrimental agents to long-term stability of the canister, buffer and backfill. For example, dissolved sulphide (HS^-) can act as a corroding agent of the canister, although considerably higher concentrations than have ever been observed in Swedish groundwaters would be required. But, in any case, it is desirable to have low groundwater concentrations of sulphide (HS^-) specially in the rock volume surrounding the deposition holes. Moreover, low groundwater concentrations of other elements, like iron and potassium are desirable.

C.1.3 Reaction processes during dilution/concentration scenarios

As it has been widely studied in coastal aquifers, salinization and freshening processes involving waters of very different salinity may trigger different types of dissolution-precipitation, redox and, specially, cation-exchange reactions.

Exchange reactions are fast and can exert an important control on the major cationic composition of the groundwaters (/Drever 1997, Appelo and Postma 2005, Andersen et al. 2005/ and references therein). Cation exchange reactions may also be effective during the concentration and dilution scenarios studied here and they have been taken into account in inverse mass balance calculations for the site characterization program. But their inclusion in direct, predictive calculations has been hampered by the absence of some key parameters like site-specific selectivity constants or, most important, cation exchange capacity (CEC) values of the fracture filling minerals (e.g. clay minerals).

The total dissolved solids (TDS) or salinity of the solution exerts a major control on the selectivity of the exchangers for the different cations. During saline (e.g. marine) intrusions into more dilute groundwaters, monovalent cations (mainly Na^+) are selectively fixed to the exchangers whereas divalent cations (Ca^{2+} and Mg^{2+}) are released to the solution. The reverse process takes place during freshening (dilution). These trends have been widely observed both in natural systems and in laboratory experiments, independently of the type of exchangers present in the systems (/Drever 1997, Appelo and Postma 2005/ and references therein). These observations allow to advance that cation exchange will favour an additional increase (to that associated to the mixing process) in the total concentration of divalent cations during concentration scenarios, assuring the safety criteria ($\sum [M^{2+}] \geq 10^{-3}$ M) even more.

These effects mainly depend on the stoichiometry of heterovalent exchange reactions (or the exponents used in the corresponding mass action equations) and, therefore, they minimize the uncertainties associated to the absence of site-specific selectivity constants or that associated to the formal convention (e.g. Gapon, Vanselow or Gaines-Thomas conventions; /Appelo and Postma 2005/) used to model exchange reactions.

Additional heterogeneous reactions have been considered in the simulations performed in this Appendix. Calcite equilibrium (calcite dissolution-precipitation) and different redox phases have been considered to better constraint pH and Eh[21].

C.2 Increase in salinity at repository depth (concentration scenario)

High salinity groundwaters are ubiquitous at depth in the Fennoscandian Shield and different processes can promote their incursions at repository depths. As such, the origin and evolution of these saline groundwaters must form an integral part of the hydrogeochemical site characterisation /Smellie et al. 2006/.

A potential increase in salinity at repository depth during the reference long term evolution is associated either to upconing or to salt rejection processes. **Upconing** promotes the ascent of pre-existent deep and saline groundwaters to shallower levels. It has occasionally been observed at borehole scale at the Laxemar/Simpevarp and Fosmark sites /Smellie et al. 2006/ and it can be effective during permafrost conditions and even during the repository construction and operational phases. **Salt rejection** is a mechanism of formation of (new) near-surface saline waters that can operate during glacial events in association with permafrost development. When water freezes slowly, most of their solutes are not incorporated into the crystal lattice of the ice and they tend to accumulate at the propagating freeze-out front. Therefore, the freezing process can give rise to an accumulation of saline water ('freeze-out" brines) at the depth reached by the perennially frozen front. These saline waters tend to sink due to density contrasts, penetrating in the bedrock and mixing with the existing groundwaters at depth.

The main consequence of these possible highly saline groundwater incursions at repository levels can be the gradual deterioration of the buffer and backfill materials[22]. Thus, both processes (upconing and salt rejection) have been considered in the SR-Can assessment /Auqué et al. 2006/). Salt rejection and formation of near-surface 'freeze-out' brines have been especially reviewed. Although these "elusive" processes have been considered since the beginning of the hydrogeochemical site characterisation program (e.g. Forsmark 1.1 and Simpevarp 1.1; /SKB 2004ab/), the possible isotopic signatures of freeze-out brines have only recently been discussed /Smellie et al. 2006/.

C.2.1 Upconing of deep saline groundwater to repository depths

The possibility of upconing of deep saline groundwater to repository depths has been suggested during the excavation and operation phase /Svensson 2005, 2006/, during glacial periods (under an advancing warm-based ice-sheet; /Jaquet and Siegel 2006/) and during permafrost conditions /King-Clayton et al. 1997/.

Modelling results by /Svenson 2005, 2006/ for ***the excavation and operation phase*** indicate that the expected upconing of saline groundwaters is negligible.

During glacial periods, salinities up to ≈ 52 g/L TDS (or ≈ 1 M Cl^-) have been predicted by /Jaquet and Siegel 2006/ to locally reach the repository depth by upconing of deep saline waters in the Oskarshamn area (Figure C-1) These high-salinity conditions would last only a few centuries and most of the waters a few kilometres under the ice upper surface may have lower salinities, between 0.1 and 1%. These values are well below the upper safety limit for maintaining buffer and backfill properties.

[21] The evaluation of the redox processes and the redox buffer capacity during the dilution scenarios has not been performed here as it was an ongoing work by Enviros /Molinero et al. 2008/.

[22] Depending on the composition of these saline waters, they may represent also a potential source of dissolved sulphate which, through sulphate reducing bacteria activity, may produce sulphide that would promote, in turn, canister corrosion.

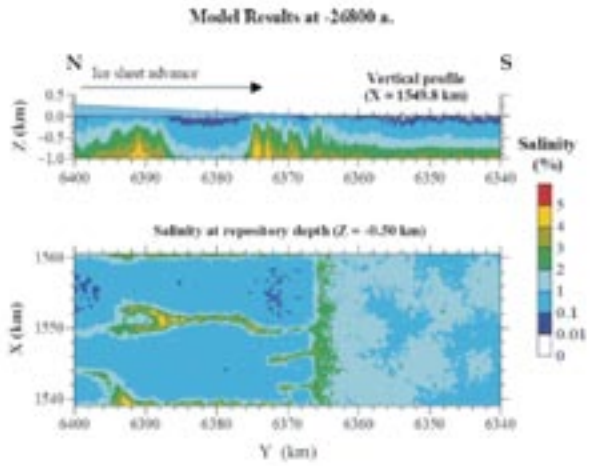

Figure C-1. *Contour plots showing the salinities of a site affected by an advancing ice sheet calculated using the model described by /Jaquet and Siegel 2006/. The plots are focused on the Oskarshamn area: the upper diagram shows a north-south depth profile centred at the site (vertically exaggerated), and the lower diagram a slice at 500 m depth.*

It can be shown from theoretical calculations with PHREEQC that the compositional characteristics of these groundwaters with salinities up to ≈ 52 g/L verify the rest of the safety criteria proposed by SKB. The detailed composition can be obtained by mixing calculations between the Deep Saline and the Glacial end-members until the prescribed salinity (52 g/L) is obtained. Simultaneous equilibration with calcite, chalcedony and several suitable redox minerals is also imposed to obtain more reliable Si, pH and Eh values.

The redox buffers considered for Eh estimation are (1) iron oxides-oxyhydroxides with different solubilities as deduced by /Grenthe et al. 1992/ and by /Banwart 1999/ in Swedish groundwater systems (in pristine or temporally O_2-altered conditions; see Section 3.5); and (2) sulphides (equilibrium with FeS or FeS_2) when sulphate reducing activity is present. Besides, the following redox initial conditions for the end-member waters have been imposed: for the Deep Saline end-member an Eh of −242 mV in equilibrium with the oxyhidroxide deduced for Swedish groundwaters by /Grenthe et al. 1992/; and for the Glacial end-member, an initial Eh controlled by equilibrium with microcrystalline $Fe(OH)_3$ (using solubility data from /Nordstrom et al. 1990/ Eh= −51 mV).

Cation exchange has not been included in these simulations. But it is well known that during saline intrusions into more dilute groundwaters monovalent cations are selectively fixed to the exchangers whereas divalent cations are liberated to the solution. Therefore, cation exchange would only produce an increase of divalent cations in solution and thus the results of these simulations are conservative.

Table C-1 gives the composition and the main physicochemical parameters of the modelled groundwaters. All waters fulfil SKB safety criteria. The obtained pH value is similar to those frequently found in the present groundwaters and the $\sum[M^{2+}]$ is much higher than the 1 mM limit prescribed to avoid chemical erosion or colloid formation from buffer and backfill.

In “mixing + reaction” calculations, equilibrium with calcite, chalcedony and different redox minerals is always imposed and the results are always reducing (around –250 mV) for all the considered alternative situations[23].

[23] Only if oxygen is allow to enter with the glacial end-member oxidizing conditions can be obtained.

Table C-1. Calculated compositions for the maximum salinity groundwaters reaching the repository depth by upconing during the glacial period. All the concentrations in mol kgw^{-1}. In the columns only the specific redox mineral used in calculations is indicated: $Fe(OH)_3$ G corresponds to the oxyhydroxide solubility deduced for the Swedish groundwaters by /Grenthe et al. 1992/; $Fe(OH)_3$ B represents the oxyhydroxide solubility deduced by /Banwart 1999/; FeS and FeS_2 correspond to equilibrium situations with respect to fresh precipitated monosulphides and pyrite, respectively.

	Only mixing	Mixing + reaction ($Fe(OH)_3$ G)	Mixing + reaction ($Fe(OH)_3$ B)	Mixing + reaction (FeS)	Mixing + reaction (FeS_2)
Temp. (ªC)	15.0	15	15	15	15
TDS	52	52	52	52	52
pH	8.387	8.04	8.16	8.15	8.04
Eh (mV)	–265	–244	–239	–258	–243
Alkalinity	7.4e–5	4.6e–5	4.6e–5	4.6e–5	4.6e–5
Cl	0.9	0.9	0.9	0.9	0.9
SO_4^{2-}	6.4e–3	6.4e–3	6.4e–3	6.4e–3	6.4e–3
Ca	0.32	0.33	0.33	0.33	0.33
Mg	6.0e–5	6.0e–5	6.0e–5	6.0e–5	6.0e–5
Na	0.25	0.25	0.25	0.25	0.25
K	5.7E–4	5.7E–4	5.7E–4	5.7E–4	5.7E–4
Si	1.7e–4	1.56e–4	1.56e–4	1.56e–4	1.55e–4
Fe^{2+}	–	6.6E–8	4.8e–6	5.95e–6	1.4e–13
S^{2-}	–	6.4E–7	1.2e–8	7.0e–6	5.6e–7

The highest predicted Fe^{2+} and S^{2-} concentrations (0.22 mg/L S^{2+} and 0.33 mg/L Fe^{2+}) are similar to the maximum concentrations found in the present groundwaters at Forsmark and below the maximum concentrations predicted for the temperate period /Auqué et al. 2006/.

The upconing of deep saline groundwater to repository depths ***during permafrost conditions*** is the last of the considered scenarios. It has not been hidrologically modelled but it may occur in the vicinity of permanent discharges such as some taliks. Such discharges mainly occur along more extensive conductive deformation zones, which are avoided in the repository design. However, it cannot be ruled out that saline waters may be transported through minor discharge zones to the repository area if the process occurs over long periods of time.

The most saline water sampled at Laxemar and Forsmark sites up to now is the sample selected as the Deep Saline end-member. It is in the limit of the safe values considered for the backfill but still well below the safe value for the buffer. Therefore, to increase salinities over the safety limits by the upconing processes, they should be more intense during permafrost conditions than what has been calculated for the glacial period. In any case, this process may require some further assessment to be conclusively ruled out.

C.2.2 Effects of freezing and salt rejection during permafrost conditions

Freeze-out processes in the permafrost can promote the formation of high density near-surface saline waters which may gradually sink, mix with the existing groundwaters at depth and, eventually, reach the repository. These processes were not considered relevant for the repository safety in SR-97 and, therefore, they were not taken into account in the safety assessment /SKB 1999/. However they have been considered in SR-Can (see the discussion in the geosphere process report, /SKB 2006c/) and in other generic calculations /Vidstrand et al. 2006/.

As stated before, these freeze-out processes have been considered in the conceptual model for groundwater evolution since the beginning of the hydrogeochemical site characterisation program but only recently some evidences of their presence at repository depths have been discovered using boron isotopes /Casanova et al. 2005, Smellie et al. 2006/.

In the reference evolution of the repository, it is estimated that the ground at Forsmark will be frozen to a depth of 50 m or more for around 30 percent of the time in the glacial cycle /SKB 2006b/. According to this scenario, the permafrost will not occur over a continuous period of time, but rather thawing will occur between more or less short periods of permafrost. Some of these permafrost periods will furthermore coincide with the time when the site is covered by an ice sheet, where "basal frozen" conditions prevail.

The effects of freezing-out during permafrost conditions have not been estimated yet in the Forsmark area. However, /Vidstrand et al. 2006/ have performed preliminary calculations on the effects of a high salinity pulse associated to freezing-out during permafrost conditions for the Laxemar-Simpevarp site. The evolution of this pulse was simulated at a regional scale, and the main results, reviewed and discussed in /Auqué et al. 2006/, are summarized here.

The salinity of the out-frozen waters was estimated by /Vidstrand et al. 2006/ assuming that, before the onset of the permafrost, the salinity distribution is linear from zero at the surface to 1.5% at 300 m depth. At the start of the simulations it was assumed that the frozen front had instantaneously reached 300 m depth and that the groundwater in a 10 m thick layer under the frozen rock had a salinity of ≈ 22%, which approximately represents the sum of all the available salt within the overlying 300 metres. This value corresponds to a groundwater with ≈ 4.2 M Cl, three times higher than the contents found in the Deep Saline end-member (the most saline groundwater sampled in the Laxemar and Forsmark sites).

At the beginning of the simulation, this highly saline 10 m thick layer is located on top of groundwaters having a salinity increasing from ≈ 1.5% (at the bottom of the permafrost) to 10% at 2,000 m depth, which is the bottom boundary of the model. The DarcyTools model was used on the Laxemar-Simpevarp site with the boundary conditions and site properties taken from the site description model SDM v.1.1.

The model calculations show that saline waters are practically immobile in the less conductive portions of the rock (outside fracture zones) during the simulated time-scale (300 years). In contrast, saline waters generated in the deformation zones will move to deeper regions due to gravitational effects in periods shorter than 300 years. In these highly conductive parts, the salinity peak at repository depth may be for a few years as high as 9% (corresponding to a groundwater with ≈ 1.6 M of Cl). This value would slightly overpass the upper safety limit for maintaining backfill properties, although it would remain below the safety limit for the buffer. However, it must be taken into account that several assumptions in these simulations can be magnifying the amount of the out-frozen salt reaching the repository:

- Permafrost formation and salt exclusion in the simulations are pessimistically assumed to take place instantaneously and homogeneously to a given depth for the whole modelled site, releasing highly saline groundwater immediately under the frozen rock (the evolution of saline waters under permafrost is performed independently of the modelling of the advance of permafrost conditions).
- The effects of regional flow fields (or the effect of taliks on the hydrological conditions at repository depth) have not been taken into account in the calculations. However, regional groundwater flows can be responsible for a "flushing" of saline waters, yielding a less saline situation in the sub-surface /Vidstrand et al. 2006/.
- The concentration of the out-frozen waters has been estimated assuming that, before the onset of the permafrost, the salinity distribution is linear from zero at the surface to 1.5% at 300 m depth. From the results obtained for the evolution during the temperate period /Auqué et al. 2006/ this seems to be an overestimation, as the groundwaters at the sites will become gradually more diluted before the start of the permafrost. Therefore, a more realistic estimate of the concentration of the saline waters out-frozen from the top 300 m and distributed into a 10 m thick layer would be ≈ 2% (≈ 0.34 M Cl^-) instead of 22% /Auqué et al. 2006/.

The calculations are so far quite generic and several factors remain to be investigated. However, they illustrate the feasibility of the downward movement of a saline pulse associated to freeze-out due to density effects reaching the repository depth (400 m).

Freeze-out scenarios may be relevant for the safety assessment and must be explored and refined in site-specific hydrological models. Theoretical calculations may be used to approximate a probable (but detailed) chemical composition for these freeze-out brines, since there are no remnants of these type of waters in the sites.

C.2.3 Discussion

Two possible scenarios with increments in salinity at the repository depth have been examined: (1) upconing, and (2) salt rejection and generation of freeze-out brines associated to permafrost conditions.

The possibility of upconing of deep saline groundwater to repository depths during the excavation and operation phase, and during glacial conditions (under an advancing warm-based ice-sheet) has been examined. Modelling results by /Svensson 2005, 2006/ obtained for the excavation and operation phase indicate that the expected upconing of saline groundwaters is negligible.

Salinities up to ≈ 52 g/L TDS (or ≈ 1 M Cl^-) have been predicted by /Jaquet and Siegel 2006/ to locally reach the repository depth by upconing of deep saline waters during glacial periods in the Oskarshamn area. This salinity value is well below the considered safety limits for maintaining backfill (up to 70 g/L) and buffer (up tp 100 g/L) properties. Geochemical calculations performed here for these saline waters reaching the repository level indicate that they easily fulfil the rest of the safety function indicators: $\sum[M^{2+}] > 1 \cdot 10^{-3}$ mol/L, reducing conditions, pH around 8 and low dissolved S^2.

Groundwaters with salinities up to 75 g/L TDS have been sampled at >1,500 m depth in the Swedish basement. 75 g/L TDS is in the limit of the safe values considered for the backfill but still well below the safe value for the buffer. Unusually intense upconing processes would be needed to push these deep brines up to repository depths and, therefore, upconing is not expected to increase the groundwater salinity to levels high enough to deteriorate the properties of backfill and buffer. In any case, this process may require some further assessment to be conclusively ruled out.

Model results and field data seem to indicate that salinity pulses associated to the sinking of shallow freeze-out brines generated during permafrost conditions can reach at least repository levels. Model calculations performed by /Vidstrand et al. 2006/ show that saline waters generated in the deformation zones may move to deeper regions due to gravitational effects in periods shorter than 300 years. In these highly conductive parts the salinity peak at repository depth may be as high as 9% for a few years (corresponding to a groundwater with ≈ 1.6 M of Cl, in the limit of the safe values for the buffer and backfill materials).

The very uncommon high $\delta^{11}B$ values found in some groundwaters of the studied sites (and in other groundwaters from the Fennoscandian Shield; /Casanova et al. 2005/) may represent freeze-out waters extending to depths greater than 500 m. Boron isotopes are, up to now, the best tool to discriminate this elusive effect. However, both the tool and its results need further verification. If the present interpretation of the anomalous $\delta^{11}B$ enrichments were incorrect, an alternative process to explain those values should be found.

For all these reasons, freeze-out scenarios should be explored and refined in site-specific hydrological models to evaluate the transient effects of the saline pulses eventually reaching the repository depth. Moreover, theoretical calculations should be used to approximate a probable (but detailed) chemical composition for these freeze-out brines.

C.3 Dilution processes at repository depth

Two main dilution scenarios can be identified during the future evolution of the repository zone at Forsmark: (1) the influx of upper bedrock-derived meteoric groundwater at the repository depth (when isostatic rebound move the Baltic shoreline away from the site), and (2) the ingress of glacial melt-water during the future climatic change.

In both cases, the influx of these dilute waters will be particularly important in the high transmissivity rock volumes. In the less transmissive rock volumes where the repository will be constructed, the effects of the incoming dilute waters may be diminished but cannot be excluded. Therefore, both meteoric water and glacial melt-water scenarios must be addressed.

The hydrodynamic evolution during the temperate period (input of meteoric waters) was coupled to geochemical calculations by /Auqué et al. 2006/ to obtain the evolution of the groundwater composition. Here this modelling tasks has been enlarged to include cation exchange reactions and to deal with some of the uncertainties detected by /Auque et al. 2006/ mainly related to the expected Ca^{2+} and Mg^{2+} concentrations during the meteoric dilution scenario.

For the remaining of the reference glacial cycle the hydrodynamic modelling is non site-specific, and the focus in SR-Can has been to estimate the importance of reactions between fracture-filling minerals and intruding glacial melt-waters /Auqué et al. 2006/ and references therein). More detailed calculations can not be made until site-specific modelling for this period is performed and therefore, this scenario is not presented here. In any case, some of the general conclusions obtained with the meteoric dilution scenario can be extrapolated to the glacial scenario.

C.3.1 Dilution process during the temperate period

The hydrogeological evolution during the temperate period (until the beginning of assumed permafrost conditions in 9000 AD) was performed by /Hartley et al. 2006/ for the Forsmark site (based on Site Description Model version 1.2) using ConnectFlow. Expected displacements of the Baltic shore line and changes in annual precipitation were included in the prediction of the future hydrological evolution.

Transport of fractions of selected component waters (meteoric, marine, glacial and deep saline) was used as a method to handle variable density flow and the modelled proportions of component waters (i.e. mixing proportions) at each spatial coordinate and time step was also used to calculate the groundwater salinity. Model results are available at specific times: years 2020, 3000, 4000, 5000, 6000, 7000, 8000 and 9000 AD.

During the temperate period after repository closure, groundwaters will be affected by increasing amounts of waters of meteoric origin. Figure C-2 displays the calculated distribution of the meteoric end-member at the repository depth for five time steps. As shown, meteoric groundwaters gradually penetrate as the shore line is slowly displaced towards the upper-right corner of the modelled domain. This leads to a decrease in salinity. Towards the end of the modelled period, over 73% of the groundwaters at Forsmark have less than 1 g/L of dissolved salts at repository depth /Auqué et al. 2006/.

The hydrological results show that, at around 3000–4000 AD, the repository level will undergone a major hydrological change and meteoric groundwaters in proportions from 90 to 100% will dominate the candidate area. At this time, the shoreline will move away from the vicinity of the repository, head gradients will be significantly modified, and the flow field around the repository area would undergo major changes /Hartley et al. 2006/.

The flow pattern in the candidate area is quite complex due to sharp changes in hydraulic properties between the very tight rock in the candidate area and the more conductive rock mass outside. This situation favours the existence of a heterogeneous zone in the northwest corner of the candidate area, with a high variability in dilute groundwater penetration, even at 9,000 AD (from less than 10% to almost 80%; Figure C-2).

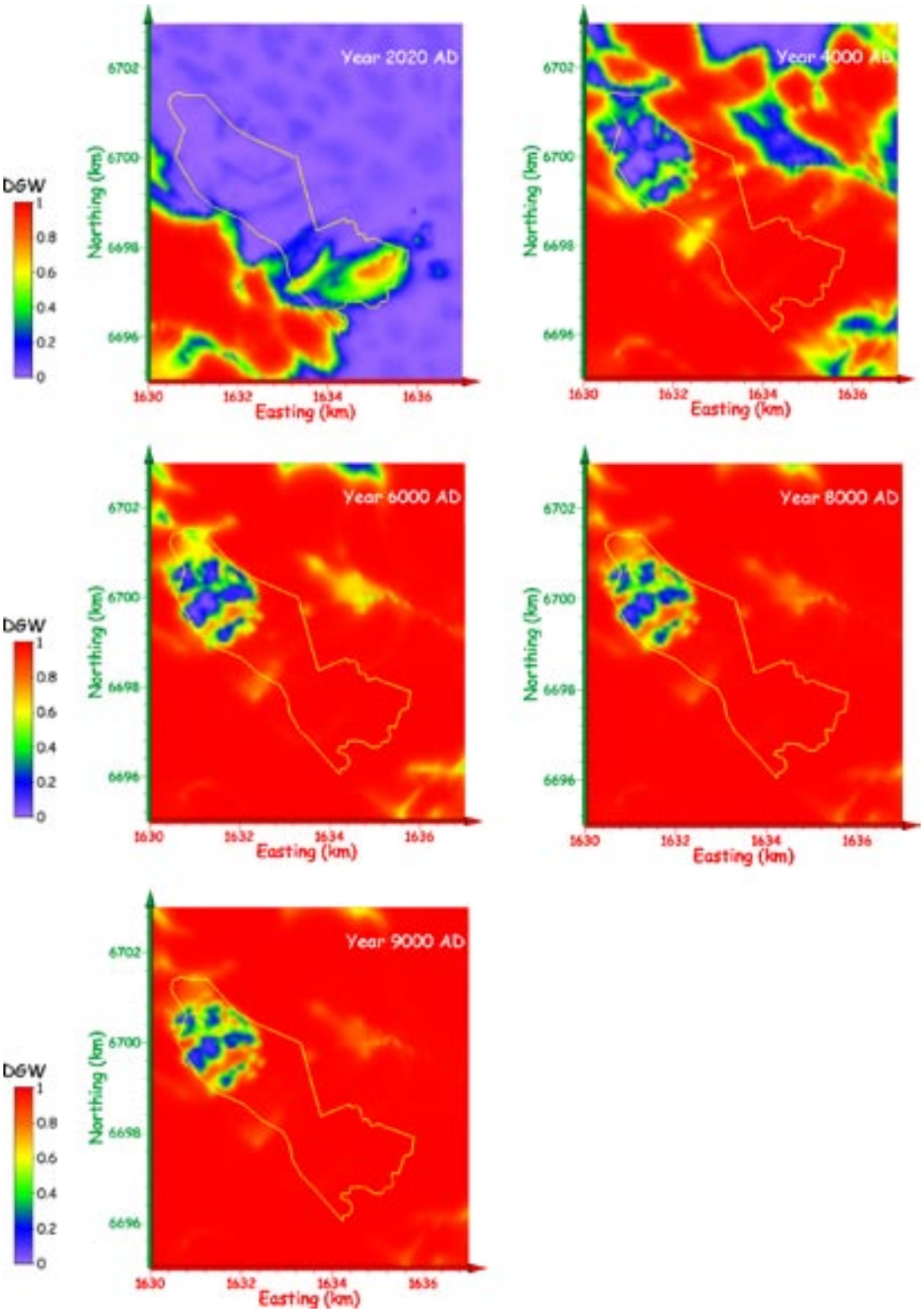

Figure C-2. *Evolution of the distribution of the meteoric end-member (dilute groundwater proportions) at the repository depth for Forsmark. Results at times 2020, 4000, 6000, 8000 and 9000 AD are shown. Plots are represented using the regional model results provided by /Hartley et al. 2006/ for SDM stage 1.2. The figure shows the progressive inflow of meteoric groundwaters as the shore line is gradually displaced towards the upper-right corner of the modelled domain.*

As a whole, these results indicate that salinities will remain very low during the temperate period following repository closure, ensuring that the swelling properties of the buffer and backfill will not be negatively affected. However, they also indicate that the inflow of superficial waters of meteoric origin will progressively flush the previous more saline groundwaters at repository depth and "soon" in the estimated evolution (3000–4000 AD) they would become dominant in some areas of the repository. At the end of the simulation period (9,000 AD) these dilute groundwaters would have almost completely replaced the previous ones in all the area.

This predicted evolution is based on Site Descriptive Modelling version 1.2 /Hartley et al. 2006/. An updated version with some new concepts for groundwater flow modelling is in preparation for the Forsmark SDM stage 2.2 /Follin et al. 2007/. These new assumptions could modify the intensity or timing of this predicted dilution scenario. In any case, the available evolution model can be used as an example of a "complete" dilution scenario to explore some important hydrochemical effects.

In geochemical terms, this evolution implies that mixing processes between the inflowing dilute groundwaters and the existing more saline groundwaters at repository depth may be transient. When these dilute groundwaters replace completely the previous ones, mixing processes are not effective anymore and the compositional features of these inflowing groundwaters will be controlled by water-rock interaction (and possibly, microbial) processes. Therefore, to evaluate SKB's suitability criteria in this dilution scenario both "mixing + reaction" (when both water types are present) and "only reaction" simulations (when only the dilute water remains) must be considered. This situation is especially relevant for the stability of the bentonite (chemical erosion and/or colloid formation, for which a total concentration of divalent cations higher than 1 mM is needed).

Methodology of geochemical calculations

To model the "mixing+reaction" stage and the "only reaction" stage during the dilution scenario in the temperate period, two types of simulations have been performed with PHREEQC /Parkhurst and Appelo 1999/ and the WATEQ4F database /Ball and Nordstrom 2001/: mixing and flush calculations.

Mixing calculations (with or without superimposed reactions) between selected groundwaters at the repository depth and an inflowing dilute groundwater of meteoric origin have been performed. Complete mixing paths are simulated between these two end-members, from 100% of the "old" groundwater (OG) to 100% of dilute groundwater (Altered Meteoric end-member, AM), in mixing steps of 10% (90% OG and 10%AM, 80% OG and 20% AM, and so on).

Flush calculations[24] /Bethke 1996/ track the evolution of a selected zone in the system from the moment when diluted groundwaters have just flushed out the last pocket of the old groundwater. Heterogeneous reactions (e.g. imposed equilibrium situations) are prescribed to occur in that portion of the aquifer (including both solids and water). At each step in the simulation a volume of diluted (and "unreacted") groundwater of fixed composition is added to the reference system, pushing the existing volume of previous groundwater and reacting with the solids. In the calculations presented here, 100 steps have been simulated and only advective transport is considered. Neither an explicit definition of time nor the spatial dimensions of the reference system have been included.

Selection of the appropriate groundwaters (the inflowing dilute groundwater and the existing groundwater at repository depth) and the appropriate heterogeneous reactions (mainly cation exchange) is necessary to perform both types of simulations.

Selected groundwaters. Most sampled groundwaters at the repository level in Forsmark candidate area are brackish (Cl between 4,500 and 5,800 mg/L;) and have an important Littorina signature (high Mg^{2+} and sulphate). However, there are also some indications of possibly more

[24] Flush calculations are a type of the classical flow-through geochemical calculations also known as solid-centred flow-through open system simulations /Wolery and Daveler 1992/.

saline groundwaters (with chloride concentrations around 14,000 mg/L) in KFM07A at the same depth /Hartley et al. 2006/. Therefore, several brackish groundwaters (from KFM01A, 2A, 3A and 6A at 300 to 450 m depth; Table C-2) and the only saline sample available at the repository level (sample #8818 from KFM07A) were selected for the simulations.

The selected dilute groundwater corresponds to sample #4167 from HFM03 borehole. Sample #8335 from HFM09 borehole has also been used to perform sensitivity calculations.

Reactions. As stated in Section 1.2, concentration and dilution processes, involving waters of very different salinity, trigger different types of reactions: dissolution-precipitation, redox and, specially, cation-exchange.

To properly include cation-exchange reactions in the simulations it would be necessary to know the cation exchange capacity (CEC) of the clay minerals in the fracture fillings and the composition of the exchange complex. Although the CEC values for the fracture fillings and the composition of the exchange complexes in the studied sites remains unreported, several indirect estimates are available, (mainly deduced from cation exchange modelling in Äspö) and the exchange complex compositions can be calculated.

/Viani and Bruton 1995, 1996/ estimated an exchange capacity of 0.1 mol_c/L for Äspö fracture minerals, whereas /Banwart et al. 1995/ proposed values between 0.083 and 0.004 mol_c/L. /Molinero 2000/ and /Molinero and Samper 2006/ deduced a CEC value of 0.6 mol_c/L as the best fit for reactive transport simulations performed in the Äspö redox zone. More recently, some CEC values for fractures at different depths in Forsmark have been measured /SGI

Table C-2. Main compositional features of the groundwaters from the repository depth (KFM01D boreholes) and diluted granitic groundwaters (HFM boreholes) used in the simulations. Samples #12354, #12002 and #8017 display major element contents similar to samples taken at the same borehole but at slightly different depths.

	Sample #12354[(1)] (KFM01D)	Sample #12002[(2)] (KFM02A)	Sample #8017[(3)] (KFM03A[25])	Sample #8809 (KFM06A)	Sample #8818 (KFM07A)	Sample #4167 (HFM03)	Sample #8335 (HFM09)
Depth (m)	445	418	441	302	379	21.25	25.5
Temp	–	–	10.7	8.94	–	–	–
pH	8.4	7.36	7.29	7.35	*7.47*[(4)]	*7.60*	*7.91*
Alk.	20.0	96.5	91.8	45.7	12.4	15.7	466.0
Cl	5,800	5,440	5,430	4,560	13,600	15.7	181.0
SO_4^{2-}	38.3	435	472	151	130	18.7	85.1
Na	1,770	1,930	2,070	1,450	2,840	64.6	274.0
K	7.67	26.30	26.8	13	15.3	9.5	5.6
Ca	1,830	1,240	975	1,300	5,150	62.0	41.1
Mg	15.2	201	202	71.2	34.5	14.0	7.5
Sr	19.8	13.3	10.1	14.9	61.1	0,28	0.38
% drilling water	0.9	2.85	0.25	7.7	2.85	–	–

(1) Very similar major composition to the sample #12316 taken at 341 m depth in borehole KFM01D.

(2) Very similar major composition to the sample #8272 taken at 415 m depth in borehole KFM02A.

(3) Very similar major composition to the sample #8012 taken at 379 m depth in borehole KFM03A.

(4) Calculated assuming calcite equilibrium. The actual measured pH is 6.46

[25] Sample 8017 in KFM03A is at the repository depth in the Forsmark candidate zone but not in the specific zone envisaged for the construction of the repository. But this brackish, Littorina-rich groundwater sample is very similar to other found in the construction zone (e.g. sample 8016 at 500 m depth in KFM02A) and it contains minor amounts of drilling water (0.25%).

2007/. Most of the available values correspond to depths of less than 200 m and are between 0.09 and 0.19 mol_c/kg. Two other CEC values correspond to a depth of 612 m and are around 0.05 mol_c/kg. (These SGI CEC values are only analytical raw data and the corresponding report is not available yet. It has been assumed that these CEC values are expressed in the most usual form, per kg of solid, and therefore additional information would be needed to express them as a per liter of groundwater basis −the values expected in PHREEQC − and properly compare these values with those deduced from modelling.)

Therefore, a value of CEC of 0.1 mol_c/L (as a sort of average for modelling tasks) has been considered in the following cation exchange calculations. However, a sensitivity analysis have been performed with a value of 0.5 mol/L. The composition of the exchangers (Table C-3) has been calculated with PHREEQC by assuming equilibrium between a generic exchanger and the selected groundwaters at repository depth. The Gaines-Thomas convention /Gaines and Thomas 1953/ has been used together with the selectivity coefficients proposed by /Appelo and Postma 1993, 2005/, both included in the WATEQ4F database /Ball and Nordstrom, 2001/ distributed with PHREEQC. All predicted exchanger compositions are almost completely saturated with Ca and Na, Ca > Na.

Although some of the selected groundwaters (samples #12002 or #8017; Table C-2) have and important Littorina component, the exchanger composition in equilibrium with these groundwaters is very different to that in equilibrium with Littorina (Table C-3). Exchanger composition in equilibrium with Littorina (or other seawater) is dominated by Na as the concentration of this element is much higher than Mg or Ca in the Littorina end-member (Na = 3,674 mg/L, Mg = 448 mg/L and Ca =151 mg/L). Therefore, the presence of a more saline end-member (deep saline) in these Littorina-rich mixtures drastically modifies the exchanger composition in equilibrium with the mixtures.

The initial conditions (Figure C-3a) are defined by the equilibrium between the groundwater existing at repository depth (one of the brackish or saline samples in Table C-2) and the exchanger in the fracture fillings (Table C-3). Is in this situation when a dilute groundwater reaches the repository and breaks the equilibrium state. The subsequent evolution is studied in two successive stages: (1) the mixing+reaction stage, when the two water types coexist, and (2) the "only reaction" stage when the old (brackish or saline) groundwater has been flushed out.

During the mixing+reaction stage the meteoric groundwater progressively mixes with the already present brackish/saline groundwater. Progressive dilution changes the groundwater composition and the exchanger reacts by cation exchange with these new water compositions. Calcite reequilibrium may also be allowed.

Once the old brackish/saline groundwater has been totally flushed out, the new volumes of dilute groundwater reaching the repository evolve only through heterogeneous reactions with the exchanger previously equilibrated with the old groundwater, or through calcite equilibrium.

Table C-3. Calculated exchanger compositions (expressed as equivalent fraction) in equilibrium with the selected brackish/saline groundwaters at the repository depth in Forsmark. Exchanger compositions in equilibrium with the selected dilute groundwater and with the Littorina end-member are also shown.

	Sample #12354 (KFM01D	Sample #12002 (KFM02A)	Sample #8017 (KFM03A)	Sample #8809 (KFM06A)	Sample #8818 (KFM07A)	DGW Forsmark (HFM03 #4167)	Littorina end-member
CaX_2	0.81	0.662	0.710	0.78	0.812	0.774	0.11
MgX_2	0.007	0.120	0.016	0.047	0.006	0.180	0.364
NaX	0.17	0.210	0.260	0.161	0.174	0.028	0.475
KX	0.002	0.008	0.009	0.004	0.002	0.012	0.0048

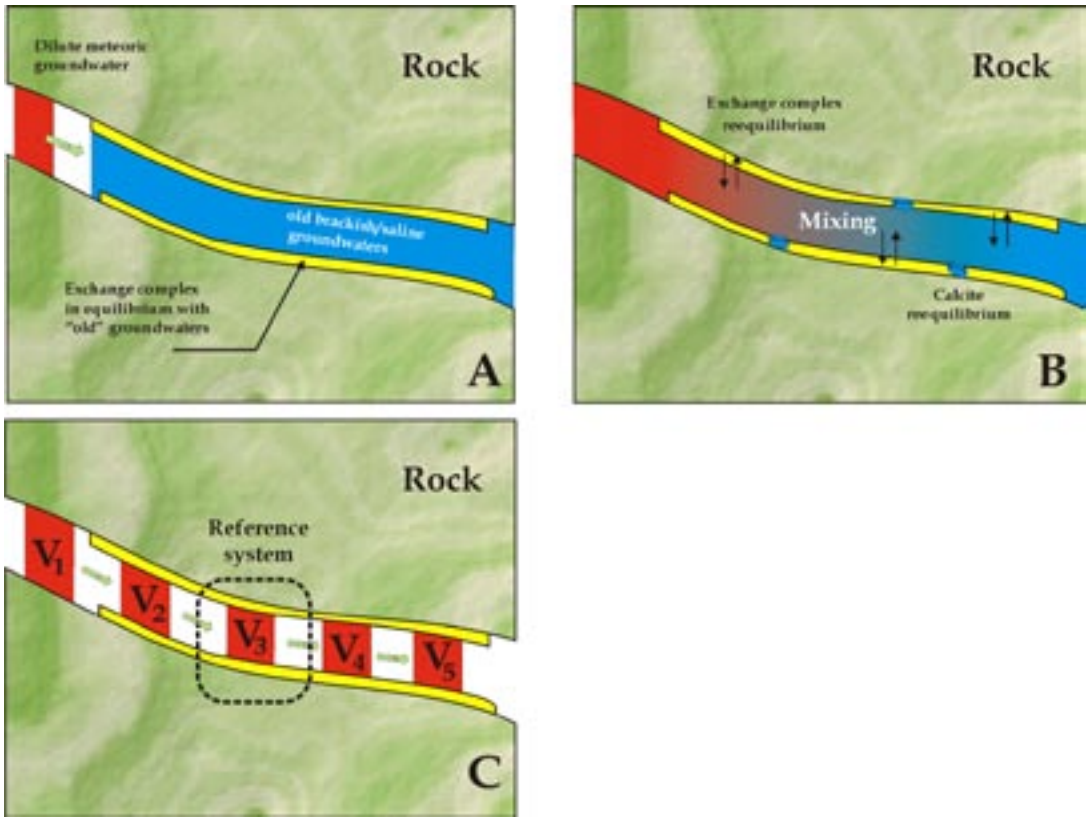

Figure C-3. *Conceptual model of the geochemical calculations performed for the dilution scenario at the repository depth. A. Initial situation; B. Mixing stage; C."Only reaction" stage.*

Within this conceptual model, several alternative evolution scenarios are analysed: pure (conservative) mixing, mixing + exchange reactions, mixing + calcite equilibrium and mixing + exchange + calcite equilibrium. In flush simulations, the effects of exchange reactions and exchange + calcite equilibrium are examined.

Results

Mixing+reaction stage: progressive dilution of the groundwaters at repository depth. Conservative mixing between dilute and brackish/saline groundwaters at repository depth always follows the same oversaturation trend with respect to calcite during the complete mixing path (Figure C-4). Maximum values in the saturation states are reached at mixing proportions of 60–80% of the dilute end-member.

The value of the calcite saturation index in the original end-members (dilute groundwaters and saline/brackish groundwaters at the repository depth) is inside the uncertainty range for equilibrium situations (0.0 ± 0.3). Mixing of these groundwaters in equilibrium with calcite results in oversaturation in the resulting mixed solutions, a classical result associated with the non linear behaviour of the ion activity product /Wigley and Plummer 1976, Appelo and Postma 2005/. This result indicates that dissolution of calcite in the fracture fillings at repository depth is not possible during mixing, and that calcite precipitation could therefore be feasible.

Cation exchange may influence mixing with brackish groundwaters (Figures C-4a and b) only for mixing proportions of the dilute groundwater end-member higher than 80%. In this situation, dissolved calcium may be retained by the exchanger in sufficient amounts to reduce the calcite oversaturation state (Figure C-5). Although a higher CEC value (0.5 mol_c/L) would have a greater impact on the calcite saturation state, it would never produce undersaturation in the mixtures.

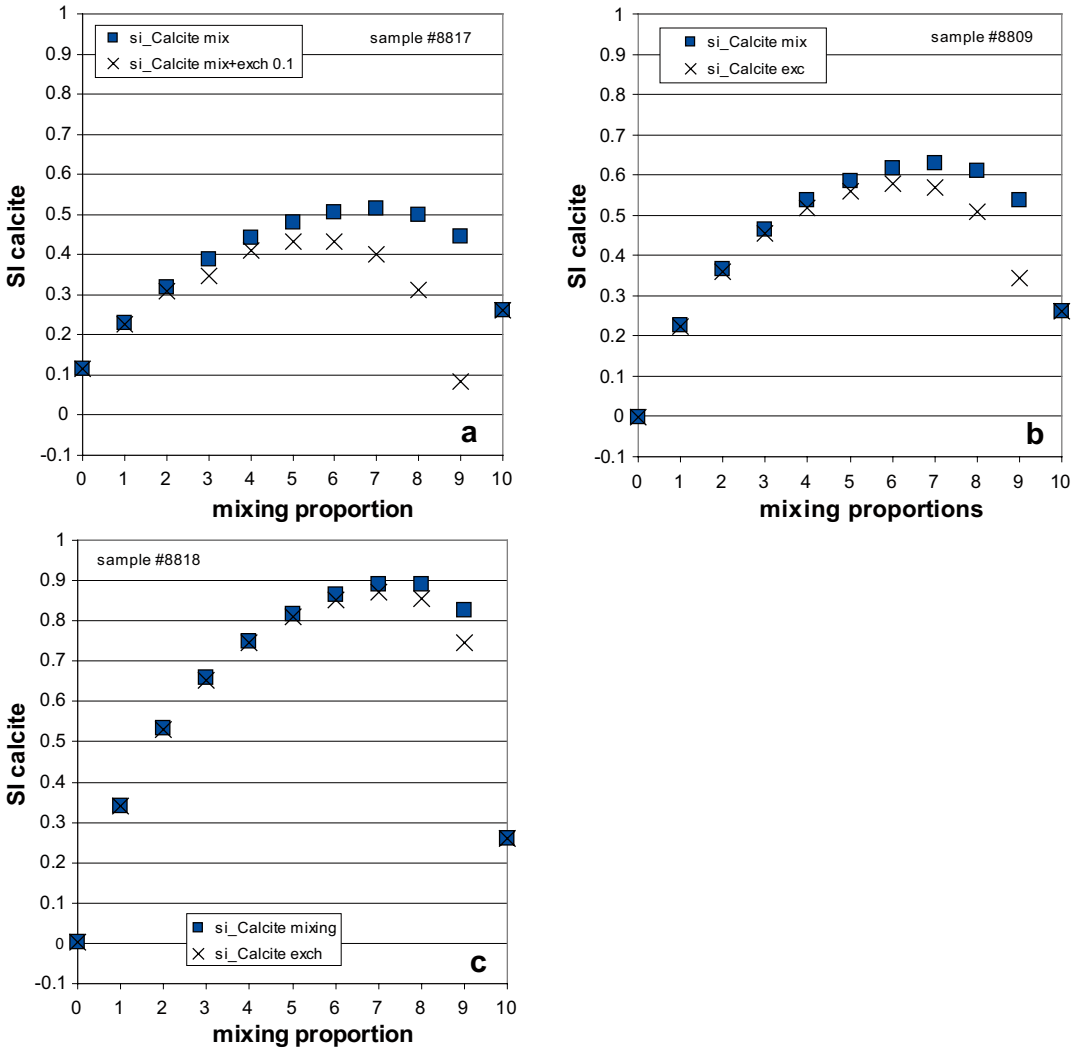

Figure C-4. *Calcite saturation indexes during conservative mixing and mixing + exchange reaction calculations using sample #8817 (a), sample #8809 (b) and sample #8818 (c) as possible groundwaters at repository depth. Sample #4167 was used as the dilute groundwater end member in all the simulations. Mixing proportions are expressed with respect to the dilute end-member.*

Calculated pH in conservative mixing and mixing+exchange calculations are similar and not very different from the pH values in the end-members (Figure C-5). If calcite equilibrium is allowed during mixing the calculated pH value decreases as calcite precipitates, but the minimum value is always higher than 7 in mixing with a brackish end-member (Figure C-5a and b) and higher than 6.6 in mixtures with a saline end-member (Figure C-5c). The pH calculated by adding exchange reactions to the calcite equilibrium during mixing with a saline groundwater do not differ much from the result obtained with just calcite equilibrium (Figure C-5c). But higher differences can be seen when dilute groundwaters dominate the mixture (> 90%) with brackish groundwaters (Figure C-4a and b).

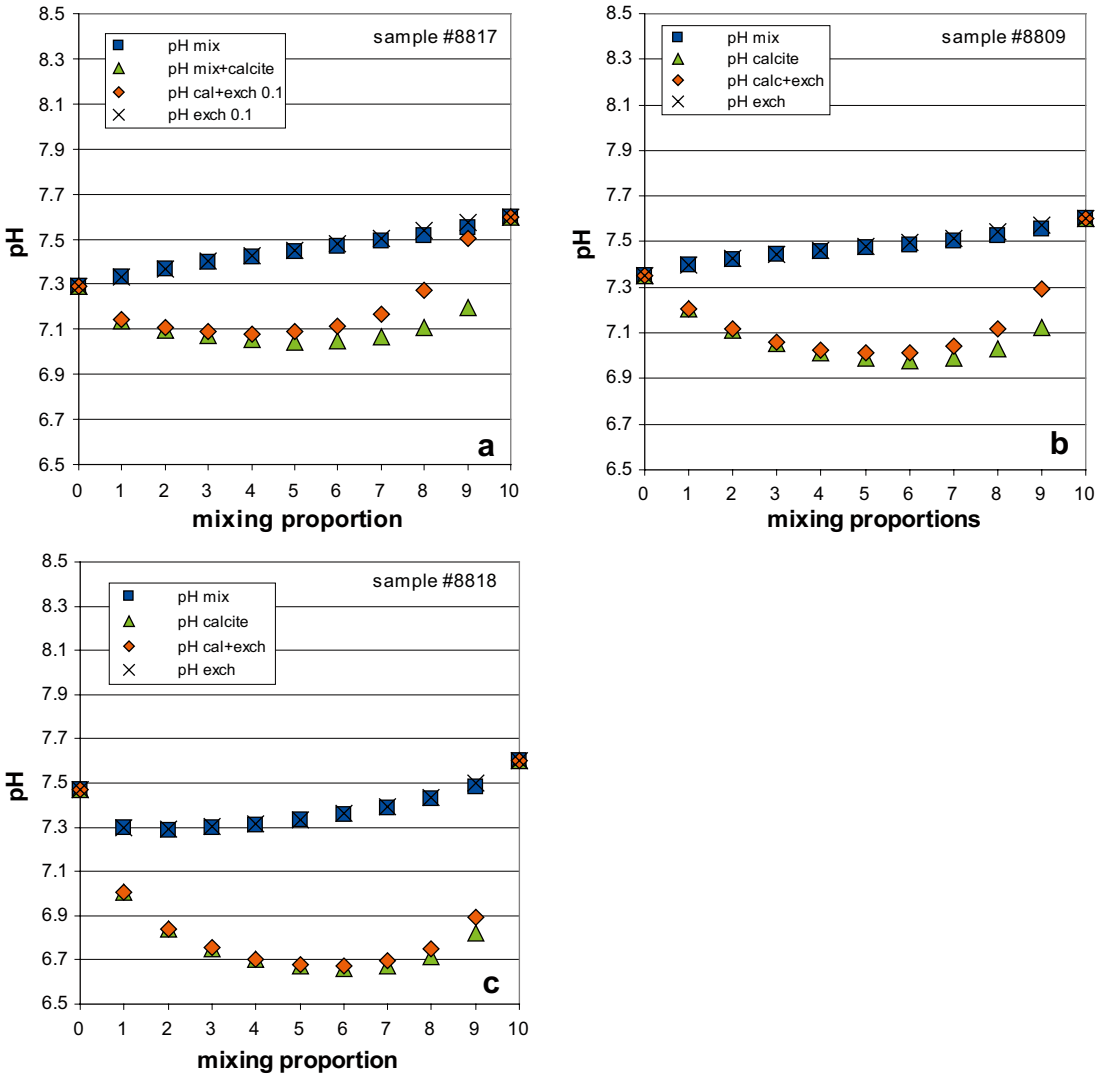

Figure C-5. *Calculated pH values during conservative mixing (pH mix), mixing + exchange reactions (pH exch), mixing+ calcite equilibrium (pH mix+calcite) and mixing+ exchange reactions + calcite equilibrium (pH cal+exch) calculations using brackish sample #8817 (a), brackish sample #8809 (b) and saline sample #8818 (c) as groundwaters at repository depth. Sample #4167 was used as the dilute groundwater end member in all the simulations. Mixing proportions are expressed with respect to the dilute end-member.*

The evolution of the concentration of the main cations (Ca^{2+}, Mg^{2+}, Na^{+} and K^{+}) during mixing and reaction is very similar for all the considered end-members (Figures C-6 and C-7). Conservative mixing defines the typical linear trend between the concentrations of the end-members. If calcite equilibrium is imposed, Ca^{2+} concentrations are slightly reduced compared to conservative mixing when dilute groundwaters dominate the mixture (Figures C-6a and C-7b). Maximum mass transfers associated to calcite precipitation are around 0.7 mmol/L but the effect of mixing clearly dominates the final Ca^{2+} concentration in the mixtures.

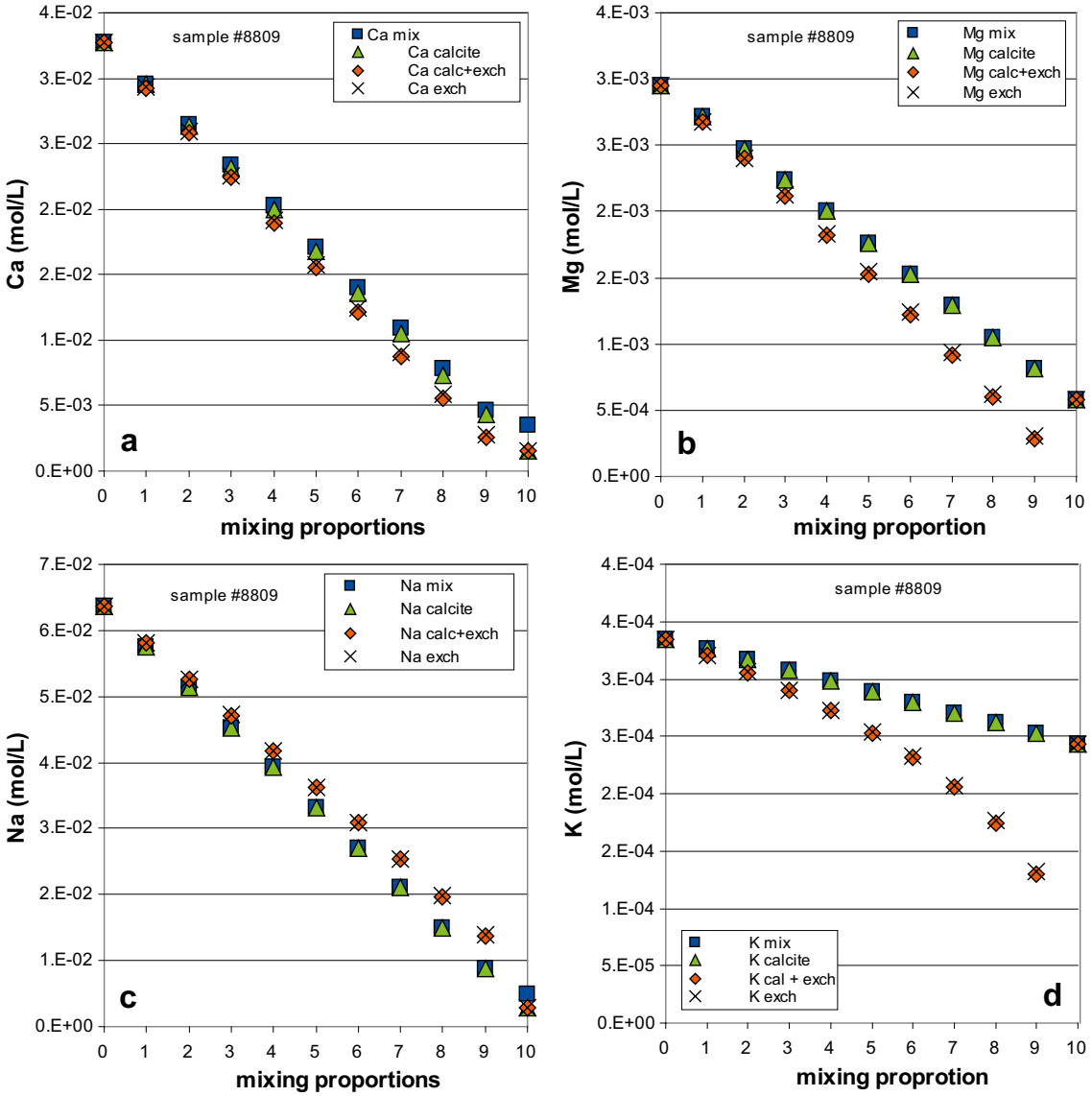

Figure C-6. *Evolution of Ca(a), Mg(b), Na(c) and K(d) concentrations during the mixing and reaction simulations between dilute groundwater (sample #4167) and brackish groundwater (sample #8809). Results of conservative mixing (mix), mixing + exchange reactions (exch), mixing+ calcite equilibrium (calcite) and mixing+ exchange reactions + calcite equilibrium (cal+exch) are shown.*

In mixing and exchange calculations, concentrations of Ca^{2+}, Mg^{2+} and K^{+} are lower than in conservative mixing, whereas sodium concentration is higher as more dilute groundwater mixes with the brackish/saline groundwaters (Figures C-6 and C-7). This indicates that Ca^{2+}, Mg^{2+} and K^{+} are selectively fixed to the exchanger whereas Na^{+} is released to the solution. Although the exchanger reacting with the mixed waters is initially saturated with calcium and magnesium (Table C-3) the incorporation of additional amounts of these elements to the exchanger can be attributed to the salinity effects on heterovalent cation exchange reactions: during a dilution processes divalent cations are preferentially adsorbed in comparison to monovalent Na^{+} /Drever, 1997, Appelo and Postma 2005/.

The effect of these exchange processes on the dissolved Ca^{2+}, Mg^{2+}, Na^{+} and K^{+} concentrations increases if higher CEC values (0.5 mol/L) are used in the simulations. However, the amounts of Mg^{2+} and Ca^{2+} is solution are always high enough as to satisfy the safety criterion $\sum[M^{2+}] > 1\times10^{-3}$ mol/L.

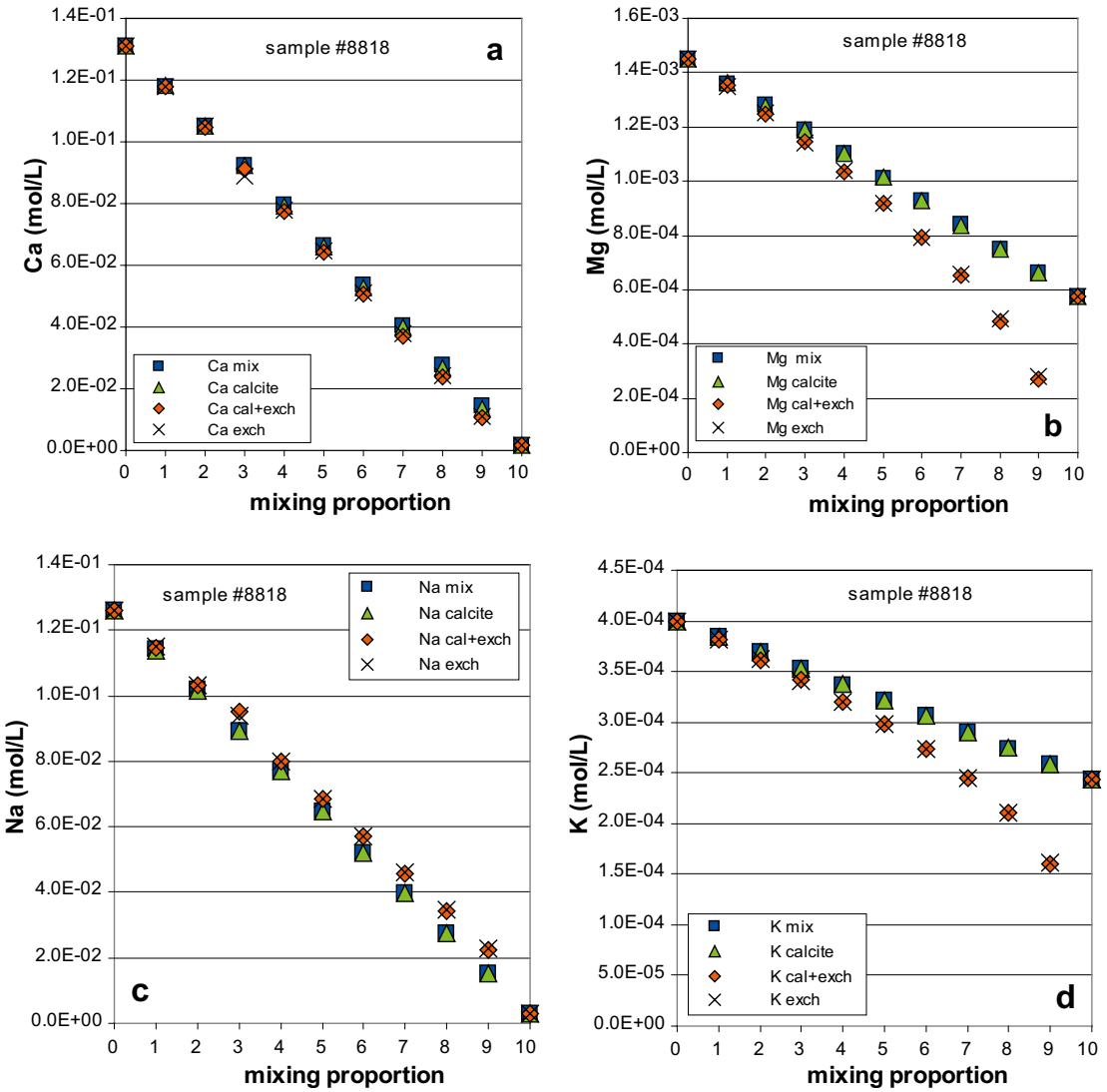

Figure C-7. *Evolution of Ca(a), Mg(b), Na(c) and K(d) concentrations during the mixing and reaction simulations between dilute groundwater (sample #4167) and saline groundwater (sample# 8818). Results of conservative mixing (mix), mixing + exchange reactions (exch), mixing+ calcite equilibrium (calcite) and mixing+ exchange reactions + calcite equilibrium (cal+exch) are shown.*

"Only reaction" stage: flush of dilute groundwater. Once brackish/saline groundwaters have been completely flushed out by the dilute groundwater, the exchanger still remains totally in dis-equilibrium with the incoming groundwater. During the mixing stage, the initial composition of the exchanger in equilibrium with the brackish/saline groundwaters is almost unchanged. Thus, the exchanger will show a high reactivity to the dilute groundwaters during flush calculations until reaching a new equilibrium composition, at which point its reactivity is exhausted.

As shown in Figures C-8, the cationic content of the first volume of dilute groundwater entering this zone is importantly affected by exchange processes. Na^+ concentration increases whereas Ca^{2+}, Mg^{2+} and K^+ decrease notably. The exchange trend is the same described in the mixing stage (Ca^{2+}, Mg^{2+} and K^+ are fixed in the exchanger whereas Na^+ are released) but now cation exchange is not buffered by mixing.

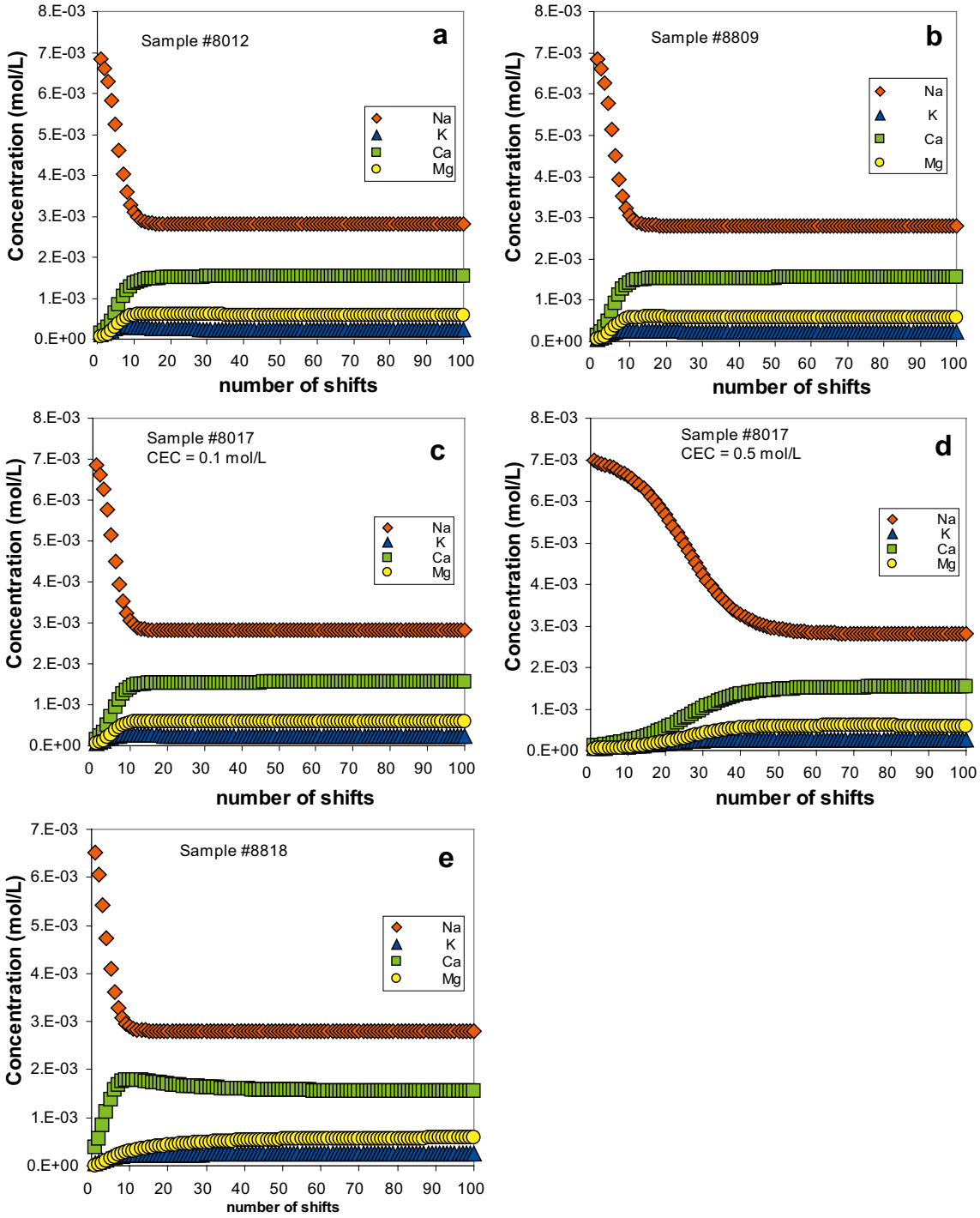

Figure C-8. *Results of flush simulations of the dilute groundwater passing through a zone with the exchanger previously equilibrated with a different water and with different CEC values. (a) equilibriated with sample #8012 and CEC = 0.1 mol/L; (b) equilibrated with sample #8809 and CEC = 0.1 mol/L; (c) and (d) equilibrated with sample #8017 but different CEC, 0.1 in (c) and 0.5 in (d); (e) equilibrated with the saline sample #8818) with a CEC = 0.1 mol/L*

As successive new volumes of dilute groundwater pass through this zone, the intensity of the exchange decreases (Na^+ concentrations decrease and Ca^{2+}, Mg^{2+} and K^+ concentrations increase towards the initial values in the inflowing groundwater). Once the exchanger reactivity is exhausted, the composition of the dilute groundwater and the concentration of cations in all subsequent volumes of water remain equal to the original concentrations in the dilute groundwater reaching the zone.

The number of dilute groundwater volumes (shifts) necessary to deplete the exchanger reactivity in zones previously occupied by brackish or saline groundwaters is around 10–15 (Figures C-8). If the CEC value considered in calculations is increased from 0.1 mol_c/L to 0.5 mol/L (Figure C-8d), the number of shifts necessary to deplete the exchanger reactivity increases in the same proportion (from 10 to 40 shifts).

If calcite equilibrium is also imposed results do not change appreciably. As a rule, calculated pH values do not pose problems to SKB's suitability criteria and, therefore, they are not discussed here.

A rough estimate of the time necessary to deplete the exchanger reactivity can be obtained from data on fracture density, kinematic porosity and flow-wetted surface area presented by /Hartley et al. 2005/ and from the effective recharge rate into the bedrock of the Forsmark zone (1 mm/year) proposed by /Molinero and Rasposo 2005/. Time periods from 100 to 4,000 years are obtained for a CEC value of 0.1 mol/L. These results must be treated with caution but they highlight the necessity of more data, since the effects of exchange reactions could be very limited in time (100 years) or either span almost half of the simulated time for the temperate period (4,000 years).

More precise estimations could be obtained with truly coupled reactive transport simulations, using multiple exchangers and/or exchangers with different types of exchange sites, site-specific selectivity coefficients, constraints on the composition of the exchange complex, changing the convention used for their formal description (e.g. Gapon, Vanselow, Gaines-Thomas, etc; /Appelo and Postma 2005/), etc.

However, the direction of the exchange reactions (with the exchanger fixing Ca^{2+} and Mg^{2+} and releasing Na^{+}) will not change in coupled reactive transport simulations as it mainly depends on the stoichiometry of the heterovalent exchange reactions during dilution processes /Drever 1997, Appelo and Postma 2005/. Therefore, a transient negative impact of these processes on the Ca^{2+} and Mg^{2+} concentrations of the groundwaters is very probable unless the CEC of the fracture fillings is very low. All these results emphasize the need for CEC values in the fracture fillings.

C.3.2 Discussion

Mixing of dilute groundwaters with the existing brackish/saline groundwaters at repository depth throughout the initial stages of dilution during the temperate period will be favourable from the point of view of SKB's suitability criteria. For instance, calcium concentrations are calculated to be around 50 mM at repository depth during the first 1,000 years /Auqué et al. 2006/. Ca^{2+} and Mg^{2+} concentrations will be higher than the stipulated safe value (1mmol/L) even when low proportions oh these brackish/saline groundwaters remain (e.g. 1%). All the simulated mixing paths predict a slight oversaturation with respect to calcite. Although calcite precipitation is feasible, this process would possibly be very limited due to the decrease in oversaturation as a result of exchange reactions.

Once brackish/saline groundwaters are totally flushed out by the incoming diluted waters, cation exchange reactions will probably lead to a decrease below the safety limit ($\sum[M^{2+}] > 1\times10-3$ mol/L) of the concentration of Ca^{2+} and Mg^{2+} in the groundwaters during a transient period, as the reactivity of the exchanger is exhausted. The duration of this transient period is not well constrained with present scoping calculations and can be as short as 100 years or as long as 4,000 years. From that moment on, the composition of the dilute groundwaters reaching the repository will not be modified and its Ca^{2+} and Mg^{2+} concentrations will depend on the previous water-rock interaction processes. This "flushed out" stage may occur "soon" in some zones of the repository in the predicted hydrological evolution for the temperate period, affecting finally to the most part of the repository.

A review of the compositional features of dilute meteoric waters in crystalline environments from Sweden and other countries (Appendix 2, /Auqué et al. 2006/) indicate that in all examined sites there exist fresh, low calcium groundwaters (i.e. Ca < 40 mg/L) in the upper 100 m of

the bedrock, irrespective of site location. Such fresh waters extend to greater depths in more hydraulically active recharge systems like the Laxemar sub-area, which mimics the future situation of Forsmark during the temperate period.

C.4 Conclusions

Two possible ***concentration scenarios*** with increments in salinity at the repository depth have been examined: (1) upconing, and (2) arrival of freeze-out brines.

(1) Upconing of deep saline groundwater to repository depths may occur during the excavation and operation phase, during permafrost conditions and during glacial periods.

Modelling results obtained for the excavation and operation phase indicate that negligible upconing of saline groundwaters is to be expected /Svensson 2005, 2006/. Salinities up to ≈ 52 g/L TDS (or ≈ 1 M Cl−) have been calculated to locally reach the repository depth by upconing of deep saline waters during glacial periods in the Oskarshamn area /Jaquet and Siegel 2006/. This salinity value is well below the safety limits for maintaining backfill (<70 g/L) and buffer (< 100 g/L) properties. Geochemical calculations performed here for these saline waters reaching the repository level indicate that they easily fulfil the rest of the safety function indicators: $\sum[M^{2+}] > 1 \cdot 10^{-3}$ mol/L to avoid colloid formation, reducing conditions, pH around 8, and low expected dissolved S^{2-} concentrations if sulphate reduction activity were present. Other possible upconing scenarios have not been modelled (e.g. upcoming during permafrost conditions) and may require further assessment to be conclusively ruled out.

(2) The possible depth reached by salinity pulses associated to the sink of shallow freeze-out brines generated during permafrost conditions has also been examined.

Both, model results /Vidstrand et al. 2006/ and field data from the reviewed sites suggest that this shallow saline pulses may reach repository depths. The generic simulations performed in SR-Can on the density-driven evolution of a high salinity pulse associated to shallow freezing-out processes suggest a transient influence of saline waters at the repository depth. Model calculations indicate that saline waters generated in deformation zones will move by gravity to deeper regions in periods shorter than 300 years. In these highly conductive parts the salinity peak at repository depth may be as high as 9% (corresponding to a groundwater with ≈ 1.6 M of Cl^-). This salinity would not be so high as to hamper the swelling capacity of the buffer and the backfill. The concentration of divalent cations (Ca^{2+}, Mg^{2+}, etc) is expected to increase in this situation, helping the accomplishment of the safety criteria concerning the indicator $\sum[M^{2+}] > 1 \times 10^{-3}$ mol/L. In any case, this freeze-out scenario should be explored and refined with site-specific hydrogeological models to evaluate the transient effect of the saline pulse that eventually would reach the repository. Moreover, theoretical calculations should be used to better approximate the chemical composition for these freeze-out brines.

In dilution scenarios, like the ones predicted during the temperate period, the initial mixing with the existing brackish/saline groundwaters at repository depth will favour the fulfilment of SKB's suitability criteria. Ca^{2+} and Mg^{2+} concentrations will be higher than the safe value (1 mmol/L), even when low proportions of brackish/saline groundwaters remain (e.g. 1%); also, salinity would be far from the limits of damage to the properties of buffer and backfill.

Once brackish/saline groundwaters are totally flushed out by the incoming diluted waters, cation exchange reactions may lead to a decrease of Ca^{2+} and Mg^{2+} concentrations below the safety limit ($\sum[M^{2+}] > 1 \times 10^{-3}$ mol/L) in the groundwaters during a more or less transient period (until the reactivity of the exchanger is exhausted). The duration of this transient period is not well constrained with present scoping calculations and can be as short as 100 years or as long as 4,000 years. From that moment on, the composition of the dilute groundwaters reaching the repository would not be modified and their Ca^{2+} and Mg^{2+} concentrations would depend on the previous water-rock interaction processes. This "flushed out" stage may occur "soon" in some zones of the repository in the predicted hydrological evolution for the temperate period, affecting finally most part of the repository.

Similar problems may arise in glacial dilution scenarios. In the site characterization studies, traces of this type of waters have been found at repository depths (400–600 m) and even at greater depths (around 1,000 m) in the Forsmark area. These melt-waters are expected to be even more diluted than present meteoric groundwaters. If these melt-waters undergo mixing with previous brackish/saline (Ca-rich) groundwaters during penetration in the bedrock, SKB's suitability criteria may be fulfilled. However, if the ingress of melt-waters completely flux out the previous brackish/saline (Ca-rich) groundwaters, similar negative situations to that described in the meteoric dilution scenario may be expected.

Therefore, in dilution scenarios it is necessary to clearly identify whether the "beneficial" mixing process is effective or either it is replaced by flushed-out situations. In this latter case, the spatial distribution of the flushing waters at the repository depth and the duration of this situation (e.g. until new saline groundwaters reach the repository) should be evaluated.

References for Appendices A, B and C

Andersen M S, Jakobsen V N R, Postma D, 2005. Geochemical processes and solute transport at the seawater/freshwater interface of a sandy aquifer. Geochim. Cosmochim Acta, 69, 3979–3994.

Appelo C A J, Postma D, 1993. Geochemistry, Groundwater and Pollution. 1st Edition. Balkema, Rotterdam, The Netherlands.

Appelo C A J, Postma D, 2005. Geochemistry, Groundwater & Pollution. Balkema, Rotterdam, The Netherlands, 2nd edition, 649 p.

Auqué L F, Gimeno M J, Gómez J, Puigdoménech I, Smellie J, Tullborg E-L, 2006. Groundwater chemistry around a repository for spent nuclear fuel over a glacial cycle Evaluation for SR-Can. SKB TR-06-31, Svensk Kärnbränslehantering AB. 123 pp.

Auqué, L, Gimeno M J, Gómez J, Nilsson A-C, 2007. Potentiometrically measured Eh in groundwaters from the Scandinavian Shield. Applied Geochemistry, in press.

Ball J W, Nordstrom D K, 2001. User's manual for WATEQ4F, with revised thermodynamic data base and test cases for calculating speciation of major, trace, and redox elements in natural waters. U.S. Geological Survey, Open File Report 91–183, USA.

Banwart S A, 1999. Reduction of iron (III) minerals by natural organic matter in groundwater. Geochim. Cosmochim. Acta, 63, 2919–2928.

Banwart S A, Laaksoharju M, Pitkänen P, Snellman M, Wallin B, 1995. Development of a site model for reactive element dynamics. In: S. Banwart (ed.), The redox experiment in block scale: final reporting of results from the three year project. SKB Äspö Hard Rock Laboratory Progress report 25-95-06, Svensk Kärnbränslehantering AB.

Bath A, 2007. Compilation and Review of Hydrochemistry Data. Memorandum, 29 p.

Berg C, Bergelin A, Wacker P, Nilsson A-N, 2006. /Forsmark site investigation. Hydrochemical characterization in borehole KFM08A. Results from the investigated section at 683.5–690.6 (690.8) m./ SKB P-06-63, Svensk Kärnbränslehantering AB. 81 p.

Bergelin A, Berg C, Wacker P, Nilsson A-C, 2006. Forsmark site investigation. Complete hydrochemical characterisation in KFM08A. Results from the investigated section at 683.5–690.6 (690.8) m. SKB P-06-63, Svensk Kärnbränslehantering AB.

Bethke C M, 1996. Geochemical reaction modelling. Concepts and applications. Oxford University Press, 397p.

Casanova J, Négrel P, Blomqvist R, 2005. Boron isotope fractionation in groundwaters as an indicator of past permafrost conditions in the fractured crystalline bedrock of the fennoscandian shield. Water Research, 39, 362–370.

Drever J I, 1997. The Geochemistry of Natural Waters: Surface and Groundwater Environments. 3rd ed., Prentice Hall, New York, USA, 436 p.

Follin S, Stigsson M, Svensson U, 2005. Regional hydrogeological simulations for Forsmark – numerical modelling using DarcyTools. Preliminary site description Forsmark area – version 1.2. SKB R-05-60, Svensk Kärnbränslehantering AB.

Follin S, Johansson P-O, Hartley L, Holton D, McCarthy R, Roberts D, 2007. Updated strategy and test of new concepts for groundwater flow modelling in Forsmark in preparation of site descriptive modelling stage 2.2. SKB R-07-20, Svensk Kärnbränslehantering AB. 100 p.

Gaines G L, Thomas H C, 1953. Adsorption studies on clay minerals. II. A formulation of the thermodynamics of exchange adsorption. J. Chem. Phys. 21, 714–718.

Gimeno M J, Auqué L F, Gómez J, 2007. PHREEQC modelling. Appendix 3. SKB R-06-70, Svensk Kärnbränslehantering AB.

Gómez J B, Laaksharju M, Skårman E, Gurban I, 2006. M3 version 3.0: Concepts, methods, and mathematical formulation. SKB TR-06-27, Svensk Kärnbränslehantering AB.

Grenthe I, Stumm W, Laaksoharju M, Nilsson A C, Wikberg P, 1992. Redox potentials and redox reactions in deep groundwater systems. Chem. Geol., 98, 131–150.

Hartley L, Cox I, Hunter F, Jackson P, Joyce S, Swift B, Gylling B, Marsic N, 2005. Regional hydrogeological simulations for Forsmark. Numerical modelling using CONNECTFLOW. Preliminary site description. Forsmark area, version 1.2. SKB R-05-32, Svensk Kärnbränslehantering AB. 254 p.

Hartley L, Hoch A, Jackson P, Joyce S, McCarthy R, Rodwell W, Swift B, Marsic N, 2006. Groundwater flow and transport modelling during the temperate period for the SR-Can assessment: Forsmark area, Version 1.2. SKB R-06-98, Svensk Kärnbränslehantering AB.

Jaquet O, Siegel P, 2006. Simpevarp 1.2. Regional groundwater flow model for a glaciation scenario. SKB R-06-100, Svensk Kärnbränslehantering AB. 55 p.

King-Clayton L, Chapman N, Ericsson L O, Kautsky F, 1997. Glaciation and Hydrogeology. Workshop on the impact of climate change and glaciations on rock stresses. Groundwater flow and hydrochemistry. Past, present and future. Workshop Proceedings. SKI-R-97:1.

Laaksoharju M, Tullborg E-L, Wikberg P, Wallin B, Smellie J, 1999. Hydrogeochemical conditions and evolution at the Äspö HRL, Sweden. Applied Geochemistry, 14, 835–859.

Langmuir D, 1997. Aqueous environmental geochemistry. Prentice Hall, 600 p.

Lindberg R D, Runnells D D, 1984. Ground water redox reactions: an analysis of equilibrium state applied to Eh measurements and geochemical modeling. Science, 22, 92 –927.

Molinero J, 2000. Testing and validation of numerical models of groundwater flow, solute transport and chemical reactions in fractured granites:a quantitative study of the hydrogeological and hydrochemical impact produced by the construction of the Äspö Underground Laboratory (Sweden). Ph. D. Dissertation. ETS De Ingenieros de Caminos, canales y Puertos. Universidad de A Coruña, 221 p.

Molinero J, Arcos D, Duro L, 2008. Coupled hydrogeochemical and solute transport, visualisation and supportive detailed reaction modelling. In Kalinowski B E (ed) Background complementary hydrogeochemical studies. SDM-Site Forsmark. SKB R-08-87, Svensk Kärnbränslehantering AB.

Molinero J, Rasposo J R, 2005. Coupled hydrological and solute transport modeling. In: Hydrogeochemical evaluation. Preliminary site description. Forsmark area, Version 1.2. SKB R-05-17, Svensk Kärnbränslehantering AB. Appendix 5, 361–397 pp.

Molinero J, Samper J, 2006. Large-scale modeling of reactive solute transport in fracture zones of granitic bedrocks. J. Contaminat. Hydrol., 82, 293–318.

Nilsson K, Bergelin A, 2006. Forsmark site investigation. Complete hydrochemical characterisation in KFM09A. Results from the investigated section at 785.1–792.2 m. SKB P-06-217, Svensk Kärnbränslehantering AB.

Nilsson K, Bergelin A, Lindquist A, Nilsson A-C, 2006. Forsmark site investigation. Complete hydrochemical characterisation in KFM01D. Results from seven investigated sections: 194.0–195.0 m, 263.8–264.8 m, 314.5–319.5 m, 354.9–355.9 m, 369.0–370.90 m, 428.5–435.6 m and 568.0–575.1 m. SKB P-06-227, Svensk Kärnbränslehantering AB.

Nordstrom D K, Munoz J L, 1985. Geochemical Thermodynamics. 2nd Ed. The Benjamin/ Cummings Publ. Co., Menlo Park, California, 477 pp.

Nordstrom D K, Ball J W, Donahoe R J, Whittemore D, 1989. Groundwater chemistry and water–rock interactions at Stripa. Geochim Cosmochim Acta, 53, 1727–1740.

Nordstrom D K, Plummer L N, Langmuir D, Busenberg E, May H M, Jones B F, Parkhurst D, 1990. Revised chemical equilibrium data for major water-mineral reactions and their limitations. In: Melchior, D.C. and Basset, R.L. (Eds.) Chemical Modeling of Aqueous Systems II. ACS Symp. Ser. pp. 398–413.

Parkhurst D L, Appelo C A J, 1999. User´s guide to PHREEQC (Version 2), a computer program for speciation, batch reaction, one dimensional transport, and inverse geochemical calculations. (Science Report WRRIR 99–4259), USGS, 312 p.

SGI, 2007. Draft laboratory results on CEC values at Forsmark. Statens Geoteknisia Institute. Linköping.Sent by e-mail by Eva Gustaffson (Geosigma).

SKB, 1999. SR-97. Processes in the repository evolution. Background report to SR-97. SKB TR-99-07, Svensk Kärnbränslehantering AB, 271 p.

SKB, 2004a. Hydrogeochemical evaluation of the Simpevarp area, model version 1.1. SKB R-04-16, Svensk Kärnbränslehantering AB, 398 p.

SKB, 2004b. Hydrogeochemical evaluation of the Forsmark site, model version 1.1. SKB R-04-05, Svensk Kärnbränslehantering AB, 342 p.

SKB, 2006a. Long-term safety for KBS- repositories at Forsmark and Laxemar. A first evaluation. Main report of the SR-Can project. SKB TR-06-09, Svensk Kärnbränslehantering AB.

SKB, 2006b. Climate and climate-related issues for the safety assessment SR-Can. SKB TR-06-23, Svensk Kärnbränslehantering AB. 186 p.

SKB, 2006c. Geosphere process report for the safety assessment SR-Can. SKB TR-06-19, Svensk Kärnbränslehantering AB, 243 p.

Smellie J, Tullborg E V, 2005. Explorative analysis and expert judgement of major components and isotopes. Contribution to the model version 1.2 In: SKB (2005), Hydrogeochemical evaluation. Preliminary site description. Forsmark area. Version 1.2. SKB R-05-17, Svensk Kärnbränslehantering AB, 403 p.

Smellie J, Tullborg E-L, Waber N, Morales T, 2006. Explorative analysis and expert judgement of major components and isotopes. In: Hydrogeochemical evaluation. Preliminary site description. Laxemar subarea, version 1.2. SKB R-06-12, Svensk Kärnbränslehantering AB. Appendix 1, pp. 83–219.

Stefánsson A, Arnórsson S, Sveinbjörnsdóttir Á E, 2005. Redox reactions and potentials in natural waters at disequilibrium. Chem. Geol., 221, 289– 11.

Svensson U, 2005. The Forsmark repository. Modelling changes in the flow, pressure and salinity fields, due to a repository for spent nuclear fuel. SKB R-05–57, Svensk Kärnbränslehantering AB.

Svensson U, 2006. The Laxemar repository. Modelling changes in the flow, pressure and salinity fields, due to a repository for spent nuclear fuel. SKB R-06-57, Svensk Kärnbränslehantering AB.

Thorstenson D C, 1984. The concept of electron activity and its relation to redox potentials in aqueous geochemical systems. USGS Open-File Report 84-072, U.S. Geol. Survey, Denver, Colorado, USA.

Viani B E, Bruton C J, 1995. The role of cation exchange in controlling groundwater chemistry at Aspo, Sweden. UCRL-JC-119724, LLNL.

Viani B E, Bruton C J, 1996. Assessing the role of cation exchange in controlling groundwater chemistry during fliud mixing in fractured granite at Äspö, Sweden. Second Äspö International Geochemistry Workshop, Äspö, Sweden, June 6–7, 1995. Lawrence Livermore National Laboratory, UCRL-JC-121527.

Vidstrand P, Svensson U, Follin S, 2006. Simulation of hydrodynamic effects of salt rejection due to permafrost. Hydrogeological numerical model of density-driven mixing, at a regional scale, due to a high salinity pulse. SKB R-06-101, Svensk Kärnbränslehantering AB, 57 p.

Wacker P, Bergelin A, Nilsson A-C, 2003. Forsmark site investigation. Complete hydrochemical characterisation in KFM01A. Results from two investigated sections: 110.1–120.8 m, 176.8–183.9 m. SKB P-03-94, Svensk Kärnbränslehantering AB.

Wacker P, Bergelin A, Nilsson A-C, 2004a. Forsmark site investigation. Complete hydrochemical characterisation in KFM02A. Results from three investigated sections: 106.5–126.5 m, 413.5–433.5 m and 509.0–516.1 m. SKB P-04-70, Svensk Kärnbränslehantering AB.

Wacker P, Bergelin A, Berg C, Nilsson A-C, 2004b. Forsmark site investigation. Complete hydrochemical characterisation in KFM03A. Results from six investigated sections: 386.0–391.0 m, 448.0–453.0 m, 445.5–455.6 m, 639.0–646.1 m, 939.5–946.6 m, and 980.0–1,001.2 m. SKB P-04-108, Svensk Kärnbränslehantering AB.

Wacker P, Bergelin A, Berg C, Nilsson A-C, 2004c. Forsmark site investigation. Complete hydrochemical characterisation in KFM04A. Results from two investigated sections: 230.5–237.6 and 354.0–361.1 m. SKB P-04-109, Svensk Kärnbränslehantering AB.

Wacker P, Berg C, Bergelin A, Nilsson A-C, 2005a. Forsmark site investigation. Complete hydrochemical characterisation in KFM05A. Results from an investigated section: 712.6–722.0 m. SKB P-05-79, Svensk Kärnbränslehantering AB.

Wacker P, Berg C, Nilsson A-C, 2005b. Forsmark site investigation. Complete hydrochemical characterisation in KFM07A. Results from the investigated section at 848.0–1,001.55 m. SKB P-05-170, Svensk Kärnbränslehantering AB.

Wacker P, Berg C, Nilsson A-C, 2005c. Forsmark site investigation. Complete hydrochemical characterisation in KFM06A. Results from the investigated sections at 353.5–360.6 m and 768.0–775.1 m. SKB P-05-178, Svensk Kärnbränslehantering AB.

Wigley T M L, Plummer L N, 1976. Mixing of carbonate waters. Geochim. Cosmochim. Acta, 40, 989–995.

Wolery T J, Daveler S A, 1992. /EQ6, a computer program for reaction path modeling of aqueous geochemical systems: theoretical manual, user's guide, and related documentation (version 7.0). /(Technical Report), LLNL, Livermore, CA, USA, 338 p.